UNIVERSITÀ DI PARMA

UNIVERSITA' DEGLI STUDI DI PARMA

DOTTORATO DI RICERCA IN
"Scienze Chimiche"

CICLO XXXIV

Metodologie catalitiche sostenibili per processi di ciclizzazione, carbonilazione e fotoossidazione

Coordinatore:
Chiar.ma Prof.ssa Alessia Bacchi Alessia Bacchi

Tutore:
Chiar.mo Prof. Nicola Della Ca'
Nicola Della Ca'

Dottorando: Aleksandr Voronov

Anni Accademici 2018/2019 – 2020/2021

Università degli studi di Parma

Doctoral Programme in Chemical Sciences

XXXIV Cycle

PhD Thesis

Catalytic Protocols for Sustainable Cyclisation, Carbonylation, and Photooxidation

Coordinator

Prof. Alessia Bacchi

Supervisor

Prof. Nicola Della Ca’

PhD Candidate

Aleksandr Voronov

Parma, 2022

Table of Contents

Abstract

Modern chemistry today is more demanding than ever. In view of the climate issues we currently face, process design must be not only simple and straightforward, but also environmentally sustainable. The development of catalytic methods that allow to curtail the release of hazardous substances and avoid energy waste is a key to a secure future. In this work five new catalytic methodologies to access valuable or previously unavailable structures under mild conditions are presented. Elaborating them, we were guided by the principles of atom economy and energy efficiency.

In **Chapter 1** a new approach to 2-aminooxazolines is described. Ligand-free silver catalysis in environmentally friendly alcoholic medium opened access to *O*-5-*exo*-dig cyclisation of propargyl ureas. The transformation is rapid and proceeds with high selectivity under mild conditions. Moreover, one-pot protocol starting from commercial propargylic amines and isocyanates was proved effective, allowing the direct formation of the desired heterocyclic compounds.

The first example of direct synthesis of optically pure hydantoins by palladium-catalysed oxidative carbonylation of unprotected α-amino acid amides is presented in **Chapter 2**. The selective carbonylation was achieved under mild conditions (1 atm of CO) in a biologically harmless solvent without the involvement of ligands and bases, overriding the formation of symmetrical ureas as by-products. The products can be obtained in a short time (2-6 h), and the palladium catalyst precipitates when the reaction is complete and can be recovered by simple filtration.

Chapter 3 contains the description of a carbonylative methodology for the synthesis of fused oxazines by using a CO surrogate in place of carbon monoxide. Extremely selective domino *6-endo-dig* carbonylative cyclisation was observed under mild conditions. The replacement of carbon monoxide by a formyl compound acting *in-situ* brought several advantages, the most important of which is the ability to safely perform the reaction in compact glassware.

Regiodivergent carbonylative cyclisation of *ortho*-alkynylphenols achieved by palladium and rhodium catalysis is described in **Chapter 4**. Previously unknown fused coumarin and 2-coumaranone-based structures were accessed for the first time starting from uniform phenolic substrates. Palladium catalyst exhibited a high selectivity in promoting *6-endo-dig* cyclisation, while rhodium catalyst exclusively provided *5-exo-dig* products. A detailed DFT study performed for the palladium catalysed process is exposed.

In **Chapter 5** a photocatalytic method for the synthesis of previously unavailable (*E*)-2-imino-1,2-dihydronaphthalen-1-ols is reported. The protocol evades the use of toxic oxidants and is promoted by oxygen. Visible light is used as an energy source for the C-O bond construction and dearomatization of naphthalene. The limitations of the process have been explored on 24 examples, and the structures of the products were unambiguously determined by NMR and X-ray analysis. Two plausible reaction mechanisms are provided.

Introduction

One of the definition of “Catalysis” is the enhancing of the chemical reaction rate by means of a compound which is not consumed during the reaction. There is an increasing demand for catalytic methods in chemical industry. Over 80% of all chemical products are manufactured involving catalysis at least in one step of their production chain. Such products include petrochemicals, edible oils, fine chemicals, fertilisers, pharmaceuticals, and polymers. The worldwide demand for catalysts was worth around €13 billion[1] in 2014, while in 2020 the market is valued at €31.5 billion[2], and further increase is foreseen in the next years. This growth is driven not only by the extraordinary versatility of catalysis, but also by its contribution to making industrial processes more sustainable by, for instance, reducing toxic by-products, allowing the access to biofuels, or implementing more efficient batteries. It took decades of thorough studies of catalyst design to achieve all the benefits the industries reap today. Optimising catalytic effects requires a deep understanding of a wide range of chemical phenomena. For these reasons working in the field of catalysis is as challenging as incredibly rewarding.

1. Historical Overview

Alchemists left behind invaluable practical knowledge, which later was successfully used by chemists. One application found its form in the mid-1700s in the production of sulfuric acid *via* the lead chamber process. As it usually happened, the actual outcome was achieved before a theoretical understanding of the reactions occurring inside. Nicolas Clément and his father-in-law Bernard Desormes were the first in 1806 to establish the quantitative relation between oxygen, sulfur dioxide, and nitrogen oxides that were involved in the process. They made it clear that nitric oxide takes part in the process and is released at the end, pointing out its catalytic effect.[3]

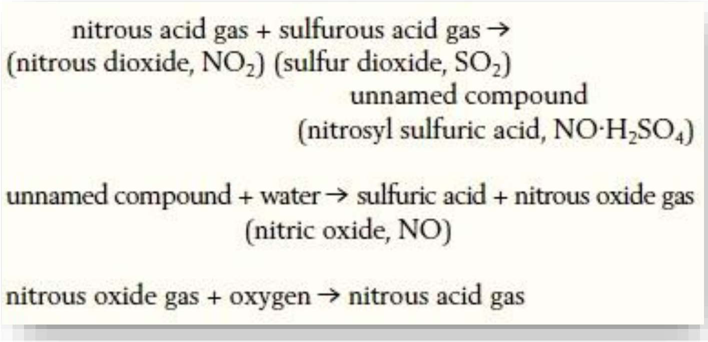

nitrous acid gas + sulfurous acid gas →
(nitrous dioxide, NO_2) (sulfur dioxide, SO_2)
unnamed compound
(nitrosyl sulfuric acid, $NO{\cdot}H_2SO_4$)

unnamed compound + water → sulfuric acid + nitrous oxide gas
(nitric oxide, NO)

nitrous oxide gas + oxygen → nitrous acid gas

Figure 1. Scheme Presented by Nicolas Clément in 1806.

The production of sulfuric acid made it possible to achieve another insight on catalysis. In 1811, one year before the Napoleon’s invasion in Russia, Gottlieb Sigismund Constantin Kirchhoff, corresponding member of Saint Petersburg Academy of Sciences, presented the samples of sugar obtained by hydrolysis of starch in sulfuric acid solutions and demonstrated that the acid was not consumed at the end of the process. The same year he published a communication in German “Bulletin of the Latest and Most

Knowledgeable in Science"[4], thus perpetuating his name as the discoverer of the first catalysed organic reaction.

The first metal-catalysed process was discovered 9 years later by Edmund Davy. He observed that finely cut platinum caused the conversion of ethanol into acetic acid and water, and during the process platinum becomes incandescent. He also showed that at only 50 ˚C platinum would ignite a mixture of hydrogen and oxygen.[6] In 1823, Johann Wolfgang Döbereiner demonstrated this reaction goes even at room temperature when spongy platinum is used.[7] The last discovery was highly praised by Jöns Jacob Berzelius who marked it as "the most brilliant of last year".

Figure 2. Picture Designed for Kirchkoff's Communication in Russian Technology Magazine[5]

Drawing on these and other works published at the beginning of the 19th century, Berzelius decided to systematise the processes that are promoted by substances that remain invariant after the reaction. He proposed the term *catalysis*, derived from Greek καταλύειν (to depose, to pick up, to put an end to), to describe them.

"*Therefore, to employ a well-known derivation in chemistry, I will call the catalytic bodies, the catalytic force, and the decomposition of other bodies by this force catalysis, just as we denote by the word analysis the separation of the constituents of bodies according to the usual chemical affinities*"[8]

Jöns Jacob Berzelius, 1835

For the next 50 years, almost no one made any further attempt to investigate the phenomenon. Catalysis found itself at a stage of complete stagnation. Mainly because the statement of Berzelius was discredited by opposition from an eminent quarter of the chemical society, headed by Justus von Liebig. Their main argument was that the only method to obtain positive knowledge is to leave the incomprehensible unexplained until sooner or later the explanation emerges on its own.[9]

It could have lasted even longer if Wilhelm Ostwald hadn't come up with his essays. As a result of thorough studies of several catalytic processes, Ostwald developed the principle that a catalyst can accelerate the reaction without being changed itself during the entire course of the reaction. At the time Ostwald received the Nobel Prize in 1909, the importance of catalysis started being widely acknowledged.[10]

Comprehension of catalysis would not have been possible without chemical thermodynamics, developed by Gibbs and Helmholtz in the 1870s, which limited the extent of chemical reactions by indicating what is possible and what is not. The principles of thermodynamics are used in studies of catalytic processes even today.

Currently, one of the most rapidly advancing areas of catalysis is transition-metal promoted transformations. Transition-metal catalysed processes have been widely employed in the bulk chemical and fine chemical industry in the last decades. They play a key role in the synthesis of a number of chemical substances, at a large-scale production too. The use of transition metals is associated with the efficiency of performing a plethora of chemical reactions with tolerance to a huge variety of functional groups and high selectivity.

2. Silver-Catalysed Cyclisation

The strategies to access valuable natural and bioactive compounds strongly rely on powerful synthetic procedures some of which would not be possible without the engagement of silver catalysis. Due to its relatively low cost, high stability and versatility, silver has taken a strong position in the industry. The first industrial application of silver was found in 1931, when Theodor Lefort discovered the direct oxidation of ethylene to oxirane by metallic silver.[11] However, it has long been believed that silver has a low catalytic efficiency, and only in the last few decades has there been a surge in the development of silver chemistry.

Silver compounds are mostly utilized as σ- or π-Lewis acids, with predominance to σ-coordination over π-coordination due to the presence of readily available empty *f* orbitals and relativistic contraction of the electron cloud. Apart from the Lewis acid behaviour, silver salts also find applications as general oxidants, single electron transfer (SET) oxidants, cocatalysts, halophiles, and radical initiators. In addition, the complete d^{10} electronic configuration of silver allows to easily coordinate with most unsaturated groups such as alkenyl, alkynyl, imino, keto, and nitrile,[12] and this property makes possible the promotion of cyclisation reactions that will be briefly reviewed in this section.

One of classic examples of silver-catalysed cyclisations is represented by the Conia-ene reaction. It involves the intramolecular addition of an enol or an enolisable moiety (typically a carbonyl group) to an alkene or an alkyne, leading to the formation of a carbocycle containing a quaternary stereocenter. Usually the cyclisation proceeds through *exo-dig* pathway to form the smaller ring, although in some cases *endo-dig* cyclisation can be favoured.

In the pioneer work of Miesch et al.,[13] silylated enol **1** was successfully cyclised by a silver salt to afford the spiro-ketones **2** and **3** (Scheme 1). It turned out that the catalyst must be dry to be active in the process and keeps the reaction medium nonacidic. As almost every silver salt is hygroscopic, the choice was made in favour of silver triflimide that is more stable and has lower tendency to catch water. The optimization study showed that its activity was comparable to that of gold(I) catalysts. The reactions produced five-membered cycles in all the entries given, but the position of the C=C bond in the final product was found to be dependent on the reaction medium: the predominant formation of the *exo*-regioisomer **2** was observed when the reaction was conducted using dichloromethane as a solvent, while the *endo*-isomer **3** was obtained as the major product in toluene.

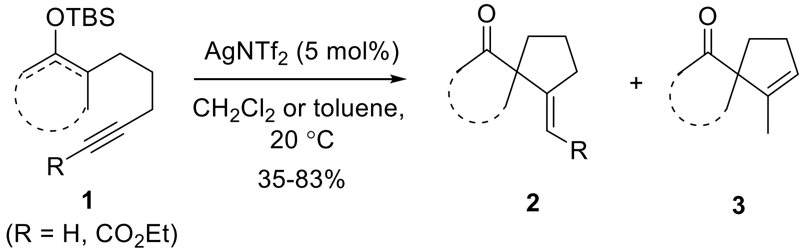

Scheme 1. Conia-Ene Reaction of Silylated Enols **1**.

Another example of silver-catalysed Conia-ene reaction was presented in 2013 by Wang and co-workers.[14] They discovered that gold catalysts failed to cyclise β-ketopropargylsulfamide **4** and only gave a hydration product, while silver triflate was extremely active in the reaction (Scheme 2). As in the previously reported work, the formation of 5-*exo-dig* cyclisation product was observed. The presence of sulfonyl groups at nitrogen atom was found to be essential as alkylated, phenylated and acylated derivatives did not give the desired product **5**.

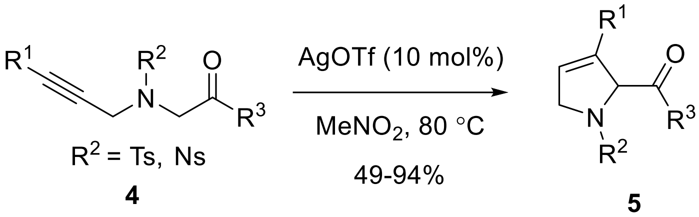

Scheme 2. Conia-Ene Reaction of β-Ketopropargylsulfamides **4**.

The ability of silver triflate to promote the 6-*endo-dig* cyclisation was reported in 2015.[15] Starting 1,3-diketones **6** bearing a 1-arylpropargylic moiety were converted into bicyclo[3.2.1]alkenes **7** at 90 ˚C in the presence of 5 mol% of the silver catalyst (Scheme 3). Weakly electron-attracting fluoro- and acetyl-substituted aromatic rings at triple bond were well-tolerated, while the presence of strong electron-withdrawing substituents as nitrile and trifluoromethyl resulted in a complete inhibition of the reaction.

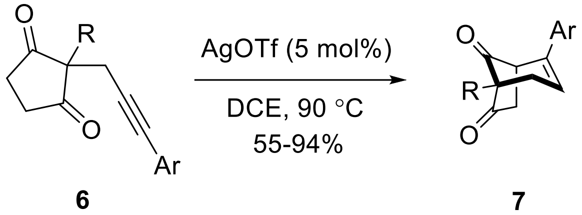

Scheme 3. Cyclisation of Diketones **6** *via* 6-*endo-dig* Pathway.

Silver(I) is known to catalyse cycloisomerisation reactions of 1,[5+*n*]-enynes (*n*=0,1,2…). The activation of C≡C bond by "carbophilic" silver catalysts facilitates the attack by the alkene to form metal carbenoid intermediates, which in turn afford diene products.

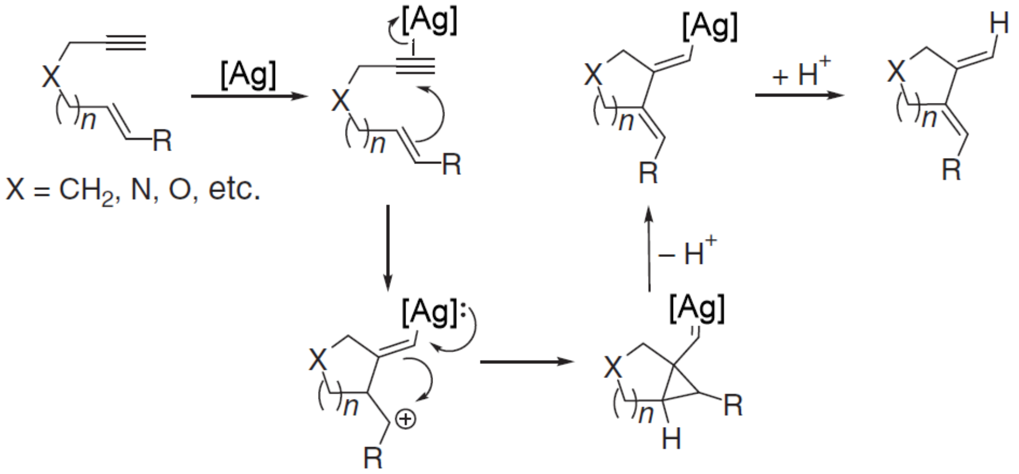

Scheme 4. Cycloisomerisation of 1,[5+n]-Enynes.

Cycloisomerisation of *N*-allylpropyolamides **8** leading to the formation 5-*exo-dig* products was first reported by Koo et al in 2013.[16] The authors underlined that silver triflide outperformed gold or platinum catalysts in terms of selectivity and reactivity, allowing to obtain 3-methylene-4-vinylpyrrolidin-2-ones **9** in high yields at room temperature.

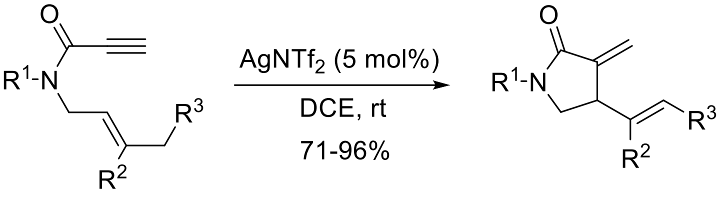

8 **9**

Scheme 5. 5-*Exo-Dig* Cycloisomerisation of Propiolamides **8**.

An example of *6-endo-dig* cycloisomerisation catalysed by silver was reported the same year.[17] In the presence of silver nitrate salt, *N*-vinylpropargylamines **10** underwent intramolecular nucleophilic attack of the α-carbon of the carbonyl group on the alkyne moiety to give 1,2-dihydropyridines **11**. It was essential for the process the presence of a terminal triple bond.

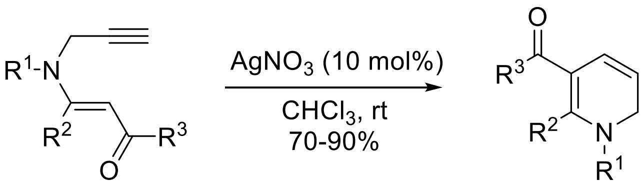

10 **11**

Scheme 6. 6-*Endo-Dig* Cycloisomerisation of *N*-Vinylpropargylamines **10**.

Cyclisation reactions involving 6-*endo-dig* route are more common for conjugated systems that can be aromatised in the process. For instance, silver precursors such as AgOTf, $AgNO_3$, AgTFA, $AgPF_6$, or $AgSbF_6$

can promote benzoannulation of quinoline, pyridine and benzene derivatives containing a silylenol ether function **12**, providing access to polysubstituted acridines **13** (Scheme 7).[18] Notably, AgOAc, Ag_2SO_4, AgF, Ag_2O, and Ag_2CO_3 did not exhibit any catalytic activity.

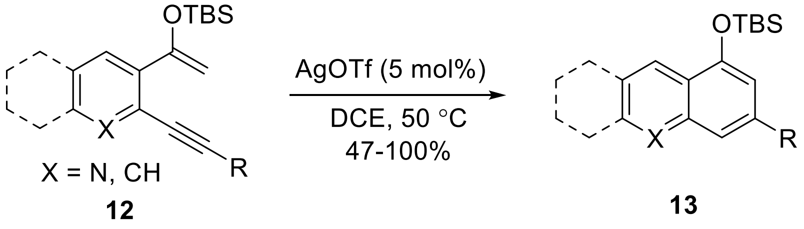

Scheme 7. Silver-Catalysed Benzoannulation.

In 2011 Garcia et al. demonstrated that silver triflate can efficiently catalyse cycloisomerisation of a large variety of allenynamides **14** giving azaheterocycles with incorporated cross-conjugated triene fragment **15** and **16**.[19] It was shown that under silver catalysis allenynes **14** react through initial triple bond activation. Sulfamide function contributes to the inherent polarization of the triple bond allowing a strong coordination of the metal, which in turn triggers a nucleophilic attack of the allene to generate highly reactive piperidine allylic intermediate. The latter evolves differently according to the substitution pattern of allene.

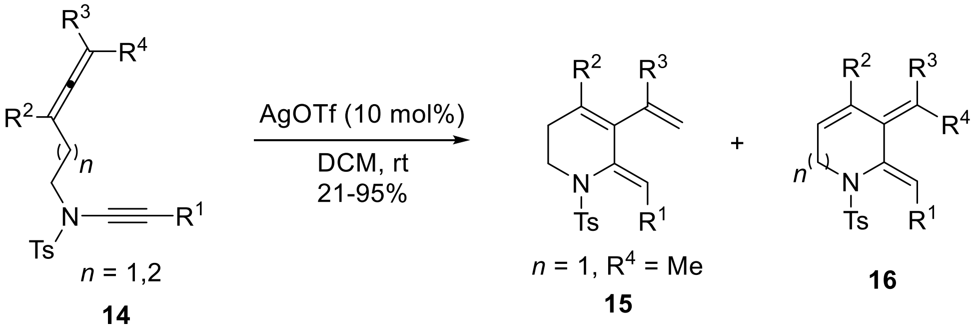

Scheme 8. Cyclisation of 1,[7+*n*]-Allenynes **14**.

A divergent reactivity of silver was reported by James and co-workers.[20] Indole-tethered propargyl alcohols **17** can undergo electrophilic cyclisation via C3 or C2 positions of the indole to afford the dearomatised spirocyclic compound **18** or the carbazole **19**, respectively (Scheme 9). The mixture of silver nitrate and silver (I) oxide in dichloromethane provided excellent selectivity towards **18**, while silver triflate in combination with THF opened access to exclusive formation of **19**.

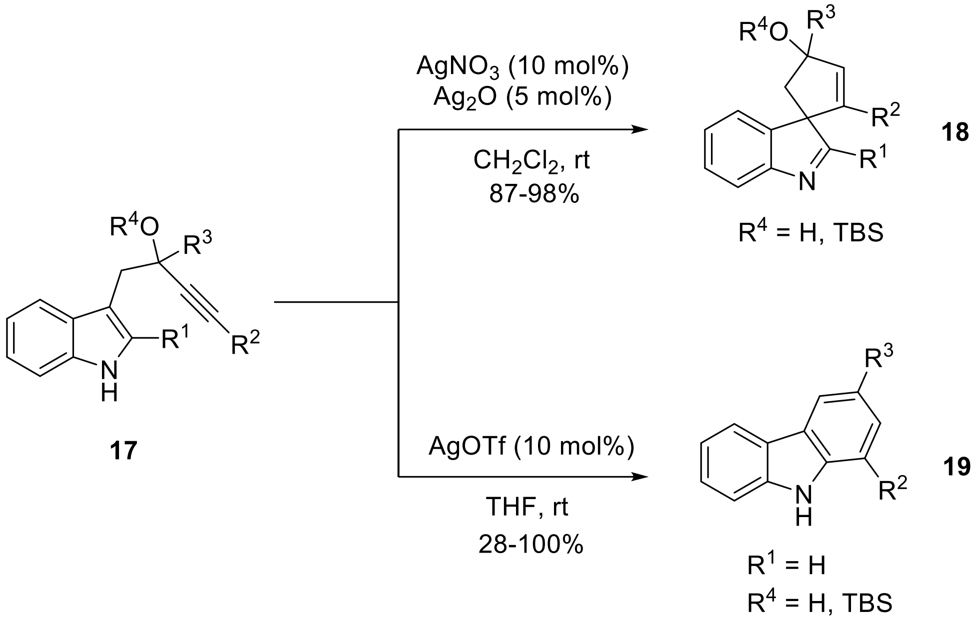

Scheme 9. Divergent Catalysis by Silver Salts.

Silver has been known for its ability to form carbon-oxygen bonds since 1987 when Pale and Chuche reported an intramolecular heterocyclisation of δ-acetylenic alcohols **20** and δ-acetylenic acids **21**.[21] The formation of the corresponding derivatives of tetrahydrofuran **22** and γ-butyrolactone **23** was optimal when silver carbonate was used as a catalyst (Scheme 10). When linear acetylenic alcohols were tested it appeared that a stoichiometric amount of Ag$_2$CO$_3$ was indispensable to reach full conversion.

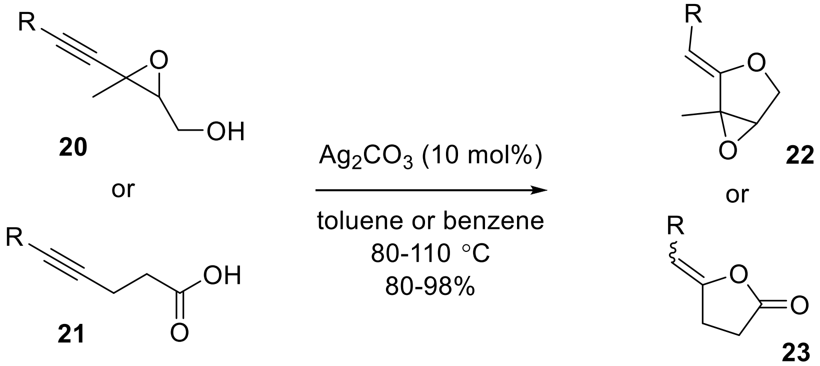

Scheme 10. First Example of Silver-Catalysed *O*-Cyclisation.

The reaction will not stop at the formation of *exo*-cyclic alkenes if propargylic diols **24** or diacids **25** are used as substrates. The intermediate alkene will immediately bare a subsequent attack of the second hydroxyl to give bridged bicyclic ketals **26** and **27** as products (Scheme 11).[22] The introduction of an extra acetylenic or allylic fragment will not alter the outcome, the formation of ketal is shown to be favorable.

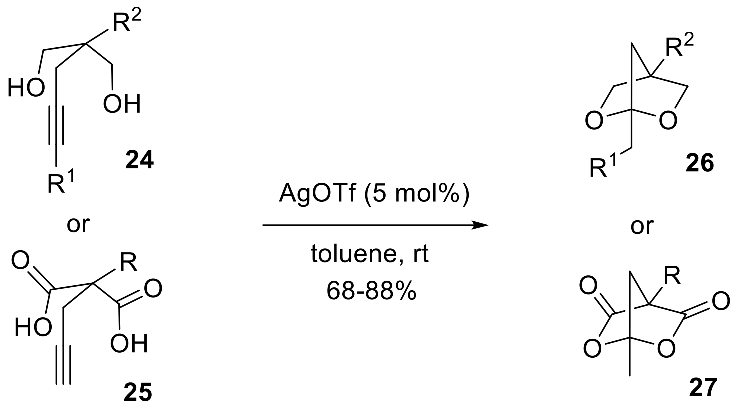

Scheme 11. Oxacyclisation of Acetylenic Diols **24** and Diacids **25**.

When phenol is a nucleophile, selective 5-*exo-dig*-cyclisation can also occur.[23] In this case a relatively high amount of silver nitrate was required to obtain aurones **29** in good yields (Scheme 12). This could be related to a lower nucleophilicity of phenol in comparison with alcohols. Flavonoids **30** were only detected in trace amounts.

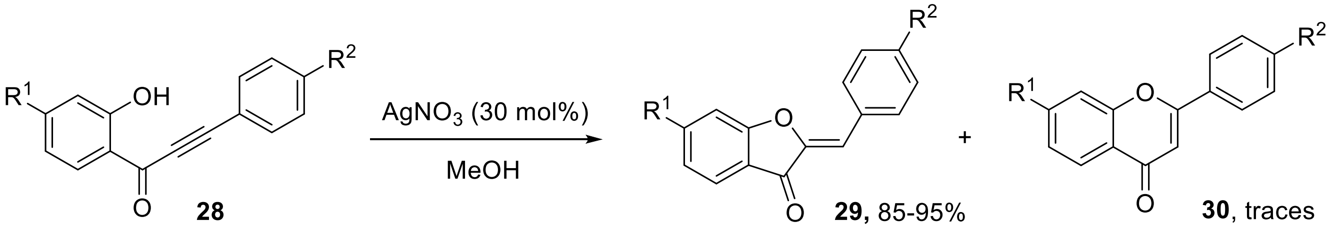

Scheme 12. Silver-Catalysed Synthesis of Aurones **29**.

Recent advances in oxacyclisations of alkynes include domino-processes, such as CO$_2$ fixation and subsequent nucleophilic attack on the triple bond reported by Dabral et al.[24] Under catalysis by silver complexes with bulky phosphinic ligands or *N*-heterocyclic carbenes (NHC), propargylic alcohols **32** reacted with gaseous CO$_2$ to give cyclic carbonates **32** (Scheme 13). Remarkably, the conversion of the reagents was reached at room temperature and by using a small catalyst loading.

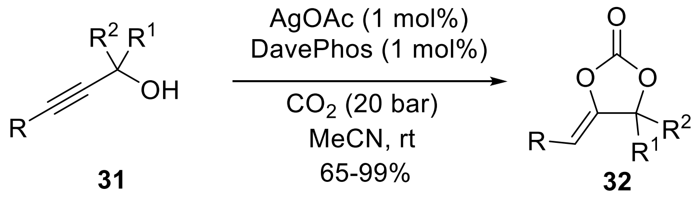

Scheme 13. CO$_2$ Incorporation and Intramolecular Cyclisation by Silver.

Besides *O*-cyclisations, there is plenty of works dedicated to *N*-cyclisation reactions catalysed by silver salts. Formation of *N*-heterocycles by Ag-catalysed 5-*endo-dig* addition of N-H to alkynes is commonplace. Silver-mediated intramolecular hydroamination of sulfamide **33** is a classic example

(Scheme 14).[25] This transformation proceeds in mild conditions and with high yields. Every silver salt tested exhibited excellent catalytic activity.

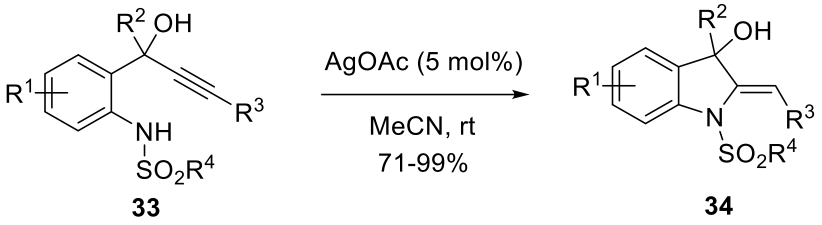

Scheme 14. Silver-Catalysed 5-*Exo-Dig* *N*-Cyclisation.

Activation of 6-*endo-dig* route for sulfamide **35** requires more drastic conditions.[26] Regioselective transformation illustrated in Scheme 12 was possible in the presence of $AgSbF_6$ in ethanol at 80 ˚C. The addition of triethylamine significantly reduced the reaction time and slightly increased the yield of **36**.

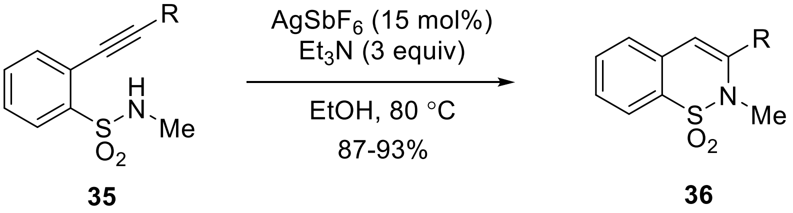

Scheme 15. Silver-Catalysed 6-*Endo-Dig* *N*-Cyclisation.

3. Palladium-Catalysed Carbonylation

Palladium has gained the reputation of a highly versatile metal in organic synthesis. Even though it is not unique in its capability of performing a variety of C-C, C-O or C-N bond forming reactions, its versatility has resulted in a constantly rising demand towards the use of palladium catalysts in chemical industries. Scientific interest in the catalytic properties of palladium does not seem to have dried up as there the number of publications related to palladium catalysis is trending upward (Figure 3).

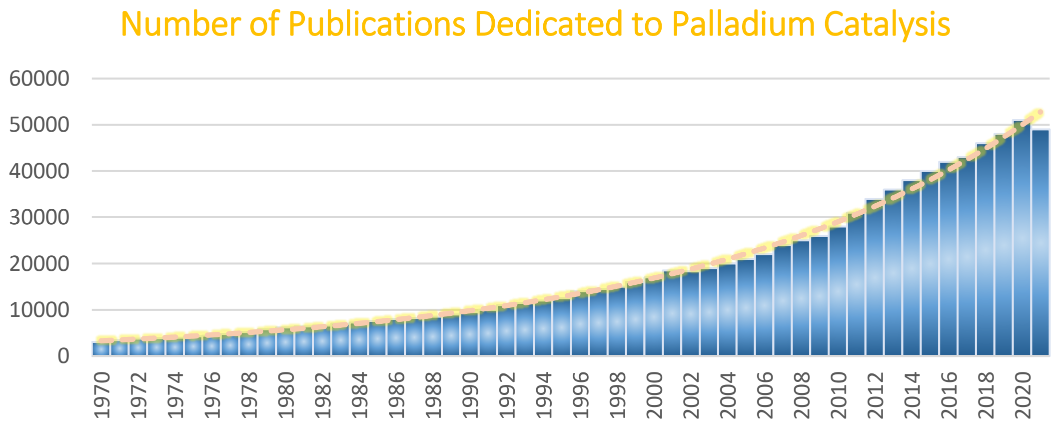

Figure 3. Trend of Publications Based on SciFinder® Search Results.

Most of the palladium-catalysed transformations are based on the interconversion of Pd^0 and Pd^{+2}, or Pd^{+2} and Pd^{+4}, that are between the d^{10} and d^8, or d^8 and d^6 electronic states, respectively. This is due to the mechanism of catalytic cycles that involve oxidative addition to, and reductive elimination from, the metal centre as essential steps. Carbonylation processes mediated by palladium are no exception. A very general sequence would consist of oxidative addition to palladium, coordination with carbon monoxide, CO incorporation with formation of acylpalladium intermediates, and reductive elimination.

It is customary to divide carbonylation reactions into substitutive, additive, reductive and oxidative.[27] Depending on the conditions applied, one of the 4 pathways can be favoured. Substitutive carbonylation necessarily includes a step in which a leaving group withdraws a proton to form an acid HX (X = Cl, Br, I, OTf…) thus, to shift the equilibrium towards the formation of the product, a base is required. Additive carbonylation processes are those in which the number of hydrogen atoms of the reagents is equal to that of the product. Reductive carbonylation proceeds in the presence of a reducing agent as molecular hydrogen or silanes, which allow the formation of aldehydes. Oxidative carbonylation relies on a dehydrogenation step and therefore requires the presence of an oxidant. The most common oxidising agents for palladium-catalysed processes are quinones, *N*-oxides, peroxides, silver or copper salts, and, in some systems, molecular oxygen (often under high pressure).

The first carbonylation reaction catalysed by palladium was discovered by Richard Heck in early 1970s. In June 1974 he launched as many as three publications on atmosphere-pressure alcoxycarbonylation and amidation, and high-pressure formylation of aryl-, vinyl-, and benzylhalides (Scheme 16).[28-30]

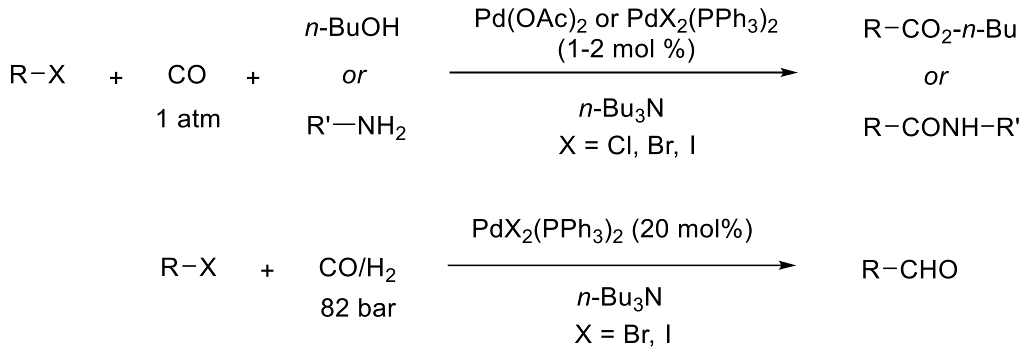

Scheme 16. Palladium-Catalysed Carbonylation Reactions Reported by Heck.

Heck's procedure had many advantages over others in use at the time, such as avoiding highly toxic nickel carbonyl that was a common carbonylating agent. Among other features, Heck noted the theoretical possibility of the acyl chloride formation under palladium catalysis could take place, as a similar nickel-catalysed reaction was known. However, under the conditions studied, no traces of acyl chloride were observed.

After almost 50 years of intense research the frontiers of palladium-catalysed carbonylation open new insights on the process. In 2020 Bruce Arndtsen et al. presented a strategy[31] that exploits visible-light excitation of palladium to overcome several problems such as the inhibitory influence of carbon monoxide. It is known that by modifying catalyst structure and reaction medium the stability of the metal complex under carbonylative conditions may be increased, but often the process still requires high temperatures in order to be efficient, setting some limitations on the use of many key substrates. Light has been shown to have multiple influences on the process, mainly contributing to lowering its energetic profile and thus offering a pathway to promote both oxidative addition and reductive elimination steps.

For the first time acyl chlorides were synthesised by palladium-catalysed carbonylation of alkyl and aryl halides (Scheme 17). Tetrabutylammonium chloride salt was selected as a chloride anion source.

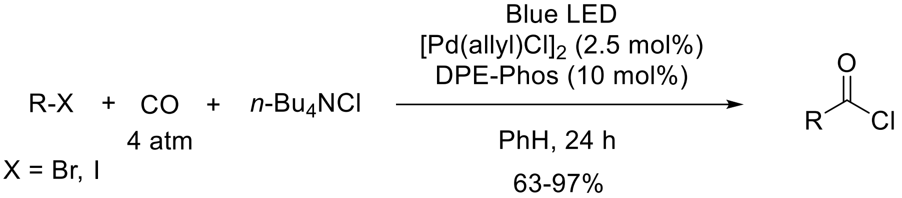

Scheme 17. Pd-Catalysed Acyl Chloride Synthesis.

Mechanistic studies showed that the driving force is given by forming *in situ* DPEphos-ligated Pd(II)-acyl complex that turned out to be photo-active and absorb blue light (λ = 330-460 nm). Irradiation even at low temperature provides the near-quantitative reductive elimination of acid chloride **38** in a few minutes (Scheme 18). When the light is switched off, the reaction equilibrium bounces back to a near 1:1 mixture of palladium-aroyl complex and aroyl chloride **37**. In addition to promoting reductive elimination, light also appears to be involved in the oxidative addition step through the excitation of intermediate (DPE-Phos)Pd$(CO)_2$.

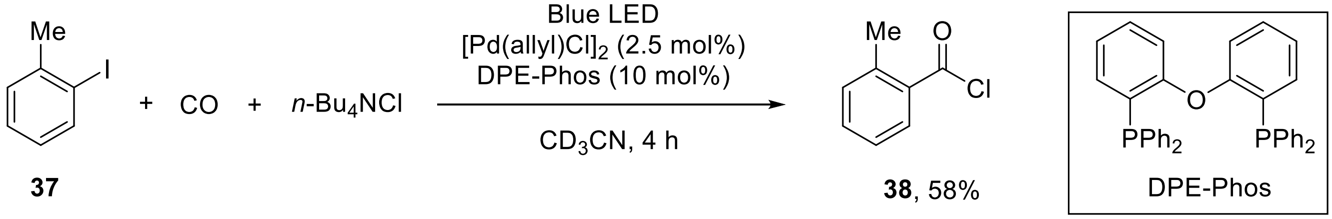

Scheme 18. Aroyl Chloride **38** Formation Under Light-Driven Palladium Catalysis.

By adding a nucleophile, the reaction can be extended for the efficient synthesis of esters, thioesters, or amides (Scheme 19). Remarkably, the reaction goes well even for highly hindered nucleophiles like 2,6-diisopropylaniline, giving up to 99% yield of the corresponding amide.

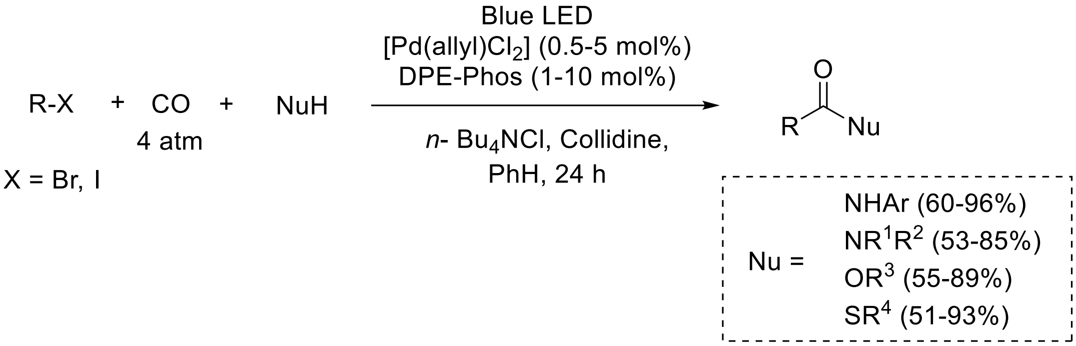

Scheme 19. Visible-Light Promoted Carbonylative Synthesis of Amides, Esters, and Thioesters.

Carbonylation of halogen-containing compounds is just one application of carbon monoxide incorporation in organic frameworks. A different kind of reaction involving CO is represented by amidocarbonylation of aldehydes. In 1989, Erhart Jaegers and Hans-Peter Koll found that bis-triphenylphosphine-palladium (II) chloride can catalyse the formation of *N*-acyl α-amino acid **39** from aldehydes and acetamide under CO pressure (120 bar) at 120 ˚C (Scheme 17).[32]

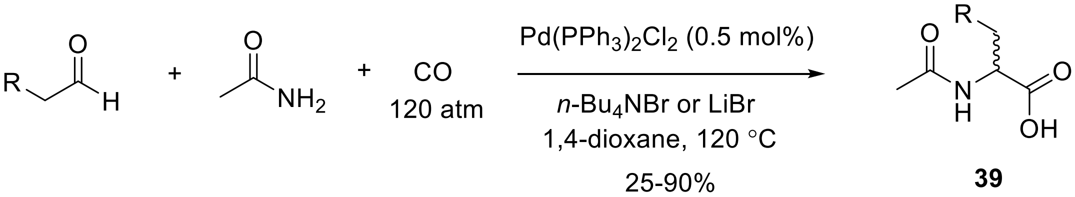

39

Scheme 20. First Amidocarbonylation of Aldehydes.

Unlike cobalt catalysts, palladium-triphenylphosphine complexes are able to catalyse even the transformation of aldehydes lacking α-hydrogen atoms. In 1998 Matthias Beller et al. extended the methodology for benzaldehyde derivatives, reducing CO pressure by half. (Scheme 21).[33]

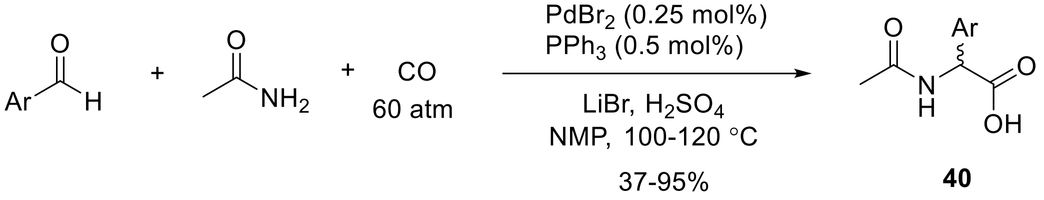

40

Scheme 21. Amidocarbonylation of Aromatic Aldehydes.

Later, Beller reported that hydantoin compounds containing various substituents at the 1-, 3-, and 5-positions can be achieved by the ureidocarbonylation reaction, when a urea is used in place of an amide (Scheme 22).[34] Remarkably, monosubstituted ureas give exclusively 3,5-substituted hydantoins. This fact aided to determine the reaction mechanism, suggesting that selective nucleophilic attack of free NH_2 to the carbonyl of the aldehyde occurs at first place, followed by the oxidative addition of Pd^0 species. The resulting complex undergoes CO insertion to give acylpalladium intermediates, which either react intramolecularly to directly give hydantoin **41** or suffer hydrolysis and form *N*-carbamoyl acid that subsequently cyclises to hydantoin **41**.

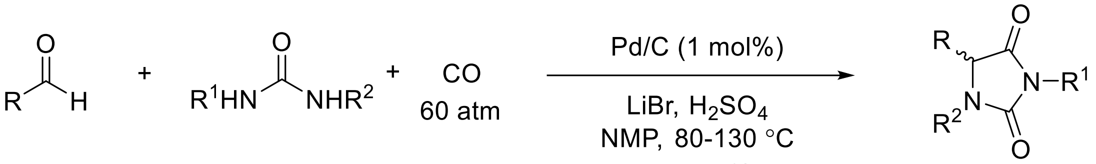

41

Scheme 22. Hydantoin Formation by Ureidocarbonylation.

Carbonylation of alkynes can give access to a spectrum of various compounds, from carboxylic acid derivatives to carbo- and heterocycles. Additive palladium-catalysed alkoxycarbonylation of mono- and di-substituted alkynes is a challenging process in terms of selectivity. Along with mono-substituted regioisomers, dicarbonylated products may form under certain conditions.

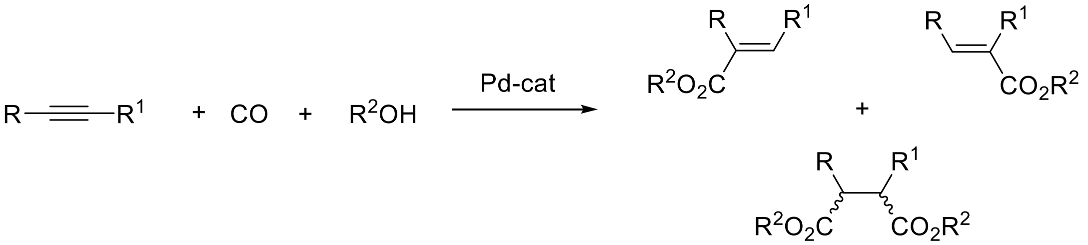

Scheme 23. Possible Products of the Additive Carbonylation of Alkynes.

One of the earliest studies of catalyst effect on alkoxycarbonylation of terminal alkynes to obtain linear and branched α,β-unsaturated esters was reported in 2000 by Akao et al.[35] The catalyst screening showed that 1-octyne can be converted into methyl *trans*-non-2-enoate **43** with high selectivity and quantitative yield when Pd(dppf)Cl_2 is used as a catalyst, whilst $[Pd(PPh_3)_2(PhCN)_2](BF_4)_2$ promotes the formation of 2-methyleneoctanoate **44**, but with rather scarce yield (Table 1). For phenylacetylene and trimethylsilylacetylene the selectivity remained high, but the yield dropped. Methyl propiolate gave a mixture of two products with low yield.

Table 1. Methoxycarbonylation of Alkynes.

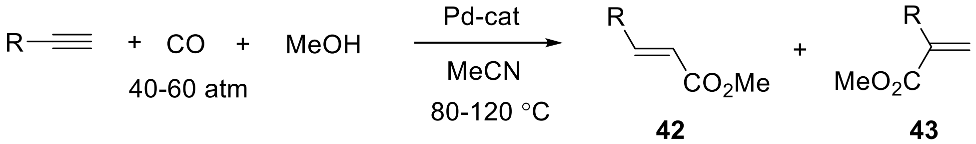

42 **43**

R	Pd-Cat	Yield **42**+**43**, %	Selectivity **42**:**43**
Hexyl	$[Pd(PPh_3)_2(PhCN)_2](BF_4)_2$	12	16:84
Hexyl	$[Pd(dppe)(PhCN)_2](BF_4)_2$	5	60:40

Hexyl	$[Pd(dppp)(PhCN)_2](BF_4)_2$	45	66:34
Hexyl	$[Pd(dppb)(PhCN)_2](BF_4)_2$	13	84:16
Hexyl	$[Pd(BINAP)(PhCN)_2](BF_4)_2$	44	76:24
Hexyl	$[Pd(dppf)(PhCN)_2](BF_4)_2$	85	85:15
Hexyl	**$Pd(dppf)Cl_2$**	**100**	**92:8**
Ph	$[Pd(dppp)(PhCN)_2](BF_4)_2$	77	44:56
Ph	**$[Pd(dppf)(PhCN)_2](BF_4)_2$**	**75**	**89:11**
Ph	$Pd(dppf)Cl_2$	41	87:13
TMS	$[Pd(dppf)(PhCN)_2](BF_4)_2$	29	100:0
CO_2Me	$[Pd(dppf)(PhCN)_2](BF_4)_2$	40	55:45d

Later, the study of El Ali et al. revealed than phenylacetylene can be efficiently converted into *trans*-cinnamic esters if a borane complex is added to the system.[36] It was shown that the presence of catalytic quantities of acids directly affects the reaction rate as well as the selectivity (Table 2). The process was extremely sensitive to changes of catalyst, ligand, and solvent.

Table 2. Acid-Mediated Alkoxycarbonylation of Phenylacetylene.

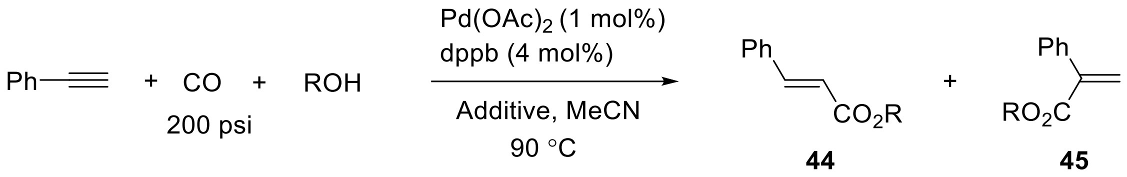

R	Additive, mol%	Yield **44**+**45**, %	Selectivity **44**:**45**
Methyl	-	0	-
Methyl	**$B(OH)_3$-salicylic acid, 15-30**	**100**	**92:8**
Methyl	Salicylic acid, 15	22	47:53
Methyl	$B(OH)_3$, 15	0	-
Methyl	PTSA, 15	100	86:14
Methyl	CH_3SO_3H, 15	100	89:11
Ethyl	$B(OH)_3$-salicylic acid, 15-30	99	91:9
Propyl	$B(OH)_3$-salicylic acid, 15-30	99	92:8
i-Propyl	$B(OH)_3$-salicylic acid, 15-30	99	91:9
Butyl	$B(OH)_3$-salicylic acid, 15-30	99	91:9
Pentyl	$B(OH)_3$-salicylic acid, 15-30	99	90:10
Heptyl	$B(OH)_3$-salicylic acid, 15-30	100	89:11

The formation of branched α,β-unsaturated esters is more common and generally can be achieved using palladium complexes with monodentate phosphine ligands.[37-40] Although, some studies involving the use of bidentate phosphines demonstrated great selectivity towards the formation of branched adducts **45**.[41] In a work published by Williams et al. Pd-catalysed methoxycarbonylation of phenylacetylene was examined making use of Lewis acids, such as aluminium triflate and several other acid-type promoters (Scheme 24).[42] The designed catalytic system consisting of sulfonated BINAP, palladium acetate and aluminium triflate displayed high activity even at low catalyst loadings and was proved to be recyclable up to 10 times.

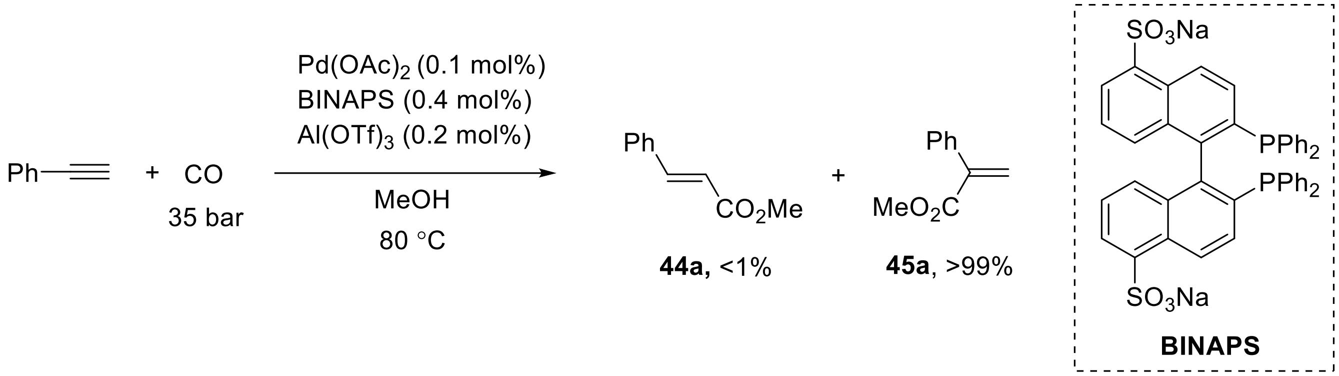

Scheme 24. Selective Methoxycarbonylation of Phenylacetylene.

Recent study conducted by Beller et al. revealed that the chemo- and regioselectivities of alkyne methoxycarbonylations can be controlled by simple changing the ligand of palladium catalyst.[43] Ligand design allowed the selective formation of a wide range of linear and branched α,β-unsaturated esters as well as 1,4-dicarboxylic acid diesters. The optimised conditions involved the use of palladium acetylacetonate, para-toluenesulfonic acid monohydrate, and the ligand under 40 bar of carbon monoxide at 120 ˚C (or 80 ˚C for **L3**).

Table 3. Ligand-Controlled Methoxycarbonylation of Phenylacetylene.

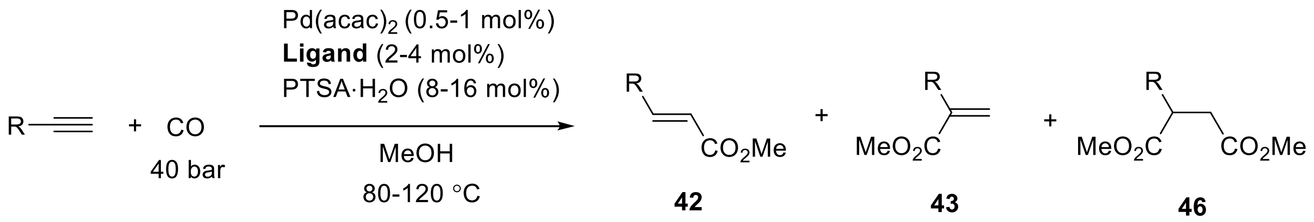

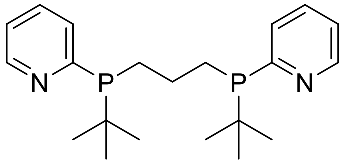 **L1**	1-24%	0%	**63-99%**

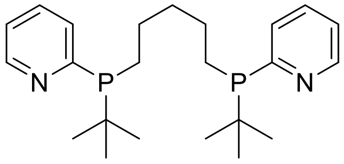 **L2**	5-16%	**55-95%**	0%
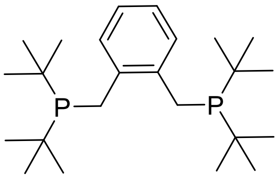 **L3**	**60-94%**	1-5%	1-12%

In 2020 Beller applied the ligand-control strategy for the selective carbonylation of propargyl alcohols to β-propiolactons.[44] In this case the use of *N*-phenyl-pyrrole-based ligand **L4** allowed to almost completely suppress the formation of furan-2(5*H*)-one derivatives and favour the 4-*exo-dig* cyclocarbonylation route to obtain **48** (Scheme 25). The presence of two substituents at 1-position of propargyl was strictly required.

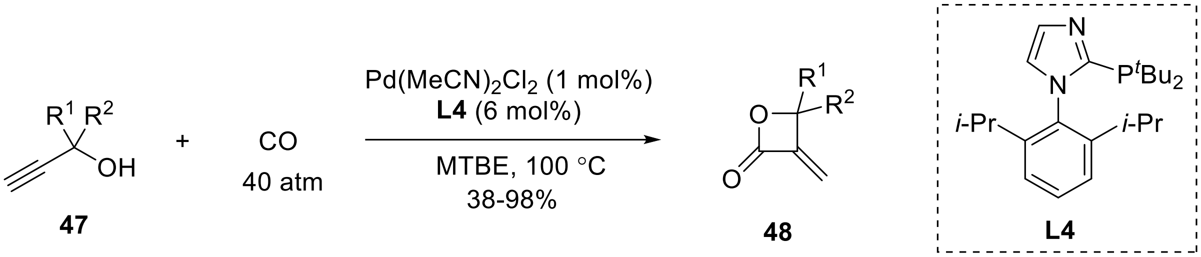

Scheme 25. Carbocyclisation of Propargylic Alcohols to β-Propiolactons.

The methodology for the *5-endo-dig* carbonylative cyclisation of propargylic alcohols has been known since 1990s.[45] Palladium dibenzylideneacetone pre-catalyst in combination with diphenylphosphinobutane can efficiently promote this transformation to afford furan-2(5*H*)-ones **49** in good yields (Scheme 26). Also here the presence of two geminal substituents is absolutely necessary.

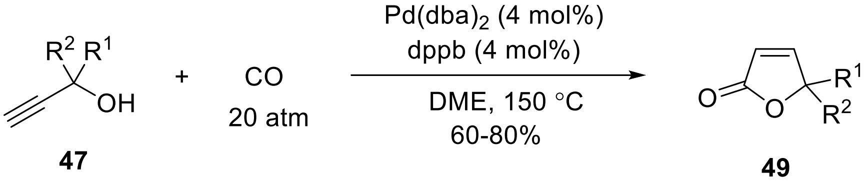

Scheme 26. Carbocyclisation of Propargylic Alcohols to Furan-2(5*H*)-ones **49**.

Along with additive carbonylations, oxidative carbonylation processes can give various types of products, the formation of which can be favoured by tuning the parameters of catalytic systems (Scheme 27). Here the classical mono-alkoxycarbonylation product can only be obtained from terminal alkynes, while di-alkoxycarbonylation can take place with both mono- and disubstituted ethyne derivatives. Moreover, a product of mono-carbonylation and nucleophilic addition can be formed.

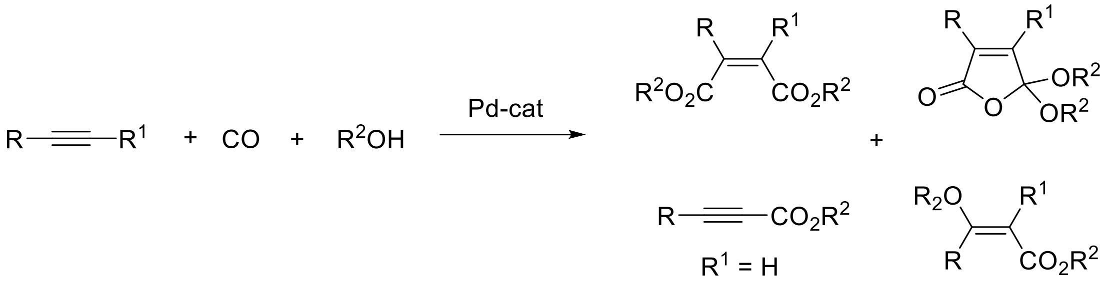

Scheme 27. Possible Products of Oxidative Carbonylation of Alkynes.

The first examples of oxidative carbonylation of alkynes were reported in 1964 by Tsuji et al., who obtained muconic, maleic, and fumaric acid chlorides from acetylene using stoichiometric amount of palladium dibenzonitrile dichloride.[46] Almost two decades later, Tsuji first disclosed the palladium-catalysed alkoxycarbonylation of alkynes to acetylenecarboxylates.[47] Atmospheric pressure of carbon monoxide was sufficient to effect the conversion of alkynes to α,β-alkynyl esters **50** (Scheme 28). It was noted that copper chloride was a better oxidant than 1,4-benzoquinone as it allowed faster conversion of the starting acetylene derivative.

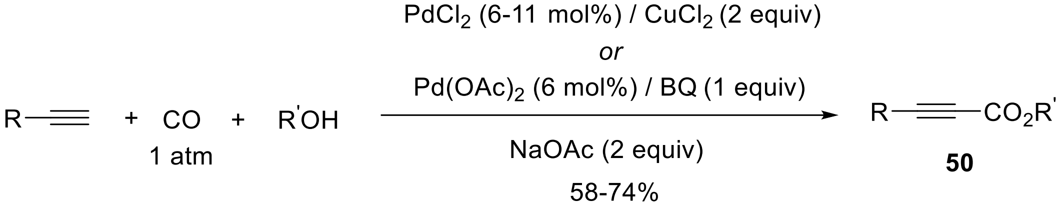

Scheme 28. Oxidative Alkoxycarbonylation of Alkynes to Acetylenecarboxylates.

Akio Yamamoto's group later demonstrated that the same reaction can occur when molecular oxygen is used as an oxidant (Scheme 29).[48] The oxidation of Pd^0 to Pd^{+2} species by oxygen is possible when triphenylphosphine ligand is present in the reaction medium. The reoxidation was rather slow, compared to the copper chloride efficiency, and the reaction required at least 48 hours to reach completion. Based on the behaviour of model complexes such as alkynylpalladium and methoxycarbonylpalladium, a mechanistic insight was given.

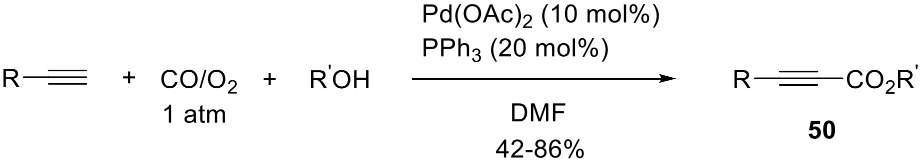

Scheme 29. Alkoxycarbonylation of Alkynes Using Molecular Oxygen as a Sole Oxidant.

A methodology for the preparation of propiolic esters and unsymmetrical maleate esters by oxidative alkoxycarbonylation of terminal alkynes was reported by Bhanage and Gadge in 2013.[49] The developed ligand-free protocol involved the use of heterogeneous and recyclable Pd/C catalyst together with tetrabutylammonium iodide under CO (5 bar) and oxygen (1 bar) atmosphere. When the reaction was conducted in 1,4-dioxane α,β-alkynyl esters **50** could be successfully obtained, while, using alcohol as a solvent, the selective formation of maleates **51** was observed. The catalyst was proved to remain active after 6 runs.

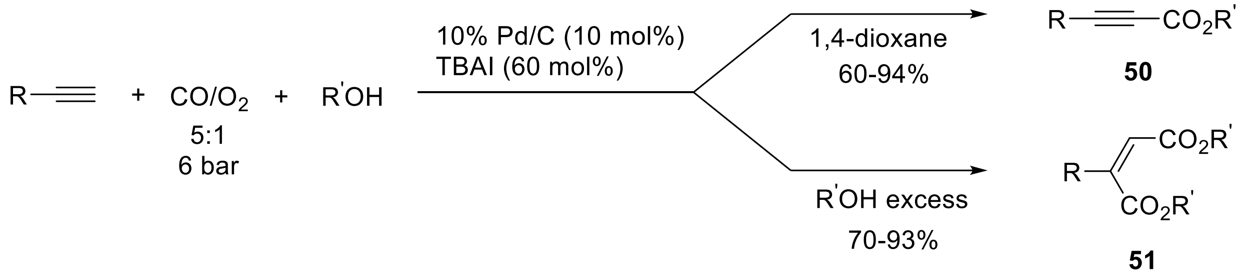

Scheme 30. Alkoxycarbonylation Reaction Catalysed by Pd/C with TBAI.

Direct conversion of alkynes into a β-methoxyacrylates can be achieved by using palladium triflate in combination with BOX-type ligand under carbonylative conditions (Scheme 31).[50] The box ligand is believed to enhance the π-electrophilicity of palladium, therefore nucleophilic addition can take place once the mono-carbonylation product is formed. Notably, acetyl, ketal, free hydroxy and glycosidic groups present in substrates were tolerated.

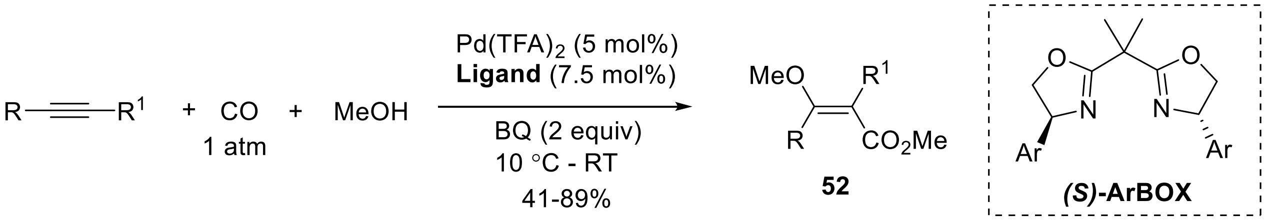

Scheme 31. Tandem Oxidative Methoxycarbonylation – Nucleophilic Methanol Addition.

The use of bis(2,6-diisopropyl)acenaphthenequinonediimine ligated palladium catalyst could be beneficial for the synthesis of maleic esters starting from disubstituted alkynes. It was demonstrated by Beltrani *et al.* that terminal alkynes can be efficiently transformed into corresponding propiolic esters under conditions illustrated on Scheme 32.[51] When these conditions are applied to internal alkynes, dicarbonylation products **53** and **54** form in various ratios. Under acidic conditions, 5,5-dimethoxyfuran-2(5H)-ones **54** can be successfully isomerised into maleic esters **55**.

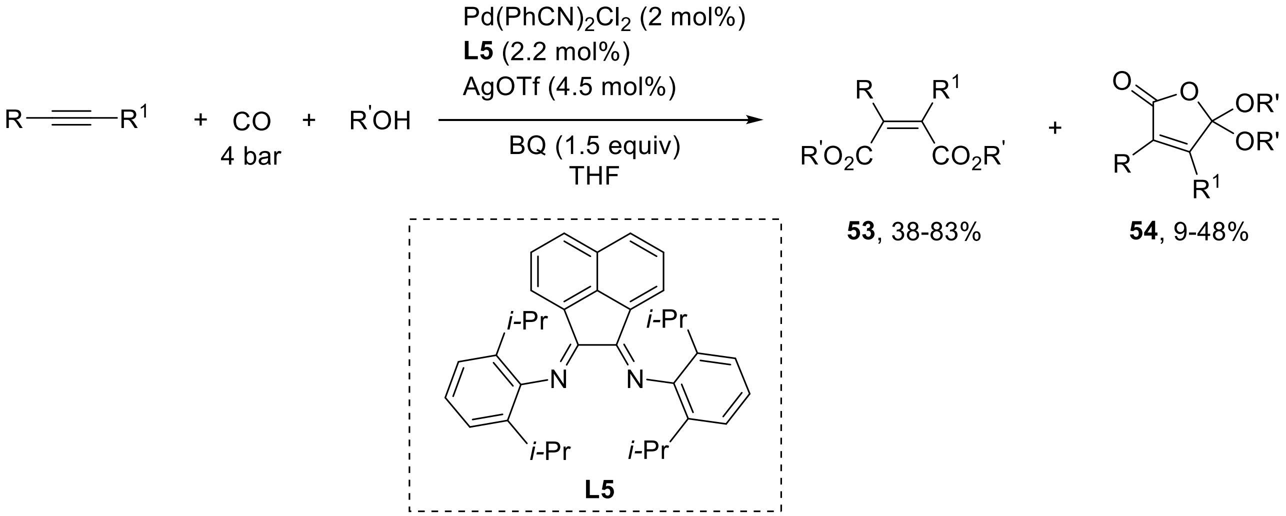

Scheme 32. Bis-Alkoxycarbonylation of Disubstituted Alkynes.

4. Rhodium-Catalysed Carbonylation

Rhodium is the rarest of all non-radioactive metals. Its ability to convert nitrogen oxides into oxygen and nitrogen has made him a star of the automotive catalyst industry. Added the constantly rising scientific interest due to the outstanding capacities of some complexes, a predictable surge in request for this metal can be testified. High demand, low abundance and difficulties in isolation inevitably lead to a price escalation. In March 2021 it resulted in touching an all-time high of €26.300 per ounce of rhodium.[52]

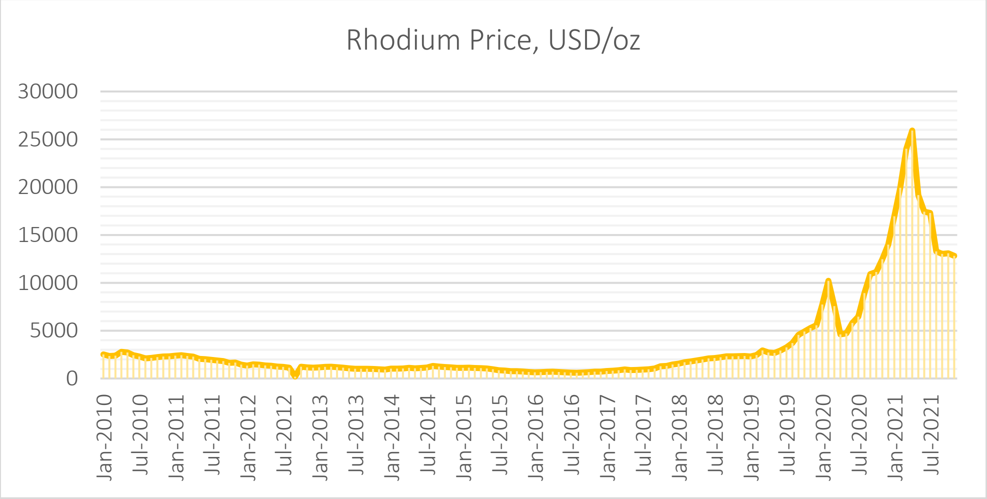

Figure 5. Rhodium Price Chart Based on Trading Statistics.

In chemical industry, rhodium catalysts find applications in several processes, including ammonia oxidation to obtain nitric acid and catalytic carbonylation of methanol to produce acetic acid by the Monsanto process.[53] The latter is now largely replaced by the Cativa process developed in 1990s, which involves the use of a similar iridium catalyst that allows to reduce water consumption and hence easier purification of the product can be achieved.[54]

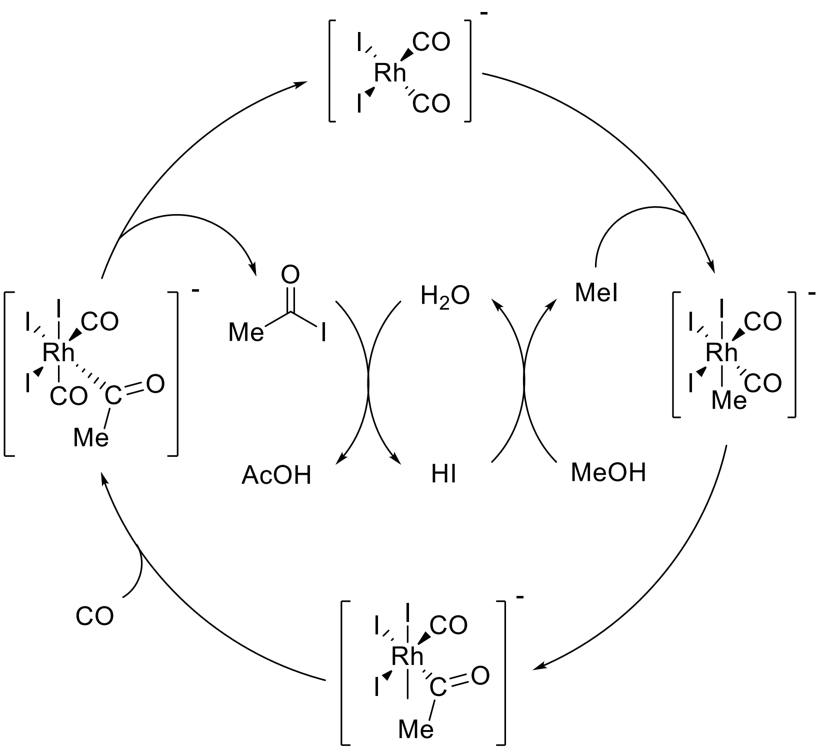

Scheme 33. The Monsanto Process.

Modern perfume and pharmaceutical industry strongly rely on rhodium. Rhodium(I) complex with (*S*)-BINAP is used in a crucial step of isomerisation to access enantiomerically pure intermediate product, in the industrial synthesis of menthol.[55] Cyclic alkyl amino carbenes (CAAC) ligated to rhodium allow highly selective hydrogenation of aromatic compounds.[56] Rhodium-based Wilkinson's catalyst is well-known for catalysing the hydrogenation and hydroboration of olefins.[57] Rhodium-catalysed transformations are essential for the synthesis of several pharmaceutical products as L-DOPA used to treat Parkinson's disease.[58]

Interactions of carbon monoxide with rhodium have been investigated for decades. Recently it was demonstrated that, in a metal-oxide cluster, a single atom of rhodium is able to promote the transfer of five oxygen atoms to oxidise carbon monoxide into carbon dioxide. Rhodium can function not only as the preferred trapping site to anchor and oxidise carbon monoxide, but also as the primarily oxidative centre to accumulate the large amounts of electrons.[59] In coordination compounds Rh(I) to Rh(III) interconversions can occur easily and in mild conditions, sometimes yielding also Rh(II) binuclear species.[60] These properties clearly demonstrate high potential of rhodium in the catalysis of carbonylative transformations.

The first example of additive double alkoxycarbonylation of acetylenes with 2-pyridinemethanol catalysed by Rh^0 species was reported by Chatani et al. in 2006 (Scheme 34).[61] It was shown that mono-carbonylation products could not be obtained starting from mono-hydroesterificated alkenes. The presence of sp^2 nitrogen of the pyridine fragment was found to be essential as no product formation was observed when different alcohols were tested. For benzyl alcohol the reaction only proceeded if pyridine was added to the reaction medium, giving a mono-benzyloxycarbonylation product **57** in 77% yield. Mechanistical studies suggested that the reaction might proceed *via* a ketene intermediate and not by two successive hydroesterifications.

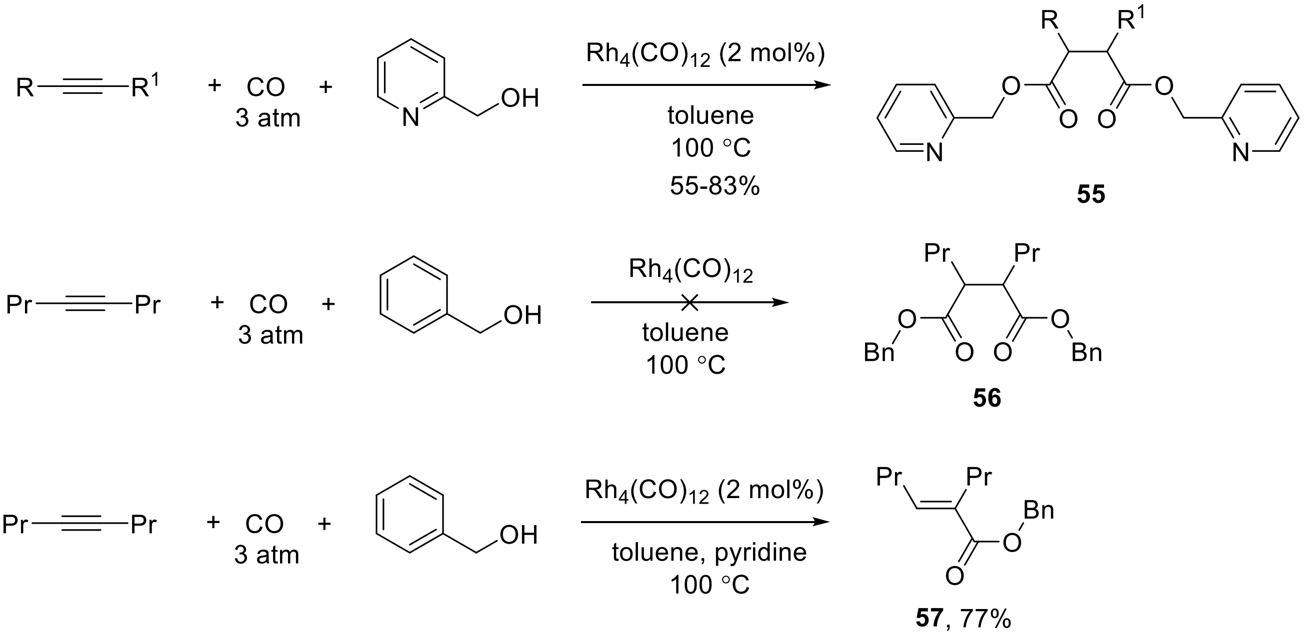

Scheme 34. Rhodium-Catalysed Alkoxycarbonylation of Alkynes.

A protocol for the rhodium-catalysed oxidative alkoxycarbonylation of arenes was presented two years later by Guan *et al.*[62] In this work, a challenging task of aromatic C-H activation and functionalization was accomplished by using $[Rh(cod)Cl]_2$ catalyst with an oxidant under low CO pressure (Scheme 35). The methodology displayed high regioselectivity and good functional group tolerance. As in the previous case, the nitrogen-containing directing group had major impact on the course of the reaction. It was shown that the efficiency of the process strongly depends on the type and the steric hindrance of the directing group of **58**. The highest yields were achieved for the 2-pyridine-substituted substrates. The proposed mechanism includes rhodium(I) oxidative addition at the *ortho*-position of the arene **58**, consecutive CO insertion, alcohol addition, oxidative dehydrogenation, and reductive elimination.

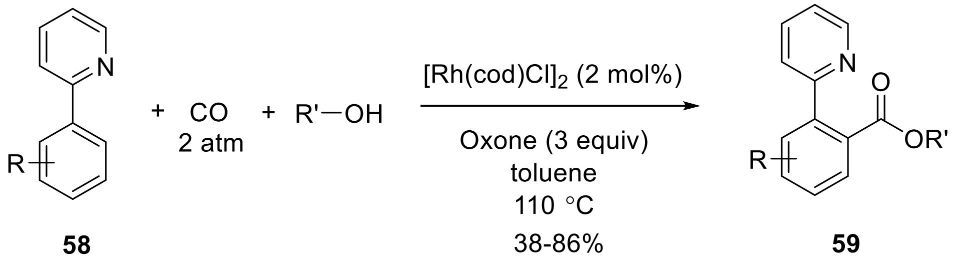

Scheme 35. Rhodium-Catalysed Alkoxycarbonylation of Arenes.

In 2020 Xiao-Feng Wu's group presented the rhodium-catalysed methodology for substitutive phenoxycarbonylation of alkylhalides.[63] The formation of Friedel-Crafts acylation products, that usually occurs for phenols under carbonylative conditions, was successfully circumvented by using $RhCl_3$-dppp (1,3-bis(diphenylphosphino)propane) catalytic system. The addition of 10 mol% NaBr, NaCl, or NaI allowed almost quantitative yields of the product in the optimisation study. The transformation proceeded at 120 ˚C under a gaseous mixture of CO and N_2 (1:5 ratio).

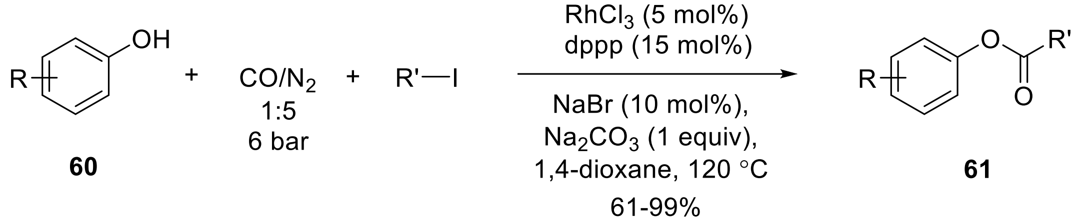

Scheme 36. Phenoxycarbonylation Catalysed by Rh(III).

Contemporarily, Wu released another publication dedicated to the selective Friedel-Crafts carbonylative acylation of phenols to aryl salicylates.[64] Altered reactivity of phenols was achieved by switching the ligand of Rh(III) to bis(dicyclohexylphosphino)ethane and the introduction of TEMPO (2,2,6,6-tetramethylpiperidinyloxy) as an oxidant (Scheme 37). Noteworthy, diphenyl carbonate was formed as the main product when dppp was used as the ligand.

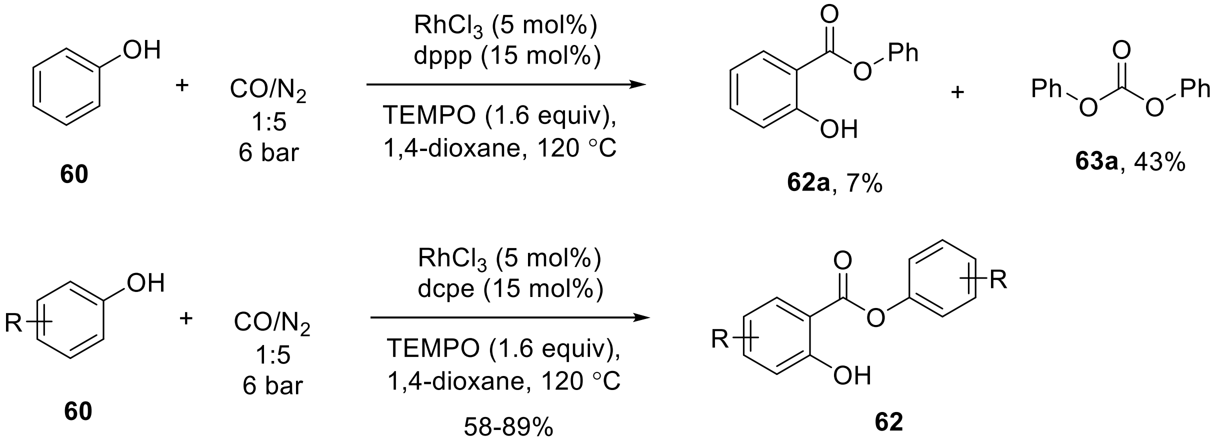

Scheme 37. Rh(III)-Catalysed Carbonylation of Phenols.

In 1990s and early 2000s Takashi's group conducted extensive studies of the catalytic properties of rhodium(0) carbonyl.[65-68] On the example of alkynylarenes containing a functional group at the *ortho*-position (CH_2OH, CH_2NHR, NHR, OH) they observed that the carbonylative cyclisation and consecutive reduction can occur at 100-175 ˚C under 30-100 atm of CO in the presence of water and a base (Scheme 38). It was demonstrated by experiments with deuterium that the reduction process involves hydrogen atoms of water and only takes place when an *exo*-double bond forms. Interestingly, benzylalcohols and anilines predominantly gave the *exo-dig*-cyclisation products **65** and **67**, while phenols led to the formation of a mixture of *exo*- and *endo*-products **69** and **70**, and benzylamines were found to undergo the unusual *7-endo-dig* transformation to afford **72**.

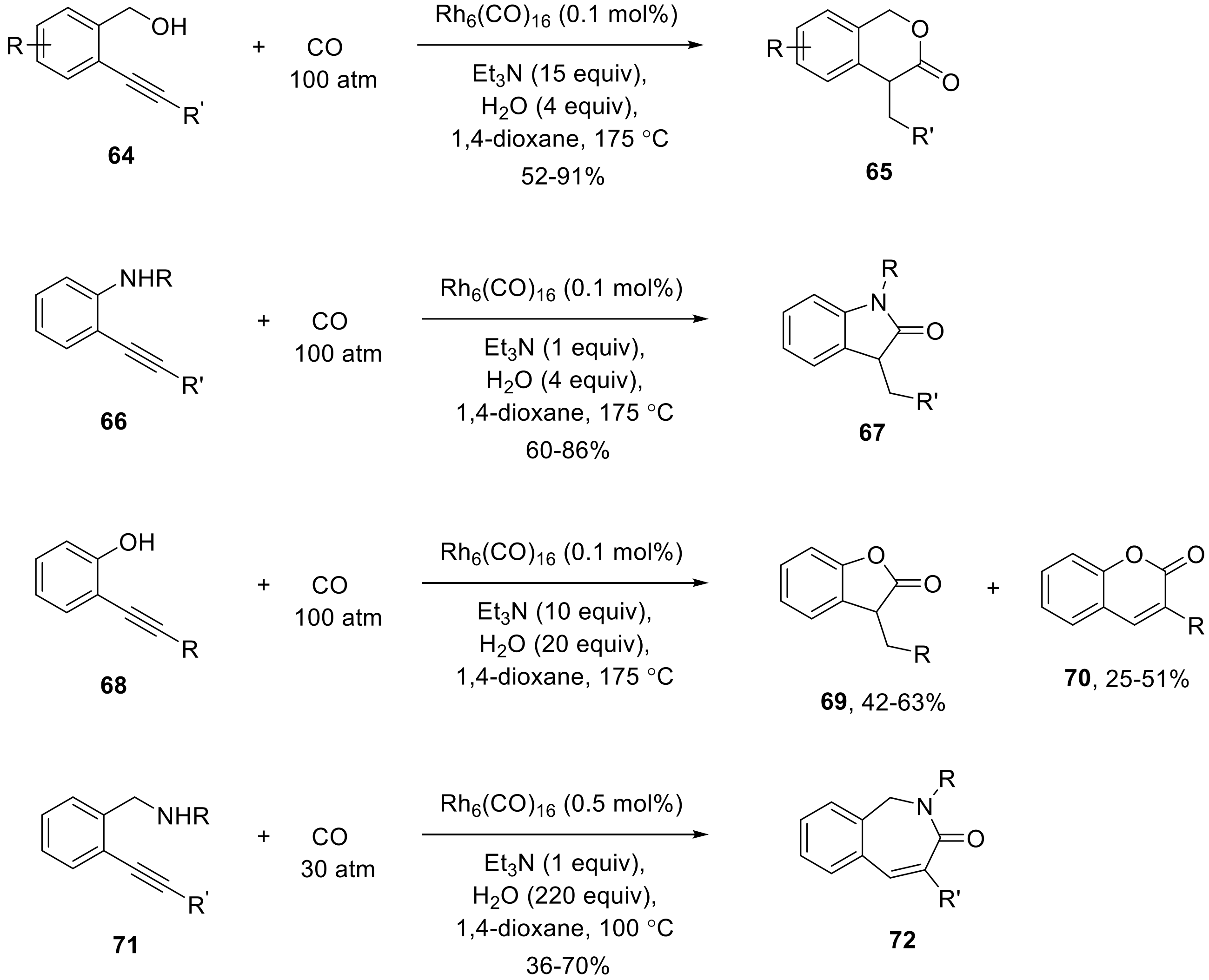

Scheme 38. Rh^0-Catalysed Carbonylative Cyclisation of Alkynylarenes.

Rhodium-catalysed carbonylative [2+2+1] cycloaddition of an alkyne (C≡C), an alkene (C=C), and carbon monoxide (CO) to a cyclopentenone is well-known as the Pauson–Khand reaction. Much effort had gone into developing a catalytic version of the process since the discovery of the original reaction of a cobalt-alkyne complex with an alkene by Pauson and Khand in early 1970s.[69] In 1998 Narasaka (Method A, Scheme 39)[70] and Jeong (Method B, Scheme 39)[71], working independently, reported a rhodium(I)-catalysed [2+2+1] cycloaddition of enynes that occurred under atmospheric pressure of CO. Since then, rhodium catalysis has been focused on the study of this chemistry because of its operation simplicity, resulting in the expanding of the scope of conforming substrates, developing enantioselective variants, and elucidating the reaction mechanism. Today there is plenty of reported versions that evade the use of molecular CO by implementing various surrogates that can produce CO *in situ*.[72]

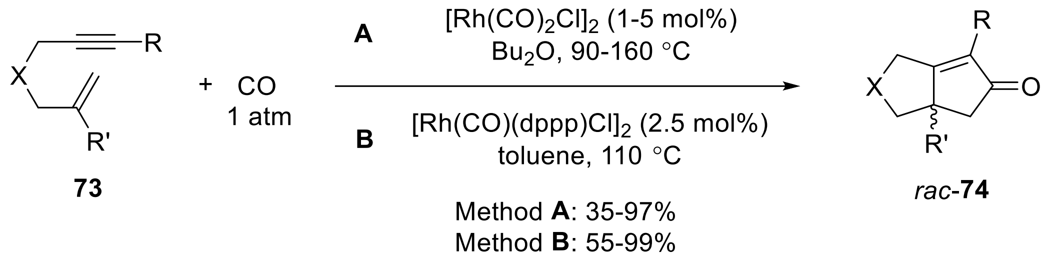

Scheme 39. Rhodium-Catalysed Intramolecular [2+2+1] Cycloaddition.

Huang and Hua were the first to report a rare example of rhodium-catalysed [2+2+1+1] cyclocarbonylation, which involves the combination of two molecules of an internal alkyne with two molecules of CO to afford tetrasubstituted *para*-benzoquinones **75** and **76** (Scheme 40).[73] A critical element in guaranteeing the success of this process was found to be slow bubbling a CO and N_2 1:1 mixture, as higher CO pressure resulted in significantly lower efficiency. The reaction of asymmetric alkynes provided poor regioselectivity.

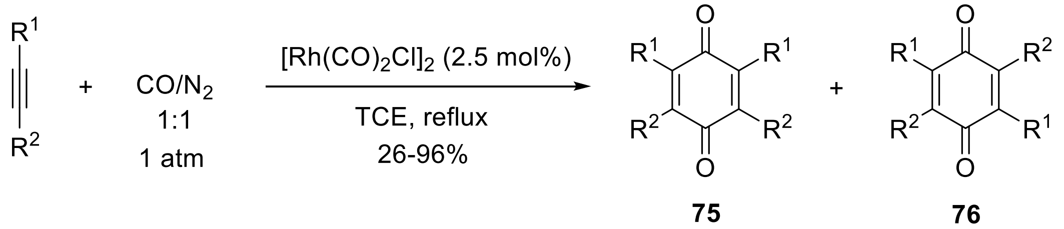

Scheme 40. Rhodium-Catalysed [2+2+1+1] Cycloaddition.

Rhodium catalysis for the carbonylative coupling of diynes had long been thought impractical to implement. In the past, the only mention of the Rh(I)-catalysed [2+2+1] alkyne-alkyne coupling emerged in 2001.[74] The formation of a cyclopentadiene derivative, starting from 1,7-diphenylhepta-1,6-diyne, proceeded at 120 ˚C with a yield of 29% when $[Rh(cod)Cl]_2$ was used as a catalyst, decreasing to 9% with the addition of triphenylphosphine.

In 2020 Morimoto *et al*. that the reaction of two alkynes with carbon monoxide fails when neutral species of rhodium (I) are used, since stoichiometric [2+2+1] cycloaddition occurs to form a rhodium ligated with cyclopentadienone, leaving no available coordination sites for two alkyne moieties.[75] Cationic rhodium(I) species, compared to neutral complexes, have an additional, more flexible coordination site on rhodium for interaction with the substrate (diyne). This allows smooth transformation even at room temperature to give cyclopentadienones **77** in good yields.

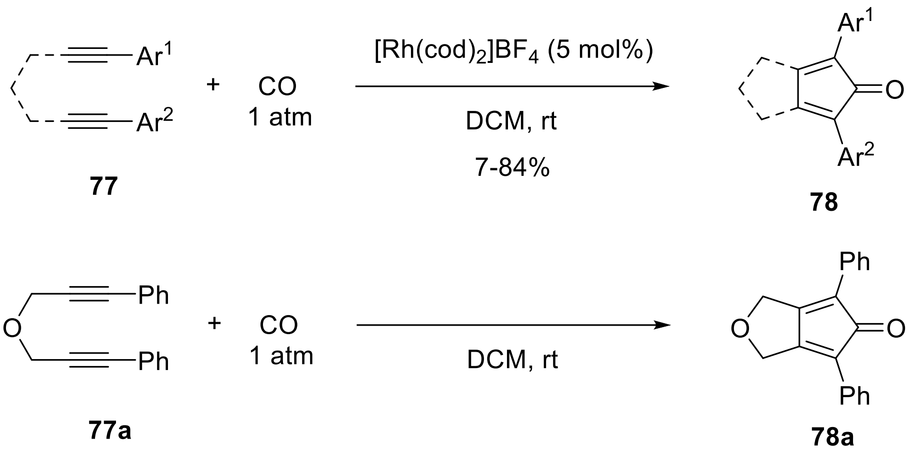

[Rh(cod)Cl]$_2$ (5 mol%)	0%
[Rh(cod)$_2$]BF$_4$ (5 mol%)	78%

Scheme 41. Intramolecular [2+2+1] Cycloaddition of Diynes **77** Catalysed by Cationic Rhodium.

Subsequent study of this process revealed that irradiation with light promotes the decomposition of rhodium-cyclopentadiene complex allowing the release of the product, thus accelerating the process by providing a vacant coordination site on rhodium centre.[76] Under photoirradiation, even the neutral rhodium(I) complex [Rh(cod)Cl]$_2$ becomes catalytically active by decoordination of cyclopentadienone from the rhodium centre. Compared to previously studied system, the yields of **78** increased by 2-34%. A plausible mechanism of the transformation was presented for [Rh(cod)Cl]$_2$ precursor (Scheme 42).

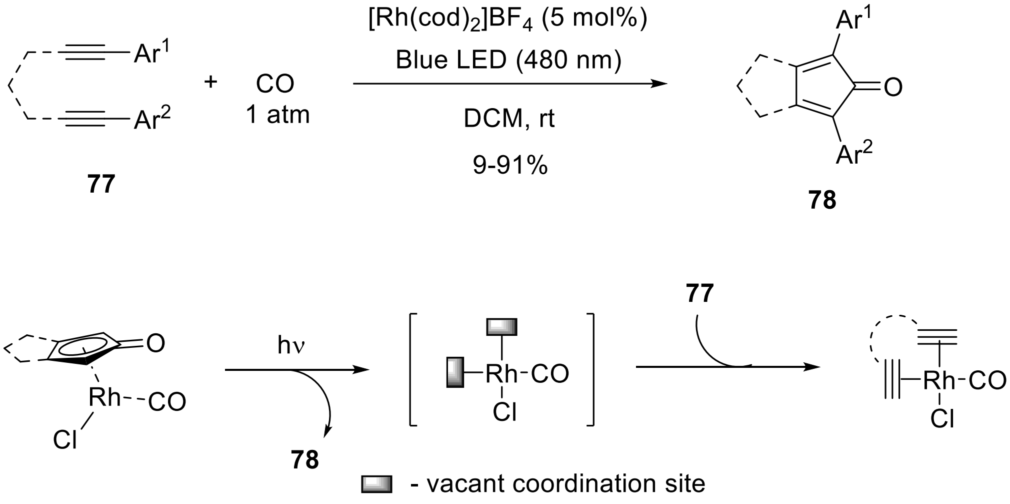

Scheme 42. Intramolecular [2+2+1] Cycloaddition of Diynes **77** Catalysed by Cationic Rhodium.

The sensitivity of rhodium complexes to photoirradiation was also investigated in the study dedicated to the catalytic production of formamides from CO and amines.[77] The potential of photoinduced rhodium-catalysed carbonylation reactions remains to be explored.

5. Ruthenium-Mediated Photooxidation

The story of ruthenium begins with the Russian mint during the reign of Tsar Nikolai I. In 1825, Nikolai I issued a decree on the minting of coins from the found "Siberian metal", alluvial platinum of the Ural Mountains. At that time, the price of platinum was much inferior to that of gold, and the mint often used it as an inexpensive means of hardening and thickening gold.[78]

Figure 6. A Russian coin made from "pure Ural platinum".

In the early 1830s, Finance Minister Count Yegor Kankrin, a major proponent of platinum coinage, began to think about how much platinum might still be in spent platinum ores. He sent samples of this waste ore to universities of the Russian Empire and to Jakob Berzelius in Stockholm. Gottfried Wilhelm Osann, a respected platinum-metal chemist who studied with Johann Döbereiner, received four pounds.[79]

Berzelius did not find any unusual metals, but Osann believed he found three new metals, which he called pluranium, polonium, and ruthenium. For the latter, Osann selected the name "ruthenium" because of the origins of the analysed samples (from Latin "Ruthenia" – Russia). The discovery caused a series of controversies between Berzelius and Osann, and eventually Osann had to relinquish his claims as he failed to repeat his isolation experiments.

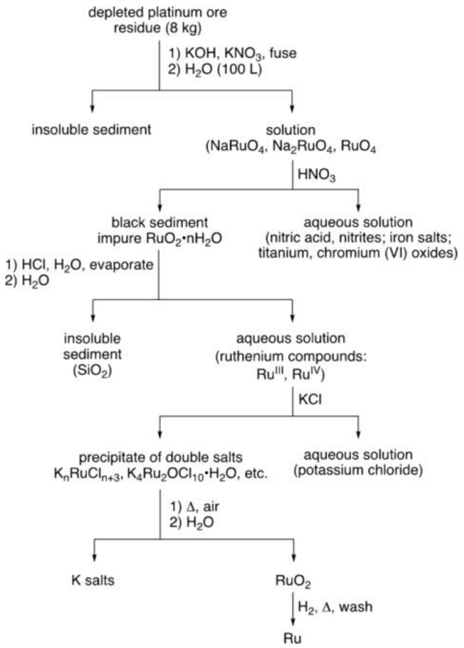

Figure 7. The Klaus' method of ruthenium isolation

In 1844, Karl Klaus who was previously working with Osann and later continued the analysis of ores, found one of his samples tasted and smelled "odd". By following this strange taste and smell, he was able to construct the reaction sequence (Figure 7) that gave him the new element. He after proved that the Osann's materials yet contained small amounts of ruthenium. Choosing the name for the new element, Klaus expressed the will to keep the name of the element given by Osann by stating: "*At the very beginning of the work, I noticed the presence of a new substance, but at first I could not find a way to separate it from impurities… This metal, which I have named ruthenium in honour of our fatherland, certainly belongs among the most interesting materials*".[80]

Ruthenium had gained great popularity in university chemistry departments in the second half of the XX^th^ century, largely due to its cheap cost compared to other metals of platinum group. The rarity these metals makes them all expensive, but unlike platinum, rhodium, and palladium, which found their applications in automotive catalytic converters, ruthenium has historically not been in high demand. Indeed, for many years Johnson Matthey, a chemical company, used a loan scheme in which they gave promising researchers about 100 grams of ruthenium trichloride to experiment with in the hope that chemists would find new potentially useful properties for the material.[81-83] The loan scheme was also available for more expensive metals such as rhodium, but only in small 5-gram packs. The loan scheme was remarkable in that the chemists would collect metal-containing residues from their experiments and send back the resulting black, smelly residue to the company for metal recovery.

Today, the chemistry of ruthenium allows multiple types of chemical reactions, as metathesis,[84] asymmetric hydrogenation,[85] or Fisher-Tropsch synthesis.[86] A special attention is now dedicated to a previously unknown ability of ruthenium complexes to promote single electron transfer (SET).[87] Visible-light-induced ruthenium catalysis has emerged as a new paradigm in organic photocatalysis, which has led to the discovery of unprecedented transformations as well as the improvement of known reactions.

Tris(bipyridine)-type ruthenium complexes have been extensively tested in areas ranging from solar cells,[88] water splitting,[89] imaging,[90] and photodynamic therapy.[91] Among them, tris(2,2-bipyridine)ruthenium(II) has occupied a privileged position on the market as it has shown high versatility and stability when exposed to air and humidity.[92] It turned out that $Ru(bpy)_3Cl_2$ and its analogues are perfectly suitable for the mediation of SET processes in various systems including organic frameworks. Photoexcitation of the ruthenium centre leads to so called metal-to-ligand charge-transfer (MLCT), the transition of an electron in t_2g orbital of Ru to a π^* orbital centred on a ligand, which is then followed by an intersystem crossing (ISC), yielding a triplet excited state (Scheme 43). For tris(bipyridine)ruthenium complexes, the maximum of MLCT is normally observed in the blue light range, at around 450 nm.

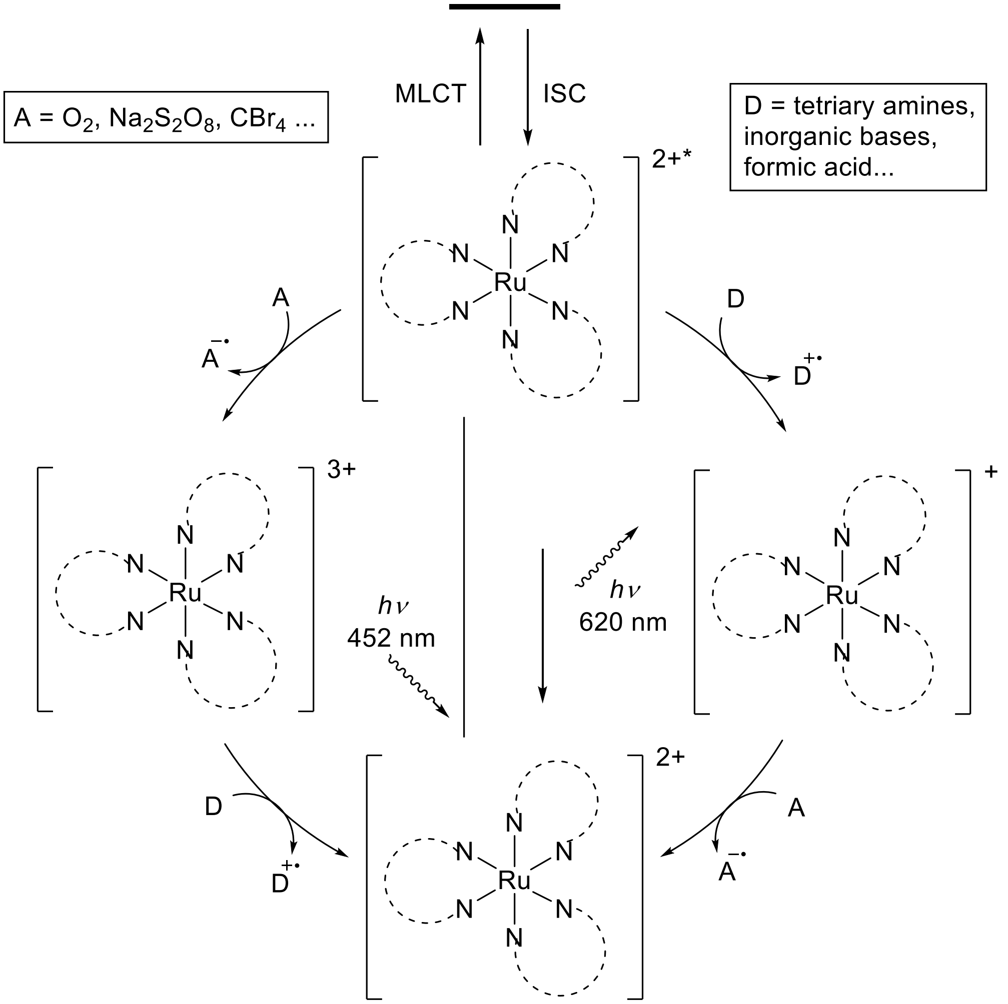

Scheme 43. Single Electron Transfer (SET) Mediated by $[Ru(bpy)_3]^{2+}$.

The lowest MLCT excited state of tris(2,2-bipyridine)ruthenium(II) lives long enough to encounter other solute molecules and possesses suitable properties to play the role of energy donor, electron donor, or electron acceptor. The energy available to $*[Ru(bpy)_3]^{2+}$ for energy transfer processes is 2.12 eV and its reduction and oxidation potentials are + 0.84 and – 0.86 V (aq. sol., vs SCE). It follows that $*[Ru(bpy)_3]^{2+}$ is simultaneously a good energy donor, electron donor, and electron acceptor.[93]

The direct observation of redox products represents the strongest evidence to support the occurrence of oxidative and reductive quenching mechanisms. The terms reductive and oxidative might be confusing and require explanation. Reductive refers to reduction of the photoexcited species, whereas the electron donor D is oxidised in the same process. Oxidative means oxidation of the photoexcited species concomitant with reduction of acceptor A.

Both oxidative and reductive quenching cycles start with the excitation of the photocatalyst to give $*[Ru(bpy)_3]^{2+}$ species. The reductive quenching consists of a sequence in which the initial step is represented by the electron transfer from an electron donor D to $*[Ru(bpy)_3]^{2+}$, leading to the formation of $[Ru(bpy)_3]^+$. The latter, being a good reducing agent, cedes an electron to acceptor A and restores its ground state $[Ru(bpy)_3]^{2+}$. Conversely, oxidative quenching can occur if the photoexcitation of the catalyst is directly followed by the electron donation to acceptor A. The resulting $[Ru(bpy)_3]^{3+}$ is a good oxidising agent for donor D. By producing $D^{+\cdot}$, it returns to its initial ground state $[Ru(bpy)_3]^{2+}$ and is ready to be excited for promoting another catalytic cycle.[94]

Until 2008, a limited number of reports were made on the $[Ru(bpy)_3]^{2+}$ photoredox catalysis of organic reactions.[95-97] Starting from 2008 an exponential upswing in publications can be observed. One of the pioneering work that undoubtedly contributed to this upward trend was carried out by Yoon's group.[98] A rare [2+2] cycloaddition was demonstrated to be accessible *via* visible-light-promoted catalysis by tris(bipyridine)ruthenium(II). Starting vinylic ketones **79** could be transformed into cyclobutanes **80** with high diastereoselectivity in just 1 h of reaction time. One critical limitation of the process is the type of substituents on carbonyls since no reaction was observed for alkyl-substituted ketones.

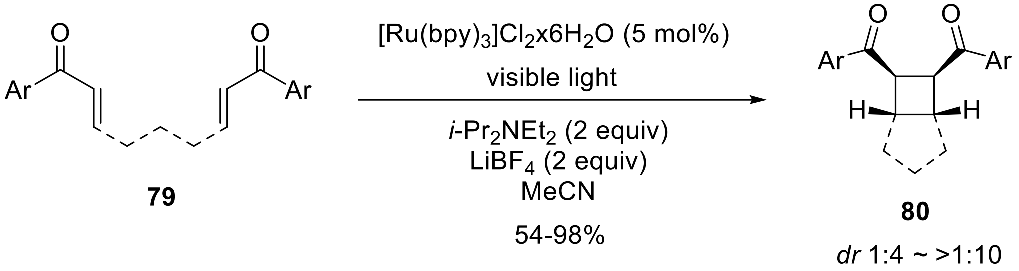

Scheme 44. Ru-Photocatalysed [2+2] Cycloaddition.

Analogous to [2+2] cycloaddition, the Diels–Alder [4+2] cycloaddition electronically mismatched dienes and dienophiles was achieved by using a similar ruthenium catalyst (Scheme 45).[99] The reaction proceeded well for a great variety of electron-rich dienophiles with moderately electron-rich dienes, while electron-deficient dienes turned out to be inert towards oxidation, due to the radical cationic nature of the process. Classic $[Ru(bpy)_3]^{2+}$ demonstrated limited reactivity that the authors associated with the propensity of oxygen to quench $*[Ru(bpy)_3]^{2+}$ by net energy transfer rather than by oxidative quenching, thus key $[Ru(bpy)_3]^{3+}$ would not be efficiently formed under air. This problem was successfully overcome by using bipyrazine ligands at ruthenium.

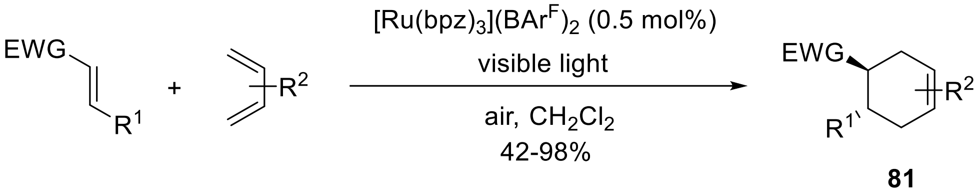

Scheme 45. Ru-Photocatalysed [4+2] Cycloaddition.

The abovementioned $[Ru(bpz)_3]^{2+}$ was used to promote [3+2] cycloaddition of alkenes with cyclopropylamines (Scheme 46).[100] In this case the mechanism of the process supposed the Ru(II)-Ru(I) transformation, following the reduction quenching cycle. Optimisation study revealed that the presence of air was damaging for the selectivity of the cycloaddition, thus solvent degassing was crucial for achieving the products in good yields. As for the aspect of substrates, 2-azabicyclo[3.1.0]hexanes **82** afforded 5 octahydrocyclopenta[*b*]pyrroles **83** in modest yield and diastereoselectivity (3:1 – >25:1), while monocyclic *N*-cyclopropylanilines **84** gave *N*-cyclopentylanilines **85** in good yields and poor diastereoselectivity. Regioselectivity remained high for both types of substrates.

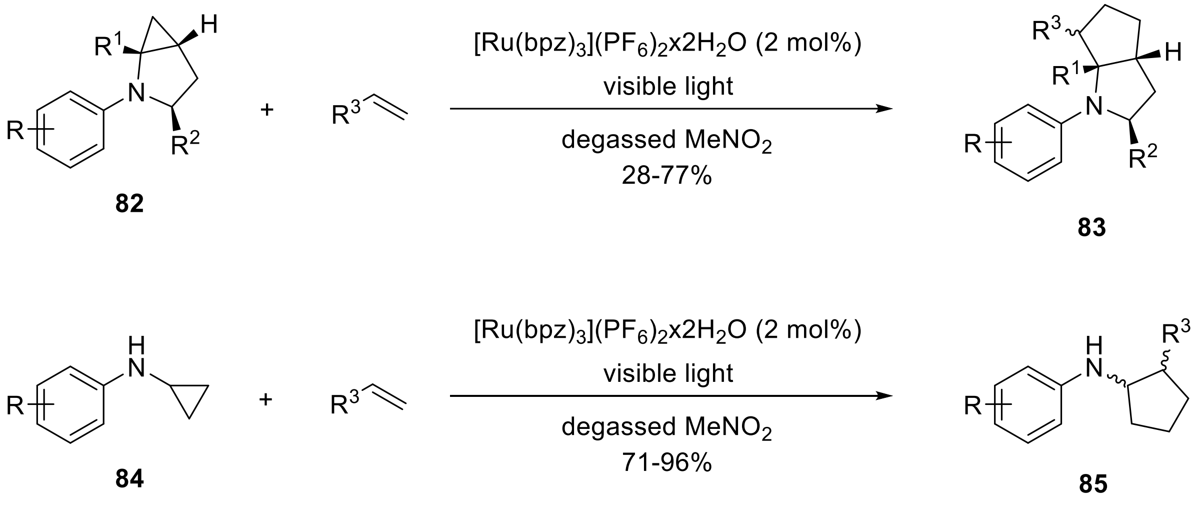

Scheme 46. Ru-Photocatalysed [3+2] Cycloaddition.

The pathway of the $[Ru(bpz)_3]^{2+}$-mediated process can be altered by carrying out the reaction under oxygen atmosphere.[101] The incorporation of oxygen opens access to the products of [2+2+2] cycloaddition (Scheme 47). Photocatalytic cyclotrimerization of bis(styrene) substrates **86** with oxygen leads to the formation of cyclic peroxides **87** that can eventually be converted to 1,4-diols or γ-hydroxyketones. The resulting mixture would always contain a certain amount of the [2+2] cycloaddition product, but the selectivity towards the cyclotrimerization product can be enhanced by changing some reaction parameters. Thus, an increase in oxygen pressure up to 4 atmospheres would lead to an increment in the yield of **87** by 14%. Lowering the concentration of the starting material from 0.1 M to 0.02 M would lead to a dramatic augmentation in the yield of the product (up to 77%). Cooling the reaction medium to 5 ˚C would allow to almost completely suppress the formation of the [2+2] cycloaddition product. The best yield reached for the model substrate was 79%. The reaction scope was limited to electron-enriched aryl substituents.

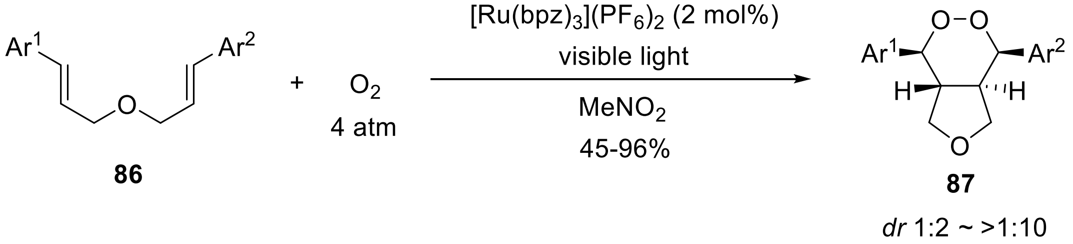

Scheme 47. Ru-Photocatalysed [2+2+2] Cycloaddition.

Electron-enriched *N*-arylanilines **88** containing a vinyl-moiety in *ortho*-position at one of the benzene rings were successfully photooxidised to afford indoles **89** (Scheme 45).[102] Similar to the mechanism of the light-mediated [3+2]-cycloaddition, the formation of the iminium radical cation is the driving force of the process. The addition of vinyl, oxidation and aromatisation sequence leads to the formation of indole derivatives. The presence of a *p*-alkoxyphenyl group at nitrogen atom was indispensable, and thus limited the substrate scope of the reaction. Interestingly, silica gel played an essential role in the reaction as the yield of the products significantly dropped (68% to 19%), when it was not added to the reaction medium. The full conversion of the substrates required from 3 to 18 hours.

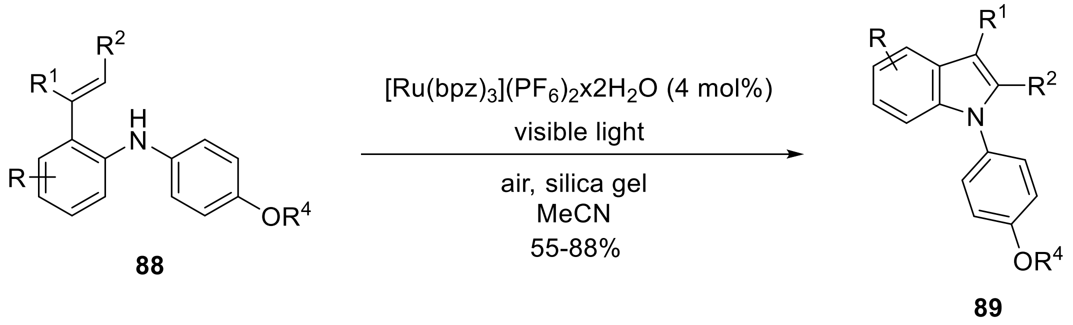

Scheme 48. Ru-catalysed Photooxidation of *N*-Arylanilines **89**.

Photocatalytic selective C–C bond cleavage represents a highly attractive and powerful chemical tool for practically useful direct transformation of complex chemical structures. Wang and co-workers applied the previously mentioned iminium ion generation strategy to enable CH-activation of sp^3 hybridised carbon atoms.[103] The C-C bond cleavage was achieved for 1,2-diaminoethane derivatives **90** thanks to the reorganization of electron density, which is induced by a β-nitrogen atom in close proximity to N-centered radical cation. The simultaneous formation of the iminium ion and α-amino radical allows the promotion of both ionic and radical processes, for instance, aza-Henry condensation and radical polymerisation. The former was investigated under photocatalytic conditions using oxygen as a terminal oxidant. The formation of aza-Henry products **92** required from 16 to 72 hours and proceeded with yields varying from 31% to 91%.

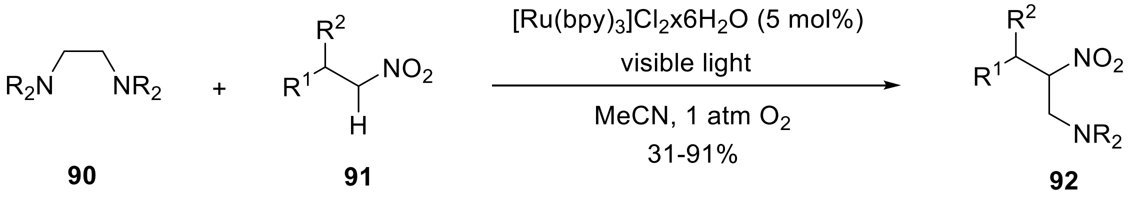

Scheme 49. Ru-Photocatalysed [2+2] Cycloaddition.

An example of light-mediated aromatic C-H activation was reported by Li and co-workers (Scheme 50).[104] An aerobic visible-light induced oxidation of thioanilides **93** led to the formation of 2-substituted benzothiazoles **94** through radical cyclisation. The sulfur radical originated from oxidation of thioimidate provided a distinct reactivity, allowing the functionalisation of the *ortho*-position of the benzene ring.

The authors stated that the mechanism of the process has to involve the oxidative quenching cycle of ruthenium as reductive quenching could not be ruled out. Interestingly, the reaction was highly sensitive to the level of the oxygen concentration. Introduction of less than a stoichiometric amount of oxygen caused a partial reaction with complete consumption of oxygen. When the reaction was carried out under air atmosphere (~21% oxygen), benzothiazole **94** formed in 74% yield, and a partial formation of the undesired benzanilide was observed. When pure oxygen was used, the intramolecular cyclisation was completely arrested, and only benzanilide formed as an outcome of the reaction. The optimal concentration of oxygen was found to be 5%.

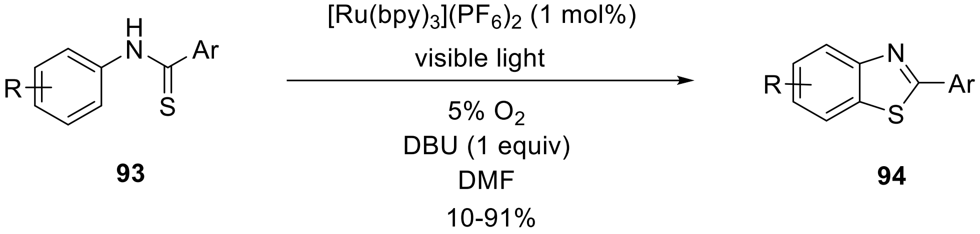

Scheme 50. Ru-Photocatalysed CH-Functionalisation of **93**.

A photocatalytic strategy for the synthesis of α-alkoxy-β-ketosulfoxides and α,β-dialkoxysulfoxides starting from alkynes, thiols, and alcohols was developed in 2020.[105] A challenging four-component oxidative addition was successfully implemented by using $[Ru(bpy)_3]Cl_2$ as a catalyst (Scheme 51).

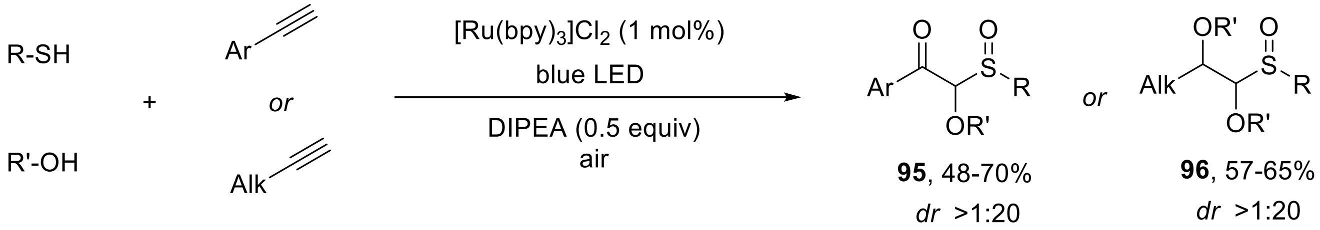

Scheme 51. Ru-Photocatalysed Synthesis of Functionalised Sulfoxides.

Aromatic and aliphatic alkynes displayed different reactivity under the same reaction conditions. Aromatic acetylenes was transformed exclusively to α-alkoxy-β-ketosulfoxides **95**, while aliphatic acetylenes gave α,β-dialkoxysulfoxides **96**, the products of double alcohol addition. Authors associated it with the lower stability of the aliphatic vinyl radicals that can render them more reactive towards the nucleophilic addition of alcohol. Both reactions proceeded with excellent regio- and high diastereoselectivity (>20:1). It should be noted that the products were obtained in moderate yields even if weak nucleophiles (phenol, trifluoroethanol) were introduced into the reaction.

References

1. World Catalysts. Industry Study with Forecasts for 2018 & 2023. *Freedonia group,* **2014**.
2. Catalyst Market by Type, Process, and Application: Global Opportunity Analysis and Industry Forecast, 2021–2030. *Allied Market Research*, **2021**.
3. Wisniak, J. Nicolas Clément. *Educación Química*, **2011**, *22(3),* 254-266.
4. Kirchhoff, G. *Bulletin des Neusten und Wissenwürdigsten aus der Naturwissenschaft...,* **1811**, *10*.
5. Kirchhoff, G. *Tekhnologichesky zhurnal,* **1812**, *9(1)*.
6. Davy, E. *Philosophical Transactions of the Royal Society of London*, **1820**, *110*, 108-125.
7. Döbereiner, J.W. *Annalen der Physik, 1st series*., **1823**, *74(3)*, 269–273
8. Berzelius, J.J*., Royal Swedish Academy of Sciences,* **1835**.
9. Ostwald, W. Nobel Lecture. **1909**.
10. Houten, J.V. *J. Chem. Educ*., **2002**, *79(2)*, 146.
11. Lefort, T. E. *Société Française de Catalyse Généralisée.* FR729 952, **1931**.
12. Li, C.-J.; Bi, X. Silver Catalysis in Organic Synthesis, vol. 1. **2018**.
13. Schfer, C.; Miesch, M.; Miesch, L. *Chem. Eur. J.*, **2012**, *18*, 8028 – 8031.
14. Boominathan, S.S.K.; Hu, W.-P.; Senadi, G.C.; Wang, J.-J. *Adv. Synth. Catal.,* **2013,** *355*, 3570 – 3574.
15. Kallepu, S.; Gollapelli, K.K.; Nanubolub, J.B.; Chegondi, R. *Chem. Commun*., **2015**, *51*, 16840 – 16843.
16. Koo, J.; Park, H.-S.; Shin, S. J. *Tetrahedron*, **2013**, *54*, 834 – 839.
17. Martins, M.A.P.; Rossatto, M.; Frizzo, C.P.; Scapin, E. et al. *Tetrahedron*, **2013**, *54*, 847–849.
18. Godet, T.; Belmont, P. *Synlett*, **2008**, *16*, 2513–2517.
19. Garcia, P.; Harrak, Y.; Diab, L. et al. *Org. Lett.*, **2011**, *13*, 2952–2955.
20. James, M.J.; Clubley, R.E.; Palate, K.Y. et al. *Org. Lett*., **2015**, *17*, 4372–4375.
21. Pale, P.; Chuche, J. *Tetrahedron*, **1987**, *28*, 6447–6448.
22. Oh, C.H.; Yi, H.J.; Lee, J.H. *New J. Chem*., **2007**, *31*, 835–837.
23. Jong, T.-T.; Leu, S.-J. J. *Chem. Soc., Perkin Trans. 1*, **1990**, 423–424.
24. Dabral, S.; Bayarmagnai, B.; Hermsen, M. et al. *Org. Lett.* **2019**, *21 (5)*, 1422–1425.
25. Susanti, D.; Koh, F.; Kothandaraman, P.; Chan, P.W.H. *J. Org. Chem*., **2012**, *77*, 7166–7175.
26. Barange, D.K.; Nishad, T.C.; Swamy, N.K. et al. *J. Org. Chem.*, **2007**, *72*, 8547–8550.
27. Gabriele, B.; Mancuso, R.; Salerno, G. *Eur. J. Org. Chem.*, **2012**, 6825-6839.
28. Schoenberg, A.; Bartoletti, I.; Heck, R.F. *J. Org. Chem*. **1974**, *39*, 3318-3326.
29. Schoenberg, A.; Heck, R.F. *J. Org. Chem.* **1974**, *39*, 3327-3330.
30. Schoenberg, A.; Heck, R.F. *J. Am. Chem. Soc*. **1974**, *96*, 7761-7764.
31. Torres, G.M.; Liu, Y.; Arndtsen, B.A. *Science*, **2020**, *368*, 318–323.
32. Jaegers, E.; Koll, H.-P. Patent EP0338330A1. Hoechst AG, **1989**.
33. Beller, M.; Eckert, M.; Holla, E.W. *J. Org. Chem*., **1998**, 63 (16), 5658–5661.
34. Beller M.; Eckert M.; Moradi W.; Neumann H. *Angew. Chem. Int. Ed.,* **1999**, *38*, 1454.
35. Akao, S.; Sugawara, K.; Inoue Amino, Y. *J. Mol. Catal.* **2000**, *157*, 117-122.

36. Tijani, J.; Suleiman, R.; El Ali, B. *Appl. Organometal. Chem.* **2008**, *22*, 553.
37. Crawford, L.E.; Cole-Hamilton, D.J.; Bühl, M. *Organometallics*, **2015**, *34 (2)*, 438–449.
38. Qiab, H.; Huang, Z.; Wang, M. et al. *J. Catal*., **2018**, *363*, 63–68.
39. Reetz M.T.; Demuth, R.; Goddard, R. *Tetrahedron*, **1998**, *39*, 7089-7092.
40. Sole, R.; Scrivanti, A.; Bertoldini, M.; Beghetto, V.; Alam, M.M. *Mol. Catal*., **2020**, *496*, 111179.
41. Yang, D.; Liu, L.; Wang, D.-L.; Lu, Y.; Zhao, X.-L.; Liu, Y. *J. Catal*., **2019**, *371*, 236–244.
42. Williams, D.B.G.; Shaw, M.L.; Hughes, T. *Organometallics*, **2011**, *30*, 4968–4973.
43. Liu, J.; Dong, K.; Beller, M. et al. *J. Am. Chem. Soc.*, **2018**, *140 (32)*, 10282–10288.
44. Ge, Y.; Ye, F.; Liu, J.; Yang, J.; Spannenberg, A.; Jiao, H.; Jackstell, R.; Beller, M. *Angew. Chem. Int. Ed*., **2020**, *59* ,21585–21590.
45. El Ali, B.; Alper, H. *J. Org. Chem.,* **1991**, *56*, 5357-5360.
46. Tsuji, J.; Morikawa, M.; Iwamoto, N. *J. Am. Chem. Soc*., **1964**, *86*, 2095.
47. Tsuji, J.; Takahashi, M.; Takahashi, T. *Tetrahedron*, **1980**, *21*, 849 – 850.
48. Izawa, Y.; Shimizu, I.; Yamamoto, A.; *Bull. Chem. Soc. Jpn.,* **2004**, *77 (11)*, 2033–2045.
49. Gadge, S.T.; Bhanage, B.M. *Synlett*, **2013**, *24 (8)*, 981–986.
50. Kato, K.; Motodate, S.; Mochida, T.; Kobayashi, T.; Akita, H. *Angew. Chem. Int. Ed.*, **2009**, *48*, 3326.
51. Beltrani, M.; Carfagna, C.; Milani, B.; Mancuso, R.; Gabriele, B.; Fini, F. *Adv. Synth. Catal.*, **2016**, *358*, 3244 –3253.
52. The data provided by Trading Economics©.
53. Paulik, F.E.; Roth, J.F. *Chem. Commun*., **1968**, *28*, 1578.
54. Sunley, G.J.; Watson, D.J. *Catal. Today*, **2000**, *58 (4)*, 293-307.
55. Akutagawa, S. *Appl. Catal. A: General*, **1995**, *128 (2),* 171-207.
56. Wiesenfeldt, M.P.; Nairoukh, Z.; Li, W.; Glorius, F. *Science*, **2017**, *357 (6354)*, 908-912.
57. Young, J.F.; Osborn, J.A.; Jardine, F.H.; Wilkinson, G.J. *Chem. Commun.*, **1965**, *7*, 131.
58. Öhrström, L. *Nature Chemistry*, **2016**, *8*, 90.
59. Li, X.-N.; Zhang, H.-M.; Yuan, Z.; He, S.-G. *Nature Commun.*, **2016**, *7*.
60. Montag, M.; Leitus, G.; Shimon, L.G.W. et al. *Chem. Eur. J.*, **2007**, *13*, 9043–9055.
61. Inoue, S.; Yokota, K.; Tatamidani, H.; Fukumoto, F.; Chatani, N. *Org. Lett.*, **2006**, *8*, 2519-2522.
62. Guan, Z.-H.; Ren, Z.-H.; Spinella, S.M. et al. *J. Am. Chem. Soc*., **2009**, *131 (2)*, 729–733.
63. Ai, H.-J.; Wang, H.; Li, C.-L.; Wu, X.-F. *ACS Catalysis,* **2020**, *10 (9)*, 5147-5152.
64. Ai, H.-J.; Zhang, Y.; Zhao, F.; Wu, X.-F. *Org. Lett.*, **2020**, *22*, 6050−6054.
65. Yoneda, E.; Kaneko, T.; Zhang, S.W.; Takahashi, S. *Tetrahedron*, **1998**, *39*, 5061–5064.
66. Yoneda, E.; Sugioka, T.; Hirao, K.; Zhang, S.W.; Takahashi, S. *J. Chem. Soc. Perkin Trans. 1*, **1998**, 477-483.
67. Hirao, K.; Morii, N.; Joh, T.; Takahashi, S. *Tetrahedron*, **1995**, *36*, 6243–6246.
68. Shiba, T.; D.Y.; Zhou, D.Y.; Onitsuka, K.; Takahashi, S. *Tetrahedron*, **2004**, *45*, 3211–3213.
69. Khand, I.U.; Pauson, P.L. et al. *J. Chem. Soc., Perkin Trans. 1*, **1973**, 977.
70. Koga, Y.; Kobayashi, T.; Narasaka, K. *Chem. Lett.,* **1998**, *27*, 249.
71. Jeong, N.; Lee, S.; Sung, B.K. *Organometallics*, **1998**, *17*, 3642.
72. Morimoto, T.; Tanaka. K. *Wiley-VCH*, **2019**, 161-182.

73. Huang Q.; Hua R. *Chem. Eur. J.*, **2007**, *13*, 8333.
74. Shibata, T.; Yamashita, K.; Ishida, H.; Takagi, K. *Org. Lett.*, ***2001**, 3 (8),* 1217–1219.
75. Morimoto, T.; Jia, J.; Yamaguchi, Y.; Tanimoto, H.; Kakiuchi, K. *Asian J. Org. Chem.* **2020***, 9,* 1778.
76. Jia, J.; Morimoto, T.; Yamaguchi, Y. et al. *Org. Lett.*, **2021**, *23 (12)*, 4893–4897.
77. Zhang, J.; Zhang, W.; Xu, M. et al. *J. Am. Chem. Soc.*, **2018**, *140 (21)*, 6656–6660.
78. Lewis, D.E. *Chem. Eur. J.*, **2019**, *25*, 11394.
79. Marshall, J.L.; Marshall, V.R., *The Hexagon*, **2009**, 20-23.
80. Klaus, K.K. *Gorn. Zh.*, **1845**, *7*, 157.
81. Hui, B.C.; Jame, B.R. *Can. J. Chem.,* **1970**, *48*, 3613-3618.
82. Bodensieck, U.; Meister, A.; Meister, G.; et al. *Chimia*, **1993**, *47 (6)*, 189-191.
83. Iengo, E.; Milani, B.; Zangrando, E. et al. *Angew. Chem. Int. Ed.,* **2000**, *39 (6)*, 1096-1099.
84. Fürstner, A. *Angew. Chem. Int. Ed*., **2000**, *39 (17),* 3012–3043.
85. Noyori, R.; Ohkuma, T.; Kitamura, M. et al. *J. Am. Chem. Soc.*, **1987**, *109 (19),* 5856–5858.
86. Schulz, H. *Appl. Catal. A: General*, **1999**, *186*, 3-12.
87. Angerani, S.; Winssinger, N. *Chem. Eur. J.*, **2019**, *25*, 6661.
88. Gratzel, M. *Acc. Chem. Res.,* **2009**, *42*, 1788-1798.
89. Huber, F.L.; Wernbacher, A.M.; Perleth, D. et al. *Inorg. Chem*., **2021**, *60 (17)*, 13299–13308.
90. Tsui, W.K.; Chung, L.H.; Wong, M.K. et al. *Sci. Rep.*, **2015**, *5*, 9070.
91. Kalyanasundaram, K.; Gratzel, M. *Coord. Chem. Rev*., **1998**, *177*, 347.
92. Prier, C.K.; Rankic, D.A.; MacMillan, D.W.C. *Chem. Rev*., **2013**, *113*, 5322.
93. Campagna, S.; Puntoriero, F.; Nastasi, F.; Bergamini, G.; Balzani, V. *Springer*, **2007**, *280*, 117-214.
94. Koike T.; Akita M. *Springer, Cham*., **2014**, *48*.
95. Pac C.; Ihama M.; Yasuda M.; Miyauchi Y.; Sakurai H. *J. Am. Chem. Soc*., **1981**, *103*, 6495–6497.
96. Ishitani O.; Pac C.; Sakurai H. *J. Org. Chem*., **1984**, *49*, 26–34.
97. Okada K.; Okamoto K.; Morita N.; Okubo K.; Oda M. *J. Am. Chem. Soc*., **1991**, *113*, 9401–9402.
98. Ischay, M.A.; Anzovino M.E.; Du, Y.; Yoon, T.P. *J. Am. Chem. Soc.*, **2008**, *130 (39),* 12886–12887.
99. Lin, S.; Ischay, M.A.; Fry C.G.; Yoon, T.P. *J. Am. Chem. Soc*., **2011**, *133*, 19350–19353.
100. Maity, S.; Zhu, M.; Shinabery, R.S.; Zheng N. *Angew. Chem., Int. Ed.*, **2012**, *51*, 222–226.
101. Parrish, J.D.; Ischay, M.A.; Yoon, T.P. et al. *Org. Lett.*, **2012**, *14 (6),* 1640-1643.
102. Maity, S.; Zheng, N. *Angew. Chem., Int. Ed.*, **2012**, *51*, 9562–9566.
103. Cai, S.; Zhao, X.; Wang, X.; Liu, Q.; Li, Z.; Wang, D.Z. *Angew. Chem. Int. Ed.*, **2012**, *51*, 8050–8053.
104. Cheng, Y.; Yang, J.; Qu, Y.; Li, P. *Org. Lett*., **2012**, *14*, 98–101.
105. Kumar, J.; Ahmad, A.; Shah, B.A. et al. *Org. Lett*., **2020**, *22*, 5661−5665.

Chapter 1. Unexpected *O-5-exo-dig* Cyclisation of Propargyl Ureas to Oxazoline-2-amines Catalysed by Silver Salts

Introduction

The intramolecular cyclisation of propargylamides has been intensively studied for decades.[1,2] Oxygen of the amide moiety can perform a nucleophilic attack on the triple bond to give heterocyclic products (Scheme 1-1). The vast majority of examples display that *5-exo-dig* cyclisation pathway, leading to the formation of oxazole derivatives, is explicitly more favourable than *6-endo-dig* route. Oxazole formation can be mediated by zinc salts in stoichiometric amounts[3] or by catalytic quantities of copper(I)[4], silver(I)[5] or gold(III)[6] precursors. If the alkynic site of the substrate is internal, the products of cyclisation would likely have *Z*-configuration.[7,8] The formation of *6-endo-dig* products, 1,3-oxazines, is rare and mainly substrate-dependent. The first example of 1,3-oxazine formation under silver catalysis was reported in 1989,[9] however the method was only valid for the substrates with two geminal CF_3 groups at 1-position of the propargyl fragment. Thirty years later, a gold(I)-promoted *6-endo-dig* cycloisomerisation was introduced.[10] Unfortunately, the method strongly depended on the substitution pattern of the triple bond: the formation of *6-endo-dig* products was only observed for internal alkyne, while terminal alkynes reacted in accordance with the *5-exo-dig* mode. Additionally, good yields were only achieved by using stoichiometric amounts of the gold catalyst.

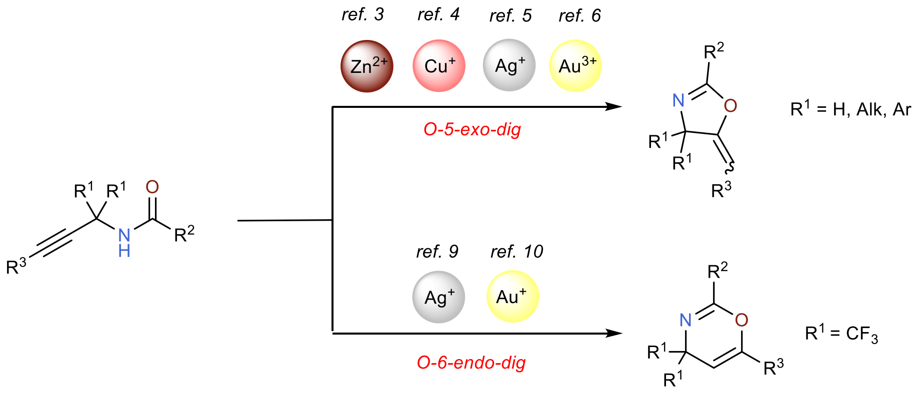

Scheme 1-1. Catalytic Cycloisomerisation of Propargylamides.

When it comes to propargylic ureas, more possible cyclisation pathways open (Scheme 1-2). Along with oxygen, nitrogen of the urea is capable of carrying out a nucleophilic attack, giving two extra products: imidazolidin-2-ones and 3,4-dihydropyrimidin-2(1*H*)-ones. Therefore, the selectivity control becomes a challenging task. Unlike for propargylamides, only few examples of catalytic cyclisation of propargylureas have been reported so far.[11,12] The main contribute to discovering the reactivity of propargylic ureas was made by Erik Van Der Eycken's group. In 2011 they presented a silver-catalysed synthesis of imidazolidin-2-ones starting from isocyanates and propargylamines,[13] and in 2013 the cycloisomerisation was directed towards the formation of oxazolidin-2-imines by gold(I) catalysis.[14] It is worth to notice that in every examined substrate a tosyl group at nitrogen atom was present.

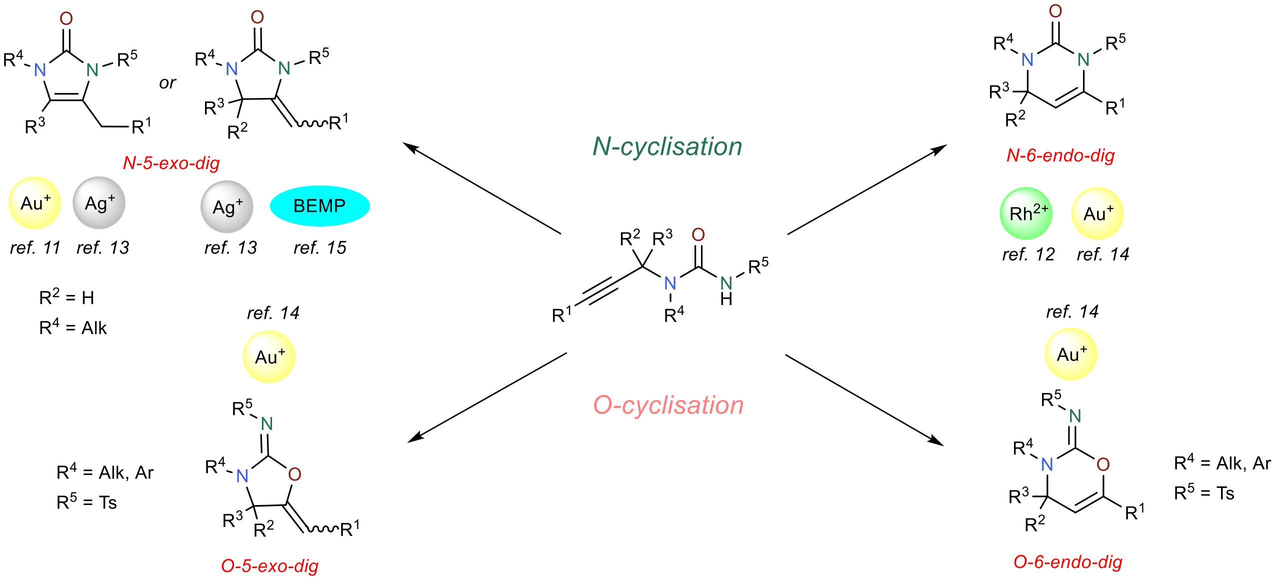

Scheme 1-2. Catalytic Cycloisomerisation of Propargylic Ureas.

In 2019 our research group conducted a study in which alkynyl ureas bore cyclisation in the presence of superbases in catalytic amounts (Scheme 1-3).[15]

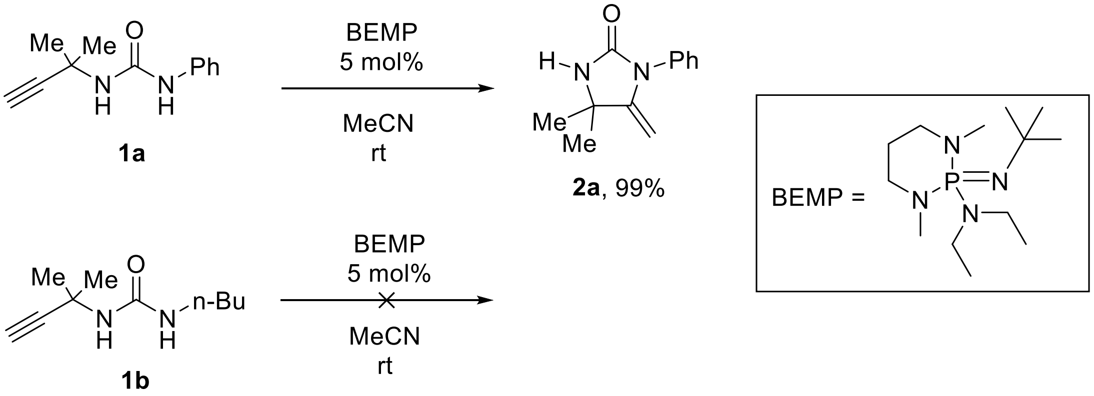

Scheme 1-3. Organocatalysed Cyclomerisation of Propargylic Ureas.

It was found that *N-exo-dig* mechanism can be easily activated when 5 mol% of a strong base is added, allowing to obtain imidazolidin-2-ones quickly and in quantitative yields. However, we testified a significant limitation of this method as the presence of an aryl group at nitrogen atom of the urea was absolutely indispensable. No reaction was observed for substrates bearing alkyl or benzyl substituents. Due to this issue, we decided to continue the research in order to find a more versatile protocol that would allow selective cycloisomerisation of propargylic ureas.

Results and Discussion

As silver has demonstrated high catalytic activity in a number of previously published works, we commenced the investigation by implementing it in the cycloisomerisation reaction. In the preliminary experiment, to promote the cyclisation of the butyl-substituted urea **1a**, silver triflate was as a catalyst (Scheme 1-4).

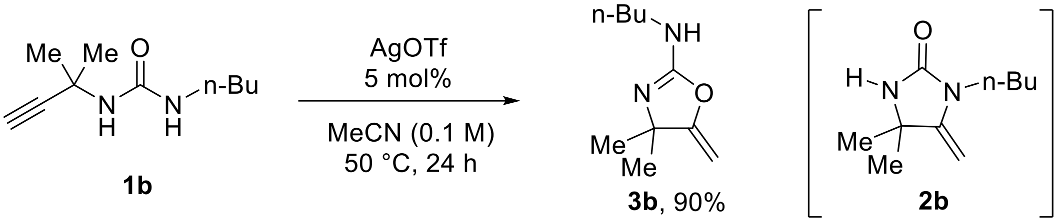

Scheme 1-4. Preliminary Experiment.

We were glad to see full conversion of **1a** in 24 hours, however, the unexpected formation of oxazoline-2-amine **3b** in place of the imidazolidinone **2b** occurred. While in the silver-catalysed process reported by Van Der Eycken[13] an *N-5-exo-dig* cyclysation pathway was described, here the *O-exo-dig* mode was observed instead. To the best of our knowledge, it is the first example of the silver-catalysed cycloisomerisation of propargylic ureas leading to the formation of an oxazoline derivative.

Once the product **3b** was obtained, we wondered whether oxazoline-2-amine fragment was common for natural or pharmaceutical products. A brief inquiry showed that oxazoline-2-amine is the structural core of several pharmaceuticals, such as rilmenidine,[16] used to treat hypertension, or sulfamoxol,[17] an antibiotic. Moreover, it is part of a compound believed to have been an intermediate in the natural nucleotide synthesis at some point in the origin of life.[18,19] Inspired by these findings, we proceeded with the optimization study for the synthesis of **3b**.

Table 1-1. Optimisation Study.

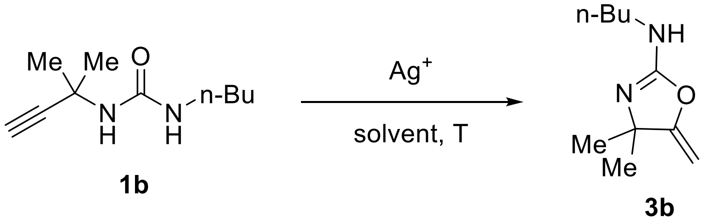

Entry	Ag-cat	Solvent	T, °C	Time, h	Yield[a] **3b**, %
1	AgOTf	CH_3CN	50	24	90
2	AgOAc	CH_3CN	50	24	94
3	Ag_2CO_3	CH_3CN	50	24	traces
4	Ag_2O	CH_3CN	50	24	traces
5	$AgPF_6$	CH_3CN	50	24	68
6	$AgBF_4$	CH_3CN	50	24	79
7	$AgSbF_6$	CH_3CN	50	24	57
8	$AgNO_3$	CH_3CN	60	18	99

9	$AgNO_3$	DMF	60	36	99
10	$AgNO_3$	DCE	60	18	99
11	$AgNO_3$	$CHCl_3$	60	24	83
12	$AgNO_3$	THF	60	16	99
13	$AgNO_3$	CH_3OH	60	4	99
14	$AgNO_3$	EtOH	60	4	74
15	$AgNO_3$	^{i}PrOH	60	4	66
16	-	CH_3OH	60	16	0

Reaction conditions: **1b** (0.2 mmol), silver salt (0.01 mmol, 5 mol%), solvent (0.1 M). ^{a}NMR yield.

Among the readily available silver(I) salts, silver nitrate exhibited the highest catalytic activity and selectivity towards **3b** (entry 8, Table 1-1). The best solvent turned out to be methanol, as the reaction reached the highest yield in only 4 hours (entry 13).

The optimised conditions (entry 13, Table 1-1) were applied to different substrates. Compared with the previously developed organocatalytic protocol[15] that was valid only for substrates with aromatic substituents at nitrogen atom, silver catalysis offered much greater versatility, allowing to obtain the desired oxazoline-2-amines starting from ureas with various types of substituents (Scheme 1-5). In most cases the yields were excellent, however the presence of allyl and ester groups were only partially tolerated as **3g** and **3i** were obtained in moderate yields (62-67%). The presence of a *p*-nitrophenyl substituent resulted in a sharp decrease in the yield of **3n** (46%). The presence of two geminal substituents at 1-position of the propargylic moiety was found to be essential for the process as products **3r**, **3s** and **3t** were not detected, and the corresponding starting ureas were almost fully recovered from the reaction mixtures. We presume that this is the evidence of the importance of Thorpe-Ingold effect of dihedral angle compression for intramolecular cyclisations.

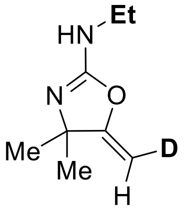

3c, 94%*, 4h

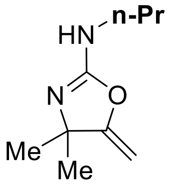

3d, quant, 5h

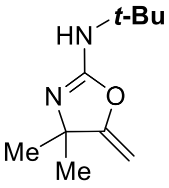

3e, 95%, 4h

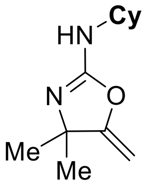

3f, quant, 4h

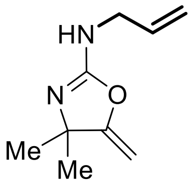

3g, 67%, 7h

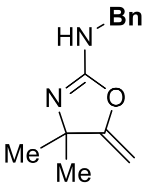

3h, 94%, 6h

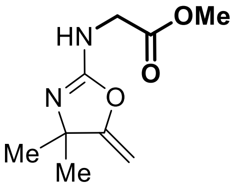

3i, 62%, 16h

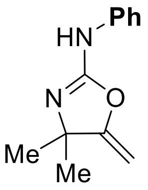

3a, quant, 3h

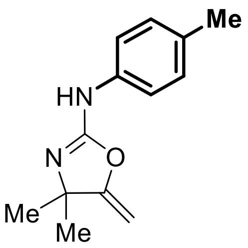

3j, quant, 3h

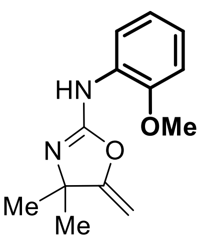

3k, quant, 4h

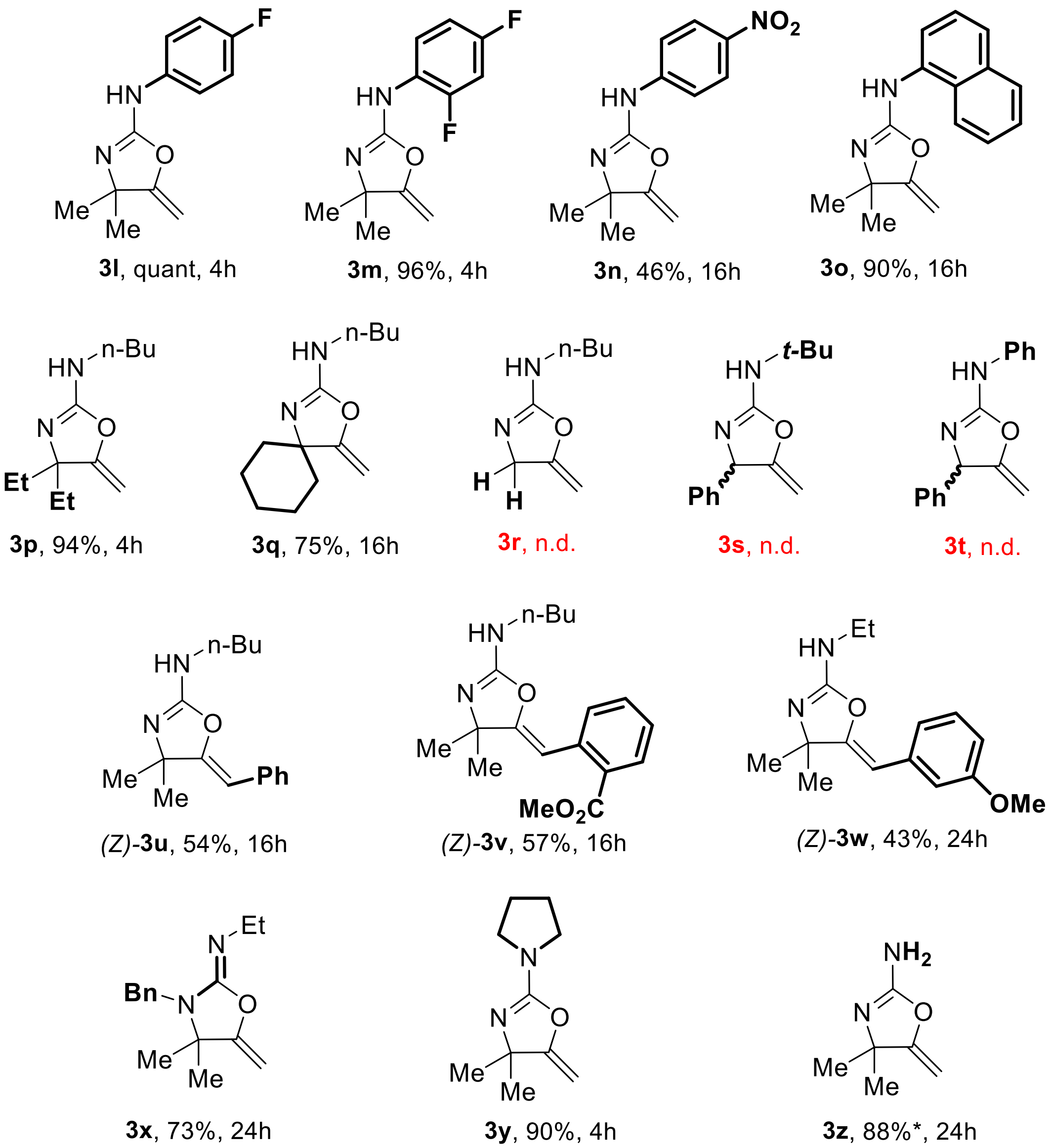

Scheme 1-5. Oxazolines Obtained by Silver Catalysis.

The products of the silver-catalysed cycloisomerisation of internal alkynes **3u**-**w** were isolated in modest yields, but their configuration was found to be exclusively *Z*. When both nitrogen atoms of the urea moiety were substituted, the product **3x** with two external double bonds formed in good 73% yield. As we discovered that compounds **3c** and **3z** are relatively volatile, their synthesis was conducted directly in NMR tubes using methanol-d_4 or DMSO as the reaction medium. Both products were obtained in good yields (88-94%), however, the reaction in methanol was followed by almost complete incorporation of one deuterium atom to the methylene fragment.

To confirm the exact structure of the obtained products, X-ray analysis was performed for selected compounds (Figure 1-1). As can be seen, **3u** is an exclusive (*Z*)-isomer.

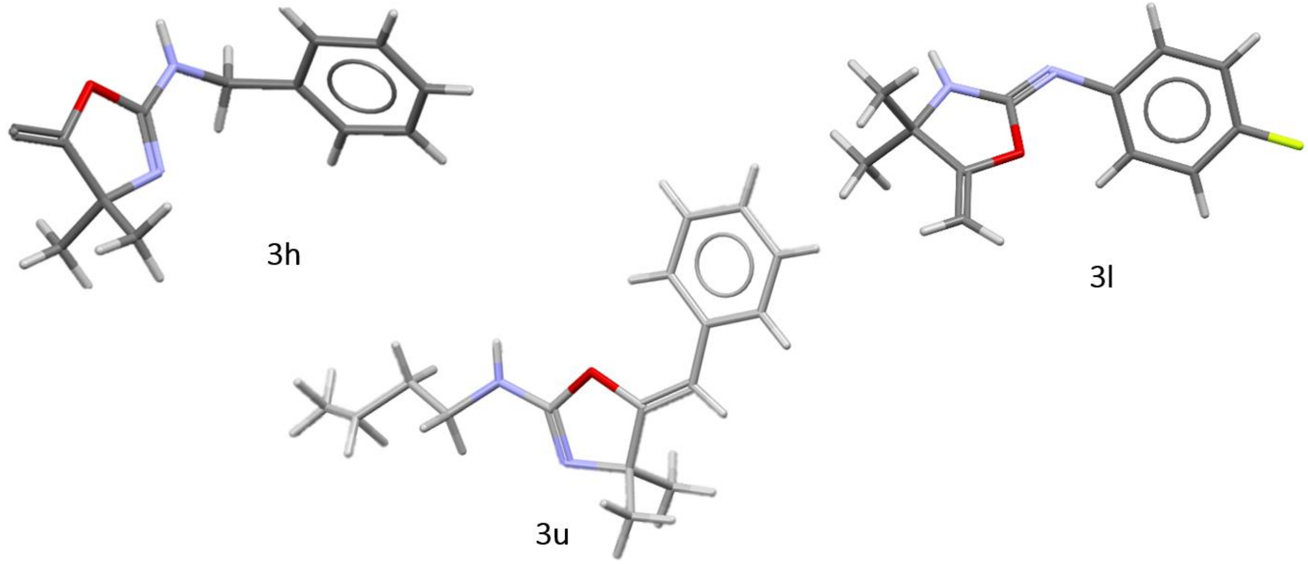

Figure 1-1. X-Ray Structures of Oxazoline-2-Amines **3h**, **3u**, and **3l**.

Under silver catalysis symmetric urea **1sym** underwent a double cyclisation affording oxazolo[3,2-*a*]pyrimidine **4** in 61% yield (Scheme 1-6). We presume that initially *O-5-exo-dig* cyclisation occurs to form the oxazoline-2-amine intermediate, which then undergoes consecutive *6-endo-dig* cyclisation through nitrogen.

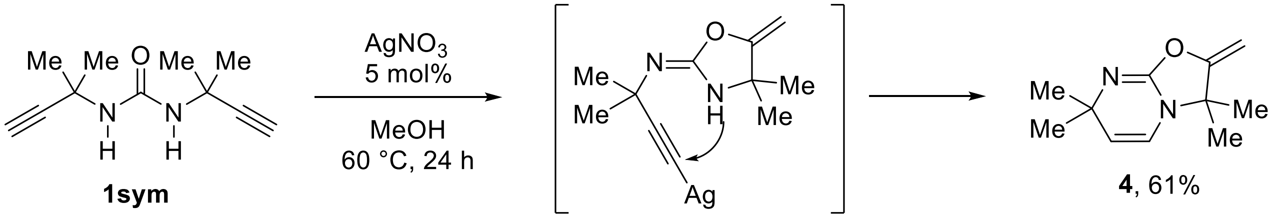

Scheme 1-6. Synthesis of Oxazolo[3,2-*a*]pyrimidine **4**.

The structure of **4** was unequivocally determined by X-ray analysis (Figure 1-2).

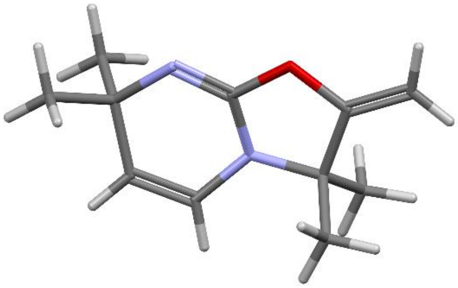

Figure 1-2. X-Ray Structure of **4**.

To further demonstrate the applicability of the developed silver-mediated protocol, we performed one-pot experiments starting from propargylic amines and isocyanates (Scheme 1-7). The *in-situ* formation of propargylic ureas was followed by the silver-catalysed intramolecular cyclisation. Products **3b** and **3c** were obtained in quantitative yields in 6 hours of reaction time.

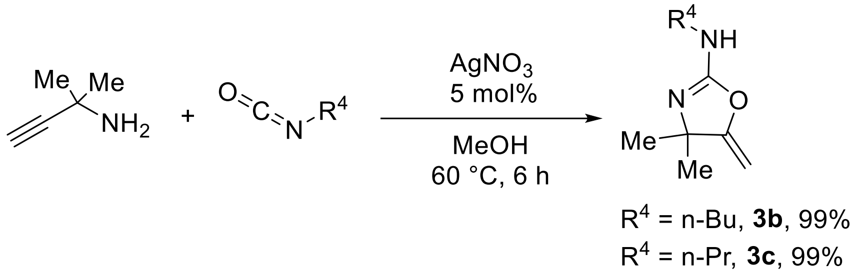

Scheme 1-7. Synthesis of **3b** and **3c** from 2-Methylbut-3-yn-2-amine and Alkyl Isocyanates.

Based on previous research and the present study, a plausible pathway of the silver-catalysed transformation is described (Scheme 1-8). Thanks to the Lewis acid character of Ag(I) along with its "carbophilicity", we assume that double coordination can possibly occur (intermediate I). The subtraction of the electron density of the alkyne moiety makes possible the nucleophilic attack of oxygen (intermediate II). Finally, proton transfer affords the desired product **3**, and silver(I) is ready to restart a new catalytic cycle. The stereoselective formation of the Z isomer can be explained through the Ag(I)-assisted nucleophilic *trans* addition of the O of the amide moiety to the activated triple bond, generating intermediate II exclusively.

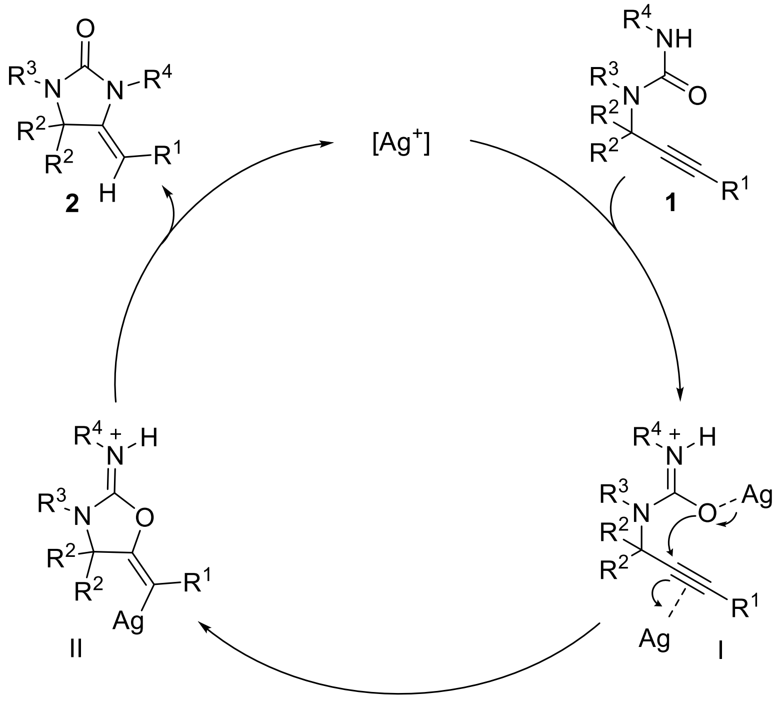

Scheme 1-8. Plausible Reaction Mechanism.

Conclusions

A new ligand-free catalytic method has been developed for the synthesis of oxazoline-2-amines. A facile and selective *O*-5-*exo*-dig cyclisation of propargyl ureas allowed the formation of the desired products in excellent to moderate yields under mild conditions (50-60 °C). Benign alcoholic medium accelerated the process reducing reaction time down to 4 hours. The one-pot protocol starting from propargylic amine and isocyanates has been proved effective. The exact structures of the obtained compounds were confirmed by X-ray diffraction analysis.

Experimental part

*General Procedure for the Preparation of Propargylic Ureas **1a-1t, 1x**:*[20]

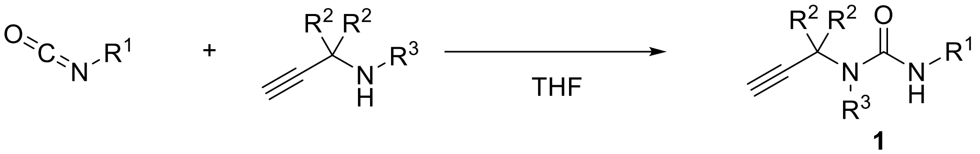

A dry 2-necked flask containing a magnetic stir bar was charged with the isocyanate (1 mmol), propargylic amine (1 mmol) and dry THF (10 mL). The resulting mixture was stirred at room temperature for 1 h. Solvent evaporation afforded propargylic urea, that was used without further purification.

*General Procedure for Sonogashira Coupling to Obtain **1u-w**:*[21]

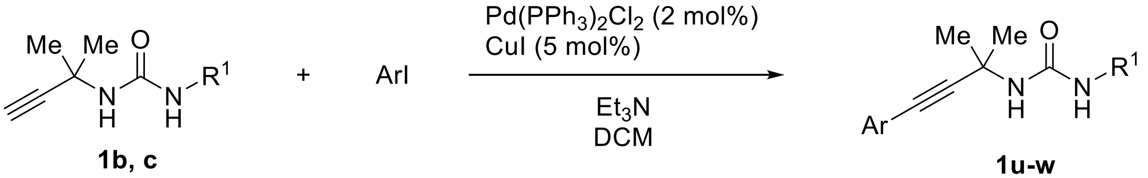

In a Schlenk tube under N_2 the starting urea (**1b** or **1c**) (1 mmol) and iodoarene (1.1 mmol) were dissolved in DCM (5 mL). Then $Pd(PPh_3)_2Cl_2$ (14 mg, 0.02 mmol) and Et_3N (5 mL) were added to the solution, followed by the addition of CuI (10 mg, 0.05 mmol). The reaction mixture was stirred at room temperature overnight. After filtration and evaporation of the solvent, the residue was poured in a NH_4Cl saturated solution (10 mL), and the organic phase was extracted with DCM (3 x 7 mL). Combined organic layers were dried over anhydrous Na_2SO_4, filtered, and concentrated under reduced pressure. Products were isolated by flash column chromatography on silica gel using a mixture of hexane-EtOAc as eluent.

Synthesis of N-Benzyl-2-methylbut-3-yn-2-amine:[22]

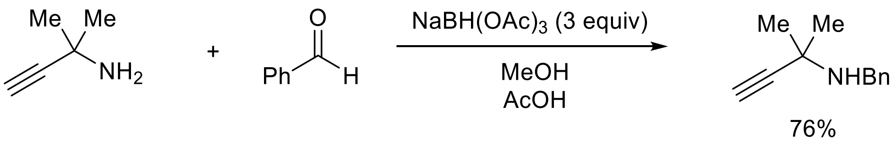

To a solution of 2-methylbut-3-yn-2-amine (210 µL, 2 mmol) in MeOH (5 mL) were added benzaldehyde (204 µL, 2 mmol) and acetic acid (171 µL, 3 mmol). After stirring for 10 minutes the mixture was cooled to 0 °C, and sodium triacetoxyborohydride (848 mg, 4 mmol) was added portionwise. The mixture was stirred for 3 hours at room temperature and then concentrated under reduced pressure. The residue was dissolved in 1 M solution of Na_2CO_3 in water (10 mL), and the extraction was performed with ethyl acetate (3 x 7 mL). Combined organic layers were dried over $MgSO_4$, filtered, and concentrated under reduced pressure. The residue was purified by silica gel column chromatography (hexane/EtOAc 10:1) to afford *N*-benzyl-2-methylbut-3-yn-2-amine in 76% yield (263 mg).

*Preparation of **1z**:*[23]

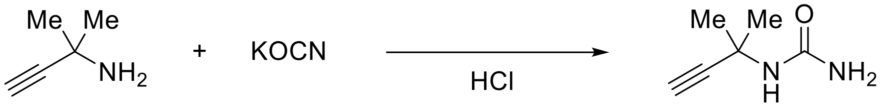

1z, 73%

To a solution of 2-methylbut-3-yn-2-amine (525 µL, 5 mmol) in aqueous HCl (1 N solution, 5 mL) was added KOCN (1.62 g, 20 mmol) at room temperature. After stirring overnight at 60 °C, the mixture was cooled at 0 °C to give white precipitate, that was filtrated with a glass filter and washed with 3 mL of water. Exsiccation under reduced afforded pure 1-(2-methylbut-3-yn-2-yl)urea in 73% yield (460 mg).

*Preparation of **1y, 1 sym**:*[24]

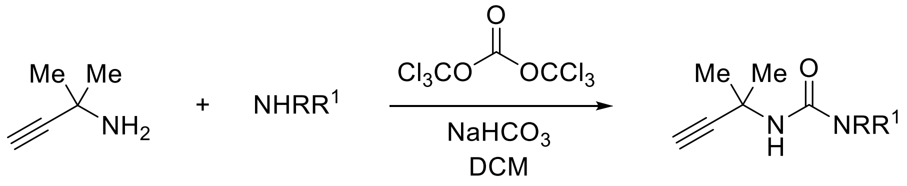

1y, **1sym**

To a stirring biphasic solution of triphosgene (54 mg, 0.18 mmol) in 25 mL of dry dichloromethane and 40 mL of saturated solution of $NaHCO_3$ was added dropwise a solution of 2-methylbut-3-yn-2-amine (53 µL, 0.5 mmol) in dry dichloromethane (25 mL). After 5 min, a solution of an amine (10 mL, 0.15 mmol) was added further into the reaction mixture and stirred for additional 3 h. The organic phase was then washed with water, dried over anhydrous Na_2SO_4, filtered, and evaporated. The residue was purified by column chromatography using a mixture of hexane and ethyl acetate as eluent.

General Procedure for the Ag-Catalysed Cyclisation of Alkyl Propargyl Ureas to Oxazoline-2-amines:

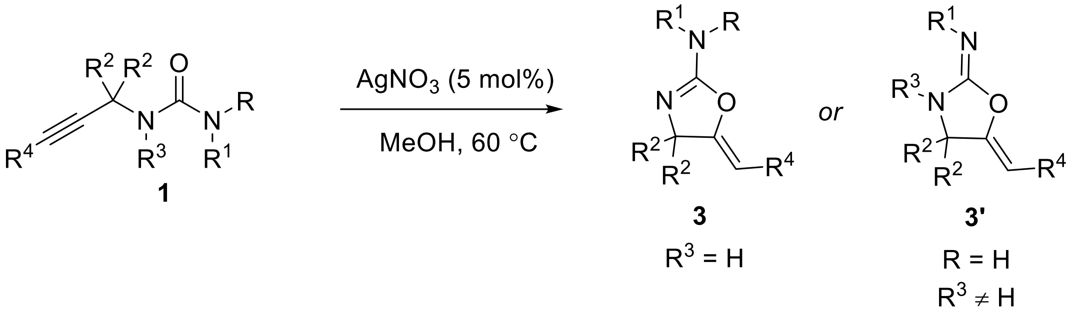

A 10 mL tube equipped with a magnetic stirrer was charged with propargylic urea (0.2 mmol) and MeOH (2 mL). Then $AgNO_3$ (1.7 mg, 0.01 mmol) was added. The reaction mixture was stirred at 60 °C and monitored by TLC. After completion of the reaction, the mixture was filtered through Celite® and concentrated in vacuo. If required, the residue was purified by silica gel column chromatography using a mixture of hexane and ethyl acetate as eluent.

Synthesis of ***4****:*

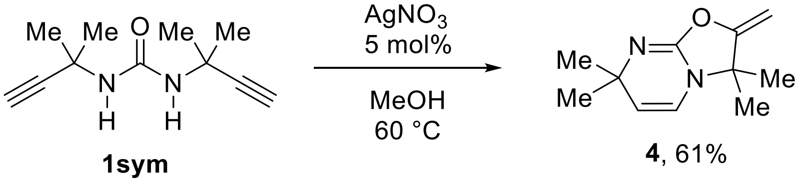

A 10 mL tube equipped with a magnetic stirrer was charged with urea **1sym** (0.2 mmol) and MeOH (2 mL). Then $AgNO_3$ (1.7 mg, 0.01 mmol) was added. The reaction mixture was stirred at 60 °C and monitored by TLC. After 24 h, the mixture was filtered through Celite® and concentrated in vacuo. The residue was purified by silica gel column chromatography using hexane/EtOAc (1:1) as eluent.

Table 1-2. Crystallographic Data and Structure Refinement.

Identification code	3h	3l	3u	4
Empirical formula	$C_{13}H_{16}N_2O$	$C_{12}H_{13}FN_2O$	$C_{16}H_{20}N_2O$	$C_{11}H_{16}N_2O$
Formula weight	216.28	220.24	256.34	192.26
Temperature/K	200.0	200.00	200.00	200.03
Crystal system	triclinic	monoclinic	orthorhombic	monoclinic
Space group	P-1	$P2_1/c$	Iba2	$P2_1/n$
a/Å	12.496(3)	6.0609(3)	9.465(6)	8.9016(2)
b/Å	12.555(3)	12.6615(10)	40.29(3)	11.2408(2)
c/Å	14.820(3)	15.1593(11)	8.097(6)	11.2554(2)
α/°	107.508(6)	90	90	90
β/°	93.963(6)	98.484(2)	90	105.0140(10)
γ/°	118.920(5)	90	90	90
Volume/Å^3	1875.6(7)	1150.60(14)	3088(4)	1087.78(4)

Z	6	4	8	4
ρ_{calc}g/cm^3	1.149	1.271	1.103	1.174
μ/mm^{-1}	0.074	0.094	0.069	0.077
F(000)	696.0	464.0	1104.0	416.0
Crystal size/mm^3	1 × 0.8 × 0.2	0.09 × 0.07 × 0.02	1.2 × 0.4 × 0.4	0.09 × 0.08 × 0.06
Radiation	MoKα (λ = 0.71073)	MoKα (λ = 0.71073)	MoKα (λ = 0.71073)	MoKα (λ = 0.71073)
2Θ range for data collection/°	3.814 to 52.826	4.21 to 52.724	4.044 to 52.698	5.212 to 54.228
Index ranges	-15 ≤ h ≤ 14, -15 ≤ k ≤ 15, -18 ≤ l ≤ 16	-6 ≤ h ≤ 7, -12 ≤ k ≤ 15, -14 ≤ l ≤ 18	-11 ≤ h ≤ 11, -49 ≤ k ≤ 50, -10 ≤ l ≤ 10	-11 ≤ h ≤ 11, -14 ≤ k ≤ 14, -13 ≤ l ≤ 14
Reflections collected	19894	6857	15004	11442
Independent reflections	7657 R_{int} = 0.1230 R_{sigma} = 0.1877	2321 R_{int} = 0.0487, R_{sigma} = 0.0534	3117 R_{int} = 0.0660, R_{sigma} = 0.0568	2397 R_{int} = 0.0226, R_{sigma} = 0.0181
Data/restraints/parameters	7657/0/439	2321/0/147	3117/1/175	2397/0/131
Goodness-of-fit on F^2	1.013	1.049	1.065	1.045
Final R indexes [I>=2σ (I)]	R_1 = 0.0918, wR_2 = 0.1526	R_1 = 0.0490, wR_2 = 0.0955	R_1 = 0.0667, wR_2 = 0.1552	R_1 = 0.0391, wR_2 = 0.1003
Final R indexes [all data]	R_1 = 0.2180, wR_2 = 0.1958	R_1 = 0.0772, wR_2 = 0.1061	R_1 = 0.1030, wR_2 = 0.1736	R_1 = 0.0426, wR_2 = 0.1034
Largest diff. peak/hole / e Å^{-3}	0.27/-0.27	0.15/-0.19	0.40/-0.20	0.23/-0.16

1-(2-Methylbut-3-yn-2-yl)-3-phenylurea (1a): Colourless solid (202 mg, quant. yield); m.p. 116.3–117.6 °C; **^{1}H NMR (400 MHz, CDCl$_3$)** δ 7.38–7.17 (m, 5H), 4.33 (bs, 2H), 2.28 (s, 1H), 1.54 (s, 6H). **^{13}C NMR (101 MHz, CDCl$_3$)** δ 157.7, 139.5, 128.6, 127.4, 127.1, 87.8, 69.9, 46.7, 44.1, 30.2 (2C). **HRMS (ESI)** *m/z* calcd for $C_{12}H_{14}N_2NaO$ [M+Na]$^+$: 225.1004, found: 225.1008.

1-Butyl-3-(2-methylbut-3-yn-2-yl)urea (1b): Colourless solid (182 mg, quant. yield); m.p. 79.5–81.3 °C; **^{1}H NMR (400 MHz, CDCl$_3$)** δ 4.88 (br s, 2H), 3.18 (t, *J* = 7.1 Hz, 2H), 2.38 (s, 1H), 1.56 (s, 6H), 1.50 – 1.42 (m, 2H), 1.37 – 1.29 (m, 2H), 0.90 (t, *J* = 7.3 Hz, 3H). **^{13}C NMR (101 MHz, CDCl$_3$)** δ 157.7, 87.8, 70.2, 46.8, 40.1, 32.3, 30.3 (2C), 20.2, 13.9. **HRMS (ESI)** *m/z* calcd for $C_{10}H_{19}N_2O$ [M+H]$^+$: 183.1493, found: 183.1493.

1-Ethyl-3-(2-methylbut-3-yn-2-yl)urea (1c): Colourless solid (154 mg, quant. yield); m.p. 84.9–85.8 °C; **^{1}H NMR (400 MHz, CDCl$_3$)** δ 4.55 (br s, 2H), 3.29 (q, *J* = 7.2 Hz, 2H), 1.61 (s, 6H), 1.17 (t, *J* = 7.2 Hz, 3H). **^{13}C NMR (101 MHz, CDCl$_3$)** δ 157.3, 87.3, 70.6, 46.8, 35.2, 30.1 (2C), 15.4. **HRMS (ESI)** *m/z* calcd for $C_8H_{15}N_2O$ [M+H]$^+$: 155.1184, found: 155.1183.

1-Ethyl-3-(2-methylbut-3-yn-2-yl-4-*d*)urea (1c-*d*): 1c-*d* was obtained by dissolving **1b** in methanol-*d$_4$*. **^{1}H NMR (400 MHz, CD$_3$OD)** δ 4.89 (s, 2H), 3.14 (q, *J* = 7.2 Hz, 2H), 1.56 (s, 6H), 1.10 (t, *J* = 7.2 Hz, 3H). **^{13}C NMR (101 MHz, CD$_3$OD)** δ 158.5, 87.2 (t, *J* = 7.0 Hz), 68.3 (t, *J* = 38.0 Hz), 46.2, 34.0, 29.1 (2C), 14.4.

1-Propyl-3-(2-methylbut-3-yn-2-yl)urea (1d): Colourless solid (168 mg, quant. yield); m.p. 80.3–81.6 °C; **^{1}H NMR (400 MHz, CDCl$_3$)** δ 5.48 (br s, 1 H), 5.18 (br s), 3.12 (t, *J* = 7.1 Hz, 2H), 2.34 (s, 1H), 1.55 (s, 6H), 1.47 (dt, *J* = 14.5, 7.3 Hz, 2H), 0.88 (t, *J* = 7.4 Hz, 3H). **^{13}C NMR (101 MHz, CDCl$_3$)** δ 157.9, 88.0, 69.8, 46.6, 42.0, 30.2 (2C), 23.5, 11.5. **HRMS (ESI)** *m/z* calcd for $C_9H_{17}N_2O$ [M+H]$^+$: 169.1341, found: 169.1340.

1-(*Tert*-butyl)-3-(2-methylbut-3-yn-2-yl)urea (1e): Colourless solid (182 mg, quant. yield); m.p. 204.1–205.7 °C; **^{1}H NMR (400 MHz, CDCl$_3$)** δ 4.57 (br s, 2H), 2.41 (s, 1H), 1.54 (s, 6H), 1.33 (s, 9H). **^{13}C NMR (101 MHz, CDCl$_3$)** δ 156.8, 87.6, 70.6, 50.7, 46.8, 30.3 (2C), 29.5 (3C). **HRMS (ESI)** *m/z* calcd for $C_{10}H_{19}N_2O$ [M+H]$^+$: 183.1493, found: 183.1494.

1-Cyclohexyl-3-(2-methylbut-3-yn-2-yl)urea (1f): Colourless solid (208 mg, quant. yield); m.p. 172.7–174.0 °C; **^{1}H NMR (400 MHz, CDCl$_3$)** δ 5.07 (br s, 1H), 4.60 (br s, 1H), 3.65 (tt, *J* = 10.1, 3.9 Hz, 1H), 2.44 (s, 1H), 1.94 (dt, *J* = 12.8, 4.0 Hz, 2H), 1.75 – 1.64 (m, 2H), 1.62 – 1.55 (m, 7H), 1.46 – 1.31 (m, 2H), 1.28 – 1.11 (m, 3H). **^{13}C NMR (101 MHz, CDCl$_3$)** δ 156.7, 87.5, 70.6, 48.8, 46.7, 33.7 (2C), 30.2 (2C), 25.7, 24.8 (2C). **HRMS (ESI)** *m/z* calcd for $C_{12}H_{21}N_2O$ [M+H]$^+$: 209.1654, found: 209.1655.

1-Allyl-3-(2-methylbut-3-yn-2-yl)urea (1g): Light yellow solid (166 mg, quant. yield); m.p. 83.8–85.4 °C; **^{1}H NMR (400 MHz, CDCl$_3$)** δ 5.82 (ddd, *J* = 22.4, 10.4, 5.3 Hz, 1H), 5.58 (t, *J* = 5.2 Hz, 1H), 5.35 (s, 1H), 5.16 (dd, *J* = 17.2, 1.5 Hz, 1H), 5.05 (dd, *J* = 10.3, 1.4 Hz, 1H), 3.79 (s, 2H), 2.33 (s, 1H), 1.56 (s, 6H). **^{13}C NMR (101 MHz, CDCl$_3$)** δ 157.7, 135.6, 115.4, 87.9, 69.8, 46.7, 42.6, 30.2 (2C). **HRMS (ESI)** *m/z* calcd for $C_9H_{15}N_2O$ [M+H]$^+$: 167.1184, found: 167.1182.

1-Benzyl-3-(2-methylbut-3-yn-2-yl)urea (1h): Colourless solid (216 mg, quant. yield); m.p. 112.7–113.8 °C; **^{1}H NMR (400 MHz, CDCl$_3$)** δ 7.30 – 7.20 (m, 5H), 6.00 (br s, 1H), 5.57 (br s, 1 H), 4.29 (s, 2H), 2.22 (s, 1H), 1.52 (s, 6H). **^{13}C NMR (101 MHz, CDCl$_3$)** δ 157.8, 139.6, 128.5 (2C), 127.3 (2C), 127.0, 88.0, 69.5, 46.6, 43.9, 30.1 (2C). **HRMS (ESI)** *m/z* calcd for $C_{13}H_{18}N_2O$ [M+H]$^+$: 217.1341, found: 217.1341.

Ethyl 2-(3-(2-methylbut-3-yn-2-yl)ureido)acetate (1i): Colourless solid (212 mg, quant. yield); m.p. 77.6–79.2 °C; **^{1}H NMR (600 MHz, DMSO)** δ 6.37 (s, 1H), 6.01 (t, *J* = 5.9 Hz, 1H), 4.04 (q, *J* = 7.1 Hz, 2H), 3.72 (d, *J* = 6.0 Hz, 2H), 1.42 (s, 6H), 1.15 (t, *J* = 7.1 Hz, 3H). **^{13}C NMR (151 MHz, DMSO)** δ 171.6, 157.1, 89.5, 71.0, 60.7, 46.4, 41.7, 30.1, 14.6. **HRMS (ESI)** *m/z* calcd for $C_{10}H_{16}N_2NaO_3$ [M+Na]$^+$: 235.1059, found: 235.1058.

1-(2-Methylbut-3-yn-2-yl)-3-(*p*-tolyl)urea (1j): Colourless solid (216 mg, quant. yield); m.p. 144.4−146.1 °C. **^{1}H NMR (400 MHz, DMSO)** δ 8.19 (br s, 1H), 7.25 (d, *J* = 8.4 Hz, 2H), 7.03 (d, *J* = 8.3 Hz, 2H), 6.34 (br s, 1H), 3.11 (s, 1H), 2.22 (s, 3H), 1.54 (s, 6H). **^{13}C NMR (101 MHz, DMSO)** δ 153.9, 137.7, 129.8, 129.0 (2C), 117.6 (2C), 88.7, 70.7, 46.0, 29.4 (2C), 20.3. **HRMS (ESI)** *m/z* calcd for $C_{13}H_{16}N_2NaO$ [M+Na]$^+$: 239.1160, found: 239.1158.

1-(2-Methoxyphenyl)-3-(2-methylbut-3-yn-2-yl)urea (1k): Colourless solid (232 mg, quant. yield); m.p. 133.0–135.2 °C; **^{1}H NMR (400 MHz, CDCl$_3$)** δ 8.12 (dd, *J* = 7.5, 2.2 Hz, 1H), 7.36 (br s, 1H), 6.97 (pt, *J* = 7.9, 4.0 Hz, 2H), 6.88 (dd, *J* = 7.3, 2.1 Hz, 1H), 4.91 (br s, 1H), 3.87 (s, 3H), 2.45 (s, 1H), 1.68 (s, 6H). **^{13}C NMR (101 MHz, CDCl$_3$)** δ 154.2, 148.2, 128.7, 122.5, 121.3, 119.7, 110.3, 87.2, 77.2, 70.2, 55.7, 47.3, 30.0 (2C). **HRMS (ESI)** *m/z* calcd for $C_{13}H_{17}N_2O_2$ [M+H]$^+$: 233.1290, found: 233.1291.

1-(4-Fluorophenyl)-3-(2-methylbut-3-yn-2-yl)urea (1l): Colourless solid (220 mg, quant. yield); m.p. 174.1–174.8 °C; **^{1}H NMR (400 MHz, DMSO)** δ 8.33 (br s, 1H), 7.41–7.30 (m, 2H), 7.09–7.01 (m, 2H), 6.38 (bs, 1H), 3.11 (s, 1H), 1.53 (s, 6H). **^{13}C NMR (101 MHz, DMSO)** δ 156.9 (d, *J*=237.2 Hz), 153.9, 136.6 (d, *J*=2.3 Hz), 119.1 (d, *J*=7.5 Hz), 115.1 (d, *J*=22.0 Hz), 88.6, 70.8, 46.0, 29.4. ^{19}F NMR (376 MHz, DMSO) δ -122.40. **HRMS (ESI)** *m/z* calcd for $C_{12}H_{13}FN_2NaO$ [M+Na]$^+$: 243.0910, found: 243.0912.

1-(2,4-Difluorophenyl)-3-(2-methylbut-3-yn-2-yl)urea (**1m**): Colourless solid (238 mg, quant. yield); m.p. 152.8–155.6 °C; **^{1}H NMR (400 MHz, CDCl$_3$)** δ 8.02 – 7.93 (m, 1H), 7.44 (br s, 1H), 6.80 (ddt, *J* = 11.0, 8.2, 2.9 Hz, 2H), 5.47 (br s, 1 H), 2.44 (s, 1 H), 1.63 (s, 6H). **^{13}C NMR (101 MHz, CDCl$_3$)** δ 159.2, 159.1, 156.8, 156.7, 154.7, 154.2, 154.1, 151.7, 151.6, 123.6, 123.4, 123.3, 123.3, 123.2, 123.0, 123.0, 122.9, 122.9, 111.1, 111.1, 110.9, 110.9, 103.6, 103.4, 103.4, 103.1, 87.0, 70.4, 47.1, 29.9 (2C). ^{19}F NMR (565 MHz, CDCl$_3$) δ -116.99, -126.01. **HRMS (ESI)** *m/z* calcd for $C_{12}H_{13}F_2N_2O$ [M+H]$^+$: 239.0996, found: 239.0993.

1-(2-Methylbut-3-yn-2-yl)-3-(4-nitrophenyl)urea (1n): Yellow solid (247 mg, quant. yield); m.p. 200.1–202.0 °C; **^{1}H NMR (600 MHz, DMSO)** δ 9.01 (s, 1H), 8.14 – 8.00 (m, 2H), 7.59 – 7.49 (m, 2H), 6.65 (s, 1H), 3.07 (s, 1H), 1.51 (s, 6H). **^{13}C NMR (151 MHz, DMSO)** δ 153.6, 147.4, 141.1, 125.6 (2C), 117.3 (2C), 88.6, 71.5, 46.8, 29.6 (2C). **HRMS (ESI)** *m/z* calcd for $C_{12}H_{14}N_3O_3$ [M+H]$^+$: 248.2620, found: 248.2617.

1-(2-Methylbut-3-yn-2-yl)-3-(naphthalen-1-yl)urea (**1o**): Colourless solid (252 mg, quant. yield); m.p. 181.0–182.5 °C; **^{1}H NMR (400 MHz, CDCl$_3$)** δ 8.07 – 7.98 (m, 1H), 7.88 – 7.79 (m, 1H), 7.67 (td, *J* = 7.6, 1.1 Hz, 2H), 7.52 – 7.37 (m, 3H), 7.31 (br s, 1H), 5.37 (br s, 1H), 2.38 (s, 1H), 1.61 (s, 6H). **^{13}C NMR (101 MHz, CDCl$_3$)** δ 155.8, 134.3, 133.4, 128.5, 126.3, 126.1, 125.8, 125.7, 121.8, 121.7, 87.6, 69.8, 47.1, 29.9 (2C). **HRMS (ESI)** *m/z* calcd for $C_{16}H_{17}N_2O$ [M+H]$^+$: 253.1341, found: 253.1342.

1-Butyl-3-(3-ethylpent-1-yn-3-yl)urea (1p): Viscous colorless oil (210 mg, quant. yield); **^{1}H NMR (400 MHz, CDCl$_3$)** δ 5.35 (bs, 1H), 4.73 (bs, 1H), 3.15 (dd, *J* = 12.7, 6.7 Hz, 2H), 2.40 (s, 1H), 1.89 (dq, *J* = 14.7, 7.4 Hz, 2H), 1.76 (dq, *J* = 14.5, 7.4 Hz, 2H), 1.50 – 1.39 (m, 2H), 1.37 – 1.26 (m, 2H), 0.95 (t, *J* = 7.4 Hz, 6H), 0.89 (t, *J* = 7.3 Hz, 3H). **^{13}C NMR (101 MHz, CDCl$_3$)** δ 157.7, 86.0, 72.4, 55.4, 40.0, 32.3, 31.8 (2C), 20.2, 13.9, 8.6 (2C). **HRMS (ESI)** *m/z* calcd for $C_{12}H_{23}N_2O$ [M+H]$^+$: 211.1810, found: 211.1811.

1-Butyl-3-(1-ethynylcyclohexyl)urea (1q): Colourless solid (222 mg; quant. yield); m.p. 71.1–73.2 °C**; ^{1}H NMR (400 MHz, CDCl$_3$)** δ 5.42 (bt, *J* = 5.0 Hz, 1H), 4.91 (bs, 1H), 3.17 (td, *J* = 7.0, 5.7 Hz, 2H), 2.45 (s, 1H), 2.12 – 2.01 (m, 2H), 1.64 – 1.50 (m, 7H), 1.49 – 1.40 (m, 2H), 1.37 – 1.28 (m, 2H), 1.27 – 1.16 (m, 1H), 0.88 (t, *J* = 7.3 Hz, 3H). **^{13}C NMR (101 MHz, CDCl$_3$)** δ 157.7, 86.4, 72.6, 50.8, 40.0, 38.2 (2C), 32.4, 25.3, 22.4 (2C), 20.2, 13.9. **HRMS (ESI)** *m/z* calcd for $C_{13}H_{22}N_2NaO$ [M+Na]$^+$: 245.1630, found: 245.1631.

1-Butyl-3-(prop-2-yn-1-yl)urea (1r): Colourless solid (154 mg, quant. yield); m.p. 86.1–87.8 °C; **^{1}H NMR (400 MHz, CDCl$_3$)** δ 4.93 (br s, 2H), 4.03 – 3.96 (m, 2H), 3.20 (t, *J* = 7.1 Hz, 2H), 2.27 – 2.19 (m, 1H), 1.50 (p, *J* = 7.1 Hz, 2H), 1.37 (dq, *J* = 14.3, 7.2 Hz, 2H), 0.94 (t, *J* = 7.3 Hz, 3H). **HRMS (ESI)** *m/z* calcd for $C_8H_{15}N_2O$ [M+H]$^+$: 155.1184, found: 155.1184.

1-(*Tert*-butyl)-3-(1-phenylprop-2-yn-1-yl)urea (1s): Yellow solid (218 mg; 95% yield); **^{1}H NMR (400 MHz, CDCl$_3$)** δ 7.51 (dd, *J* = 7.3, 1.8 Hz, 2H), 7.38 – 7.25 (m, 3H), 5.75 (d, *J* = 2.4 Hz, 1H), 4.82 (br s, 2H), 2.42 (d, *J* = 2.4 Hz, 1H), 1.32 (s, 9H). **^{13}C NMR (101 MHz, CDCl$_3$)** δ 156.4, 139.5, 128.6 (2C), 127.8 (2C), 126.9, 83.1, 72.6, 50.6, 45.5, 29.5 (3C). **HRMS (ESI)** *m/z* calcd for $C_{14}H_{18}N_2NaO$ [M+Na]$^+$: 253.1317, found: 253.1315.

1-Phenyl-3-(1-phenylprop-2-yn-1-yl)urea (1t): Colourless solid (245 mg; 98% yield); m.p. 177.7–178.7 °C; **^{1}H NMR (400 MHz, CD$_3$OD)** δ 7.62 – 7.50 (m, 2H), 7.44 – 7.20 (m, 7H), 7.00 (tt, *J* = 7.3, 1.2 Hz, 1H), 5.81 (d, *J* = 2.5 Hz, 1H), 4.89 (s, 2H), 2.95 (d, *J* = 2.5 Hz, 1H), 2.16 (s, 1H). **^{13}C NMR (101 MHz, CD$_3$OD)** δ 155.5, 139.4, 139.2, 128.5 (2C), 128.3 (2C), 127.6, 126.5 (2C), 122.3, 118.8 (2C), 82.1, 72.8, 44.9. **HRMS (ESI)** *m/z* calcd for $C_{16}H_{15}N_2O$ [M+H]$^+$: 251.1184, found: 251.1184.

1-Butyl-3-(2-methyl-4-phenylbut-3-yn-2-yl)urea (1u): Colourless oil (255 mg, 99% yield); **^{1}H NMR (400 MHz, CDCl$_3$)** δ 7.43 – 7.35 (m, 2H), 7.32 – 7.24 (m, 3H), 5.47 (br s, 1H), 4.99 (br s, 1H), 3.21 (t, *J* = 7.0 Hz, 2H), 1.63 (s, 6H), 1.50 – 1.40 (m, 2H), 1.36 – 1.26 (m, 2H), 0.84 (t, *J* = 7.3 Hz, 3H). **^{13}C NMR (101 MHz, CDCl$_3$)** δ 157.9, 131.7 (2C), 128.5, 128.4 (2C), 122.5, 92.6, 82.7, 47.5, 40.1, 32.3, 30.4 (2C), 20.2, 13.8. **HRMS (ESI)** *m/z* calcd for $C_{16}H_{22}N_2NaO$ [M+Na]$^+$: 281.1630, found: 281.1631.

Methyl 2-(3-(3-butylureido)-3-methylbut-1-yn-1-yl)benzoate (**1v**): Colourless oil (288 mg, 91% yield); **^{1}H NMR (400 MHz, CDCl$_3$)** δ 7.87 (dd, *J* = 7.9, 1.1 Hz, 1H), 7.45 (dd, *J* = 7.7, 1.2 Hz, 1H), 7.37 (td, *J* = 7.6, 1.4 Hz, 1H), 7.28 (td, *J* = 7.6, 1.4 Hz, 1H), 6.09 (br s, 1H), 5.41 (s, 1H), 3.83 (s, 3H), 3.19 (dd, *J* = 12.8, 6.9 Hz, 2H), 1.60 (s, 6H), 1.47 – 1.38 (m, 2H), 1.29 – 1.19 (m, 2H), 0.78 (t, *J* = 7.3 Hz, 3H). **^{13}C NMR (101 MHz, CDCl$_3$)** δ 166.3, 158.1, 134.1, 131.7, 131.4, 130.2, 127.9, 123.2, 97.6, 81.0, 51.9, 47.2, 39.9, 32.3, 30.0 (2C), 20.0, 13.7. **HRMS (ESI)** *m/z* calcd for $C_{18}H_{24}N_2NaO_3$ [M+Na]$^+$: 339.1685, found: 339.1682.

1-Ethyl-3-(4-(3-methoxyphenyl)-2-methylbut-3-yn-2-yl)urea (1w): Colourless solid (255 mg, 98% yield); m.p. 78.8–79.8 °C; **^{1}H NMR (400 MHz, CDCl$_3$)** δ 7.15 (t, *J* = 8.0 Hz, 1H), 6.98 (dt, *J* = 7.6, 1.2 Hz, 1H), 6.93-6.90 (m, 1H), 6.80 (ddd, *J* = 8.3, 2.7, 1.0 Hz, 1H), 5.87 (br s, 1H), 5.77 (br s, 1H), 3.74 (s, 3H), 3.18 (q, *J* = 7.6 Hz, 2H), 1.63 (s, 6H), 1.07 (t, *J* = 7.2 Hz, 3H). **^{13}C NMR (101 MHz, CDCl$_3$)** δ 159.2, 158.1, 129.2, 124.2, 124.1, 116.4, 114.7, 93.5, 81.1, 77.4, 55.2, 47.2, 34.7, 30.3 (2C), 15.6. **HRMS (ESI)** *m/z* calcd for $C_{15}H_{25}N_2O_2$ [M+H]$^+$: 289.1916, found: 289.1915.

1-Benzyl-3-ethyl-1-(2-methylbut-3-yn-2-yl)urea (1x): Colourless oil (225 mg, 92%); **^{1}H NMR (400 MHz, CDCl$_3$)** δ 7.37 – 7.27 (m, 4H), 7.27 – 7.19 (m, 1H), 4.85 (br t, *J* = 5.2 Hz, 1H), 4.68 (s, 2H), 3.19 (qd, *J* = 7.2, 5.3 Hz, 2H), 1.75 (s, 6H), 1.02 (t, *J* = 7.2 Hz, 3H). **^{13}C NMR (101 MHz, CDCl$_3$)** δ 158.7, 139.9, 128.7 (2C), 127.0, 126.2 (2C), 88.3, 72.0, 54.0, 49.6, 35.5, 29.1 (2C), 15.3. **HRMS (ESI)** *m/z* calcd for $C_{15}H_{21}N_2O$ [M+H]$^+$: 245.1654, found: 245.1655.

***N*-(2-Methylbut-3-yn-2-yl)pyrrolidine-1-carboxamide (1y):** Colourless solid (49 mg, 54% yield); m.p. 127.3–128.5 °C; **^{1}H NMR (400 MHz, CDCl$_3$)** δ 4.32 (br s, 1H), 3.37 – 3.28 (m, 4H), 2.33 (s, 1H), 1.95 – 1.85 (m, 4H), 1.66 (s, 6H). **^{13}C NMR (101 MHz, CDCl$_3$)** δ 155.5, 88.6, 68.4, 47.4, 45.5 (2C), 29.9 (2C), 25.6 (2C). **HRMS (ESI)** *m/z* calcd for $C_{10}H_{16}N_2NaO$ [M+Na]$^+$: 203.1160, found: 203.1162.

1-(2-Methylbut-3-yn-2-yl)urea (1z): Colourless solid (460 mg, 73% yield); m.p. 151.4–152.9 °C; **^{1}H NMR (600 MHz, DMSO)** δ 6.13 (br s, 1H), 5.32 (br s, 2H), 2.97 (s, 1H), 1.41 (s, 6H). **^{13}C NMR (151 MHz, DMSO)** δ 158.1, 89.7, 70.8, 46.2, 30.1 (2C). **HRMS (ESI)** *m/z* calcd for $C_6H_{10}N_2KO$ [M+K]$^+$: 165.0430, found: 165.0429.

1,3-Bis(2-methylbut-3-yn-2-yl)urea (1sym): Colourless solid (69 mg, 72% yield); m.p. 177.3–176.6 °C; **^{1}H NMR (400 MHz, $CDCl_3$)** δ 5.34 (br s, 2H), 2.35 (s, 2H), 1.57 (s, 12H). **^{13}C NMR (101 MHz, $CDCl_3$)** δ 156.5, 87.8 (2C), 69.9 (2C), 47.0 (2C), 30.1 (4C). **HRMS (ESI)** *m/z* calcd for $C_{11}H_{16}N_2NaO$ $[M+Na]^+$: 215.1160, found: 215.1162.

4,4-Dimethyl-5-methylene-*N*-phenyl-4,5-dihydrooxazol-2-amine (3a): Colourless solid (40 mg, quant. yield); m.p. 114.8–115.8 °C; **^{1}H NMR (400 MHz, $CDCl_3$)** δ 7.42 – 7.20 (m, 5H), 7.07 – 7.02 (m, 1H), 4.64 (d, *J* = 3.1 Hz, 1H), 4.21 (d, *J* = 3.0 Hz, 1H), 1.47 (s, 6H). **^{13}C NMR (101 MHz, $CDCl_3$)** δ 166.1, 152.8, 140.9, 129.0 (2C), 122.7, 120.1 (2C), 82.1, 64.9, 30.3 (2C). **HRMS (ESI)** *m/z* calcd for $C_{12}H_{14}N_2NaO$ $[M+Na]^+$: 225.1004, found: 225.1005.

***N*-Butyl-4,4-dimethyl-5-methylene-4,5-dihydrooxazol-2-amine (3b):** Light yellow oil (36 mg, quant. yield); **^{1}H NMR (400 MHz, $CDCl_3$)** δ 4.47 (d, *J* = 2.8 Hz, 1H), 4.06 (d, *J* = 2.8 Hz, 1H), 3.60 (bs, 1H), 3.20 (t, *J* = 7.1 Hz, 2H), 1.52 (dt, *J* = 14.9, 7.4 Hz, 2H), 1.38 – 1.30 (s, 1.32, 6H; m, 2H), 0.91 (t, *J* = 7.3 Hz, 3H). **^{13}C NMR (101 MHz, $CDCl_3$)** δ 168.2, 156.5, 80.9, 67.0, 42.5, 31.9, 30.6 (2C), 20.0, 13.9. **HRMS (ESI)** *m/z* calcd for $C_{10}H_{19}N_2O$ $[M+H]^+$: 183.1493, found: 183.1492.

***N*-Ethyl-4,4-dimethyl-5-(methylene-d)-4,5-dihydrooxazol-2-amine (3c):** ***3c** was obtained performing the reaction in methanol-d_4 in an NMR tube*. Volatile colourless oil (94% NMR yield). **^{1}H NMR (400 MHz, CD_3OD)** δ 4.94 (br s, 2H), 3.21 (q, *J* = 7.2 Hz, 2H), 1.35 (s, 6H), 1.19 (t, *J* = 7.2 Hz, 3H). **^{13}C NMR (101 MHz, CD_3OD)** δ 167.2, 167.1, 157.8, 80.25 (t, *J* = 24.4), 65.8, 36.6, 29.6 (2C), 13.6.

***N*-Propyl-4,4-dimethyl-5-methylene-4,5-dihydrooxazol-2-amine (3d):** Colourless oil (33 mg, quant. yield). **^{1}H NMR (400 MHz, $CDCl_3$)** δ 4.47 (d, *J* = 2.8 Hz, 1H), 4.07 (d, *J* = 2.8 Hz, 1H), 3.93 (br s, 1H), 3.16 (t, *J* = 7.2 Hz, 2H), 1.55 (dt, *J* = 14.6, 7.3 Hz, 2H), 1.32 (s, 6H), 0.92 (t, *J* = 7.4 Hz, 3H). **^{13}C NMR (101 MHz, $CDCl_3$)** δ 168.1, 156.5, 80.9, 67.0, 44.5, 30.6 (2C), 23.1, 11.3. **HRMS (ESI)** *m/z* calcd for $C_9H_{17}N_2O$ $[M+H]^+$: 169.1341, found: 169.1341.

***N-Tert*-butyl-4,4-dimethyl-5-methylene-4,5-dihydrooxazol-2-amine (3e):** Light yellow solid (34.5 mg, 95% yield); m.p. 177.6–179.3 °C; **^{1}H NMR (400 MHz, $CDCl_3$)** δ 4.42 (d, *J* = 2.7 Hz, 1H), 4.05 (br s, 1H), 4.01 (d, *J* = 2.7 Hz, 1H), 1.31 (s, 6H), 1.29 (s, 9H). **^{13}C NMR (101 MHz, $CDCl_3$)** δ 167.7, 154.4, 80.2, 67.5, 51.0, 30.5 (2C), 29.1 (3C). **HRMS (ESI)** *m/z* calcd for $C_{10}H_{19}N_2O$ $[M+H]^+$: 183.1493, found: 183.1494.

***N*-Cyclohexyl-4,4-dimethyl-5-methylene-4,5-dihydrooxazol-2-amine (3f):** Colourless solid (41 mg, quant. yield); m.p. 99.8–101.5 °C; **^{1}H NMR (400 MHz, $CDCl_3$)** δ 4.47 (d, *J* = 2.8 Hz, 1H), 4.06 (d, *J* = 2.8 Hz, 1H), 3.97 (br s, 1H), 3.45 (tt, *J* = 10.4, 3.9 Hz, 1H), 2.07 – 1.96 (m, 2H), 1.76 – 1.63 (m, 2H), 1.63 – 1.53 (m, 1H), 1.41-1.30 (m, 8H), 1.23 – 1.07 (m, 3H). **^{13}C NMR (101 MHz, $CDCl_3$)** δ 168.1, 155.3, 80.5, 67.1, 50.8, 33.4 (2C), 30.5 (2C), 25.6, 24.7 (2C). **HRMS (ESI)** *m/z* calcd for $C_{12}H_{21}N_2O$ $[M+H]^+$: 209.1654, found: 209.1649.

***N*-Allyl-4,4-dimethyl-5-methylene-4,5-dihydrooxazol-2-amine (3g):** Light yellow oil (22 mg, 67% yield); **^{1}H NMR (400 MHz, $CDCl_3$)** δ 5.88 (ddt, *J* = 17.2, 10.4, 5.5 Hz, 1H), 5.20 (ddd, *J* = 17.2, 3.1, 1.7 Hz, 1H), 5.12 (dq, *J* = 10.3, 1.4 Hz, 1H), 4.48 (d, *J* = 2.8 Hz, 1H), 4.07 (d, *J* = 2.8 Hz, 1H), 3.96 (br s, 1H), 3.82 (dt, *J* = 5.5, 1.6 Hz, 2H), 1.32 (s, 6H). **^{13}C NMR (101 MHz, $CDCl_3$)** δ 168.2, 156.3, 134.3, 116.3, 81.1, 67.1, 45.0, 30.5 (2C). **HRMS (ESI)** *m/z* calcd for $C_9H_{15}N_2O$ $[M+H]^+$: 167.1184, found: 167.1183.

***N*-Benzyl-4,4-dimethyl-5-methylene-4,5-dihydrooxazol-2-amine (3h):** Colourless solid (40 mg, 94% yield); m.p. 93.3–94.6 °C; **^{1}H NMR (400 MHz, CDCl$_3$)** δ 7.34 – 7.28 (m, 4H), 7.27 – 7.22 (m, 1H), 4.97 (br s, 1H), 4.48 (d, *J* = 2.8 Hz, 1H), 4.37 (s, 2H), 4.08 (d, *J* = 2.8 Hz, 1H), 1.32 (s, 6H). **^{13}C NMR (101 MHz, CDCl$_3$)** δ 168.1, 156.6, 138.5, 128.6 (2C), 127.6 (2C), 127.5, 81.0, 66.9, 46.6, 30.4 (2C). **HRMS (ESI)** *m/z* calcd for $C_{13}H_{18}N_2O$ [M+H]$^+$: 217.1341, found: 217.1341.

Methyl (4,4-dimethyl-5-methylene-4,5-dihydrooxazol-2-yl)glycinate (3i): Colourless solid (25 mg, 62% yield); m.p. 82–84.4 °C. **^{1}H NMR (400 MHz, CDCl$_3$)** δ 4.63 (br s, 1H), 4.50 (d, *J* = 2.9 Hz, 1H), 4.08 (d, *J* = 2.9 Hz, 1H), 4.00 (s, 2H), 3.74 (s, 3H), 1.31 (s, 6H). **^{13}C NMR (101 MHz, CDCl$_3$)** δ 170.7, 168.0, 156.0, 81.4, 66.9, 52.4, 44.1, 30.3 (2C). **HRMS (ESI)** *m/z* calcd for $C_9H_{15}N_2O_3$ [M+H]$^+$: 199.1083, found: 199.1082.

4,4-Dimethyl-5-methylene-*N*-(*p*-tolyl)-4,5-dihydrooxazol-2-amine (3j): Colourless solid (43 mg, quant. yield); m.p. 147.2–148.5 °C; **^{1}H NMR (400 MHz, CDCl$_3$)** δ 7.21 (d, *J* = 8.2 Hz, 2H), 7.11 (d, *J* = 8.2 Hz, 2H), 7.02 (br s, 1H), 4.62 (d, *J* = 3.0 Hz, 1H), 4.20 (d, *J* = 3.0 Hz, 1H), 2.33 (s, 3H), 1.46 (s, 6H). **^{13}C NMR (101 MHz, CDCl$_3$)** δ 166.3, 153.0, 138.2, 132.2, 129.5 (2C), 120.2 (2C), 82.0, 64.9, 30.3 (2C), 20.8. **HRMS (ESI)** *m/z* calcd for $C_{13}H_{16}N_2NaO$ [M+Na]$^+$: 239.1160, found: 239.1160.

***N*-(2-Methoxyphenyl)-4,4-dimethyl-5-methylene-4,5-dihydrooxazol-2-amine (3k)**: Colourless oil (46 mg, quant. yield); **^{1}H NMR (400 MHz, CDCl$_3$)** δ 8.19-8.17 (m, 1H), 7.03 – 6.94 (m, 2H), 6.91 – 6.84 (m, 1H), 6.12 (br s, 1H), 4.61 (d, *J* = 2.9 Hz, 1H), 4.19 (d, *J* = 2.9 Hz, 1H), 3.89 (s, 3H), 1.46 (s, 6H). **^{13}C NMR (101 MHz, CDCl$_3$)** δ 166.9, 152.1, 147.4, 128.3, 122.0, 121.2, 117.8, 109.9, 81.2, 68.2, 55.7, 30.4 (2C). **HRMS (ESI)** *m/z* calcd for $C_{13}H_{17}N_2O_2$ [M+H]$^+$: 233.1290, found: 233.1288.

***N*-(4-Fluorophenyl)-4,4-dimethyl-5-methylene-4,5-dihydrooxazol-2-amine (3l):** Colourless solid (43 mg, 98% yield); m.p. 158.5–159.7 °C; **^{1}H NMR (400 MHz, CDCl$_3$)** δ 7.28 – 7.10 (m, 3H), 7.05 – 6.91 (m, 2H), 4.62 (d, *J* = 3.2 Hz, 1H), 4.21 (d, *J* = 3.1 Hz, 1H), 1.45 (s, 6H). **^{13}C NMR (101 MHz, CDCl$_3$)** δ 165.6, 159.9, 157.5, 152.9, 137.7, 122.1, 122.0, 115.6, 115.4, 82.5, 63.8, 30.2 (2C). **^{19}F NMR (565 MHz, CDCl$_3$)** δ -120.8. HRMS (ESI) *m/z* calcd for $C_{12}H_{13}FN_2NaO$ [M+Na]$^+$: 243.0910, found: 243.0911.

***N*-(2,4-Difluorophenyl)-4,4-dimethyl-5-methylene-4,5-dihydrooxazol-2-amine (3m):** Colourless solid (46 mg, 96% yield); m.p. 131.1–132.6 °C; **^{1}H NMR (400 MHz, CDCl$_3$)** δ 7.46 (td, *J* = 9.3, 5.8 Hz, 1H), 6.89 – 6.79 (m, 2H), 6.53 (br s, 1H), 4.62 (d, *J* = 3.3 Hz, 1H), 4.21 (d, *J* = 3.3 Hz, 1H), 1.44 (s, 6H). **^{13}C NMR (101 MHz, CDCl$_3$)** δ 164.8, 159.3, 159.2, 156.8, 156.7, 155.5, 155.4, 153.0, 152.9, 152.8, 128.1, 124.2, 124.1, 111.0, 110.9, 110.8, 110.7, 104.1, 103.8, 103.6, 83.1, 61.7, 29.7 (2C).**^{19}F NMR (565 MHz, CDCl$_3$)** δ -122.61, -127.74. **HRMS (ESI)** *m/z* calcd for $C_{12}H_{13}F_2N_2O$ [M+H]$^+$: 239.0996, found: 239.0994.

4,4-Dimethyl-5-methylene-*N*-(4-nitrophenyl)-4,5-dihydrooxazol-2-amine (3n): Light yellow solid (23 mg, 46%); m.p. 147.8–148.4 °C; **^{1}H NMR (400 MHz, CDCl$_3$)** δ 8.22 – 8.12 (m, 2H), 7.40 – 7.32 (m, 2H), 6.92 – 6.66 (m, 1H), 4.70 (d, *J* = 3.4 Hz, 1H), 4.30 (d, *J* = 3.5 Hz, 1H), 1.48 (s, 6H). **^{13}C NMR (101 MHz, CDCl$_3$)** δ 164.6, 152.4, 149.1, 142.6, 125.1 (2C), 120.8 (2C), 83.9, 63.0, 30.0 (2C). **HRMS (ESI)** *m/z* calcd for $C_{12}H_{14}N_3O_3$ [M+H]$^+$: 248.2620, found: 248.2619.

4,4-Dimethyl-5-methylene-*N*-(naphthalen-1-yl)-4,5-dihydrooxazol-2-amine (3o): Colourless solid (45 mg, 90% yield); m.p. 139.5–135.2 °C; **^{1}H NMR (400 MHz, CD$_3$OD)** δ 8.06 – 7.95 (m, 1H), 7.88 – 7.82 (m, 1H), 7.62 (d, *J* = 8.2 Hz, 1H), 7.52 – 7.42 (m, 2H), 7.37 (t, *J* = 7.8 Hz, 1H), 7.19-7.17 (m, 1H), 5.00 (br s, 1H), 4.87 (d, *J* = 3.2 Hz, 1H), 4.67 (d, *J* = 3.2 Hz, 1H), 4.33 (d, *J* = 3.2 Hz, 1H), 1.35 (s, 6H). **^{13}C NMR (101 MHz, CD_3OD)** δ 164.5, 155.1, 140.5, 134.7, 128.6, 127.9, 125.9, 125.8, 125.4, 124.1, 122.8, 119.1, 82.2, 61.2, 28.6 (2C). **HRMS (ESI)** *m/z* calcd for $C_{16}H_{17}N_2O$ $[M+H]^+$: 253.1341, found: 253.1343.

_N_-Butyl-4,4-diethyl-5-methylene-4,5-dihydrooxazol-2-amine (3p): Light yellow oil (39.5 mg, 94% yield). **^{1}H NMR (400 MHz, $CDCl_3$)** δ 4.54 (d, *J* = 2.6 Hz, 1H), 4.14 (bs, 1H), 3.91 (d, *J* = 2.6 Hz, 1H), 3.18 (t, *J* = 7.1 Hz, 2H), 1.66 (dq, *J* = 14.6, 7.3 Hz, 2H), 1.50 (dt, *J* = 14.9, 7.3 Hz, 2H), 1.44 – 1.36 (m, 2H), 1.31 (dt, *J* = 14.5, 7.4 Hz, 2H), 0.87 (t, *J* = 7.3 Hz, 3H), 0.74 (t, *J* = 7.3 Hz, 6H). **^{13}C NMR (101 MHz, $CDCl_3$)** δ 164.3, 156.6, 81.4, 74.7, 42.4, 34.5 (2C), 31.9, 19.9, 13.8, 8.1 (2C). **HRMS (ESI)** *m/z* calcd for $C_{12}H_{23}N_2O$ $[M+H]^+$: 211.1810, found: 211.1809.

_N_-Butyl-4-methylene-3-oxa-1-azaspiro[4.5]dec-1-en-2-amine (3q): Colourless oil (33 mg, 75% yield). **^{1}H NMR (400 MHz, $CDCl_3$)** δ 4.49 (d, *J* = 2.7 Hz, 1H), 4.09 (d, *J* = 2.7 Hz, 1H), 3.79 (bs, 1H), 3.20 (t, *J* = 7.1 Hz, 2H), 1.75 – 1.68 (m, 2H), 1.67 – 1.54 (m, 6H), 1.52 – 1.44 (m, 3H), 1.39 – 1.29 (m, 3H), 0.91 (t, *J* = 7.3 Hz, 3H). **^{13}C NMR (101 MHz, $CDCl_3$)** δ 168.4, 156.4, 81.4, 69.7, 42.5, 39.5 (2C), 32.1, 25.6, 22.3 (2C), 20.0, 13.9. **HRMS (ESI)** *m/z* calcd for $C_{13}H_{22}N_2NaO$ $[M+Na]^+$: 245.1630, found: 245.1630.

(_Z_)-5-Benzylidene-_N_-butyl-4,4-dimethyl-4,5-dihydrooxazol-2-amine (3u): Colourless solid (28 mg, 54% yield); m.p. 135.4–137.0 °C; **^{1}H NMR (400 MHz, $CDCl_3$)** δ 7.53 – 7.47 (m, 2H), 7.34 – 7.28 (m, 2H), 7.19 – 7.10 (m, 1H), 5.39 (s, 1H), 3.86 (br s, 1H), 3.29 (t, *J* = 7.2 Hz, 2H), 1.62 – 1.54 (m, 2H), 1.46 – 1.36 (m, 8H: 1.42, s, 6H), 0.94 (t, *J* = 7.3 Hz, 3H). **^{13}C NMR (101 MHz, $CDCl_3$)** δ 161.1, 156.5, 135.2, 128.5 (2C), 127.8 (2C), 126.0, 98.1, 68.8, 42.7, 31.9, 30.5 (2C), 20.1, 13.9. **HRMS (ESI)** *m/z* calcd for $C_{16}H_{23}N_2O$ $[M+H]^+$: 259.1810, found: 259.1811.

Methyl (_Z_)-2-((2-(butylamino)-4,4-dimethyloxazol-5(4_H_)-ylidene)methyl)benzoate (3v): Light yellow oil (36 mg, 57% yield); **^{1}H NMR (400 MHz, $CDCl_3$)** δ 7.91 (dd, *J* = 7.9, 1.3 Hz, 1H), 7.81 (dd, *J* = 8.0, 0.9 Hz, 1H), 7.47 (td, *J* = 7.7, 1.4 Hz, 1H), 7.27 – 7.20 (m, 1H), 6.41 (s, 1H), 3.89 (s, 3H), 3.28 (t, *J* = 7.2 Hz, 2H), 1.58 (dd, *J* = 8.2, 6.3 Hz, 2H), 1.47 (s, 6H), 1.37 (dd, *J* = 10.4, 4.8 Hz, 2H), 0.92 (t, *J* = 7.4 Hz, 3H). **^{13}C NMR (101 MHz, $CDCl_3$)** δ 168.1, 160.2, 158.2, 135.4, 131.9, 130.8, 129.8, 128.0, 126.2, 97.3, 67.8, 52.1, 42.7, 32.1, 31.0 (2C), 20.0, 13.8. **HRMS (ESI)** *m/z* calcd for $C_{18}H_{24}N_2O_3$ $[M+H]^+$: 317.1865, found: 317.1862.

(_Z_)-_N_-ethyl-5-(3-methoxybenzylidene)-4,4-dimethyl-4,5-dihydrooxazol-2-amine (3w): Colourless solid (22 mg, 43% yield); m.p. 171.3–172.7 °C; **^{1}H NMR (400 MHz, $CDCl_3$)** δ 7.26 (t, *J* = 7.9 Hz, 1H), 7.14 – 7.06 (m, 2H), 6.79 – 6.72 (m, 1H), 5.42 (s, 1H), 3.91-3.75 (m, 4H), 3.37 (q, *J* = 7.2 Hz, 2H), 1.43 (d, *J* = 2.5 Hz, 6H), 1.27 (t, *J* = 7.2 Hz, 3H). **^{13}C NMR (101 MHz, $CDCl_3$)** δ 160.9, 159.6, 156.3, 136.2, 129.3, 120.5, 113.5, 111.5, 98.3, 68.5, 55.2, 37.7, 30.4 (2C), 15.0. **HRMS (ESI)** *m/z* calcd for $C_{15}H_{25}N_2O_2$ $[M+H]^+$: 289.1916, found: 289.1916.

3-Benzyl-_N_-ethyl-4,4-dimethyl-5-methyleneoxazolidin-2-imine (3x): Colourless oil (36 mg, 73% yield); **^{1}H NMR (400 MHz, $CDCl_3$)** δ 7.37 – 7.21 (m, 5H), 4.59 (d, *J* = 3.1 Hz, 1H), 4.45 (s, 2H), 4.14 (d, *J* = 3.0 Hz, 1H), 3.37 (q, *J* = 7.2 Hz, 2H), 1.28 (s, 6H), 1.18 (t, *J* = 7.2 Hz, 3H). **^{13}C NMR (101 MHz, $CDCl_3$)** δ 163.1, 150.2, 139.3, 128.3 (2C), 127.5 (2C), 127.0, 81.9, 61.0, 44.1, 40.7, 27.3 (2C), 17.2. **HRMS (ESI)** *m/z* calcd for $C_{15}H_{21}N_2O$ $[M+H]^+$: 245.1654, found: 245.1652.

4,4-Dimethyl-5-methylene-2-(pyrrolidin-1-yl)-4,5-dihydrooxazole (3y): Colourless oil (32 mg, 90% yield); **^{1}H NMR (400 MHz, $CDCl_3$)** δ 4.50 (d, *J* = 2.7 Hz, 1H), 4.06 (d, *J* = 2.7 Hz, 1H), 3.43 – 3.34 (m, 4H), 1.91 – 1.86 (m, 4H), 1.33 (s, 6H). **^{13}C NMR (101 MHz, $CDCl_3$)** δ 168.9, 155.6, 80.6, 66.8, 46.9 (2C), 30.8 (2C), 25.5 (2C). **HRMS (ESI)** *m/z* calcd for $C_{10}H_{16}N_2NaO$ $[M+H]^+$: 181.1341, found: 181.1340.

4,4-Dimethyl-5-methylene-4,5-dihydrooxazol-2-amine (3z): Volatile colourless oil (88% NMR yield). **^{1}H NMR (400 MHz, $CDCl_3$)** δ 5.09 (br s, 2H), 4.57 (d, *J* = 3.1 Hz, 1H), 4.16 (d, *J* = 3.1 Hz, 1H), 1.36 (s, 6H). **^{13}C NMR (101 MHz, $CDCl_3$)** δ 167.4, 156.9, 82.0, 66.5, 30.2 (2C).

3,3,7,7-Tetramethyl-2-methylene-2,3-dihydro-7*H*-oxazolo[3,2-a]pyrimidine (4): Light yellow solid (23 mg, 61% yield); m.p. 121.8–123.1 °C; **^{1}H NMR (400 MHz, $CDCl_3$)** δ 5.87 (d, *J* = 7.8 Hz, 1H), 4.70 (d, *J* = 7.8 Hz, 1H), 4.57 (d, *J* = 3.2 Hz, 1H), 4.14 (d, *J* = 3.2 Hz, 1H), 1.36 (s, 6H), 1.20 (s, 6H). **^{13}C NMR (101 MHz, $CDCl_3$)** δ 161.9, 151.0, 118.4, 111.7, 83.6, 60.7, 54.8, 32.6 (2C), 26.9 (2C). **HRMS (ESI)** *m/z* calcd for $C_{11}H_{16}N_2NaO$ $[M+Na]^+$: 215.1160, found: 215.1161.

References

1. Hu, Y.; Xin, X.; Wan, B. *Tetrahedron*, **2015**, *56 (1),* 32-52.
2. Farshbaf, S.; Sreerama, L.; Khodayari, T.; Vessally, E. *Chem. Rev. Lett.,* **2018**, *1 (2)*, 56-67.
3. Senadi, G.C.; Wang, J.-J. et al. *Org. Lett.,* **2012**, *14 (7)*, 4478 – 4481.
4. Alhalib, Ali; Moran, W.J. *Org. Biomol. Chem.*, **2014**, *12 (5)*, 795 – 800.
5. Wong, V.H.L.; White, A.J.P.; Hor, H. *Adv. Synth. Catal.,* **2015**, *357 (18)*, 3943 – 3948.
6. Hashmi, A. et al. *Org. Lett.*, **2004**, *6 (23)*, 4391 – 4394.
7. Bacchi, A.; Costa, M.; Gabriele, B.; Pelizzi, G.; Salerno, G. *J. Org. Chem.* **2002,** *67,* 4450-4457.
8. Wong, V.H.L.; Vummaleti, S.V.C.; Cavallo, L. et al. *Chem. Eur. J.*, **2016**, *22*, 13320.
9. Burger, K. et al. *Zeitschrift fur Naturforschung, B: Chemical Sciences*, **1989**, *44 (10)*, 1298 – 1312.
10. Ma, J.W.; Wang, Q.; Wang, X.-G.; Liang, Y.-M. *J. Org. Chem.*, **2018**, *83*, 13296−13307.
11. Testero, S.A. et al. *ACS Comb. Sci.,* **2016**, *18*, 482 – 489.
12. Yang, M. et al. *Tetrahedron*, **2013**, *69*, 5744 – 5750.
13. Peshkov, V.A.; Van der Eycken, E.V. et al. *J. Org. Chem.,* **2011**, *76*, 5867–5872.
14. Pereshivko, O.; Van Der Eycken, E.V. et al. *Adv. Synth. Catal.*, **2013**, *355 (4)*, 781–789.
15. Casnati, A.; Perrone, A.; Della Ca’, N. et al. *J. Org. Chem.,* **2019**, 84 (6), 3477–3490.
16. Reid, J.L. *Am. J. Hypertens*., **2000**, *13 (4S)*, 106S-111S.
17. Hingst V.; Sonntag H.G. *Med. Welt*., **1979**, *30 (33)*. 1199-1201.
18. Powner, M.W.; Gerland, B.; Sutherland, J.D. *Nature,* **2009**, 459, p. 239 – 242.
19. Szostak J.W. et al. *J. Am. Chem. Soc*., **2017**, 139, p. 8780 − 8783.
20. Liu, J.; Shen, M.; Zhang, Y. et al. *Org. Lett.,* **2006**, 8, 3573–3575.
21. Sonogashira, K.; Tohda, Y.; Hagihara, N. *Tetrahedron*. **1975**, 16, 4467–4470.
22. Brak, K.; Doyle, P.S.; McKerrow, J.H.; Ellman. J.A. *J. Am. Chem. Soc*., **2008**, 130, 6404–6410.
23. Lee, C.-M.; Horrom, B.W.; Michaels, R.J. et al. *J. Med. Chem*., **1972**, 15 (12), 1252-1255.
24. Verma, R. P.; Shandilya, A.; Haridas, V. *Tetrahedron*, **2015**, 71 (46), 8758–8765.

Chapter 2. Palladium-Catalysed Oxidative Carbonylation of Alpha-Amino Amides to Hydantoins Under Mild Conditions

The content of this chapter was published as:

Voronov, A.; Botla, V.; Montanari, L.; Carfagna, C.; Mancuso, R.; Bartolo, G.; Maestri, G.; Motti, E., and Della Ca', N. ***Chem. Commun.***, 2022, ***58***, 294-297.

Introduction

Chiral hydantoin derivatives are widespread among natural products[1] and have shown great potential in the treatment of various deseases.[2-4] Some of hydantoin-based compounds are registered drugs commercialized d by companies like Galapagos[5] and Novartis[6] (Scheme 2-1).

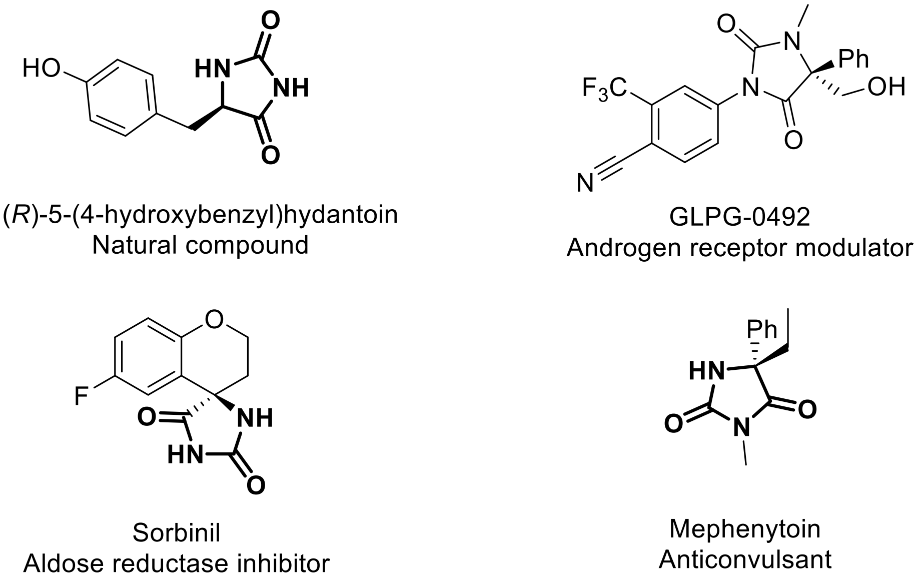

(*R*)-5-(4-hydroxybenzyl)hydantoin
Natural compound

GLPG-0492
Androgen receptor modulator

Sorbinil
Aldose reductase inhibitor

Mephenytoin
Anticonvulsant

Scheme 2-1. Biologically Active Chiral Hydantoins.

Also, imidazolidine-2,4-diones (hydantoins) display an array of utilities that include their application as ligands,[7] directing groups,[8] organocatalysts,[9] intermediates in organic synthesis[10], and functional moieties in specialty polymers.[11] Traditional routes to hydantoin scaffold include the Bucherer–Bergs reaction,[12] the Urech,[13] and the Read[14] syntheses and the Biltz reaction.[15] Enantiopure hydantoins can provide additional key properties, which can be exploited in medicinal chemistry[16] as well as in organic chemistry.[17] Besides the well-established Urech and Read syntheses, the most common strategy to chiral imidazolidine-2,4-diones rely on the use of optically pure building blocks[18] mainly by cyclisation of ureido compounds generated from the reaction of α-amino acid derivatives with isocyanates or other unfriendly acylating agents (i.e. phosgene, triphosgene, and 1,1-carbonyldiimidazole (CDI)) and an amine.[1] Despite their high efficiency, these non-catalytic protocols suffer from limited atom-economy, low generality and functional group tolerance. Alternatively, optically enriched hydantoins can be accessed by elegant enantioselective transformations,[19] but their applicability is weakened by the high cost of the catalytic system, availability of the starting reagents or limited enantioselectivity values. Therefore, catalytic protocols for the synthesis of chiral hydantoins featuring improved efficiency, atom-economy and versatility are still in high demand.[20] Catalytic carbonylative approaches to hydantoins should be highly attractive from the abovementioned points of view, however, only few examples have been reported so far.

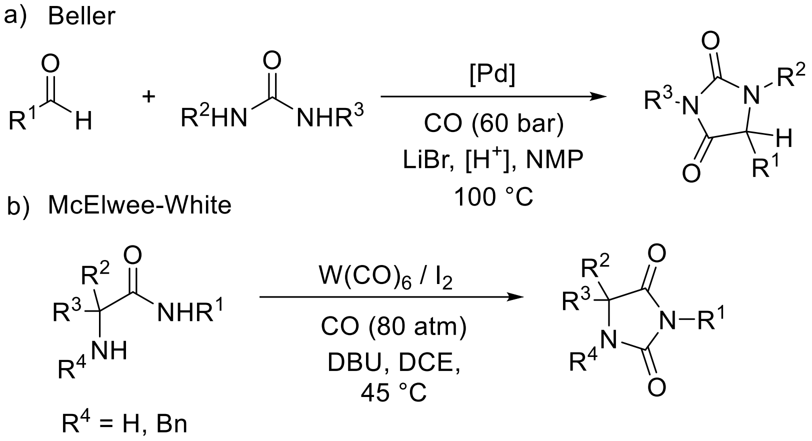

Scheme 2-2. Previously Reported Carbonylative Protocols For the Synthesis of Hydantoins.

In 1994, Beller and coworkers presented a simple but remarkable example of the synthesis of hydantoins by palladium-catalysed carbonylation of aldehydes with urea derivatives (row a, Scheme 2-2).[21] More recently, McElwee-White *et al.* reported the first example of carbonylation of primary amino amides to hydantoins by means of $W(CO)_6$ catalyst (row b, Scheme 2-2).[22] Although, high pressure of CO (80 atm) and the stoichiometric amount of base (DBU) were indispensable. This is the unique example of catalytic carbonylative synthesis of hydantoins, probably because the carbonylation of primary amino acids *via* catalytic CO insertion, leads exclusively to the formation of the urea[23] or benzolactam derivatives,[24] especially under palladium catalysis.

Here, we describe the first example of palladium-catalysed carbonylative transformation of α-amino acid amides to enantiomerically pure hydantoins under mild conditions and atmospheric CO pressure. Competitive pathways to urea and benzolactam derivatives were successfully circumvented, and the carbonylation took place without racemisation of the chiral centre.

Results and Discussion

Initially, in the context of our work on the carbonylation of amines to ureas[25] in the presence of the PdI_2/KI catalytic system,[26] we examined to what extent amino amides can be used as hydantoins precursors under palladium catalysis. The easily accessible butylamide of L-phenylalanine (*S*)-**1a**, was selected as a model compound. The primal attempts to direct the carbonylation of amino amide (*S*)-**1a** to imidazolidine-2,4-dione **2a** were completely unsuccessful. In fact, the PdI_2/KI catalytic system turned out to be as efficient in the synthesis of ureas as ineffective in the formation of hydantoins (Table 2-1).

All experiments performed under various conditions, using different solvents and concentrations afforded urea **3a** in quantitative yield and no traces of hydantoins were detected.

Table 2-1. Carbonylation of (*S*)-**1a** Using PdI_2/KI Catalytic System.

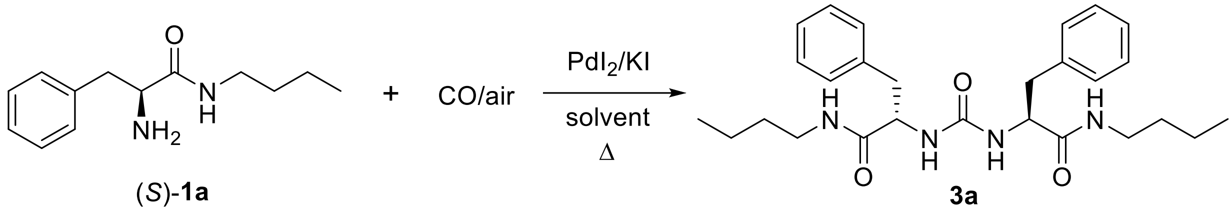

Entry	PdI_2, mol%	KI, mol%	p(CO), bar	p(air), bar	T, °C	Solvent	Yield[a] **3a**, %
1	2	20	16	4	115	1,4-dioxane	72
2	2	20	16	4	100	1,4-dioxane	84
3	2	20	16	4	80	1,4-dioxane	92
4	2	20	4	16	80	1,4-dioxane	94
5	5	50	4	16	80	1,4-dioxane	99
6	5	50	8	2	80	1,4-dioxane	99
7	5	50	8	2	70	1,4-dioxane	99
8	5	50	8	2	70	MeCN	93
9	5	50	8	2	70	DME	88
10	5	100	16	4	80	DMF	94

Reaction conditions: (*S*)-**1a** (0.4 mmol), PdI_2, KI, solvent (0.1 M). [a]Isolated yield.

The formation of urea derivatives is also the most preferred pathway when primary amines, including unprotected amino esters, are carbonylated under milder palladium-based conditions.[23] Exceptions to this behaviour include the palladium-catalysed oxidative carbonylation of *N*-protected amino acids to 3,4-dihydroisoquinolinones[27] and the synthesis of benzolactams by palladium-catalysed carbonylation of *N*-unprotected amino esters.[24]

Inspired by the work of Albert et al.,[24] that were successful in preventing the formation of urea in favour of benzolactam derivatives, we initially submitted substrate (*S*)-**1a** to similar carbonylative conditions, that imply the use of $Pd(OAc)_2$ as a catalyst, benzoquinone (BQ) as an oxidant, 1 atm of carbon monoxide, and acetic acid as a solvent (Table 2-2).

Table 2-2. Optimisation Study.

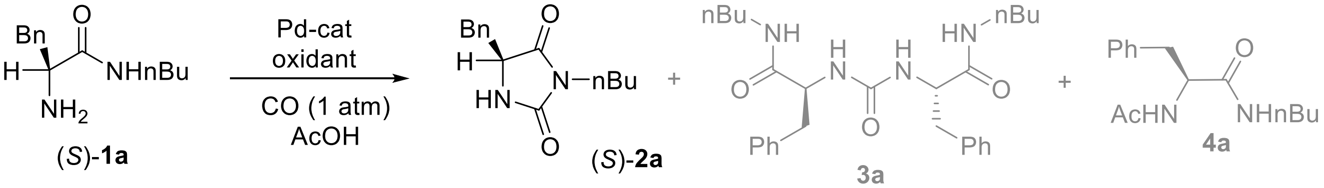

Entry	Pd-cat (mol%)	Oxidant (equiv)	T (°C)	t, (h)	Yield[a] **2a**, %
1	$Pd(OAc)_2$ (10)	BQ (2.0)	120	6	74 (70)[b,d]
2	$Pd(OAc)_2$ (10)	BQ (2.0)	80	6	86 (83)[b,d]
3	$Pd(OAc)_2$ (10)	BQ (1.2)	80	6	80 (76)[b,d]
4	$Pd(OAc)_2$ (10)	MBQ (1.2)	80	6	19[b,d]
5	$Pd(OAc)_2$ (10)	DMBQ (1.2)	80	6	23[b,d]
6	$Pd(OAc)_2$ (10)	$Cu(OAc)_2$ (2.2)	80	6	16[b,e]
7	$Pd(OAc)_2$ (10)	$Cu(OAc)_2$ (1.0)[f]	80	6	64[b,g]
8	$Pd(OAc)_2$ (10)	AgOAc (2.2)	80	6	81[b]
9	**$Pd(OAc)_2$ (10)**	**TEMPO (2.2)**	**80**	**2**	**84[b]**
10	$Pd(MeCN)_2Cl_2$ (10)	TEMPO (2.2)	80	2	77[b]
11	$Pd(TFA)_2$ (10)	TEMPO (2.2)	80	2	60[b]
12	$Pd_2(dba)_3$ (10)	TEMPO (2.2)	80	2	68[b]
13	$Pd(OAc)_2$ (5)	TEMPO (2.2)	80	3	81[b]
14	$Pd(OAc)_2$ (2)	TEMPO (2.2)	80	5	74[b]
15	$Pd(OAc)_2$ (10)	TEMPO (2.2)	60	3	65[b]

Reaction conditions: (*S*)-**1a** (0.3 mmol), CO (balloon, 1 atm), Pd-cat, oxidant, acetic acid (0.1 M). [a]NMR yield. [b]Isolated yield. [c]NMR yield. [d]Impure of quinone. [e]Compounds **3a** and **4a** were isolated in 15% and 27% yield, respectively. [f] Under atmosphere of CO and air (3:1 ratio). [g] Compounds **4a** was isolated in 11% yield and traces of **3a** were detected.

Gladly, both urea **3a** and acetylamide **4a** were not observed. Similarly, the formation of the benzolactam derivative *via* C-H activation was not detected, and hydantoin **2a** was obtained in 74% NMR yield (entry 1, Table 2-2). Importantly, the absolute configuration of the chiral centre of **2a** was found to be *S*, confirming the enantiospecificity of this transformation. Unfortunately, the ultimate purification of the target product was unsatisfactory due to the presence of traces of BQ derivatives. A possible adduct of BQ and the product[28] was difficult to remove by chromatographic separation. We were pleased to find that the yield increased lowering the reaction temperature to 80 °C (entry 2), but the isolation issues persisted even though the BQ was employed in near stoichiometric amount (entry 3). This prompted us to consider alternative oxidants. Other BQ derivatives, such as methyl-*p*-benzoquinone (MBQ) and 2,6-dimethyl-*p*-benzoquinone (DMBQ), were less efficient in the reoxidation of palladium (entries 4 and 5).

Copper (II) acetate, a common oxidant in palladium-catalysed reactions, gave satisfactory results only in combination with air (entries 6 and 7). The purification of the final product was successfully performed, but compound **4a** was formed in not negligible amount, suggesting that the competitive acetylation of (*S*)-**1a** might be accelerated by copper (II) species.[29] High yield and selectivity were achieved when 2.2 equivalents of silver acetate were used (entry 8). However, despite its efficiency, we intended to find a more sustainable oxidation system. Satisfyingly, TEMPO provided the highest yield of compound (*S*)-**2a** which in this case could be easily isolated (entry 9). Remarkably, the use of TEMPO caused a significant reduction of the reaction time (from 6 to 2 hours), and the complete suppression of the acetylated compound **4a** was also achieved. In all reactions carried out with TEMPO, the selectivity reached values close to 99%, as only reduced amount of the starting material was recovered. Other palladium precursors behaved nicely but were less efficient (entries 10-12). The reduction of $Pd(OAc)_2$ from 10% to 5 and 2% was still acceptable in terms of yield, but longer reaction times were required (entries 13 and 14). The optimal reaction temperature was 80 °C since at 60 °C a lower performance was observed (entry 15, Table 2-2). Alternative polar solvents, such as MeCN and DMF, provided less satisfactory results only in combination with acetic acid.

Then, to explore the reaction scope, an array of α-amino amides was smoothly prepared from the corresponding esters and tested under the optimised reaction conditions (entry 9, Table 2-2).

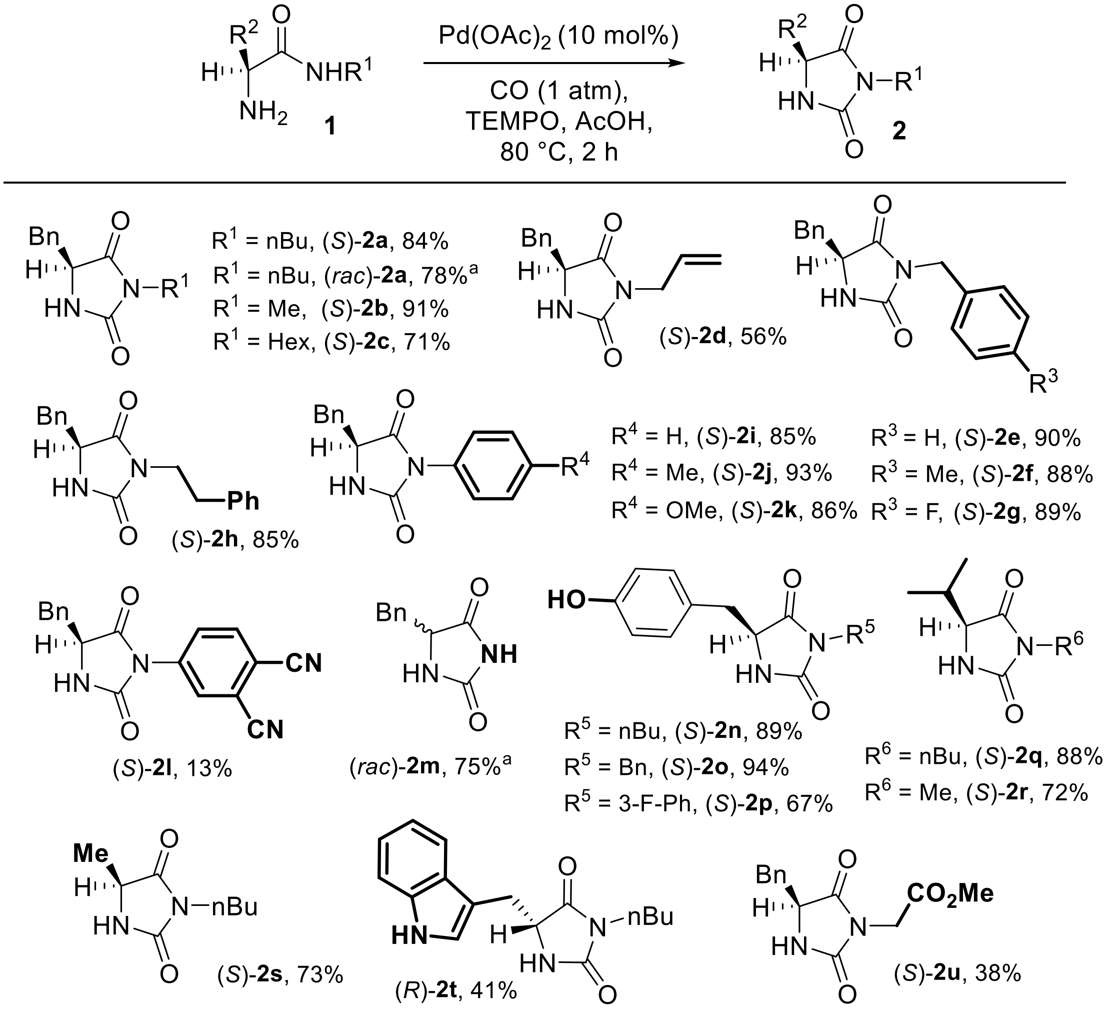

[a]From the corresponding (*RS*)-aminoamides.

Scheme 2-3. Hydantoins Obtained by Palladium-Catalysed Carbonylation.

Firstly, the catalytic process was successfully extended to the racemic phenylalanine amide (*RS*)-**1a** that was converted to (*RS*)-**2a** in 78% yield (Scheme 2-3). Different R^1 substituents were then explored. The methyl group on the amide nitrogen (R^1 = Me) provided excellent yield of compound **2b**, while a longer alkyl chain (R^1 = Hex) seems to decrease the efficiency of the reaction (**2c**, 71%). The allyl substituent is only partially tolerated being the corresponding hydantoin **2d** obtained in 56% yield. The benzyl moiety was particularly beneficial to this transformation and yield near to 90% were achieved with both electron withdrawing and electron releasing groups (**2e-g**, 88-90%). Substrate **1h**, bearing the phenylethyl unit, afforded the desired product **2h** in 85% yield. Aryl amides were also compatible with this process and allowed to prepare 2-arylhydantoins **2i-k** in excellent yields (85-93%). The unsubstituted amide of the (*RS*)-phenylalanine **1l** was successfully converted to the hydantoin scaffold in good yield (**2l**, 75%). Different natural amino acids were then considered. The hydroxyl function of tyrosine amides was well tolerated, delivering the expected carbonylated products **2m** and **2n** in 89% and 94% yield, respectively. A comparable outcome was observed for valine derivatives (**2o-p**, 72-88%) and alanine amide **1q** (**2q**, 73%), while the *N*-butyl amide of tryptophan led to the desired product **2r** in poor 41% yield as the C-H activation at the C-2 position of indole turned out to be a competitive pathway.[30]

To gain preliminary insights on the reaction mechanism some control experiments were performed (Scheme 2-4). Firstly, an attempt to carbonylate the secondary amino amide (*S*)-**1s** was performed under the standard conditions and, surprisingly, the expected product (*S*)-**2s** was detected only in traces, while the hydantoin (*S*)-**2a** was isolated in limited amount.

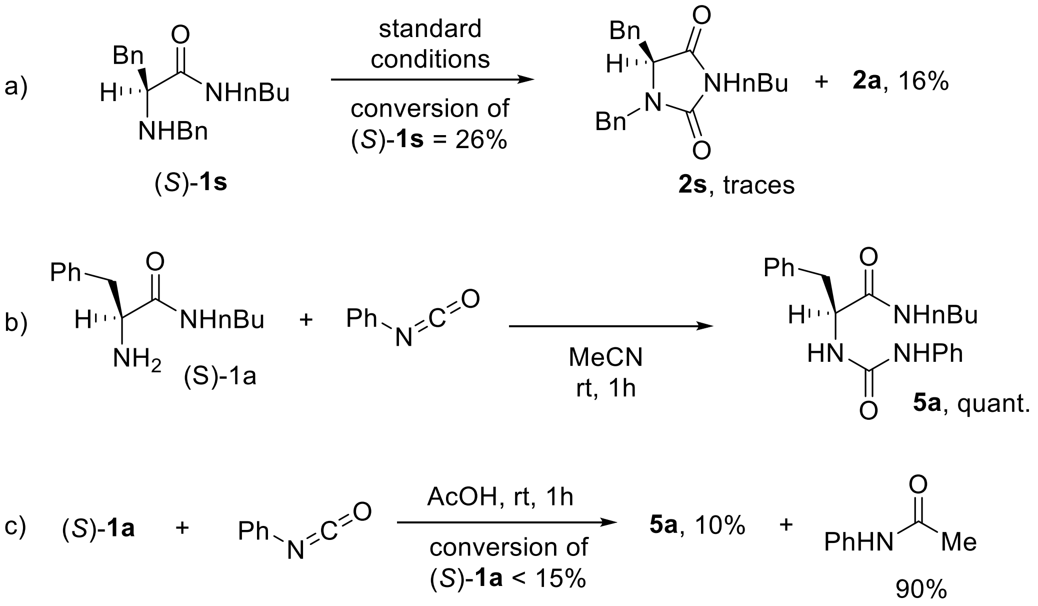

Scheme 2-4. Control Experiments.

This would suggest the intermediacy of an isocyanate species that can be formed only from primary amines.[31,32] Considering this, the reaction of amino amide (*S*)-**1a** with phenyl isocyanate was performed in MeCN and in AcOH. While the corresponding urea **5a** was quantitatively obtained in MeCN, only 10% of **5a** was observed in AcOH together with *N*-phenylacetamide in 90% yield.[33] This would explain the complete suppression of the urea derivatives **3** in the presence of acetic acid and the formation of small amount of acetamide **4**, derived from the reaction of isocyanate intermediate with acetic acid[33] under not optimised conditions (Table 2-2).

Summarising, two reaction pathways are in principle possible, one involving the isocyanate intermediate (pathway *a*, Scheme 2-5) and the other passing through palladacycle species (pathway *b*, Scheme 2-5).

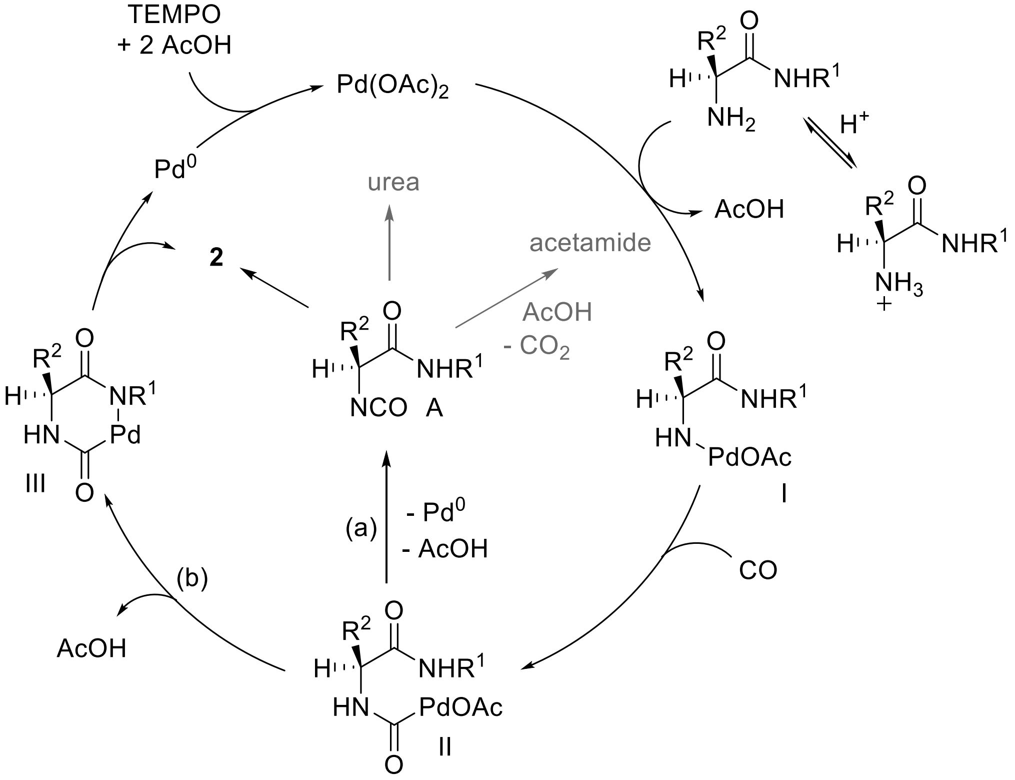

Scheme 2-5. Plausible Reaction Pathways.

Initially, $Pd(OAc)_2$ coordinates the free amino group leading to complex **I**. Insertion of CO leads to intermediate **II** which can evolve to isocyanate **A** (pathway *a*), that in its turn can justify all the observed products. Compound **4** is generated by the reaction of intermediate **A** with acetic acid[33] or under acetate/acetic acid conditions directly from the free amino group.[34] Product **2** can be formed again from **A** by intermolecular attack of amide moiety to isocyanate group.[35] Formation of **3**, that usually is the preferred product in conventional reaction media (row b, Scheme 2-4),[36,1] is here completely prevented mainly by the reaction medium (row c, Scheme 2-4). Additionally, considering that amino amide **1** is mostly in its protonated form, the reaction with the isocyanate to afford **3** should be disfavoured in acidic media. The alternative pathway *b*, where **II** leads to palladacycle **III**, that undergoes reductive elimination to hydantoin **2** cannot be ruled out. Finally, in both pathways *a* and *b*, Pd^0 species are promptly re-oxidised by TEMPO to $Pd(OAc)_2$.

Conclusions

A new palladium-catalysed carbonylative protocol to access hydantoins from α-amino amides with excellent yields under very mild conditions was developed. Importantly, the quick formation of urea derivatives under palladium catalysis is here circumvented in favour of hydantoin products. Some important features include the use of largely available starting materials and acetic acid as an environmentally friendly reaction medium, together with the absence of bases and ligands. The retention of the chiral information in the target compounds is unequivocally beneficial.

Experimental Part

Preparation of 2-Iodophenylacetates

General Procedure for the Synthesis of Amino Acid Amides ***1a-h, 1n, 1o, 1q-t****:*

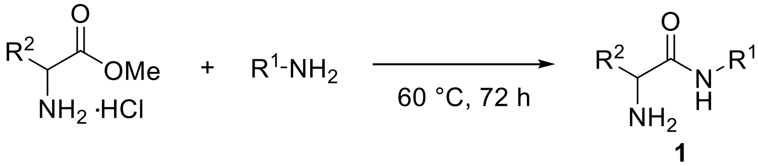

A 10 mL Schlenk tube was charged with the amino acid methyl ester hydrochloride (2 mmol) and an amine (8 mmol) under N_2. The Schlenk tube was sealed, and the mixture was stirred at 60 °C for 72 h. The crude mixture was transferred to a 50 mL flask and the excess of amine was removed under vacuum (in case of high-boiling amines the evaporation step was skipped). The residue was washed with brine and extracted with ethyl acetate (3x10 mL). The organic phase was dried over anhydrous Na_2SO_4, filtered and concentrated in vacuo. The residue was then purified by silica gel column chromatography (ethyl acetate/hexane/methanol (5:10:1)) to afford the pure amino acid amide **1**.

General Procedure for the Synthesis of Amino Acid Amides ***1i-k 1i-k, 1l, 1p****:*[37]

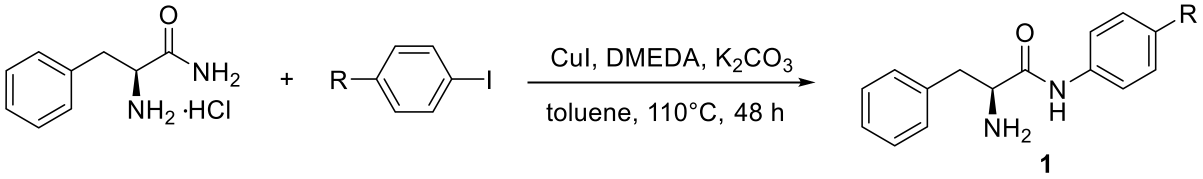

An oven-dried ground test tube with a stir bar was charged with an amino acid amide or its hydrochloride (1.2 mmol), K_2CO_3 (3 mmol), and CuI (0.05 mmol) before sealing. Under argon atmosphere, an aryl halide (1 mmol) and toluene (6 mL) were added by a syringe. The tube was put into an oil bath pot preheated at 110 °C and kept stirring at the temperature for 24 h. The reaction mixture was then cooled to room temperature, quenched with water, and extracted with ethyl acetate (20 mL) three times. The organic layer was combined, dried over anhydrous sodium sulfate, and filtrated. The filtrate was condensed under reduced pressure. The residual was purified with silica gel column chromatography with a solution of petroleum ether and ethyl acetate (1:5 to 2:1) to afford pure amino acid amide.

*Synthesis of Amino Acid Amide **1v**:*

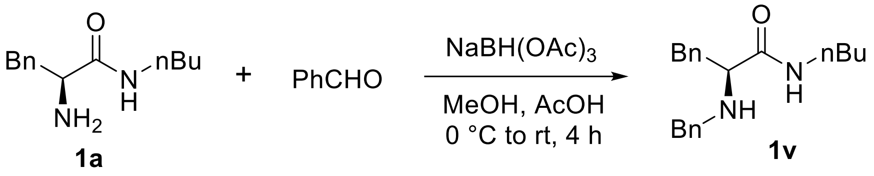

To a solution of **1a** (330 mg, 1.5 mmol) in dry MeOH (8.0 mL), benzaldehyde (0.158 mL, 1.55 mmol) and acetic acid (2 mL) were added. The reaction mixture was stirred at room temperature for 10 min and cooled to 0 °C, then NaBH(OAc)$_3$ (650 mg, 3 mmol) was added portionwise. After stirring at room temperature for additional 4 h, the solvent was evaporated, and the residue was extracted with ethyl acetate and washed with brine. The organic layer was dried over Na$_2$SO$_4$, filtered, and concentrated in vacuo. The residue was purified by silica gel column chromatography (ethyl acetate/hexane/methanol (5:15:1)).

*Synthesis of Methyl L-Phenylalanylglycinate **1u**:*[38]

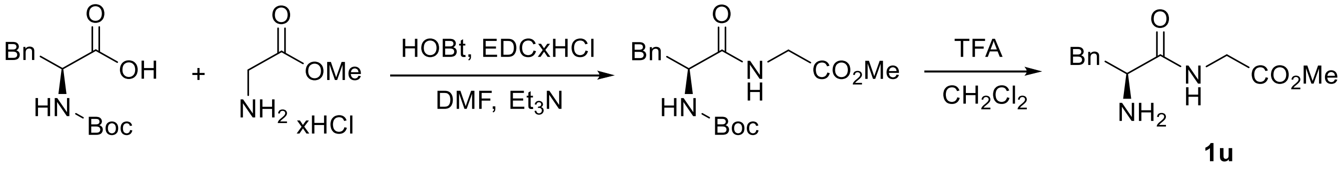

N-Boc-Phenylalanine (292 mg, 1.1 mmol) and HOBt (203 mg, 1.5 mmol) were dissolved in cooled at 0˚C DMF (10 mL) and maintained under stirring for 15 minutes. To a resulting solution methyl glycinate hydrochloride (125 mg, 1.0 mmol) and EDCxHCl (287 mg, 1.5 mmol), and 5 minutes later TEA (0.67 mL, 5 mmol) were added. Reaction mixture was stirred at room temperature for 24 hours and monitored by TLC until the complete consume of methyl glycinate. The mixture was filtered through a pad of SiO$_2$, and the solvent was evaporated under reduced pressure. The residue was purified by column chromatography using ethyl acetate/hexane (2:3) mixture as eluent. Obtained colourless oil (317 mg, 0.94 mmol) was dissolved in 3 mL of DCM, and TFA (0.72 mL, 9.4 mmol) was added dropwise to the solution. After stirring for 8 hours at room temperature, the excess of TFA was removed under reduced pressure, the residue was dissolved in ethyl acetate (3 mL), and potassium carbonate (414 mg, 3 mmol) was added. The solution was then filtered through a pad of SiO$_2$ and concentrated in vacuo. The product (219 mg, 93% yield) did not require any further purification.

*Synthesis of Urea **5a**:*

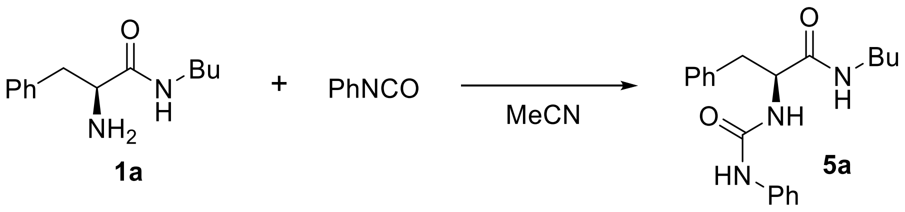

In a 25 ml Schlenk tube, **1a** (66 mg, 0.3 mmol) was dissolved in dry acetonitrile (3 mL) under N_2. Phenyl isocyanate was added (0.033 mL, 0.3 mmol), and the mixture was stirred for 1 min. Solvent evaporation afforded **5a** in quantitative yield, and no further purification was required.

*PdI_2/KI Oxidative Carbonylation of Amino Amide **1a**:*

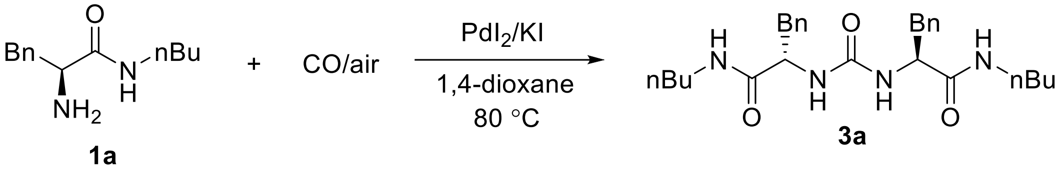

A 45 mL stainless steel autoclave was charged with substrate **1a** (110 mg, 0.5 mmol), PdI_2 (2-5 mol%), KI (20-100%) and 1,4-dioxane (5 mL). The autoclave was sealed and pressurized with CO and air, heated at 80 °C (oil bath) under stirring for 18 h. Then the autoclave was cooled, degassed, and opened. The mixture was passed through a pad of Celite®, and the solvent was removed in vacuo affording product **3a** in quantitative yield.

*Pd-catalysed Oxidative Carbonylation of Amino Amides **1a-r** to Hydantoins **2a-r**:*

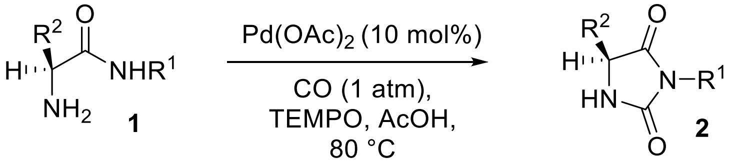

A 25 mL Schlenk tube was charged with a solution of amino acid amide **1** (0.3 mmol) in glacial acetic acid (3 mL), palladium acetate (6.7 mg, 0.03 mmol) and TEMPO (104 mg, 0.66 mmol) under N_2. The tube was sealed, and the mixture was stirred for 5 minutes at 80 °C. The reaction then was purged for ~ 30 seconds with CO and, finally, a balloon charged with CO (1 atm) was attached to the Schlenk tube. The reaction mixture was kept at 80 °C under stirring and CO atmosphere for 2-6 h. Then the reaction mixture was cooled down to room temperature and passed through a Celite® path. Acetic acid was evaporated under reduced pressure at 60 °C, and the residue was neutralized with K_2CO_3 powder (400 mg, 2.9 mmol), dissolved in ethyl acetate (5 mL) and filtered. The product was purified by silica gel column chromatography (ethyl acetate/dichloromethane (1:8)).

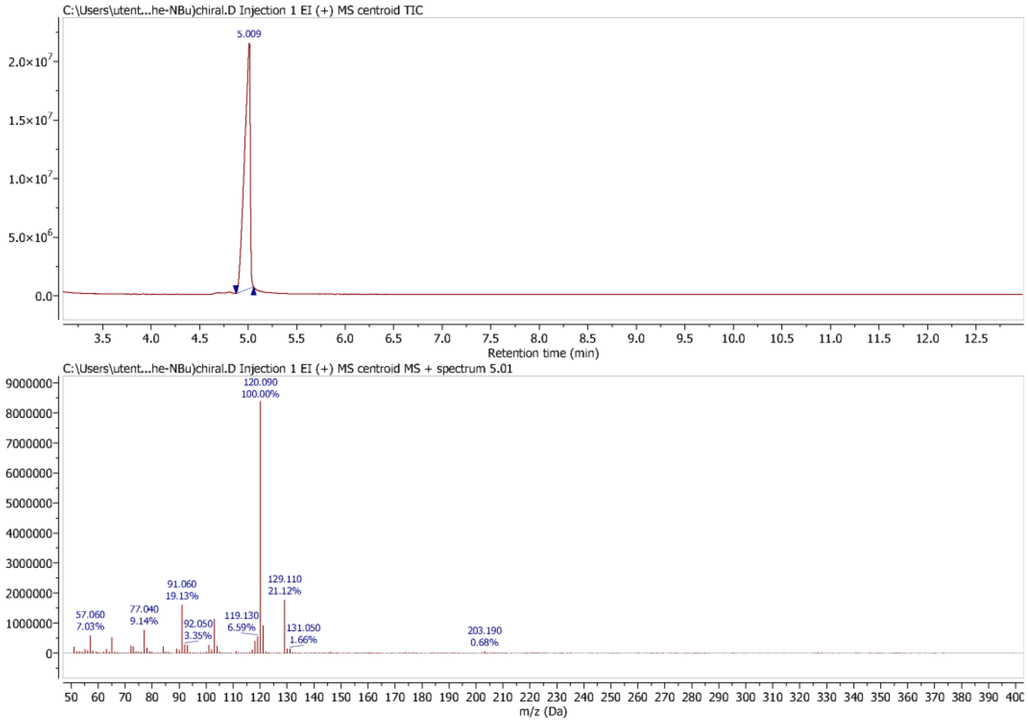

Figure 2-1. Gas Chromatogram and Mass Spectrum of (*S*)-**1a**.

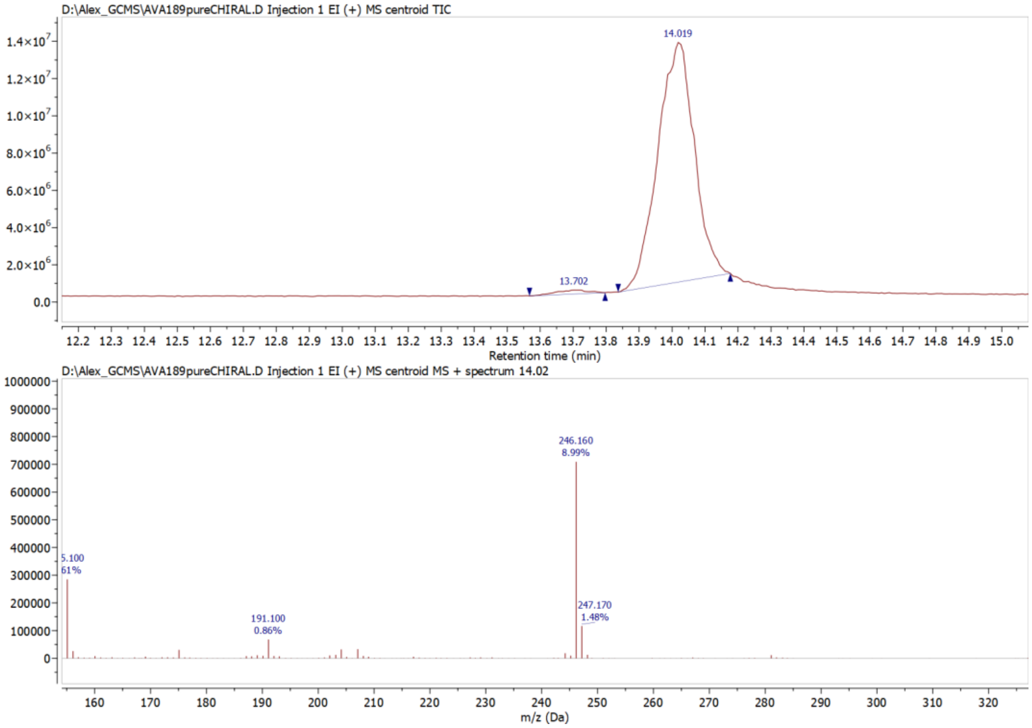

Figure 2-2. Gas Chromatogram and Mass Spectrum of (*S*)-**2a**.

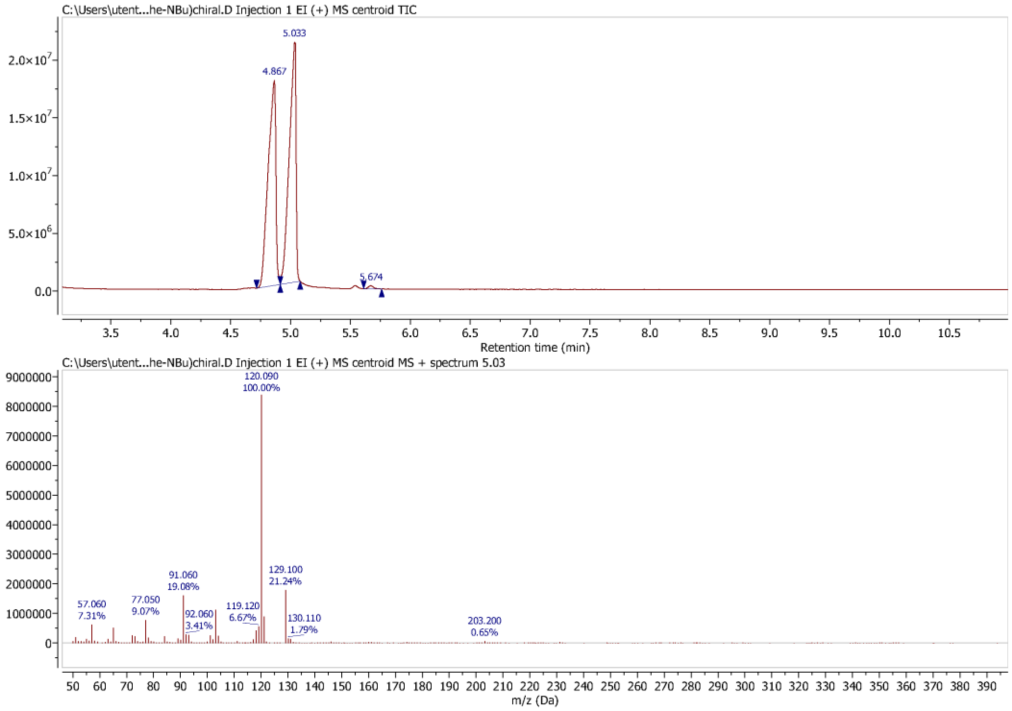

Figure 2-3. Gas Chromatogram and Mass Spectrum of (*rac)*-1a.

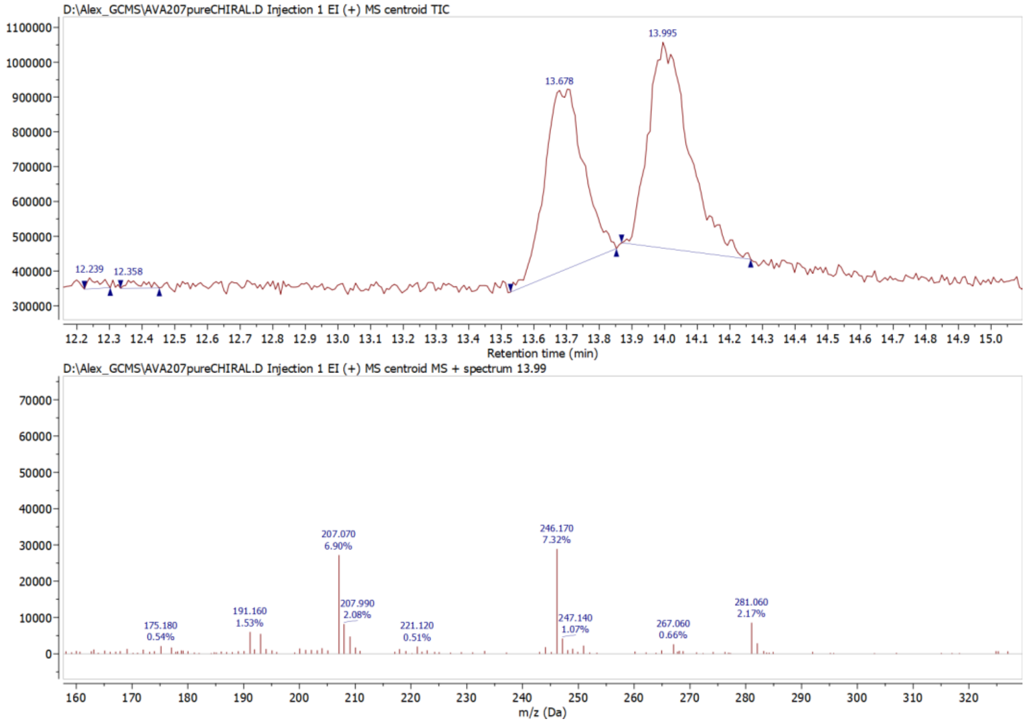

Figure 2-4. Gas Chromatogram and Mass Spectrum of (*rac)*-2a.

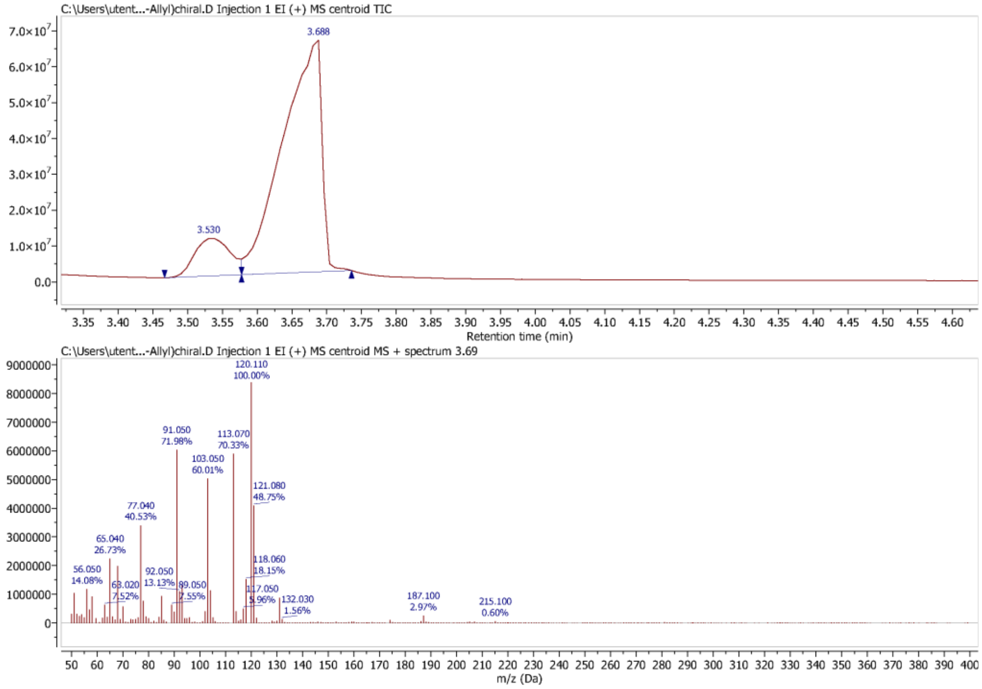

Figure 2-5. Gas Chromatogram and Mass Spectrum of (*S*)-**1d**.

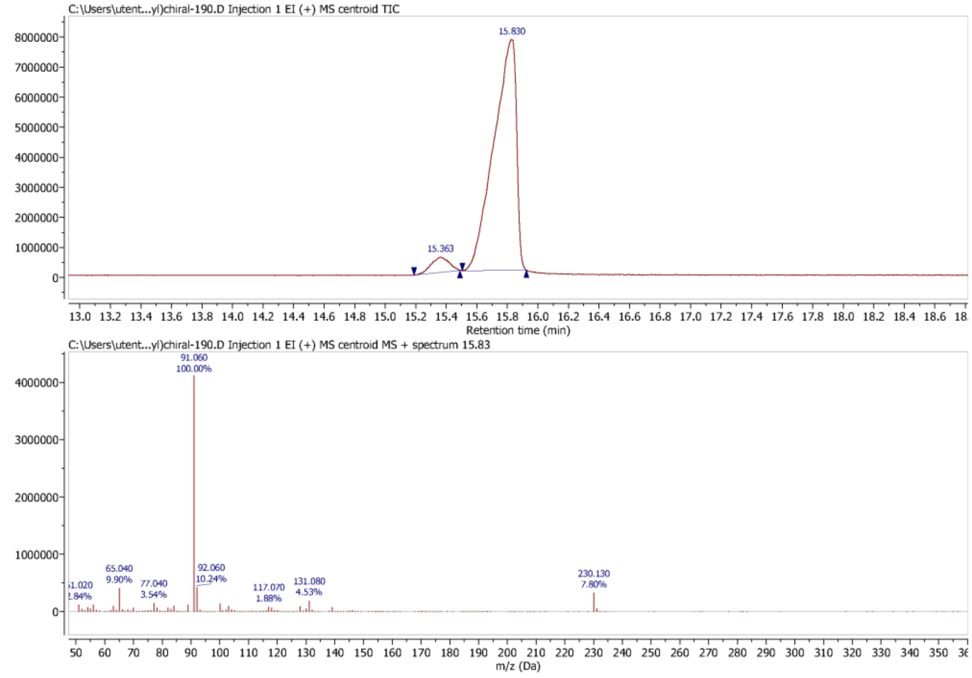

Figure 2-6. Gas Chromatogram and Mass Spectrum of (*S*)-**2d**.

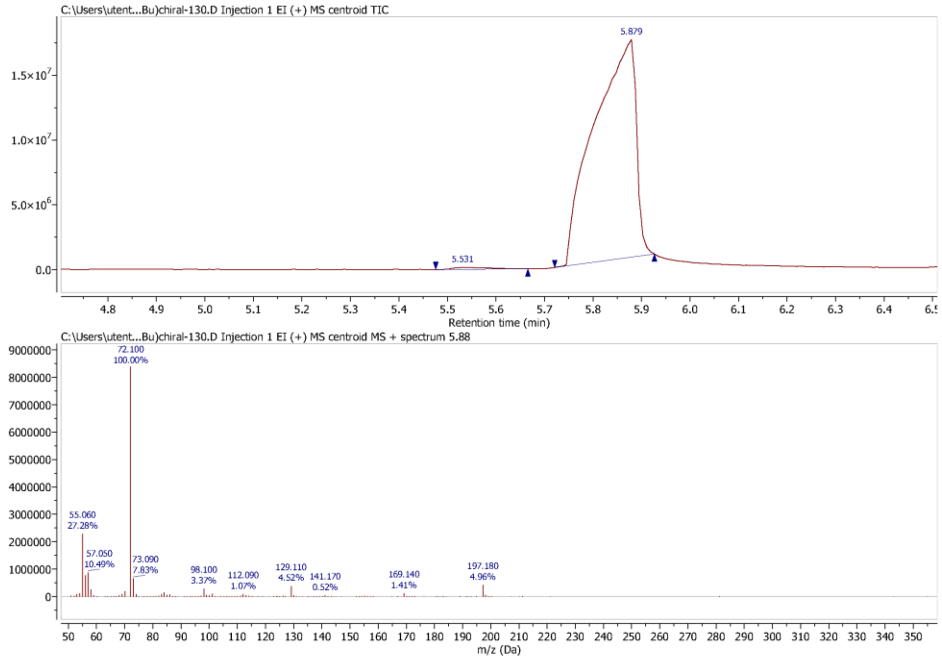

Figure 2-7. Gas Chromatogram and Mass Spectrum of (*S*)-**1o**.

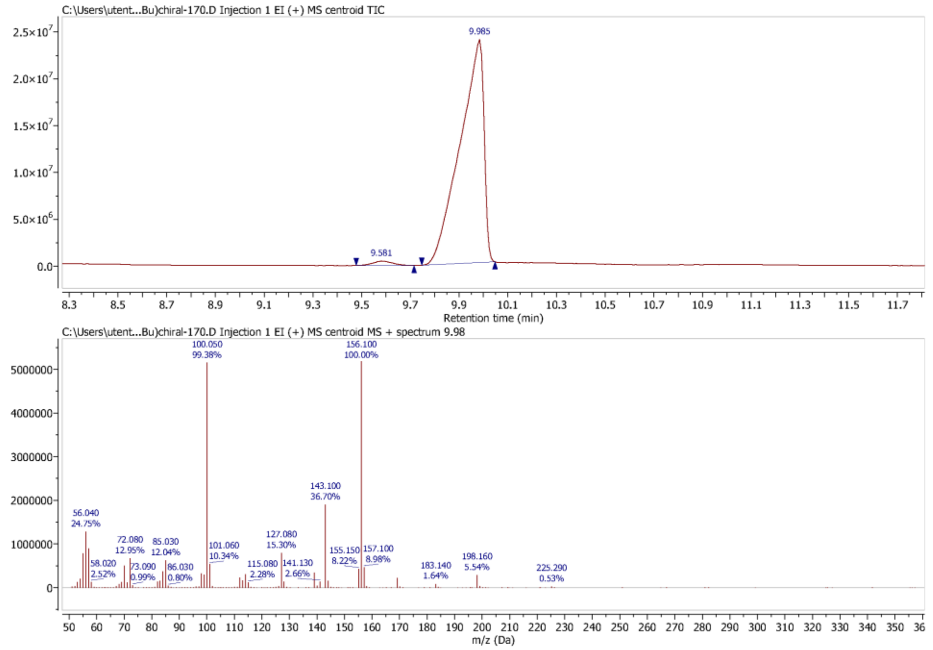

Figure 2-8. Gas Chromatogram and Mass Spectrum of (*S*)-**2o**.

(*S*)-2-Amino-*N*-butyl-3-phenylpropanamide (1a): Colourless oil (414 mg, 94% yield); **^{1}H NMR (400 MHz, CDCl$_3$)** *δ* 7.32-7.20 (m, 5H), 3.59 (br s, 2H), 3.25-3.22 (m, 3H), 2.70 (dd, *J* = 13.7, 9.1 Hz, 1H), 1.65-1.42 (m, 3H), 1.35-1.24 (m, 2H), 0.91 (t, *J* = 7.3 Hz, 3H). **^{13}C NMR (100 MHz, CDCl$_3$)** *δ* 174.2, 138.0, 129.3 (2C), 128.6 (2C), 126.7, 56.4, 41.1, 38.8, 31.6, 20.0, 13.7. **HRMS (ESI)** *m/z* calculated for $C_{13}H_{20}N_2O$ [M+H]$^+$: 221.1468, found: 221.1466. **IR (ATR diamond, neat):** *v* 3299.8, 3063.5, 3027.6, 2956.9, 2929.4, 2871.3, 2358.9, 2337.9, 1647.2, 1522.3, 1454.0, 741.7, 698.8 cm^{-1}.

(*S*)-2-Amino-*N*-methyl-3-phenylpropanamide (1b): Colourless solid (328 mg, 92% yield); m.p. 58.5-60.6 °C; **^{1}H NMR (400 MHz, CDCl$_3$)** *δ* 7.37 (br s, 1H), 7.30 – 7.09 (m, 5H), 3.55 (br s, 1H), 3.19 (dd, *J* = 13.6, 3.9 Hz, 1H), 2.73 (d, *J* = 5.0 Hz, 3H), 2.63 (dd, *J* = 13.7, 9.2 Hz, 1H), 1.57 (br s, 2H). **IR (ATR diamond, neat):** *v* 3372, 3344, 3291, 2939, 2914, 2876, 1644, 1522, 1455, 1439, 744, 698 cm^{-1}.

(*S*)-2-Amino-*N*-hexyl-3-phenylpropanamide (1c): Light yellow solid (432 mg, 87% yield); m.p. 39.2-39.6 °C; **^{1}H NMR (600 MHz, CDCl$_3$)** *δ* 7.30 – 7.22 (m, 3H), 7.17 (d, *J* = 6.7 Hz, 2H), 5.99 (s, 1H), 4.21 (dd, *J* = 4.2, 1.2 Hz, 1H), 3.38 (dd, *J* = 7.9, 7.0 Hz, 2H), 3.22 (dd, *J* = 14.0, 3.9 Hz, 1H), 2.87 (dd, *J* = 14.0, 8.0 Hz, 1H), 1.43 (t, *J* = 7.1 Hz, 2H), 1.29 – 1.13 (m, 6H), 0.86 (t, *J* = 7.0 Hz, 3H). **^{13}C NMR (151 MHz, CDCl$_3$)** *δ* 174.2, 138.1, 129.3 (2C), 128.6 (2C), 126.7, 56.5, 41.2, 39.1, 31.5, 29.6, 26.6, 22.6, 14.0. **HRMS (ESI)** *m/z* calculated for $C_{15}H_{24}N_2O$ [M+H]$^+$: 249.1961, found: 249.1660. **IR (ATR diamond, neat):** *v* 3304.1, 2956.8, 2921.4, 2987.6, 1638.4, 1545.8, 1491.0, 1453.8, 744.2, 697.2 cm^{-1}.

(*S*)-*N*-Allyl-2-amino-3-phenylpropanamide (1d): Colourless oil (384 mg, 94% yield); **^{1}H NMR (400 MHz, CDCl$_3$)** *δ* 7.50 – 7.18 (m, 6H), 5.83 (ddt, *J* = 17.3, 10.7, 5.6 Hz, 1H), 5.21 – 5.09 (m, 2H), 3.90 (td, *J* = 5.8, 1.6 Hz, 2H), 3.64 (dd, *J* = 9.3, 4.1 Hz, 1H), 3.29 (dd, *J* = 13.7, 4.1 Hz, 1H), 2.73 (dd, *J* = 13.7, 9.3 Hz, 1H), 1.41 (br s, 2H). **^{13}C NMR (101 MHz, CDCl$_3$)** *δ* 174.0, 137.9, 134.3, 129.3, 128.7, 126.8, 116.1, 56.5, 41.5, 41. **HRMS (ESI)** *m/z* calculated for $C_{12}H_{16}N_2O$ [M+H]$^+$: 205.1335, found: 205.1334. **IR (ATR diamond, neat):** *v* 3299.1, 3082.8, 3027.2, 2919.3, 1652.5, 1640.9, 1517.3, 1496.0, 1453.8, 1419.3, 1254.5, 989.9, 918.2, 743.6, 699.7 cm^{-1}.

(*S*)-2-Amino-*N*-benzyl-3-phenylpropanamide (1e): Colourless oil (437 mg, 86% yield); **^{1}H NMR (400 MHz, CDCl$_3$)** *δ* 7.64 (t, *J* = 5.8 Hz, 1H), 7.41 – 7.22 (m, 10H), 4.47 (dd, *J* = 5.9, 4.0 Hz, 2H), 3.80 – 3.63 (m, 1H), 3.33 (dd, *J* = 13.7, 4.2 Hz, 1H), 2.79 (dd, *J* = 13.7, 9.1 Hz, 1H), 1.61 (br s, 2H).

(*S*)-2-Amino-*N*-(4-methylbenzyl)-3-phenylpropanamide (1f): Yellow solid (488 mg, 91% yield); m.p. 70.1-71.5 °C; **^{1}H NMR (400 MHz, CDCl$_3$)** *δ* 7.59 (s, 1H), 7.37 – 7.09 (m, 9H), 4.41 (dd, *J* = 5.9, 2.6 Hz, 2H), 3.67 (s, 1H), 3.30 (dd, *J* = 13.7, 4.2 Hz, 1H), 2.79 (dd, *J* = 13.7, 8.9 Hz, 1H), 2.36 (s, 3H), 1.64 (s, 2H). **^{13}C NMR (100 MHz, CDCl$_3$)** *δ* 174.0, 137.9, 137.0, 135.4, 129.4 (2C), 129.3 (2C), 128.7 (2C), 127.8 (2C), 126.8, 56.5, 42.9, 41.0, 21.1. **HRMS (ESI)** *m/z* calculated for $C_{17}H_{20}N_2O$ [M+H]$^+$: 269.1648, found: 269.1650. **IR (ATR diamond, neat):** *v* 3284.9, 3022.7, 2915.4, 2857.7, 1637.5, 1530.2, 1515.0, 1493.1, 743.3, 697.1 cm^{-1}.

(*S*)-2-Amino-*N*-(4-fluorobenzyl)-3-phenylpropanamide (1g): Yellow solid (501 mg, 92% yield); m.p. 59.4-60.0 °C; **^{1}H NMR (600 MHz, CDCl$_3$)** *δ* 7.60 (br s, 1H), 7.29 (t, J = 7.4 Hz, 2H), 7.26-7.21 (m, 1H), 7.20 – 7.15 (m, 4H), 6.97 (t, J = 8.6 Hz, 2H), 4.38 (qd, J = 14.8, 6.0 Hz, 2H), 3.64 (dd, J = 9.1, 4.3 Hz, 1H), 3.25 (dd, J =

13.7, 4.2 Hz, 1H), 2.75 (dd, J = 13.7, 9.0 Hz, 1H), 1.42 (br s, 2H). **^{13}C NMR (151 MHz, CDCl$_3$)** *δ* 174.2, 137.9, 134.3 (2C), 129.5 (2C), 128.8 (2C), 126.9 (2C), 115.6, 115.5, 56.5, 42.5, 41.1. **HRMS (ESI)** *m/z* calculated for $C_{16}H_{17}FN_2O$ [M+H]$^+$: 273.1398, found: 273.1395. **IR (ATR diamond, neat):** ν 3350.2, 3297.0, 3271.2, 1654.1, 1601.7, 1526.3, 1507.3, 1220.8, 723.5, 703.2 cm^{-1}.

(*S*)-2-Amino-*N*-phenethyl-3-phenylpropanamide (1h): Yellow solid (494 mg, 92% yield); m.p. 58.6-60.7 °C; **^{1}H NMR (400 MHz, CDCl$_3$)** *δ* 7.40 (d, *J* = 5.9 Hz, 1H), 7.35 – 7.11 (m, 10H), 3.51 (dq, *J* = 19.9, 6.7 Hz, 3H), 3.22 (dd, *J* = 13.7, 4.1 Hz, 1H), 2.78 (t, *J* = 7.1 Hz, 2H), 2.69 (dd, *J* = 13.6, 9.1 Hz, 1H), 1.33 (br s, 2H). **^{13}C NMR (101 MHz, CDCl$_3$)** *δ* 174.2, 139.0, 137.9, 129.3 (2C), 128.8 (2C), 128.7 (2C), 128.5 (2C), 126.8, 126.4, 56.4, 41.0, 35.8. **HRMS (ESI)** *m/z* calculated for $C_{17}H_{20}N_2O$ [M+H]$^+$: 269.1648, found: 269.1649. **IR (ATR diamond, neat):** *v* 3360.5, 3331.3, 3062.4, 3026.7, 2918.8, 1644.4, 1522.9, 1494.2, 1453.8, 740.9, 695.7 cm^{-1}.

(*S*)-2-Amino-*N*,3-diphenylpropanamide (1i): Colourless solid (374 mg, 78% yield); **^{1}H NMR (400 MHz, CDCl$_3$)** *δ* 9.44 (s, 1H), 7.66 – 7.58 (m, 2H), 7.42 – 7.23 (m, 7H), 7.13 (t, *J* = 7.4 Hz, 1H), 3.77 (dd, *J* = 9.5, 4.0 Hz, 1H), 3.41 (dd, *J* = 13.8, 3.9 Hz, 1H), 2.82 (dd, *J* = 13.8, 9.5 Hz, 1H), 1.61 (s, 2H).

(*S*)-2-Amino-3-phenyl-*N*-(*p*-tolyl)propanamide (1j): Colourless solid (532 mg, 75% yield); **^{1}H NMR (400 MHz, CDCl$_3$)** *δ* 9.37 (br s, 1H), 7.50 (m, 2H), 7.35–7.24 (m, 5H), 7.18-7.06 (m, 2H), 3.83–3.63 (m, 1H) 3.47–3.31 (dd, J = 14, 4.8 Hz, 1H), 2.88–2.73 (m ,1H), 2.35 (s, 3H), 1.56 (br s, 2H).

(*S*)-2-Amino-3-phenyl-*N*-(4-methoxyphenyl)propanamide (1k): Colourless solid (516 mg, 77% yield); **^{1}H NMR (400 MHz, CDCl$_3$)** *δ* 9.26 (br s, 1H), 7.55-7.52 (m, 2H), 7.25-7.04 (m, 7H), 3.38-3.35 (m, 1H), 3.23 (m, 4H), 2.82-2.76 (br s, 1H), 1.91 (br s, 2H).

(*S*)-2-Amino-*N*-(3,4-dicyanophenyl)-3-phenylpropanamide (1l): Light green oil (69 mg, 33% yield); **^{1}H NMR (600 MHz, CDCl$_3$)** *δ* 10.03 (br s, 1H), 8.21 (d, *J* = 2.2 Hz, 1H), 7.88 (dd, *J* = 8.6, 2.2 Hz, 1H), 7.72 (d, *J* = 8.5 Hz, 1H), 7.36 – 7.30 (m, 2H), 7.30 – 7.24 (m, 1H), 7.24 – 7.19 (m, 2H), 3.78 (dd, *J* = 9.3, 4.0 Hz, 1H), 3.32 (dd, *J* = 13.9, 4.1 Hz, 1H), 2.83 (dd, *J* = 13.9, 9.2 Hz, 1H), 1.61 (br s, 2H). **^{13}C NMR (151 MHz, CDCl$_3$)** *δ* 173.5, 156.0, 142.2, 136.9, 134.6, 129.3 (2C), 129.1 (2C), 127.4, 123.4, 122.8, 117.0, 115.6, 115.3, 110.0, 56.7, 40.3. **HRMS (ESI)** *m/z* calculated for $C_{17}H_{14}N_4O$ [M+H]$^+$: 290.1168, found: 290.1164. **IR (ATR diamond, neat):** *v* 3385.8, 3265.1, 3028.3, 2923.5, 2230.9, 1693.9, 1597.3, 1568.7, 1497.2, 1407.5, 1315.3, 1253.1, 1187.7, 1098.4, 906.4, 837.9, 727.5, 699.7 cm^{-1}.

(*S*)-2-Amino-*N*-butyl-3-(4-hydroxyphenyl)propanamide (1n): Colourless solid (455 mg, 96% yield); m.p. 140.7-141.2 °C; **^{1}H NMR (600 MHz, DMSO)** *δ* 7.71 (t, *J* = 5.8 Hz, 1H), 6.99 – 6.87 (m, 2H), 6.68 – 6.55 (m, 2H), 3.26 (dd, *J* = 7.8, 5.5 Hz, 1H), 3.05 – 2.91 (m, 2H), 2.73 (dd, *J* = 13.4, 5.5 Hz, 1H), 2.52 – 2.47 (m, 1H), 2.37 (d, *J* = 5.5 Hz, 1H), 1.35 – 1.22 (m, 2H), 1.22 – 1.08 (m, 2H), 0.80 (t, *J* = 7.3 Hz, 3H). **^{13}C NMR (151 MHz, DMSO)** *δ* 174.4, 156.3, 130.7 (2C), 129.0, 115.4 (2C), 56.9, 40.8, 38.5, 31.7, 20.0, 14.2. **HRMS (ESI)** *m/z* calculated for $C_{13}H_{20}N_2O_2$ [M+H]$^+$: 237.1598, found: 237.1560. **IR (ATR diamond, neat):** *v* 3338.5, 3322.0, 3281.5, 2952.1, 2925.8, 2871.7, 2854.0, 2669.3, 2585.8, 1635.9, 1554.8, 1516.7, 1455.4, 1381.2, 1250.4, 1098.8, 996.6, 825.1, 700.0, 557.8 cm^{-1}.

(*S*)-2-Amino-*N*-benzyl-3-(4-hydroxyphenyl)propanamide (1o): Colourless solid (496 mg, 92% yield); m.p. 144.5-145.3 °C; **^{1}H NMR (600 MHz, DMSO)** *δ* 9.25 – 9.03 (m, 1H), 8.23 (t, *J* = 6.1 Hz, 1H), 7.32 – 7.11 (m, 3H), 7.14 – 7.03 (m, 2H), 7.00 – 6.89 (m, 2H), 6.68 – 6.56 (m, 2H), 4.22 (ddd, *J* = 50.0, 15.1, 6.0 Hz, 2H), 3.34 (dd, *J* = 7.7, 5.8 Hz, 1H), 2.77 (dd, *J* = 13.4, 5.7 Hz, 1H), 2.53 (dd, *J* = 13.4, 7.7 Hz, 1H), 1.94 – 1.69 (m, 2H). **^{13}C NMR (151 MHz, DMSO)** *δ* 174.9, 156.3, 140.0, 130.8 (2C), 129.1 (2C), 128.7 (2C), 127.7, 127.2, 115.5 (2C), 57.1, 42.4, 41.0. **HRMS (ESI)** *m/z* calculated for $C_{16}H_{18}N_2O_2$ [M+H]$^+$: 271.1441, found: 271.1440. **IR (ATR diamond, neat):** *v* 3334.3, 3276.5, 2950.1, 2926.6, 2856.5, 2669.3, 2580.7, 1636.3, 1542.9, 1515.2, 1453.9, 1243.6, 1098.9, 998.2, 825.5, 696.7, 536.8 cm^{-1}.

(*S*)-2-Amino-*N*-(3-fluorophenyl)-3-(4-hydroxyphenyl)propanamide (1p): Light yellow waxy solid (139 mg, 50% yield); **^{1}H NMR (400 MHz, CD_3OD)** *δ* 7.51 (dt, *J* = 11.2, 2.2 Hz, 1H), 7.30 – 7.17 (m, 2H), 7.09 – 7.01 (m, 2H), 6.81 (tdd, *J* = 8.3, 2.6, 1.1 Hz, 1H), 6.77 – 6.71 (m, 2H), 4.93 (br s, 1H), 3.64 (dd, *J* = 7.2, 6.4 Hz, 1H), 2.99 (dd, *J* = 13.6, 6.4 Hz, 1H), 2.86 – 2.75 (dd, *J* = 13.6, 7.2 Hz, 1H). **^{13}C NMR (101 MHz, CD_3OD)** *δ* 173.9, 164.0, 161.6, 156.0, 139.8, 139.6, 130.1 (2C), 129.9, 129.8, 127.8, 115.4, 115.3, 115.1 (2C), 110.5, 110.2, 107.1, 106.8, 57.1, 47.5, 47.3, 47.1, 40.4. **HRMS (ESI)** *m/z* calculated for $C_{15}H_{15}FN_2O_2$ [M+H]$^+$: 274.1118, found: 258.1117. **IR (ATR diamond, neat):** *v* 3270.2, 3029.1, 2920.7, 2397.7, 1667.5, 1610.0, 1551.4, 1512.7, 1491.7, 1443.0, 1423.3, 1249.9, 1016.4, 954.7, 858.3, 814.4, 774.9, 678.4 cm^{-1}.

(*S*)-2-Amino-*N*-butyl-3-methylbutanamide (1q): Colourless oil (320 mg, 93% yield); **^{1}H NMR (400 MHz, DMSO)** *δ* 7.99 (br t, 1H), 3.92 (s, 2H), 3.20 – 2.93 (m, 3H), 1.99 – 1.80 (m, 1H), 1.45 – 1.34 (m, 2H), 1.28 (dp, *J* = 9.0, 7.0 Hz, 2H), 0.87 (dt, *J* = 7.3, 3.9 Hz, 6H), 0.82 (d, *J* = 6.8 Hz, 3H). **^{13}C NMR (101 MHz, DMSO)** *δ* 173.0, 59.9, 38.5 (2C), 31.7, 20.0, 19.7, 17.9, 14.1. **HRMS (ESI)** *m/z* calculated for $C_9H_{20}N_2O$ [M+H]$^+$: 173.1648, found: 173.1650. **IR (ATR diamond, neat):** *v* 3675.4, 3280.3, 3071.0, 2958.6, 2931.4, 2872.7, 1642.8, 1531.5, 1465.2, 1370.7, 1299.9, 1242.0, 1076.3, 980.0, 686.1 cm^{-1}.

(*S*)-2-Amino-*N*,3-dimethylbutanamide (1r): Colourless oil (234 mg, 90% yield); **^{1}H NMR (400 MHz, DMSO)** *δ* 7.94 (br s, 1H), 3.78 (s, 2H), 3.05 (d, *J* = 5.4 Hz, 1H), 2.61 (d, *J* = 4.6 Hz, 3H), 1.89 (pd, *J* = 6.9, 5.4 Hz, 1H), 0.87 (d, *J* = 6.9 Hz, 3H), 0.81 (d, *J* = 6.8 Hz, 3H). **^{13}C NMR (101 MHz, DMSO)** *δ* 173.8, 60.0, 31.6, 25.8, 19.7, 17.9. **HRMS (ESI)** *m/z* calculated for $C_6H_{14}N_2O$ [M+H]$^+$: 131.1179, found: 131.1176. **IR (ATR diamond, neat):** *v* 3265.3, 3084.0, 2962.4, 2901.5, 2876.8, 1641.9, 1563.0, 1466.5, 1410.9, 1371.8, 1301.1, 1251.2, 1160.9, 1056.7, 977.8, 885.7, 586.7 cm^{-1}.

(*S*)-2-Amino-*N*-butylpropanamide (1s): Colourless oil (252 mg, 88% yield); **^{1}H NMR (400 MHz, $CDCl_3$)** *δ* 7.37 (t, *J* = 6.0 Hz, 1H), 3.47 (qt, *J* = 6.9, 2.6 Hz, 1H), 3.23 – 3.10 (m, 2H), 2.12 (d, *J* = 6.6 Hz, 2H), 1.52 – 1.35 (m, 2H), 1.35 – 1.21 (m, 5H), 0.94 – 0.77 (m, 3H). **^{13}C NMR (101 MHz, $CDCl_3$)** *δ* 175.2, 50.6, 38.7, 31.6, 21.5, 20.0, 13.7. **HRMS (ESI)** *m/z* calculated for $C_7H_{16}N_2O$ [M+H]$^+$: 145.1335, found: 145.1336. **IR (ATR diamond, neat):** *v* 3287.2, 3082.6, 2959.3, 2931.4, 2873.0, 1643.6, 1536.2, 1455.7, 1368.8, 1259.0, 1229.0, 1130.0, 1074.3, 956.8, 856.4, 665.4 cm^{-1}.

(*R*)-2-Amino-*N*-butyl-3-(1*H*-indol-3-yl)propanamide (1t): Colourless solid (471 mg, 91% yield); **^{1}H NMR (600 MHz, DMSO)** *δ* 10.80 (s, 1H), 7.75 (d, *J* = 5.7 Hz, 1H), 7.52 (dd, *J* = 7.9, 2.8 Hz, 1H), 7.32 – 7.25 (m, 1H), 7.10 (d, *J* = 2.4 Hz, 1H), 7.02 (ddd, *J* = 8.1, 6.9, 1.3 Hz, 1H), 6.93 (td, *J* = 7.4, 6.9, 1.1 Hz, 1H), 3.43 –

3.35 (m, 1H), 3.07 – 2.94 (m, 3H), 2.72 (dd, *J* = 14.1, 8.1 Hz, 1H), 2.08 – 1.71 (m, 2H), 1.34 – 1.24 (m, 2H), 1.22 – 1.11 (m, 2H), 0.80 (s, 3H).

Methyl L-phenylalanylglycinate (1u): Colourless oil (221 mg, 94% yield); **^{1}H NMR (400 MHz, CD_3OD)** δ 7.41 – 7.26 (m, 5H), 4.98 (br s, 1H), 4.23 (dd, *J* = 7.7, 6.4 Hz, 1H), 4.00 (s, 2H), 3.74 (s, 3H), 3.28 (dd, *J* = 14.1, 6.4 Hz, 1H), 3.13 (dd, *J* = 14.1, 7.8 Hz, 1H). **^{13}C NMR (101 MHz, CD_3OD)** δ 170.2, 169.1, 134.2, 129.2 (2C), 128.7 (2C), 127.4, 54.3, 51.5, 40.6, 37.1.

(*S*)-2-(Benzylamino)-*N*-butyl-3-phenylpropanamide (1v): Colourless solid (395 mg, 85% yield); m.p. 58.6-61.4 °C; **^{1}H NMR (400 MHz, $CDCl_3$)** δ 7.39 – 7.22 (m, 7H), 7.22 – 7.16 (m, 2H), 7.14 – 7.04 (m, 2H), 3.72 (d, *J* = 13.3 Hz, 1H), 3.59 (d, *J* = 13.3 Hz, 1H), 3.51 – 3.18 (m, 5H), 2.78 (dd, *J* = 13.8, 9.2 Hz, 1H), 1.48 (ddd, *J* = 14.3, 7.6, 5.0 Hz, 2H), 1.41 – 1.25 (m, 2H), 0.94 (t, *J* = 7.3 Hz, 3H). **^{13}C NMR (100 MHz, $CDCl_3$)** δ 173.2, 138.9, 137.3, 129.1 (2C), 128.8 (2C), 128.9 (2C), 128.0 (2C), 127.3, 126.9, 63.2, 52.6, 39.2, 38.8, 31.7, 20.1, 13.8. **HRMS (ESI)** *m/z* calculated for $C_{20}H_{26}N_2O$ $[M+H]^+$: 311.2118, found: 311.2115. **IR (ATR diamond, neat):** ν 3314.7, 3286.1, 3059.7, 3027.0, 2958.4, 2930.0, 2872.9, 1626.5, 1542.3, 1496.1, 1472.2, 1453.2, 1301.1, 1126.4, 750.1, 740.0, 695.0 cm^{-1}.

(*S*)-5-Benzyl-3-butylimidazolidine-2,4-dione (2a): Colourless solid (62 mg, 84% yield); $[\alpha]_D^{27}$ –72.52° (c 0.3, MeOH); **^{1}H NMR (600 MHz, $CDCl_3$)** δ 7.30-7.21 (m, 3H), 7.21-7.13 (m, 2H), 6.21 (s, 1H), 4.21 (ddd, *J* = 7.8, 3.9, 1.2 Hz, 1H), 3.47-3.29 (m, 2H), 3.21 (dd, *J* = 14.0, 4.0 Hz, 1H), 2.89 (dd, *J* = 14.0, 7.7 Hz, 1H), 1.46-1.37 (m, 2H), 1.19-1.09 (m, 2H), 0.86 (t, *J* = 7.4 Hz, 3H).

(*S*)-5-Benzyl-3-methylimidazolidine-2,4-dione (2b): Colourless solid (56 mg, 91% yield); $[\alpha]_D^{27}$–87.75° (c 0.3, MeOH); **^{1}H NMR (400 MHz, $CDCl_3$)** δ 7.31 – 7.20 (m, 3H), 7.17 (m, 2H), 6.08 (s, 1H), 4.21 (ddd, *J* = 8.8, 3.9, 1.2 Hz, 1H), 3.25 (dd, *J* = 14.0, 3.8 Hz, 1H), 2.91 (s, 3H), 2.86 – 2.78 (m, 1H).

(*S*)-5-Benzyl-3-hexylimidazolidine-2,4-dione (2c): Colourless solid (58 mg, 71% yield); $[\alpha]_D^{23}$ –58.81° (c 0.3, MeOH); **^{1}H NMR (600 MHz, $CDCl_3$)** δ 7.30 – 7.22 (m, 3H), 7.17 (d, *J* = 6.7 Hz, 2H), 5.99 (s, 1H), 4.21 (dd, *J* = 4.2, 1.2 Hz, 1H), 3.38 (dd, *J* = 7.9, 7.0 Hz, 2H), 3.22 (dd, *J* = 14.0, 3.9 Hz, 1H), 2.87 (dd, *J* = 14.0, 8.0 Hz, 1H), 1.43 (t, *J* = 7.1 Hz, 2H), 1.29 – 1.13 (m, 6H), 0.86 (t, *J* = 7.0 Hz, 3H).

(*S*)-3-Allyl-5-benzylimidazolidine-2,4-dione (2d): Colourless solid (39 mg, 85% yield); $[\alpha]_D^{20}$ –69.6° (c 0.3, MeOH); m.p. 94.5-95.3 °C; **^{1}H NMR (400 MHz, $CDCl_3$)** δ 7.38 – 7.24 (m, 3H), 7.20 (dd, *J* = 7.7, 1.8 Hz, 2H), 6.33 (s, 1H), 5.68 (ddt, *J* = 17.1, 10.2, 5.6 Hz, 1H), 5.11 (dp, *J* = 10.3, 1.3 Hz, 1H), 5.02 (dq, *J* = 17.1, 1.5 Hz, 1H), 4.28 (ddd, *J* = 7.8, 4.0, 1.3 Hz, 1H), 4.13 – 3.95 (m, 2H), 3.26 (dd, *J* = 14.0, 3.9 Hz, 1H), 2.94 (dd, *J* = 14.0, 7.9 Hz, 1H). **^{13}C NMR (101 MHz, $CDCl_3$)** δ 172.8, 157.1, 135.0, 130.9, 129.5, 128.8, 127.4, 117.6, 58.4, 40.5, 37.8. **HRMS (ESI)** *m/z* calculated for $C_{13}H_{14}N_2O_2$ $[M+H]^+$: 231.1288, found: 231.1289. **IR (ATR diamond, neat):** ν 3284.7, 2926.2, 1750.3, 1697.5, 1452.2, 1421.5, 1355.7, 1334.7, 1142.0, 1094.8, 964.5, 700.2 cm^{-1}.

(*S*)-3,5-Dibenzylimidazolidine-2,4-dione (2e): Colourless solid (76 mg, 90% yield); $[\alpha]_D^{27}$ –36.18° (c 0.3, MeOH); **^{1}H NMR (600 MHz, $CDCl_3$)** δ 7.29 – 7.07 (m, 10H), 6.43 (s, 1H), 4.63 – 4.48 (m, 2H), 4.22 (dd, *J* = 7.6, 5.3 Hz, 1H), 3.18 (dd, *J* = 14.1, 4.0 Hz, 1H), 2.89 (dd, *J* = 14.0, 7.7 Hz, 1H).

(*S*)-5-Benzyl-3-(4-methylbenzyl)imidazolidine-2,4-dione (2f): Colourless solid (78 mg, 88% yield); $[\alpha]_D^{23}$ −38.40° (c 0.3, MeOH); m.p. 125.6-127.1 °C; **^{1}H NMR (400 MHz, CDCl$_3$)** *δ* 7.30-7.27 (m, 3H), 7.19-7.17 (m, 4H), 7.11-7.10 (m, 2H), 5.50 (br s, 1H), 4.58 (d, *J* = 6.5 Hz, 2H), 4.25 (ddd, *J* = 8.7, 3.8, 1.2 Hz, 1H), 3.28 (dd, *J* = 13.9, 3.8 Hz, 1H), 2.85 (dd, *J* = 13.9, 8.7 Hz, 1H), 2.34 (s, 3H). **^{13}C NMR (101 MHz, CDCl$_3$)** *δ* 172.7, 156.6, 137.6, 135.2, 132.8, 129.3 (2C), 129.2 (2C), 128.9 (2C), 128.4 (2C), 127.4, 58.4, 41.9, 37.9, 21.2. **HRMS (ESI)** *m/z* calculated for $C_{18}H_{18}N_2O_2$ [M+H]$^+$: 295.1441, found: 295.1442. **IR (ATR diamond, neat):** *v* 3240.0, 3031.0, 2922.4, 1769.6, 1707.0, 1446.7, 1349.2, 1196.8, 906.8, 725.2 cm^{-1}.

(*S*)-5-Benzyl-3-(4-fluorobenzyl)imidazolidine-2,4-dione (2g): Colourless solid (80 mg, 89% yield); $[\alpha]_D^{23}$ −15.49° (c 0.4, MeOH); **^{1}H NMR (400 MHz, CDCl$_3$)** *δ* 7.18-7.02 (m, 7H), 6.88-6.83 (m, 2H), 5.29 (br s, 1H), 4.43 (dd, *J* = 15.0, 11.5 Hz, 2H), 4.18 (ddt, *J* = 7.6, 4.1, 1.1 Hz, 1H), 3.11 (ddd, *J* = 14.0, 4.0, 1.3 Hz, 1H), 2.83 (ddd, *J* = 14.0, 7.5, 1.1 Hz, 1H).

(*S*)-5-Benzyl-3-phenethylimidazolidine-2,4-dione (2h): Colourless solid (75 mg, 85% yield); $[\alpha]_D^{27}$ −89.90° (c 0.3, MeOH); m.p. 126.1-126.4 °C; **^{1}H NMR (400 MHz, CDCl$_3$)** *δ* 7.26-7.09 (m, 10H), 5.78 (br s, 1H), 4.09 (ddd, *J* = 8.8, 3.8, 1.1 Hz, 1H), 3.66-3.52 (m, 2H), 3.13 (dd, *J* = 13.9, 3.8 Hz, 1H), 2.74-2.63 (m, 3H). **^{13}C NMR (101 MHz, CDCl$_3$)** *δ* 172.9, 157.0, 137.8, 135.3, 128.3 (2C), 129.0 (2C), 128.9 (2C), 128.6 (2C), 127.5, 126.7, 58.2, 38.6, 38.0, 33.8. **HRMS (ESI)** *m/z* calculated for $C_{18}H_{18}N_2O_2$ [M+H]$^+$: 295.1441, found: 295.1443. **IR (ATR diamond, neat):** *v* 3286.0, 2985.3, 1764.3, 1683.3, 1453.2, 1423.6, 1355.5, 1130.1, 749.0, 726.0, 696.4 cm^{-1}.

(*S*)-5-Benzyl-3-phenylimidazolidine-2,4-dione (2i): Colourless solid (68 mg, 85% yield); $[\alpha]_D^{27}$ −109.72° (c 0.3, MeOH); **^{1}H NMR (400 MHz, CDCl$_3$)** *δ* 7.37-7.08 (m, 10H), 6.55 (br s, 1H), 4.30 (ddd, *J* = 7.1, 4.0, 1.2 Hz, 1H), 3.16 (dd, *J* = 13.9, 4.1 Hz, 1H), 2.99 (dd, *J* = 13.9, 7.0 Hz, 1H).

(*S*)-5-Benzyl-3-(*p*-tolyl)imidazolidine-2,4-dione (2j): Colourless solid (78 mg, 93% yield); $[\alpha]_D^{23}$ −163.89° (c 0.3, MeOH); m.p. 124.9-127.0 °C; **^{1}H NMR (400 MHz, CDCl$_3$)** *δ* 7.38 – 7.22 (m, 7H), 7.06 (dd, *J* = 8.4, 2.0 Hz, 2H), 6.55 (d, *J* = 7.6 Hz, 1H), 4.40 (ddd, *J* = 7.1, 4.0, 1.1 Hz, 1H), 3.26 (dt, *J* = 13.9, 3.7 Hz, 1H), 3.17 – 3.01 (m, 1H), 2.39 (s, 3H). **^{13}C NMR (101 MHz, CDCl$_3$)** *δ* 172.3, 156.7, 138.5, 134.7, 129.8 (2C), 129.6 (2C), 128.8 (2C), 128.6, 127.5, 126.2 (2C), 58.1, 37.9, 37.8, 21.2. **HRMS (ESI)** *m/z* calculated for $C_{17}H_{16}N_2O_2$ [M+H]$^+$: 281.1285, found: 281.1283. **IR (ATR diamond, neat):** *v* 3325.0, 3116.2, 2920.0, 2848.8, 1774.8, 1711.8, 1513.1, 1404.3, 1358.1, 1162.8, 818.1, 746.8, 695.4 cm^{-1}.

(*S*)-5-Benzyl-3-(4-methoxyphenyl)imidazolidine-2,4-dione (2k): Colourless solid (76 mg, 86% yield); $[\alpha]_D^{27}$ −143.07° (c 0.3, MeOH); **^{1}H NMR (400 MHz, CDCl$_3$)** *δ* 7.38 – 7.30 (m, 3H), 7.27 – 7.21 (m, 2H), 7.09 – 7.03 (m, 2H), 7.00 – 6.92 (m, 2H), 6.76 (s, 1H), 4.39 (ddd, *J* = 6.8, 4.1, 1.2 Hz, 1H), 3.83 (s, 3H), 3.24 (dd, *J* = 13.9, 4.1 Hz, 1H), 3.10 (dd, *J* = 13.9, 6.7 Hz, 1H).

(*S*)-4-(4-Benzyl-2,5-dioxoimidazolidin-1-yl)phthalonitrile (2l): Yellow solid (10 mg, 13% yield); $[\alpha]_D^{20}$ −101.3° (c 0.1, MeOH); m.p. 165.1-167.2 °C; **^{1}H NMR (600 MHz, CDCl$_3$)** *δ* 7.96 – 7.91 (m, 1H), 7.89 – 7.81 (m, 2H), 7.37 – 7.28 (m, 3H), 7.21 (dt, *J* = 6.1, 1.6 Hz, 2H), 6.06 (br s, 1H), 4.48 (ddd, *J* = 7.9, 3.9, 1.2 Hz, 1H), 3.34 (dd, *J* = 14.0, 3.9 Hz, 1H), 3.05 (dd, *J* = 14.0, 7.8 Hz, 1H). **^{13}C NMR (151 MHz, CDCl$_3$)** *δ* 181.7, 170.8, 154.0, 141.5, 136.3, 134.2, 134.1, 134.1, 129.5, 129.4 (2C), 129.2 (2C), 129.1, 128.1, 116.8, 115.0, 114.7, 114.3, 58.1, 38.1. **HRMS (ESI)** *m/z* calculated for $C_{18}H_{12}N_4O_2$ $[M+H]^+$: 316.3200, found: 316.3197. **IR (ATR diamond, neat):** *v* 3327.9, 3116.2, 3030.2, 2925.7, 2853.0, 2235.3, 1784.7, 1720.1, 1599.4, 1494.2, 1392.7, 1348.1, 1186.1, 1160.7, 1112.8, 1030.1, 907.7, 841.6, 727.7 cm^{-1}.

(*rac)*-5-Benzylimidazolidine-2,4-dione (2m): Colourless solid (43 mg, 75% yield); **^{1}H NMR (400 MHz, DMSO)** δ 10.43 (s, 1H), 7.93 (s, 1H), 7.35 – 7.13 (m, 5H), 4.39 – 4.29 (m, 1H), 2.93 (dd, *J* = 5.0, 3.7 Hz, 2H). **^{13}C NMR (101 MHz, DMSO)** δ 180.4, 162.4, 140.9, 135.0, 133.3, 131.9, 63.6, 41.7.

(*S*)-3-Butyl-5-(4-hydroxybenzyl)imidazolidine-2,4-dione (2n): Light yellow solid (70 mg, 89% yield); $[\alpha]_D^{23}$ –50.81° (c 0.3, MeOH); m.p. 173.5-174.2 °C; **^{1}H NMR (400 MHz, DMSO)** δ 9.21 (s, 1H), 8.26 – 8.03 (m, 1H), 7.07 – 6.85 (m, 2H), 6.71 – 6.53 (m, 2H), 4.27 (d, *J* = 1.1 Hz, 1H), 3.14 (d, *J* = 18.5 Hz, 2H), 2.84 (dd, *J* = 4.6, 2.2 Hz, 2H), 1.29 – 1.08 (m, 2H), 1.03 – 0.82 (m, 2H), 0.75 (t, *J* = 7.2 Hz, 3H). **^{13}C NMR (101 MHz, DMSO)** δ 174.0, 157.1, 156.7, 131.2 (2C), 125.3, 115.2 (2C), 57.6, 37.5, 35.9, 29.9, 19.5, 14.0. **HRMS (ESI)** *m/z* calculated for $C_{14}H_{18}N_2O_3$ $[M+H]^+$: 263.1690, found: 262.1689. **IR (ATR diamond, neat):** *v* 3285.8, 2954.1, 2926.0, 2866.0, 1742.6, 1689.1, 1613.9, 1515.3, 1448.7, 1204.9, 1175.0, 1109.2, 1081.3, 864.0, 824.1, 766.0, 566.5 cm^{-1}.

(*S*)-3-Benzyl-5-(4-hydroxybenzyl)imidazolidine-2,4-dione (2o): Light yellow solid (83 mg, 94% yield); $[\alpha]_D^{23}$ –19.71° (c 0.3, MeOH); m.p. 149.4-150.2 °C; **^{1}H NMR (600 MHz, DMSO)** δ 9.29 (s, 1H), 8.28 (s, 1H), 7.17 – 7.13 (m, 3H), 6.91 (d, *J* = 8.5 Hz, 2H), 6.72 – 6.64 (m, 2H), 6.63 – 6.56 (m, 2H), 4.44 – 4.22 (m, 3H), 2.92 – 2.78 (m, 2H). **^{13}C NMR (151 MHz, DMSO)** δ 173.9, 156.9, 156.8, 136.8, 131.5 (2C), 128.7 (2C), 127.4, 126.9 (2C), 125.4, 115.5 (2C), 58.0, 41.2, 35.7. **HRMS (ESI)** *m/z* calculated for $C_{17}H_{16}N_2O_3$ $[M+H]^+$: 296.1234, found: 296.1233. **IR (ATR diamond, neat):** *v* 3304.8, 3190.2, 3028.7, 2927.8, 1759.8, 1693.9, 1599.9, 1514.7, 1451.3, 1422.9, 1360.7, 1240.3, 1131.5, 961.9, 818.6, 755.0, 715.3, 694.9, 631.5, 569.1 cm^{-1}.

(*S*)-3-(3-Fluorophenyl)-5-(4-hydroxybenzyl)imidazolidine-2,4-dione (2p): Colourless solid (60 mg, 67% yield); $[\alpha]_D^{20}$ –92.3° (c 0.2, MeOH); m.p. 150.0-151.5 °C; **^{1}H NMR (400 MHz, CD_3OD)** δ 7.40 (td, *J* = 8.2, 6.3 Hz, 1H), 7.15 – 7.04 (m, 3H), 6.90 (ddd, *J* = 8.0, 1.9, 1.0 Hz, 1H), 6.84 (dt, *J* = 9.8, 2.3 Hz, 1H), 6.79 – 6.71 (m, 2H), 4.88 (br s, 2H) 4.46 (dd, *J* = 4.5 Hz, *J* = 4.5 Hz, 1H), 3.15 – 3.01 (m, 2H). **^{13}C NMR (101 MHz, CD_3OD)** δ 173.1, 163.6, 161.2, 156.5, 156.3, 133.2, 133.1, 130.8 (2C), 129.9, 129.8, 125.0, 122.2, 122.2, 114.8 (2C), 114.7, 114.5, 113.6, 113.4, 58.0, 36.0. **HRMS (ESI)** *m/z* calculated for $C_{16}H_{13}FN_2O_3$ $[M+H]^+$: 300.0910, found: 300.0913. **IR (ATR diamond, neat):** *v* 3260.9, 2426.2, 1771.9, 1599.0, 1600.4, 1514.0, 1492.1, 1422.2, 1348.8, 1238.6, 1185.9, 1166.8, 1015.1, 802.0, 781.5, 735.6 cm^{-1}.

(*S*)-3-Butyl-5-isopropylimidazolidine-2,4-dione (2q): Colourless oil (52 mg, 88% yield); $[\alpha]_D^{20}$ –36.91° (c 0.3, MeOH); **^{1}H NMR (400 MHz, $CDCl_3$)** δ 6.71 (s, 1H), 3.93 (dd, *J* = 3.7, 1.1 Hz, 1H), 3.59 – 3.40 (m, 2H), 2.28-2.20 (m, 1H), 1.66 – 1.49 (m, 2H), 1.41 – 1.27 (m, 2H), 1.06 (d, *J* = 7.0 Hz, 3H), 0.99 – 0.87 (m, 6H). **^{13}C NMR (101 MHz, $CDCl_3$)** δ 173.7, 158.7, 62.3, 38.3, 30.2, 30.1, 20.0, 18.8, 15.9, 13.6. **HRMS (ESI)** *m/z* calculated for $C_{10}H_{18}N_2O_2$ $[M+H]^+$: 199.1441, found: 199.1440. **IR (ATR diamond, neat):** *v* 3662.0, 3283.9, 2961.3, 2934.6, 2874.9, 1770.9, 1696.4, 1449.4, 1421.1, 1353.1, 1294.6, 1200.1, 1103.5, 1042.3, 922.1, 765.2, 624.1 cm^{-1}.

(*S*)-5-Isopropyl-3-methylimidazolidine-2,4-dione (2r): Colourless solid (34 mg, 72% yield); $[\alpha]_D^{20}$ –59.80° (c 0.3, MeOH); m.p. 127.1-128.6 °C; **^{1}H NMR (400 MHz, CDCl$_3$)** δ 6.68 (s, 1H), 3.95 (dd, *J* = 3.9, 1.2 Hz, 1H), 3.01 (s, 3H), 2.29-2.20 (m, 1H), 1.07 (d, *J* = 7.0 Hz, 3H), 0.92 (d, *J* = 6.8 Hz, 3H). **^{13}C NMR (101 MHz, CDCl$_3$)** δ 173.7, 158.6, 62.6, 30.2, 24.4, 18.8, 16.1. **HRMS (ESI)** *m/z* calculated for $C_7H_{12}N_2O_2$ [M+H]$^+$: 157.0972, found: 157.0972. **IR (ATR diamond, neat):** *v* 3283.6, 2966.0, 2874.7, 1745.7, 1693.8, 1470.0, 1392.2, 1355.2, 1305.7, 1280.3, 1197.4, 1143.9, 1115.1, 1100.2, 1041.6, 947.3, 832.6, 761.5, 719.9 cm^{-1}.

(*S*)-3-Butyl-5-methylimidazolidine-2,4-dione (2s): Colourless oil (37 mg, 73% yield); $[\alpha]_D^{20}$ –14.06° (c 0.3, MeOH); **^{1}H NMR (400 MHz, CDCl$_3$)** δ 6.66 (s, 1H), 4.08 (qd, *J* = 6.9, 1.0 Hz, 1H), 3.49 (td, *J* = 7.2, 1.5 Hz, 2H), 1.67 – 1.53 (m, 2H), 1.45 (d, *J* = 7.0 Hz, 3H), 1.41 – 1.26 (m, 2H), 0.93 (t, *J* = 7.3 Hz, 3H). **^{13}C NMR (101 MHz, CDCl$_3$)** δ 174.9, 158.0, 52.8, 38.4, 30.1, 19.9, 17.6, 13.6. **HRMS (ESI)** *m/z* calculated for $C_8H_{14}N_2O_2$ [M+H]$^+$: 171.1128, found: 171.1126. **IR (ATR diamond, neat):** *v* 3299.8, 2959.1, 2935.1, 2874.0, 1771.7, 1695.0, 1449.4, 1421.2, 1370.9, 1344.4, 1321.6, 1200.9, 1133.8, 1045.4, 936.2, 772.0, 594.5 cm^{-1}.

(*R*)-5-((1*H*-Indol-3-yl)methyl)-3-butylimidazolidine-2,4-dione (2t): Brown solid (35 mg, 41% yield); $[\alpha]_D^{20}$ +2.6° (c 0.1, MeOH); m.p. 129.0-130.8 °C; **^{1}H NMR (400 MHz, CDCl$_3$)** δ 8.26 (s, 1H), 7.61 (dt, *J* = 7.9, 1.0 Hz, 1H), 7.35 (dt, *J* = 8.2, 0.9 Hz, 1H), 7.22 (ddd, *J* = 8.2, 7.0, 1.2 Hz, 1H), 7.13 (ddd, *J* = 8.0, 7.0, 1.1 Hz, 1H), 7.00 (d, *J* = 1.9 Hz, 1H), 6.07 (s, 1H), 4.26 (ddd, *J* = 8.1, 3.8, 1.0 Hz, 1H), 3.50 – 3.31 (m, 3H), 3.07 (dd, *J* = 14.8, 8.1 Hz, 1H), 1.40 (p, *J* = 7.4 Hz, 2H), 1.27 – 1.11 (m, 2H), 0.86 (t, *J* = 7.3 Hz, 3H). **^{13}C NMR (101 MHz, CDCl$_3$)** δ 173.8, 157.8, 136.2, 127.1, 123.3, 122.4, 119.9, 118.7, 111.4, 109.3, 57.8, 38.4, 29.9, 27.9, 19.8, 13.6. **HRMS (ESI)** *m/z* calculated for $C_{16}H_{19}N_3O_2$ [M+H]$^+$: 286.1550, found: 286.1553. **IR (ATR diamond, neat):** *v* 3313.6, 2956.6, 2929.3, 2879.6, 1767.4, 1692.8, 1452.5, 1422.1, 1341.9, 1232.6, 1096.5, 739.5, 553.1 cm^{-1}.

Methyl (*S*)-2-(4-benzyl-2,5-dioxoimidazolidin-1-yl)acetate (2u): Colourless solid (30 mg, 38% yield); $[\alpha]_D^{20}$ –94.5° (c 0.2, MeOH); m.p. 132.9-135.4 °C; **^{1}H NMR (400 MHz, CDCl$_3$)** δ 7.39 – 7.30 (m, 2H), 7.34 – 7.26 (m, 1H), 7.26 – 7.18 (m, 2H), 5.96 (br s, 1H), 4.34 (ddd, *J* = 9.4, 3.8, 1.2 Hz, 1H), 4.22 (d, *J* = 1.0 Hz, 2H), 3.77 (s, 3H), 3.34 (dd, *J* = 14.0, 3.8 Hz, 1H), 2.88 (dd, *J* = 13.9, 9.3 Hz, 1H). **^{13}C NMR (101 MHz, CDCl$_3$)** δ 172.6, 167.4, 156.1, 135.4, 129.2 (2C), 129.0 (2C), 127.5, 58.8, 52.7, 39.2, 38.0. **HRMS (ESI)** *m/z* calculated for $C_{13}H_{14}N_2O_4$ [M+H]$^+$: 262.0954, found: 262.0950. **IR (ATR diamond, neat):** *v* 3232.1, 3108.9, 3031.5, 2954.5, 1774.6, 1716.3, 1498.8, 1455.4, 1431.9, 1344.6, 1221.7, 1157.4, 1084.9, 924.6, 729.0 cm^{-1}.

2,2'-(Carbonylbis(azanediyl))bis(*N*-butyl-3-phenylpropanamide) (3a): Colourless solid (116 mg, quant. yield); m.p. 210.5-211.7 °C; **^{1}H NMR (400 MHz, DMSO)** δ 7.76 (t, *J* = 5.6 Hz, 2H), 7.33 – 7.11 (m, 10H), 6.33 (d, *J* = 8.3 Hz, 2H), 4.27 (td, *J* = 7.8, 6.2 Hz, 2H), 3.03 (dt, *J* = 13.1, 6.6 Hz, 2H), 2.95 (dt, *J* = 12.7, 6.2 Hz, 2H), 2.85 (dd, *J* = 13.5, 6.2 Hz, 2H), 2.73 (dd, *J* = 13.6, 7.6 Hz, 2H), 1.37 – 1.24 (m, 4H), 1.24 – 1.10 (m, 4H), 0.82 (t, *J* = 7.2 Hz, 6H). **^{13}C NMR (101 MHz, DMSO)** δ 171.8 (2C), 157.1, 138.3 (2C), 129.7 (4C), 128.4 (4C), 126.6 (2C), 54.9 (2C), 39.3 (2C), 38.5 (2C), 31.5 (2C), 19.9 (2C), 14.1 (2C). **HRMS (ESI)** *m/z* calculated for $C_{27}H_{38}N_4O_3$ [M+H]$^+$: 467.3017, found: 467.3014. **IR (ATR diamond, neat):** *v* 3381.2, 3280.0, 2960.8, 2934.8, 2885.3, 1632.6, 1548.6, 1495.0, 1449.2, 1372.9, 1283.7, 1225.6, 1077.6, 1031.9, 740.2, 701.2, 615.5 cm^{-1}.

(*S*)-*N*-Butyl-3-phenyl-2-(3-phenylureido)propanamide (5a): Colourless solid (101 mg, quant. yield); m.p. 181.7-183.1 °C; **^{1}H NMR (400 MHz, DMSO)** *δ* 8.66 (s, 1H), 8.05 (t, *J* = 5.6 Hz, 1H), 7.39 – 7.15 (m, 9H), 6.89 (t, *J* = 7.3 Hz, 1H), 6.36 (d, *J* = 8.3 Hz, 1H), 4.47 (td, *J* = 7.8, 5.9 Hz, 1H), 3.18 – 2.91 (m, 3H), 2.84 (dd, *J* = 13.6, 7.5 Hz, 1H), 1.44 – 1.28 (m, 2H), 1.28 – 1.15 (m, 2H), 0.85 (t, *J* = 7.2 Hz, 3H). **^{13}C NMR (101 MHz, DMSO)** *δ* 171.6, 155.0, 140.8, 138.0, 129.8 (2C), 129.1 (2C), 128.5 (2C), 126.7, 121.6, 117.9 (2C), 54.4, 39.6, 38.6, 31.6, 20.0, 14.1. **HRMS (ESI)** *m/z* calculated for $C_{20}H_{25}N_3O_2$ $[M+H]^+$: 340.2020, found: 340.2017. **IR (ATR diamond, neat):** *v* 3279.3, 3089.2, 3062.7, 2957.2, 2929.4, 2870.3, 1634.0, 1544.3, 1497.3, 1440.9, 1312.2, 1225.9, 1030.9, 742.6, 691.6, 503.0 cm^{-1}.

References

1. Konnert, L.; Lamaty, F.; Martinez, J.; Colacino, E. *Chem. Rev.*, **2017**, *117*, 13757.
2. Mudit, M.; Khanfar M.; Muralidharan, A. et al. *Bioorg. Med. Chem.,* **2009**, *17 (4)*, 1731-1738.
3. Meusel, M.; Gütschow, M. *Org. Prep. Proced. Int.*, **2004**, *36*, 391.
4. Chang K.C.; Shieh B.; Petrash J.M. *Chem. Biol. Interact.*, **2017**, *276*, 149-154.
5. Nique, F.; Hebbe, S.; Triballeau, N. *J. Med. Chem.,* **2012**, *55 (19),* 8236–8247.
6. Kupfer, A.; Preisig, R. *Eur. J. Clin. Pharmacol.*, **1984**, *26*, 753-759.
7. Sabounchei, S.J.; Sayadi, M.; Hashemi, M.S. et al. *Appl. Organomet. Chem.*, **2017**, *31*, e3716.
8. Leitch, J.A.; Cook, H.P.; Bhonoah, Y.; Frost, C.G. *J. Org. Chem*., **2016**, *81*, 10081.
9. Kheirabadi, M.; Çelebi-Ölçüm, N.; Parker, M.F.L. et al. *J. Am. Chem. Soc.*, **2012**, *134*, 18345.
10. Oliveira, V.C.; Oliveira, J.M.; Menezes da Silva, V.H. et al. *Adv. Synth. Catal.*, **2020**, *362*, 3395.
11. Ravichandran, V.; Rai, R.L. et al. *Biomater. Sci. Polym. Ed.*, **2017**, *28*, 2131.
12. Kalník, M.; Gabko, P.; Bella, M.; Koóš, M. *Molecules*, **2021**, *26*, 4024.
13. Urech, F. *Justus Liebigs Ann. Chem. Pharm*., **1873**, *165*, 99.
14. Read, W.T. *J. Am. Chem. Soc*., **1922**, *44*, 1746.
15. Biltz, H. *Ber. Dtsch. Chem. Ges.*, **1908**, *41*, 1379.
16. Hotha, S.; Yarrow, J.C.; Yang, J.G. et al. *Angew. Chem. Int. Ed.*, **2003**, *42*, 2379.
17. Chen, F.; Lu, C.-F.; Nie, J.Q. et al. *Tetrahedron: Asymmetry*, **2015**, *26*, 180.
18. Konnert, L.; Gonnet, L.; Halasz, I. et al. *J. Org. Chem.*, **2016**, *81*, 9802.
19. Song, J.; Zhang, Z.-J.; Chen, S.-S.; Fan, T.; Gong, L.-Z. *J. Am. Chem. Soc.*, **2018**, *140*, 3177.
20. Briones, J.F.; Basarab, G.S. *Chem. Commun.*, **2016**, *52*, 8541.
21. Beller, M.; Eckert, M.; Moradi, W.A.; Neumann, H. *Angew. Chem. Int. Ed.* **1999**, *38*, 1454.
22. Dumbris, S.M.; Díaz, D.J.; McElwee-White, L. *J. Org. Chem*., **2009**, *74*, 8862.
23. Orito, K.; Miyazawa, M.; Nakamura, T. et al. *J. Org. Chem*., **2006**, *71*, 5951.
24. Albert, J.; Ariza, X.; Calvet, T. et al. *Organometallics*, **2013**, *32*, 649.
25. Mancuso, R.; Raut, D.S.; Della Ca', N. et al. *ChemSusChem*, **2015**, *8*, 2204.
26. Mancuso, R.; Della Ca', N.; Veltri, L.; Ziccarelli, I.; Gabriele, B. *Catalysts*, **2019**, *9*, 610.
27. Zhang, L.; Wang, C.; Han, J.; Huang, Z.-B.; Zhao, Y. *J. Org. Chem*., **2016**, *81*, 5256.
28. Bittner, S. *Amino Acids*, **2006**, *30*, 205.
29. Yamada, S.; Terashima, S.; Wagatsuma, M. *Tetrahedron*, **1970**, *11*, 1501.
30. Han, H.; Yang, S.-D.; Xia, J.-B. *J. Org. Chem.*, **2019**, *84*, 3357.
31. Gabriele, B.; Mancuso, R.; Salerno G.; Costa, M. *Chem. Commun*., **2003**, *2003*, 486.
32. Gabriele, B.; Salerno, G.; Mancuso R.; Costa, M. *J. Org. Chem*., **2004**, 69, 4741.
33. Sorenson, W.R. *J. Org. Chem*., **1959**, *24*, 978.
34. Prasad, H.S.; Srinivasa, G.R.; Channe Gowda, D. *Synth. Commun.*, **2005**, *35*, 1189.
35. Nowick, J.S.; Holmes, D.L.; Noronha, G. et al. *J. Org. Chem*., **1996**, *61*, 3929.
36. Chen, Y.; Su, L.; Yang, X.; Pan, W.; Fang, H. *Tetrahedron*, **2015**, *71*, 9234.
37. Dong, J.; Wang, Y.; Xiang, Q. et al. *Adv. Synth. Catal.*, **2013**, *355 (4)*, 692-696.
38. Kaur, B.; Kaur, M.; Kaur, N. et al. *J. Med. Chem*., **2019**, *62 (13)*, 6363–6376.

Chapter 3. Palladium-Catalysed Domino Carbonylation Cycloisomerisation of *ortho*-Alkynylanilines Bearing an Amide Moiety using CO-Surrogates

Introduction

The replacement of toxic carbon monoxide by easier-to-handle surrogates brings significant advantages for the implementation of carbonylation processes as it allows to perform syntheses without special equipment, thus making carbonylation reactions more accessible for scientific laboratories. Generally, the strategies for carbonylation by using alternative CO-sources can be grouped into two categories based on where the CO is generated: *ex situ* and *in situ*. The *ex situ* CO production involves the use of the two-chamber system, in which decarbonylation takes place in one vessel and carbonylation in another.[1] The *in situ* CO generation supposes that the CO release by a surrogate and consecutive carbonylation occur in the same pot.[2] The latter method is more attractive as it minimises the number of necessary manipulations and allows better control of the macroscopic reaction parameters (temperature, pressure, etc.), however, the compatibility of the reagents may impose certain limitations.[3]

Metal carbonyls as $Mo(CO)_6$[4] and $Co_2(CO)_8$[5] have been used for decades to promote carbonylation reactions, but their high toxicity by skin contact, inhalation or ingestion make them fairly difficult to handle, and the formation of large metal waste at the end of the process renders their use not sustainable. Known organic CO precursors as formamides[6], chloroform[7], polyoxymethylenes[8], formic acid[9], aryl formates[10], etc. are greener but usually require a specific activator. Taking into consideration the concepts of atom economy and sustainable chemistry, the choice of CO surrogate might be challenging.

In recent years, our research group has reported palladium-catalysed carbonylative cascade double-cyclisation processes to afford indole-fused furanones,[11] furobenzofuranones,[12] and oxazinoquinolinone derivatives[13] starting from easily accessible precursors. Specifically, anilines functionalised with alkyne moieties were successfully converted into polycyclic products through a sequence of intramolecular cyclisation and oxidative carbonylation steps under PdI_2/KI catalysis. Palladium iodide in combination with potassium iodide represents an efficient and stable catalytic system that can promote oxidative processes using molecular oxygen as a terminal oxidant. However, it is only active under high pressure of gaseous mixtures of CO and O_2 and, as a consequence, requires the use of autoclave and explosivity limits control.[14]

In the present study, the possibility of replacing carbon monoxide with CO surrogates for carbonylative cyclisation under palladium catalysis was considered. The employment of a CO surrogate implied the use of catalytic systems that can function efficiently with low concentrations of CO. Palladium acetate, a widely commercialised precursor, in combination with phosphine- and pyridine-based ligands is known to promote diverse oxidative carbonylation reactions at atmospheric pressure of CO,[15-17] as well as in the presence of CO surrogates.[18-20] We envisioned that this type of catalyst can be suitable for the carbonylative cyclisation of 2-alkynylanilines by *in situ* generated CO.

Results and Discussion

We commenced the optimisation study with testing the palladium-based catalysts under atmospheric pressure of carbon monoxide. *N*-benzylaniline **1a** bearing a propargylamide moiety in *ortho*-position was selected as a model substrate. Using 5 mol% of palladium acetate in combination with 1,10-phenanthroline in acetonitrile, we were pleased to observe full conversion of **1a** at room temperature in six hours (entry 1, Table 3-1). A reduced catalyst loading afforded the quantitative formation of the product **2a** in extended reaction time. Remarkably, the transformation proceeded selectively *via* 6-*endo*-*dig* cyclisation pathway.

Table 3-1. Optimisation Study for the Synthesis of **2a**.

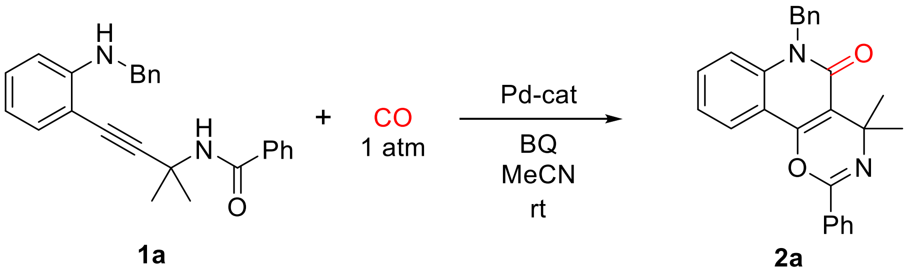

Entry	Deviation from Standard[a]	Reaction time	Yield[b] **2a**, %
1	none	6 h	99 (95)[c]
2	$Pd(OAc)_2$/1,10-phen 2 mol %	16 h	99
3	$Pd(OAc)_2$/1,10-phen 1 mol %	24 h	96
4	$Pd(TFA)_2$/1,10-phen 5 mol %	6 h	99
5	$Pd(OAc)_2$/bpy 5 mol %	8 h	95

[a] Standard conditions: **1a** (0.3 mmol, 1 equiv), $Pd(OAc)_2$ (0.015 mmol, 5 mol%), 1,10-phenanthroline (0.015 mmol, 5 mol%), 1,4-benzoquinone (0.36 mmol, 1.2 equiv) in acetonitrile (3 mL) with CO balloon at RT for 6 hours. [b] NMR yield. [c] Isolated yield.

Delighted by the obtained results, we continued with the investigation of CO surrogates. Aryl formate were proven to be interesting and practical CO surrogates.[21] They can be decomposed to CO and phenols by heating or in the presence of a small amount of base. The most robust analogue, benzene-1,3,5-triyl triformate (TFBen),[22-26] contains three formyl functions and thus can potentially generate higher amount of CO. Additionally, TFBen decomposes easily due to the keto-enolic tautomeric resonance of the decarbonylation product, phloroglucinol. This resonance significantly decreases the nucleophilicity of the hydroxygroups, which makes phloroglucinol almost non-reactive with metal catalyst intermediates. A considerable disadvantage of TFBen implementation is that its preparation proceeds in low yields (36-

40% obtained for this work), and the prepared compound displays low stability at room temperature. Partial degradation can be noticed after a couple of days.

Freshly prepared TFBen was reacted with **1a** at room temperature under inert atmosphere of nitrogen. Unfortunately, the formation of **2a** was not detected neither with 1.2 times excess nor with 3 equivalents of TFBen (Entries 1 and 2, Table 3-2). The major product of the reaction was formamide **3a**, which was formed as a result of TFBen deformylation. Therefore, CO generation did not occur under these conditions. Heating the reaction at 60 ˚C allowed the formation of the desired product **2a**, which was isolated in 50% yield. Rising the temperature to 80 ˚C increased the yield of **2a** to 95% (NMR). An attempt to halve the amount of TFBen resulted in a 33% drop in yield of the carbonylation product.

Table 3-2. Optimisation Study for the Carbonylation of **1a** Using TFBen.

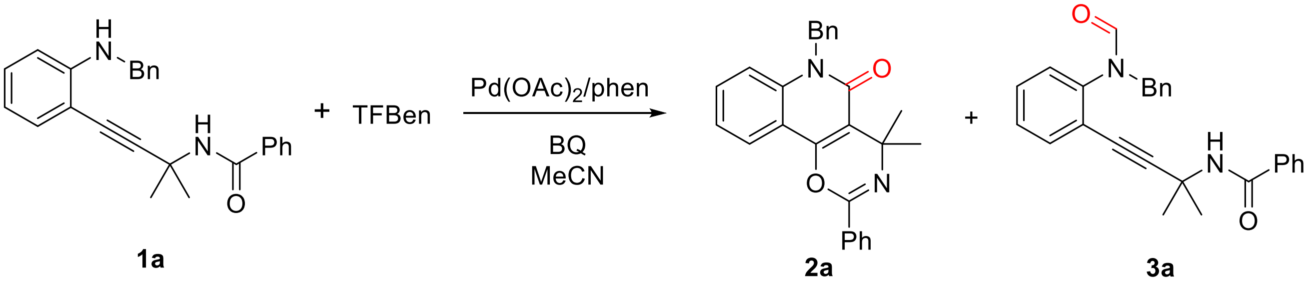

Entry	TFBen, equiv	Temperature	Yield^a **2a**, %	Yield^a **3a**, %	Conv.^{a} **1a**, %
1	1.2	RT	-	31	38
2	3	RT	-	36	44
3	3	60 ˚C	56 (50)^b	22	100
4	3	80 ˚C	95 (90)^b	traces	100
5	1.5	80 ˚C	64 (59)^b	traces	82

Reaction conditions: Under N_2, **1a** (0.3 mmol, 1 equiv), TFBen, $Pd(OAc)_2$ (0.015 mmol, 5 mol%), 1,10-phenanthroline (0.015 mmol, 5 mol%), 1,4-benzoquinone (0.36 mmol, 1.2 equiv) in acetonitrile (3 mL) for 24 hours. ^{a}NMR yield. ^{b}Isolated yield.

In collaboration with Baldini's group novel calix[6]arene hexaformates that contain six formyl functions, were prepared for the optimisation study. We suggested that calixarene-based surrogates should be more stable than TFBen and therefore can be stored for a longer time before use, even at room temperature. Additionally, greater number of formyl groups implies that more CO can potentially be released, and consequently the surrogate load can be reduced.

The *O*-formylation of hydroxy-groups of calixarenes was carried out with mixed anhydride of acetic and formic acids. The corresponding fully formylated products **4-6** were obtained with the yields ranging from 52 to 92%. The electronic effect of the substituents in *para* position to hydroxyls turned out to directly affect the efficiency of the formylation. The electron-donating *tert*-butyl provided excellent product formation, while the electron-attracting bromine, by reducing the nucleophilicity of the oxygen atom of phenol moieties, dramatically decreased the yield of the formylated product (Scheme 3-1).

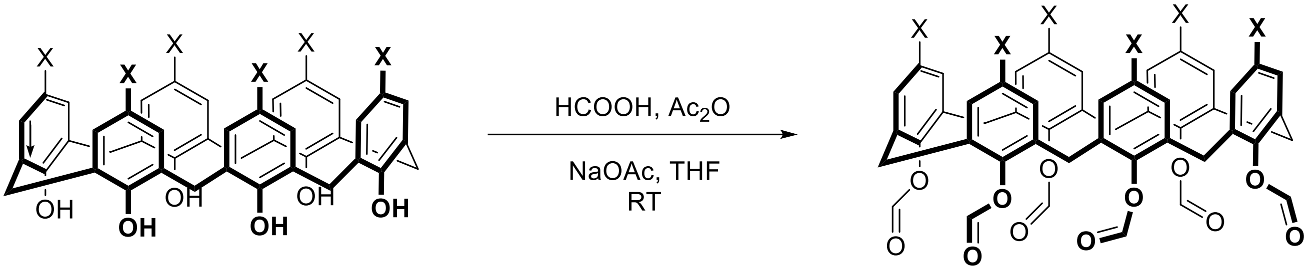

4, 84% X = H
5, 92% X = ^{t}Bu
6, 52% X = Br

Scheme 3-1. Synthesis of Calixarene-Based CO Surrogates **4-6**.

The obtained calix[6]arene hexaformates were introduced into the carbonylation reaction. Unfortunately, their low solubility did not allow the reaction to be carried out in acetonitrile. Therefore, 1,4-dioxane, in which calix[6]arenes can be dissolved upon heating, was selected as an alternative reaction medium.

Table 3-3. Optimisation Study for the Carbonylation of **1a** Using Calix[6]arene-Based Surrogates.

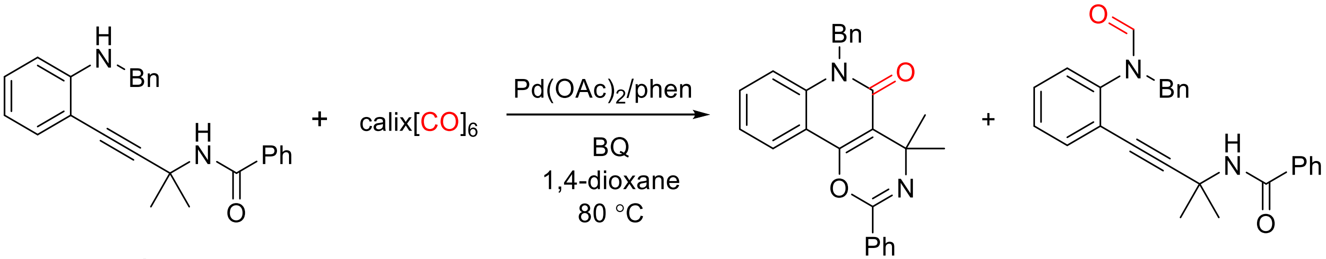

1a **2a** **3a**

Entry	CO surrogate	Additive	Yield[a] **2a**, %	Yield[a] **3a**, %	Conv.[a] **1a**, %
1	**4**	-	-	traces	8
2	**4**	Et$_3$N, 3 equiv	21 (15)[b]	14	39
3	**5**	Et$_3$N, 3 equiv	10	13	30
4	**6**	Et$_3$N, 3 equiv	62 (58)[b]	7	74

Reaction conditions: Under N$_2$, **1a** (0.3 mmol, 1 equiv), calix[6]arene hexaformate (0.45 mmol, 1.5 equiv), Pd(OAc)$_2$ (0.015 mmol, 5 mol%), 1,10-phenanthroline (0.015 mmol, 5 mol%), 1,4-benzoquinone (0.36 mmol, 1.2 equiv) in acetonitrile (3 mL) at 80 ˚C for 24 hours. [a]NMR yield. [b]Isolated yield.

Heating of the calix[6]arene hexaformate **4** at 80 ˚C was insufficient to initiate the CO generation. However, the presence of a base aided to promote the decarbonylation of **4** and thus to launch the process of the oxidative carbonylation of **1a**. It turned out that the decarbonylation of calix[6]arene hexaformates proceeds more smoothly when an electon-attracting group is present in the para-position of phenolic fragments. In fact, the best yield of the desired product **2a** was obtained when the surrogate **6** was used as a CO source.

As calixarene-based CO surrogates required the presence of an excess of base and did not improve the yield of **2a**, TFBen was the final choice as the CO surrogate for the oxidative carbonylation of 2-alkynylanilines. The optimised conditions (Entry 4, Table 3-2) were applied to compounds **1b-l**. The transformation proceeded with excellent yields for the majority of substrates. Weak electron-withdrawing substituent in *para* position to nitrogen of the aniline moiety (examples **2g** and **2h**) did not have major effect of the yield of the product, while strong electron-attracting groups as CF_3 and CO_2Me (**2i** and **2j**, respectively) dramatically decreased the nucleophilicity of the nitrogen, which led to a reduced formation of the product.

Table 3-4. Scope of the Substrates Obtained Using TFBen as a CO Source.

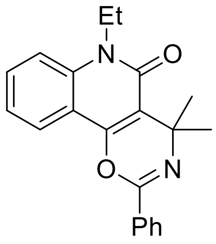 **2b**, 84%	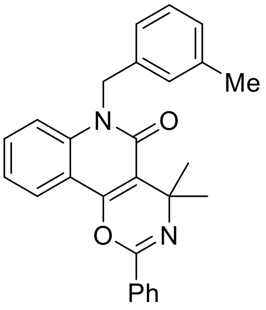 **2c**, 94%	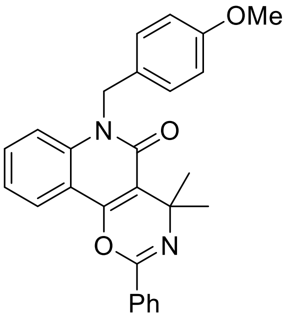 **2d**, 82%	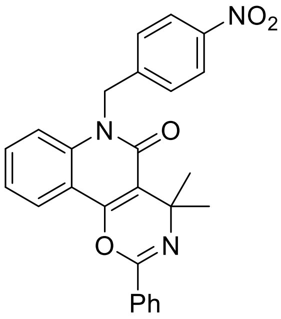 **2e**, 97%
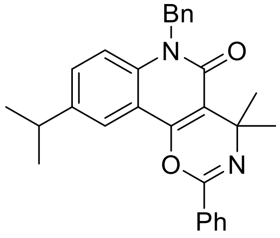 **2f**, 78%	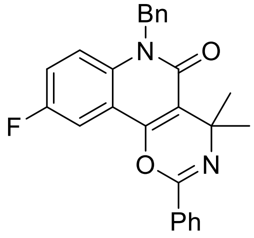 **2g**, 92%	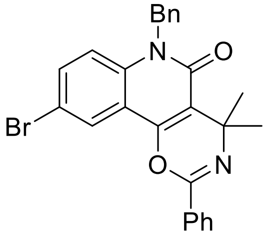 **2h**, 88%	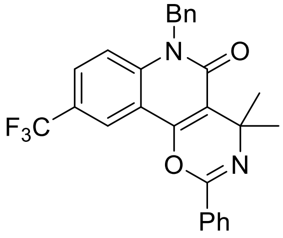 **2i**, 65%
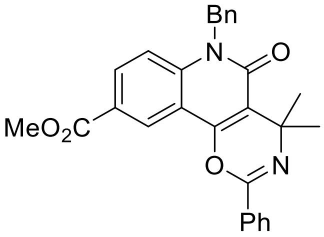 **2j**, 23%	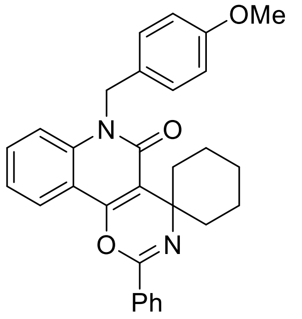 **2k**, 64%	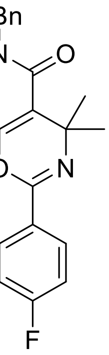 **2l**, 90%	

Based on the previous studies,[11-13,22] a mechanism of the reaction is proposed (Scheme 3-2). Initially, the triple bond of amide **1** coordinates Pd(II) to give complex **A**. The most favourable route lays in the nucleophilic attack of the oxygen of the amide group on the activated triple bond following the *6-endo-dig* cyclisation pathway to afford the σ-vinylpalladium complex **B**. At this point, carbon monoxide generated thanks to the thermal decarbonylation of TFBen, coordinates to palladium to form the complex **C**. Consecutive CO insertion and reductive elimination of the Pd^0 species allow the formation of the product **2**. The final step of the catalytic cycle the reoxidation of palladium by 1,4-benzoquinone to restore active palladium(II) species.

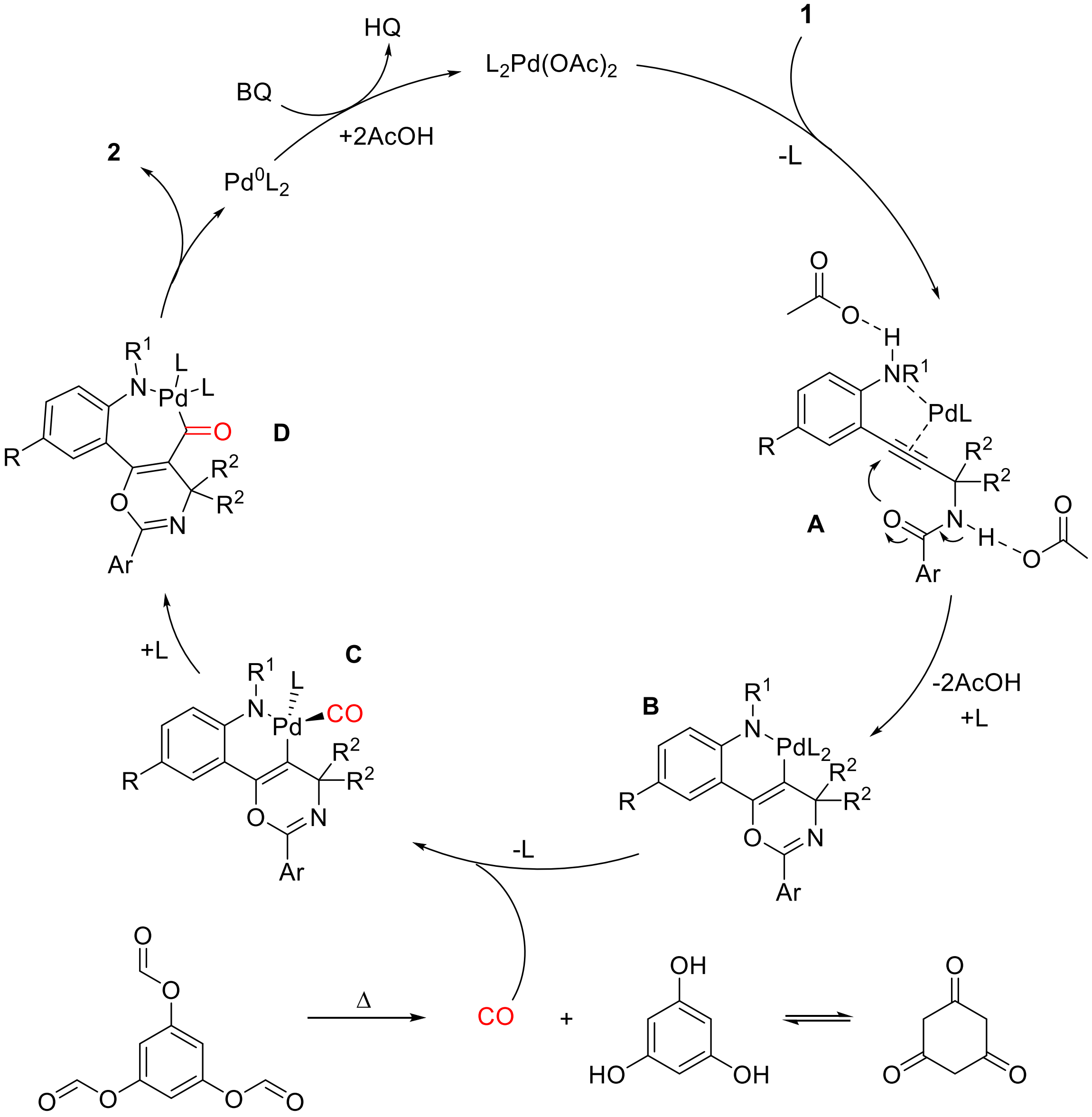

Scheme 3-2. Plausible Mechanism of the Pd-Catalysed Oxidative Carbonylation of **1**.

Conclusions

In the present study a new carbonylative methodology for the synthesis of fused oxazines has been developed. Selective domino *6-endo-dig* cyclisation and carbonylation has been achieved in mild conditions. Toxic and difficult-to-handle carbon monoxide has been successfully replaced with a handier analogue TFBen, that is able to generate CO *in situ* without any activators required. The presence of label substituents such as bromine is well tolerated. The efficiency of the process strongly depends on the nucleophilicity of the nitrogen atom of the aniline moiety. A mechanism of the described transformation is proposed.

Experimental part

General Procedure for the Reductive Amination of Aldehydes:[27]

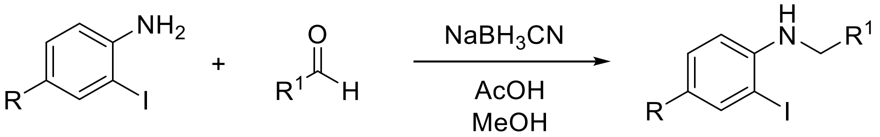

A solution of 2-iodoaniline (4 mmol) in 8 mL of methanol was introduced into a 25 mL flask. Aldehyde (6 mmol) and acetic acid (6 mmol) were added, and the mixture was cooled to 0 °C. Sodium cyanoborohydrate (8 mmol) was added to the solution portionwise within 30 minutes. Once the addition was finished, the reaction was left stirring at room temperature for 16 hours. When full conversion of the starting 2-iodoaniline was reached, the mixture was poured to a cooled 1 M Na_2CO_3 solution (25 mL), and the organic phase was extracted with ethyl acetate (4x10 mL) and dried over anhydrous Na_2SO_4. After filtration, the solvent was then removed under reduced pressure. The final secondary amine was purified by silica gel column chromatography using hexane/ethyl acetate mixtures as eluent.

General Procedure for the Synthesis of Propargylic Amides (N-Acylation):[13]

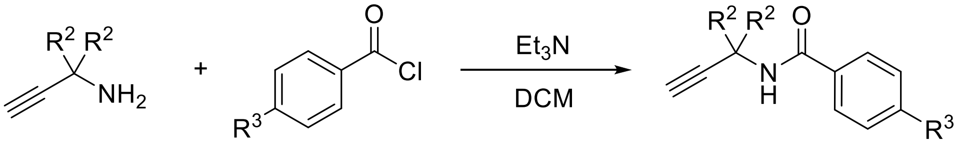

A solution of a propargylamine (10 mmol) and Et_3N (10.5 mmol, 1.46 mL) in 25 mL of DCM was added to a 100 mL flask and cooled to 0 °C. Aroyl chloride (10.1 mmol) was added dropwise to the solution, and the reaction mixture was stirred at room temperature for 1 h. The resulting mixture was poured into a 1 M solution of NH_4Cl (30 mL), and the organic phase was extracted with DCM (2x10 mL) and dried over anhydrous Na_2SO_4. After filtration, the solvent was then removed under reduced pressure. The obtained propargylic amide was purified by flash chromatography on SiO_2 using hexane/ethyl acetate mixtures as eluent.

*General Procedure for the Synthesis of Substrates **1** (Sonogashira Coupling):*[13]

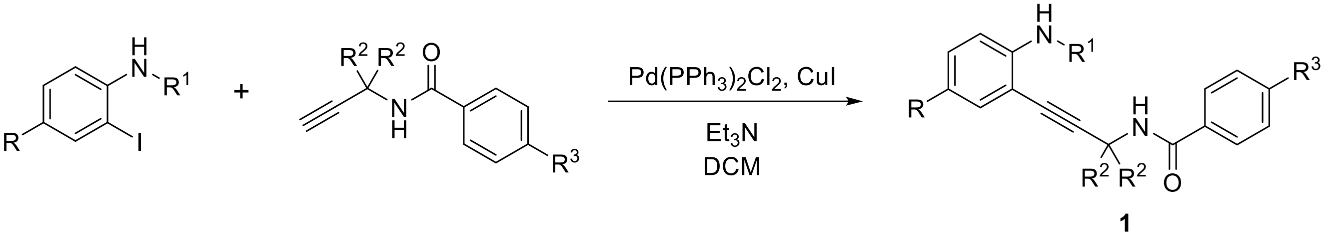

1

In a 100 mL Schlenk tube under nitrogen, $Pd(PPh_3)_2Cl_2$ (0.02 mmol, 14 mg) was added to a solution of *N*-substituted 2-iodoaniline (1 mmol) and propargylic amide (1.05 mmol) in 8 mL of DCM. Then Et_3N (57.5 mmol, 8 mL) and finally CuI (0.07 mmol, 13 mg) were added. The tube was sealed, and the reaction was stirred at room temperature for 4-24 h until the full conversion of the 2-iodoaniline. After filtration and concentration in vacuo, the residue was diluted with ethyl acetate (40 mL) and washed with 1 M NH_4Cl solution (25 mL). The organic layer was dried over anhydrous Na_2SO_4, filtered and concentrated under reduced pressure. Products **1** were isolated by flash column chromatography on SiO_2 using mixtures of hexane/ethyl acetate as eluent.

*General Procedure for the Oxidative Carbonylation of **1** Using Carbon Monoxide:*

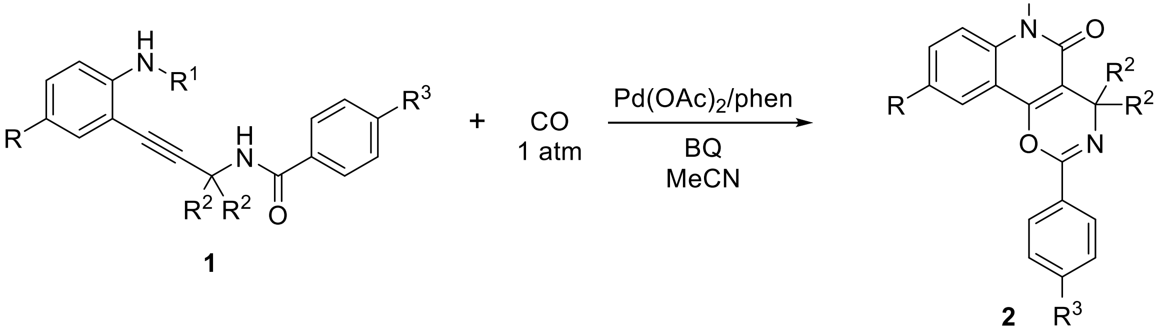

1

2

In a 45 mL Schlenk tube under nitrogen, palladium acetate (0.015 mmol, 3.4 mg) and 1,10-phenanthroline (0.015 mmol, 2.7 mg) were dissolved in 3 mL of acetonitrile. The solution was stirred for 5 minutes, and then **1** (0.3 mmol) and 1,4-benzoquinone (0.36 mmol) were added. The reaction then was purged with CO for ~30 seconds and, finally, a balloon charged with CO (1 atm) was attached to the tube. Full conversion of **1** was observed after 2-6 hours of reaction time. The resulting mixture was filtered through a Celite® pad and concentrated in vacuo. The product **2** was isolated by flash column chromatography on SiO_2 using mixtures of hexane/ethyl acetate as eluent.

*General Procedure for the Synthesis of Arylformates (TFBen[26], **4**-**6**):*

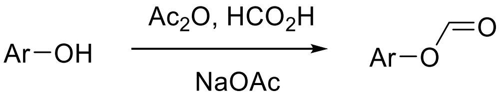

Under nitrogen, acetic anhydride (265 mmol, 10 mL) and formic acid (210 mmol, 20 mL) were added to a 100 mL three-necked flask, and the mixture was stirred for an hour at 60 °C. The mixture was cooled down to room temperature, and the solution of hydroxyaryl (1 mmol) together with CH_3OONa (1.2 mmol, 1 g) in 6 mL of THF was added. The reaction was monitored by TLC using hexane/ethyl acetate mixtures as eluents. When the reaction was complete (4-72 h), a 2 M Na_2CO_3 solution (50 ml) was added. The organic phase was extracted with DCM (3x25 ml), washed with brine (2x15 ml) and dried over anhydrous Na_2SO_4. After filtration, the solvent was then removed under reduced pressure. The residue was dissolved in methanol (30 mL), and the insoluble precipitate was filtered off. The evaporation of methanol afforded pure aryl formate as a colourless solid.

*General Procedure for the Oxidative Carbonylation of **1** Using TFBen as a CO Source:*

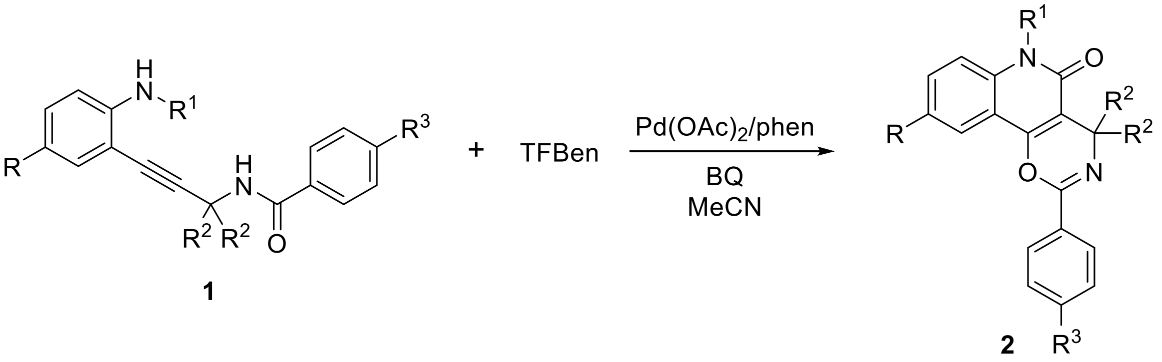

In a 10 mL tube under nitrogen, palladium acetate (0.015 mmol, 3.4 mg) and 1,10-phenanthroline (0.015 mmol, 2.7 mg) were dissolved in 3 mL of acetonitrile. The solution was stirred for 5 minutes, and then **1** (0.3 mmol), 1,4-benzoquinone (0.36 mmol) and TFBen (0.9 mmol) were added. The tube was immediately sealed, and the reaction mixture was heated at 80 °C. After 24 hours of stirring, the mixture was cooled to room temperature, filtered through a pad of Celite®, and concentrated under reduced pressure. The product **2** was isolated by flash column chromatography on SiO_2 using mixtures of hexane/ethyl acetate as eluent.

***N*-(4-(2-(Benzylamino)phenyl)-2-methylbut-3-yn-2-yl)benzamide (1a):** Yellow solid (331 mg, 90% yield); m.p. 106.5-108.5 °C; **^{1}H NMR (400 MHz, $CDCl_3$)** δ 7.74–7.66 (m, 2H), 7.55–7.47 (m, 1H), 7.46–7.37 (m, 4H), 7.34–7.20 (m, 4H), 7.15–7.07 (m, 1H), 6.58 (td, *J* = 7.4, 0.9 Hz, 1H), 6.53 (d, *J* = 8.3 Hz, 1H), 6.34 (s, 1H), 6.31 (bs, 1H), 4.58 (s, 2H), 1.85 (s, 6H). **^{13}C NMR (101 MHz, $CDCl_3$)** δ 166.8, 149.9, 140.0, 134.8, 131.5, 131.2, 129.8, 128.6, 128.4, 127.1, 126.9, 126.7, 115.5, 109.6, 106.9, 98.1, 78.8, 48.4, 47.3, 29.6. **IR (ATR)** ν 3407, 3365, 3021, 2982, 1636, 1601, 1575, 1518, 1484, 1287, 1182, 750, 737, 721 cm^{-1}. **HRMS (ESI)** *m/z* calcd for $C_{25}H_{24}N_2O$ $[M+H]^+$ 369.1967, found 369.1971.

***N*-(4-(2-(Ethylamino)phenyl)-2-methylbut-3-yn-2-yl)benzamide (1b):** Yellow solid (269 mg, 88% yield); m.p. 115.4-125.2 °C; **^{1}H NMR (400 MHz, $CDCl_3$)** δ 7.84 – 7.75 (m, 2H), 7.55 – 7.39 (m, 4H), 7.32 – 7.25 (m, 1H), 7.21 (ddd, *J* = 8.8, 7.3, 1.6 Hz, 1H), 6.66 – 6.53 (m, 2H), 6.42 (s, 1H), 5.47 (s, 1H), 3.28 (q, *J* = 7.2 Hz, 2H), 1.85 (s, 6H), 1.42 (t, *J* = 7.2 Hz, 3H). **^{13}C NMR (101 MHz, $CDCl_3$)** δ 166.6, 150.1, 135.1, 134.9, 134.9, 131.6, 131.4, 130.9, 129.9, 128.6, 128.3, 128.2, 127.7, 127.0, 115.2, 109.1, 106.7, 97.9, 78.6, 54.5, 48.4, 38.1, 29.7, 14.7, 14.5. **IR (ATR):** ν 3348.2, 3250.0, 3059.7, 2973.4, 2855.2, 1634.6, 1600.0, 1538.5, 1509.0, 1455.3, 1312.9, 1277.6, 1160.5, 743.3, 714.2, 691.3, 533.7 cm^{-1}. **HRMS (ESI)** *m/z* calcd for $C_{20}H_{22}N_2O$ $[M+H]^+$ 307.1810, found 307.1811.

***N*-(4-(2-((3-Methylbenzyl)amino)phenyl)-2-methylbut-3-yn-2-yl)benzamide (1c):** Yellow solid (340 mg, 89% yield); m.p. 89.2-92.3 °C; **^{1}H NMR (400 MHz, CDCl$_3$)** δ 7.74 – 7.66 (m, 2H), 7.54 – 7.48 (m, 1H), 7.44 – 7.37 (m, 2H), 7.27 – 7.15 (m, 5H), 7.13 – 7.07 (m, 1H), 7.07 – 7.01 (m, 1H), 6.58 – 6.47 (m, 2H), 6.30 (s, 1H), 6.19 (d, *J* = 39.8 Hz, 1H), 4.51 (s, 2H), 2.29 (s, 3H), 1.84 (s, 6H). **^{13}C NMR (101 MHz, CDCl$_3$)** δ 166.7, 149.9, 140.0, 138.0, 134.8, 131.5, 131.2, 129.8, 128.6, 128.3, 127.8, 127.5, 126.9, 124.1, 115.5, 109.6, 106.8, 98.0, 78.8, 48.5, 47.3, 29.6, 21.4 ppm. **IR (ATR)** ν 3421, 3334, 3021, 2983, 2968, 2923, 2860, 1638, 1602, 1572, 1514, 1458, 1434, 1290, 1249, 1177, 1162, 742, 733, 711, 689 cm^{-1}. **HRMS (ESI)** *m/z* calcd for $C_{26}H_{26}N_2O$ $[M+H]^+$ 383.2123, found 383.2119.

***N*-(4-(2-((4-Methoxybenzyl)amino)phenyl)-2-methylbut-3-yn-2-yl)benzamide (1d):** Yellow solid (374 mg, 94% yield); m.p. 128.5-130.0 °C; **^{1}H NMR (400 MHz, CDCl$_3$)** δ 7.73–7.67 (m, 2H), 7.51 (t, *J* = 7.4 Hz, 1H), 7.41 (t, *J* = 7.5 Hz, 2H), 7.34 (d, *J* = 8.5 Hz, 2H), 7.26 (dd, *J* = 7.5, 1.5 Hz, 1H), 7.14–7.08 (m, 1H), 6.83 (d, *J* = 8.6 Hz, 2H), 6.60–6.50 (m, 2H), 6.33 (s, 1H), 6.18 (s, 1H), 4.49 (s, 2H), 3.79 (s, 3H), 1.84 (s, 6H). **^{13}C NMR (101 MHz, CDCl$_3$)** δ 166.7, 158.5, 149.8, 134.8, 132.0, 131.5, 131.2, 129.8, 128.6, 128.3, 126.9, 115.5, 113.8, 109.6, 106.9, 98.1, 78.8, 55.2, 48.4, 46.7, 29.6. **IR (ATR)**: ν 3406, 3329, 2991, 2970, 1659, 1601, 1512, 1289, 1247, 1177, 1031, 755, 716 cm^{-1}. **HRMS (ESI)** *m/z* calcd for $C_{26}H_{26}N_2O_2$ $[M+H]^+$ 399.2073, found 399.2072.

***N*-(4-(2-((4-Nitrobenzyl)amino)phenyl)-2-methylbut-3-yn-2-yl)benzamide (1e):** Yellow solid (376 mg, 91% yield); m.p. 131.0-135.8 °C; **^{1}H NMR (400 MHz, CDCl$_3$)** δ 8.12 – 8.05 (m, 2H), 7.71 – 7.63 (m, 2H), 7.57 – 7.52 (m, 2H), 7.52 – 7.46 (m, 1H), 7.38 (dd, *J* = 8.3, 7.1 Hz, 2H), 7.28 (dd, *J* = 7.6, 1.6 Hz, 1H), 7.09 (ddd, *J* = 8.7, 7.4, 1.6 Hz, 1H), 6.67 (t, *J* = 6.3 Hz, 1H), 6.60 (td, *J* = 7.5, 1.0 Hz, 1H), 6.46 (s, 1H), 6.39 (dd, *J* = 8.4, 1.0 Hz, 1H), 4.66 (d, *J* = 5.1 Hz, 2H), 1.85 (s, 6H). **^{13}C NMR (101 MHz, CDCl$_3$)** δ 167.0, 149.4, 148.4, 146.9, 134.6, 131.8, 131.1, 129.8, 128.6, 127.7, 126.8, 123.7, 116.1, 109.3, 107.4, 98.4, 48.2, 46.8, 29.7. **IR (ATR)** ν 3398, 3338, 3079, 2974, 2929, 2851, 1639, 1598, 1575, 1515, 1484, 1450, 1347, 1293, 1282, 741, 736, 715 cm^{-1}. **HRMS (ESI)** *m/z* calcd for $C_{25}H_{23}N_3O_3$ $[M+H]^+$ 414.1818, found 414.1814.

***N*-(4-(2-(Benzylamino)-5-isopropylphenyl)-2-methylbut-3-yn-2-yl)benzamide (1f):** Yellow solid (320 mg, 78% yield); m.p. 115.3-117.9 °C; **^{1}H NMR (400 MHz, CDCl$_3$)** δ 7.74–7.69 (m, 2H), 7.54–7.48 (m, 1H), 7.46–7.38 (m, 4H), 7.34–7.28 (m, 2H), 7.27–7.22 (m, 1H), 7.17 (d, *J* = 2.1 Hz, 1H), 7.00 (dd, *J* = 8.5, 2.1 Hz, 1H), 6.49 (d, *J* = 8.5 Hz, 1H), 6.35 (bs, 1H), 6.08 (bs, 1H), 4.55 (s, 2H), 2.78 (hept, *J* = 6.9 Hz, 1H), 1.86 (s, 6H), 1.21 (d, *J* = 6.9 Hz, 6H). **^{13}C NMR (101 MHz, CDCl$_3$)** δ 166.8, 148.1, 140.3, 136.0, 134.9, 131.5, 128.9, 128.6, 128.4, 128.1, 127.1, 126.9, 126.7, 109.7, 106.7, 97.8, 79.0, 48.5, 47.6, 33.0, 29.6, 24.2. **IR (ATR)** ν 3410, 3347, 2987, 2973, 1664, 1597, 1513, 1288, 1252, 1178, 755 cm^{-1}. **HRMS (ESI)** *m/z* calcd for $C_{28}H_{30}N_2O$ $[M+H]^+$ 411.2436, found 411.2431.

***N*-(4-(2-(Benzylamino)-5-fluorophenyl)-2-methylbut-3-yn-2-yl)benzamide (1g):** Yellow solid (363 mg, 94% yield); m.p. 150.2-150.5 °C; **^{1}H NMR (400 MHz, CDCl$_3$)** δ 7.74–7.67 (m, 2H), 7.54–7.48 (m, 1H), 7.45–7.37 (m, 4H), 7.34–7.20 (m, 3H), 6.98 (dd, *J* = 8.9, 3.0 Hz, 1H), 6.82 (td, *J* = 8.7, 3.0 Hz, 1H), 6.41 (dd, *J* =

9.1, 4.6 Hz, 1H), 6.32 (bs, 1H), 6.22 (bs, 1H), 4.53 (s, 2H), 1.84 (s, 6H). **^{13}C NMR (101 MHz, CDCl$_3$)** δ 166.8, 153.9 (d, $J_{C,F}$ = 233.4 Hz), 146.6, 139.9, 134.7, 131.6, 128.6, 128.4, 127.0, 126.9, 126.8, 117.2 (d, $J_{C,F}$ = 23.6 Hz), 116.5 (d, $J_{C,F}$ = 22.2 Hz), 110.2 (d, $J_{C,F}$ = 7.9 Hz), 107.4 (d, $J_{C,F}$ = 9.2 Hz), 98.7, 77.9, 48.2, 47.7, 29.5. **IR (ATR)** ν 3403, 3332, 2954, 2917, 1644, 1602, 1511, 1489, 1324, 1297, 1172, 732, 710 cm^{-1}. **HRMS (ESI)** *m/z* calcd for $C_{25}H_{23}FN_2O$ [M+H]$^+$ 387.1873, found 387.1894.

***N*-(4-(2-(Benzylamino)-5-bromophenyl)-2-methylbut-3-yn-2-yl)benzamide (1h):** Brown solid (362 mg, 81% yield); m.p. 136.8-138.5 °C; **^{1}H NMR (400 MHz, CDCl$_3$)** δ 7.72–7.67 (m, 2H), 7.54–7.48 (m, 1H), 7.44–7.34 (m, 5H), 7.32–7.23 (m, 3H), 7.15 (dd, *J* = 8.8, 2.4 Hz, 1H), 6.46 (bs, 1H), 6.37 (d, *J* = 8.9 Hz, 1H), 6.32 (bs, 1H), 4.54 (d, *J* = 2.7 Hz, 2H), 1.83 (s, 6H). **^{13}C NMR (101 MHz, CDCl$_3$)** δ 166.8, 148.9, 139.5, 134.6, 133.2, 132.3, 131.6, 128.6, 128.5, 127.0, 126.89, 126.86, 111.1, 108.9, 106.4, 99.0, 77.6, 48.2, 47.2, 29.6. **IR (ATR)** ν 3410, 3347, 2951, 2908, 1649, 1600, 1565, 1514, 1481, 1331, 1293, 1170, 802, 729 cm^{-1}. **HRMS (ESI)** *m/z* calcd for $C_{25}H_{23}BrN_2O$ [M+H]$^+$ 447.1072, found 447.1078.

***N*-(4-(2-(Benzylamino)-5-(trifluoromethyl)phenyl)-2-methylbut-3-yn-2-yl)benzamide (1i):** Yellow solid (375 mg, 86% yield); m.p. 133.5-134.5 °C; **^{1}H NMR (400 MHz, CDCl$_3$)** δ 7.69 (d, *J* = 7.4 Hz, 2H), 7.55–7.47 (m, 2H), 7.45–7.37 (m, 4H), 7.33–7.21 (m, 4H), 6.93 (bs, 1H), 6.51 (d, *J* = 8.8 Hz, 1H), 6.31 (bs, 1H), 4.61 (d, *J* = 5.3 Hz, 2H), 1.84 (s, 6H). **^{13}C NMR (101 MHz, CDCl$_3$)** δ 166.9, 152.1, 139.2, 134.5, 131.7, 128.6, 128.5, 128.2 (q, $J_{C,F}$ = 3.4 Hz), 126.95, 126.87, 126.7 (q, $J_{C,F}$ = 3.3 Hz), 124.7 (q, $J_{C,F}$ = 270.3 Hz), 117.0 (q, $J_{C,F}$ = 32.8 Hz), 108.8, 106.8, 98.9, 77.7, 48.1, 46.9, 29.6. **IR (ATR)** ν 3397, 3325, 2965, 2910, 1634, 1604, 1508, 1488, 1322, 1300, 1169, 734 cm^{-1}. **HRMS (ESI)** *m/z* calcd for $C_{26}H_{24}F_3N_2O$ [M+H]$^+$ 437.1841, found 437.1893.

Methyl 3-(3-benzamido-3-methylbut-1-yn-1-yl)-4-(benzylamino)benzoate (1j): Yellow solid (320 mg, 75% yield); m.p. 161.2-163.0 °C; **^{1}H NMR (400 MHz, CDCl$_3$)** δ 7.96 (d, *J* = 1.9 Hz, 1H), 7.77 (dd, *J* = 8.7, 1.8 Hz, 1H), 7.68 (d, *J* = 7.6 Hz, 2H), 7.49 (t, *J* = 7.1 Hz, 1H), 7.42–7.35 (m, 4H), 7.32–7.21 (m, 3H), 7.08 (b t, *J* = 5.9 Hz, 1H), 6.49 (d, *J* = 8.8 Hz, 1H), 6.42 (bs, 1H), 4.63 (d, *J* = 5.9 Hz, 2H), 3.83 (s, 3H), 1.83 (s, 6H). **^{13}C NMR (101 MHz, CDCl$_3$)** δ 167.0, 153.3, 139.1, 134.6, 133.1, 131.7, 131.6, 128.6, 128.5, 126.98, 126.96, 126.9, 116.7, 108.5, 106.6, 98.4, 77.9, 51.5, 48.1, 46.9, 29.6. **IR (ATR)** ν 3400, 3323, 2955, 2915, 1709, 1641, 1554, 1504, 1484, 1328, 1298, 1172, 734 cm-1. **HRMS (ESI)** *m/z* calcd for $C_{27}H_{26}N_2O_3$ [M+H]$^+$ 427.2022, found 427.2026.

***N*-(1-((2-((4-Methoxybenzyl)amino)phenyl)ethynyl)cyclohexyl)benzamide (1k):** Yellow solid (346 mg, 79% yield); m.p. 96.1-102.3 °C; **^{1}H NMR (400 MHz, CDCl$_3$)** δ 7.76 – 7.65 (m, 2H), 7.55 – 7.45 (m, 1H), 7.41 (ddt, *J* = 8.2, 6.5, 1.2 Hz, 2H), 7.34 – 7.30 (m, 2H), 7.29 – 7.24 (m, 2H), 7.11 (ddd, *J* = 8.2, 7.4, 1.6 Hz, 1H), 6.86 – 6.76 (m, 2H), 6.62 – 6.52 (m, 2H), 6.21 (s, 2H), 4.47 (s, 2H), 3.79 (s, 3H), 2.43 – 2.29 (m, 2H), 1.96 – 1.51 (m, 8H), 1.39 (dd, *J* = 10.2, 6.3 Hz, 1H). **^{13}C NMR (101 MHz, CDCl$_3$)** δ 166.6, 146.0, 135.1, 131.5, 131.3, 129.6, 129.4, 128.6, 128.6, 128.4, 126.9, 116.8, 114.1, 113.8, 111.1, 55.3, 55.3, 47.7, 46.8, 37.5, 25.4, 22.7, 21.2. **IR (ATR)** ν 3393, 3346, 3335, 3061, 2930, 2845, 1646, 1600, 1574, 1508, 1483, 1301, 1247, 1172, 1030, 819, 739, 710 cm^{-1}. **HRMS (ESI)** *m/z* calcd for $C_{29}H_{30}N_2O_2$ [M+H]$^+$ 439.2386, found 439.2383.

N-(4-(2-(Benzylamino)phenyl)-2-methylbut-3-yn-2-yl)-4-fluorobenzamide (1l): Yellow solid (355 mg, 92% yield); m.p. 100.1-101.0 °C; **^{1}H NMR (400 MHz, CDCl$_3$)** δ 7.73–7.67 (m, 2H), 7.45 (d, *J* = 7.2 Hz, 2H), 7.36–7.25 (m, 4H), 7.18–7.11 (m, 1H), 7.09–7.02 (m, 2H), 6.62 (td, *J* = 7.5, 0.9 Hz, 1H), 6.58 (d, *J* = 8.3 Hz, 1H), 6.48 (bs, 1H), 6.31 (bs, 1H), 4.60 (s, 2H), 1.86 (s, 6H). **^{13}C NMR (101 MHz, CDCl$_3$)** δ 165.9, 164.7 (d, $J_{C,F}$ = 251.8 Hz), 149.9, 140.0, 131.3, 131.0 (d, $J_{C,F}$ = 3.1 Hz), 129.9, 129.4 (d, $J_{C,F}$ = 8.9 Hz), 128.5, 127.1, 126.9, 115.6, 115.5 (d, $J_{C,F}$ = 24.8 Hz), 109.7, 107.0, 98.2, 78.8, 48.5, 47.3, 29.6. **IR (ATR)** ν 3343, 3027, 2979, 2917, 1654, 1602, 1574, 1491, 1288, 1226, 1157, 848, 731 cm^{-1}. **HRMS (ESI)** *m/z* calcd for $C_{25}H_{23}FN_2O$ [M+H]$^+$ 387.1873, found 387.1836.

6-Benzyl-4,4-dimethyl-2-phenyl-4,6-dihydro-5*H*-[1,3]oxazino[5,6-c]quinolin-5-one (2a): Colourless solid (106 mg, 90% yield); m.p. 211.2-212.0 °C; **^{1}H NMR (400 MHz, CDCl$_3$)** δ 8.22 (dd, *J* = 7.9, 1.7 Hz, 2H), 8.13 (dd, *J* = 8.2, 1.4 Hz, 1H), 7.58–7.47 (m, 4H), 7.38–7.24 (m, 7H), 5.60 (bs, 2H), 1.90 (s, 6H). **^{13}C NMR (101 MHz, CDCl$_3$)** δ 161.0, 150.4, 146.1, 138.7, 136.6, 131.9, 131.2, 131.1, 128.9, 128.4, 127.5, 127.3, 126.5, 122.9, 122.1, 114.9, 114.0, 112.0, 52.9, 45.9, 30.1. **IR (ATR)** ν 3013, 2948, 1684, 1631, 1512, 1452, 1297, 1262, 1247, 1136, 1018, 743 cm^{-1}. **HRMS (ESI)** *m/z* calcd for $C_{26}H_{22}N_2O_2$ [M+H]$^+$ 395.1760, found 395.1762.

6-Ethyl-4,4-dimethyl-2-phenyl-4,6-dihydro-5*H*-[1,3]oxazino[5,6-c]quinolin-5-one (2b): Colourless solid (80 mg, 84% yield); m.p. 142.2-145.7 °C; **^{1}H NMR (400 MHz, CDCl$_3$)** δ 8.21 – 8.15 (m, 2H), 8.10 (dd, *J* = 8.1, 1.6 Hz, 1H), 7.63 (ddd, *J* = 8.7, 7.1, 1.6 Hz, 1H), 7.58 – 7.44 (m, 3H), 7.41 (d, *J* = 8.6 Hz, 1H), 7.33 (ddd, *J* = 8.1, 7.1, 0.9 Hz, 1H), 4.38 (q, *J* = 7.1 Hz, 2H), 1.82 (s, 6H), 1.40 (t, *J* = 7.1 Hz, 3H). **^{13}C NMR (101 MHz, CDCl$_3$)** δ 160.3, 150.0, 146.1, 138.1, 131.9, 131.3, 131.1, 128.4, 127.4, 123.0, 121.8, 113.9, 112.0, 52.9, 37.4, 30.0, 12.9. **IR (ATR)** ν 3660, 3366, 2988, 2968, 2923, 2900, 1692, 1627, 1597, 1579, 1366, 1316, 1276, 1249, 1147, 1110, 1074, 1042, 1022, 761, 695, 686 cm^{-1}. **HRMS (ESI)** *m/z* calcd for $C_{21}H_{20}N_2O_2$ [M+H]$^+$ 333.1603, found 333.1603.

6-(3-Methylbenzyl)-4,4-dimethyl-2-phenyl-4,6-dihydro-5*H*-[1,3]oxazino[5,6-c]quinolin-5-one (2c): Colourless solid (115 mg, 94% yield); m.p. 144.2-149.6 °C; **^{1}H NMR (400 MHz, CDCl$_3$)** δ 8.28 – 8.16 (m, 2H), 8.13 (dd, *J* = 8.2, 1.5 Hz, 1H), 7.62 – 7.45 (m, 4H), 7.36 – 7.27 (m, 2H), 7.27 – 7.18 (m, 1H), 7.12 – 6.98 (m, 3H), 5.56 (s, 2H), 2.34 (s, 3H), 1.89 (s, 6H) ppm. **^{13}C NMR (101 MHz, CDCl$_3$)** δ 161.02, 150.42, 146.13, 138.71, 138.53, 136.55, 131.84, 131.23, 131.18, 128.75, 128.45, 128.09, 127.49, 127.18, 123.53, 122.82, 122.10, 114.93, 113.93, 111.96, 52.96, 45.94, 30.10, 21.56 ppm. **IR (ATR)** ν 3368, 3177, 2928, 2847, 1641, 1600, 1569, 1505, 1448, 1351, 1313, 1239, 754, 739, 682 cm^{-1}. **HRMS (ESI)** *m/z* calcd for $C_{27}H_{24}N_2O_2$ [M+H]$^+$ 409.1916, found 409.1414.

6-(4-Methoxybenzyl)-4,4-dimethyl-2-phenyl-4,6-dihydro-5*H*-[1,3]oxazino[5,6-c]quinolin-5-one (2d): Colourless solid (104 mg, 82% yield); m.p. 155.1-158.8 °C; **^{1}H NMR (400 MHz, CDCl$_3$)** δ 8.23 – 8.16 (m, 2H), 8.11 (dd, *J* = 8.0, 1.5 Hz, 1H), 7.59 – 7.48 (m, 4H), 7.38 – 7.26 (m, 2H), 7.24 – 7.16 (m, 2H), 6.91 – 6.83 (m, 2H), 5.74 – 5.37 (m, 2H), 3.78 (s, 3H), 1.87 (s, 6H). **^{13}C NMR (101 MHz, CDCl$_3$)** δ 161.0, 158.8, 150.3, 146.2, 138.6, 136.5, 131.8, 131.2, 131.1, 128.6, 128.4, 127.9, 127.5, 122.8, 122.1, 114.9, 114.3, 113.9, 112.0, 55.3, 53.0, 45.4, 30.1. **IR (ATR)** ν 3663, 3388, 3184, 2988, 2970, 2902, 2829, 2535, 1639, 1596, 1567, 1538, 1505, 1448, 1361, 1289, 1241, 1176, 1020, 761, 744, 679 cm^{-1}. **HRMS (ESI)** *m/z* calcd for $C_{27}H_{24}N_2O_3$ [M+H]$^+$ 425.1865, found 425.1866.

6-(4-Nitrobenzyl)-4,4-dimethyl-2-phenyl-4,6-dihydro-5*H*-[1,3]oxazino[5,6-c]quinolin-5-one (2e): Colourless solid (128 mg, 97% yield); m.p. 224.5-233.4 °C; **^{1}H NMR (400 MHz, $CDCl_3$)** δ 8.27 – 8.10 (m, 5H), 7.61 – 7.49 (m, 4H), 7.43 – 7.31 (m, 3H), 7.17 (d, *J* = 8.5 Hz, 1H), 5.67 (s, 2H), 1.85 (s, 6H). **^{13}C NMR (101 MHz, $CDCl_3$)** δ 160.9, 150.8, 147.3, 146.0, 144.2, 138.2, 131.6, 131.5, 131.4, 128.5, 127.5, 127.4, 124.2, 123.3, 122.7, 114.3, 114.1, 111.9, 77.3, 52.9, 45.6, 30.1. **IR (ATR)** ν 3393, 3335, 3184, 2973, 2930, 2845, 1692, 1641, 1600, 1575, 1511, 1483, 1484, 1455, 1343, 1313, 1246, 739, 710, 690 cm^{-1}. **HRMS (ESI)** *m/z* calcd for $C_{26}H_{21}N_3O_4$ [M+H]$^+$ 440.1610, found 440.1607.

6-Benzyl-9-isopropyl-4,4-dimethyl-2-phenyl-4,6-dihydro-5*H*-[1,3]oxazino[5,6-c]quinolin-5-one (2f): Colourless solid (102 mg, 78% yield); m.p. 183.5-183.9 °C; **^{1}H NMR (400 MHz, CDCl3)** δ 8.25–8.18 (m, 2H), 7.94 (d, *J* = 2.0 Hz, 1H), 7.61–7.52 (m, 3H), 7.40 (dd, *J* = 8.8, 2.1 Hz, 1H), 7.35 (t, *J* = 7.3 Hz, 2H), 7.31–7.24 (m, 4H), 5.59 (bs, 2H), 3.08 (hept, *J* = 6.9 Hz, 1H), 1.87 (s, 6H), 1.35 (d, *J* = 6.9 Hz, 6H). **^{13}C NMR (101 MHz, CDCl3)** δ 160.9, 150.4, 146.1, 142.7, 137.0, 136.8, 132.0, 131.2, 129.9, 128.8, 128.5, 127.4, 127.2, 126.6, 119.9, 115.0, 113.8, 111.8, 53.0, 45.9, 33.7, 30.1, 24.1. **IR (ATR)** ν 3024, 2948, 1691, 1645, 1568, 1500, 1435, 1322, 1269, 1129, 1013, 808, 728 cm^{-1}. **HRMS (ESI)** *m/z* calcd for $C_{29}H_{28}N_2O_2$ [M+H]$^+$ 437.2229, found 437.2233.

6-Benzyl-9-fluoro-4,4-dimethyl-2-phenyl-4,6-dihydro-5*H*-[1,3]oxazino[5,6-c]quinolin-5-one (2g): Colourless solid (114 mg, 92% yield); m.p. 219.7-220.1 °C; **^{1}H NMR (400 MHz, $CDCl_3$)** δ 8.20–8.15 (m, 2H), 7.75 (dd, *J* = 8.6, 2.6 Hz, 1H), 7.60–7.50 (m, 3H), 7.37–7.32 (m, 2H), 7.31–7.19 (m, 5H), 5.58 (bs, 2H), 1.86 (s, 6H). **^{13}C NMR (101 MHz, $CDCl_3$)** δ 160.6, 157.9 (d, *J*C,F = 242.7 Hz), 149.7 (d, *J*C,F = 3.1 Hz), 145.8, 136.3, 135.1, 131.5, 131.3, 128.9, 128.5, 127.4, 126.4, 119.0 (d, *J*C,F = 24.0 Hz), 116.6 (d, *J*C,F = 8.0 Hz), 114.9 (d, *J*C,F = 8.5 Hz), 113.1, 108.4 (d, *J*C,F = 24.3 Hz), 53.0, 46.1, 30.0. **IR (ATR)** ν 3038, 2949, 2902, 1642, 1605, 1573, 1512, 1485, 1324, 1281, 1174, 809, 729 cm^{-1}. **HRMS (ESI)** *m/z* calcd for $C_{26}H_{21}FN_2O_2$ [M+H]$^+$ 413.1665, found 413.1591.

6-Benzyl-9-bromo-4,4-dimethyl-2-phenyl-4,6-dihydro-5*H*-[1,3]oxazino[5,6-c]quinolin-5-one (2h): Colourless solid (125 mg, 88% yield); m.p. 209.1-211.5 °C; **^{1}H NMR (400 MHz, $CDCl_3$)** δ 8.21–8.14 (m, 3H), 7.60–7.51 (m, 4H), 7.35 (t, *J* = 7.3 Hz, 2H), 7.28 (t, *J* = 7.2 Hz, 1H), 7.24–7.19 (m, 2H), 7.16 (d, *J* = 9.0 Hz, 1H), 5.55 (bs, 2H), 1.86 (s, 6H). **^{13}C NMR (101 MHz, $CDCl_3$)** δ 160.6, 149.4, 145.8, 137.5, 136.1, 133.9, 131.5, 131.4, 129.0, 128.5, 127.49, 127.47, 126.4, 125.3, 116.6, 115.5, 115.2, 113.0, 53.0, 46.0, 30.0. **IR (ATR)** ν 3041, 2955, 2915, 1643, 1599, 1547, 1485, 1327, 1283, 1179, 801, 724 cm^{-1}. **HRMS (ESI)** *m/z* calcd for $C_{26}H_{21}BrN_2O_2$ [M+H]$^+$ 473.0865, found 473.0868.

6-Benzyl-4,4-dimethyl-2-phenyl-9-(trifluoromethyl)-4,6-dihydro-5*H*-[1,3]oxazino[5,6-c]quinolin-5-one (2i): Colourless solid (90 mg, 65% yield); m.p. 222.1-224.2 °C; **^{1}H NMR (400 MHz, $CDCl_3$)** δ 8.35 (d, *J* = 1.2 Hz, 1H), 8.19 (dd, *J* = 7.8, 1.8 Hz, 2H), 7.72 (dd, *J* = 8.9, 1.9 Hz, 1H), 7.62–7.52 (m, 3H), 7.43–7.34 (m, 3H), 7.33–7.27 (m, 1H), 7.24 (d, *J* = 7.2 Hz, 2H), 5.61 (bs, 2H), 1.87 (s, 6H). **^{13}C NMR (101 MHz, $CDCl_3$)** δ 160.9, 150.1, 145.7, 140.5, 135.9, 131.43, 131.41, 129.0, 128.6, 127.6, 127.48 (q, $J_{C,F}$ = 3.5 Hz), 127.43, 126.4, 124.3 (q, $J_{C,F}$ = 33.4 Hz), 124.0 (q, $J_{C,F}$ = 271.7 Hz), 120.5 (q, $J_{C,F}$ = 4.1 Hz), 115.4, 113.8, 113.3, 52.9, 46.1, 30.0. **IR (ATR)** ν 3049, 2966, 2942, 2912, 1644, 1601, 1559, 1519, 1488, 1328, 1295, 1177, 803, 730 cm^{-1}. **HRMS (ESI)** *m/z* calcd for $C_{27}H_{21}F_3N_2O_2$ $[M+H]^+$ 463.1633, found 463.1610.

Methyl 6-benzyl-4,4-dimethyl-5-oxo-2-phenyl-5,6-dihydro-4*H*-[1,3]oxazino[5,6-c]quinoline-9-carboxylate (2j): Colourless solid (31 mg, 23% yield); m.p. 258.1-259.9 °C; **^{1}H NMR (400 MHz, CDCl$_3$)** δ 8.78 (d, *J* = 2.0 Hz, 1H), 8.23–8.18 (m, 2H), 8.12 (dd, *J* = 8.9, 2.0 Hz, 1H), 7.61–7.51 (m, 3H), 7.37–7.25 (m, 4H), 7.23 (d, *J* = 7.1 Hz, 2H), 5.60 (bs, 2H), 3.99 (s, 3H), 1.84 (s, 6H). **^{13}C NMR (101 MHz, CDCl$_3$)** δ 166.2, 161.0, 150.5, 145.9, 141.4, 136.0, 131.8, 131.5, 131.3, 129.0, 128.5, 127.5 (2C), 126.5, 125.2, 123.9, 114.9, 113.7, 112.6, 52.9, 52.4, 46.1, 30.0. **IR (ATR)** ν 3053, 2956, 2923, 1639, 1601, 1562, 1503, 1486, 1330, 1291, 1165, 789, 727 cm^{-1}. **HRMS (ESI)** *m/z* calcd for $C_{28}H_{24}N_2O_4$ $[M+H]^+$ 453.1814, found 453.1802.

6'-(4-Methoxybenzyl)-2'-phenylspiro[cyclohexane-1,4'-[1,3]oxazino[5,6-c]quinolin]-5'(6'*H*)-one (2k): Colourless solid (89 mg, 64% yield); m.p. 206.5-209.6 °C; **^{1}H NMR (400 MHz, CDCl$_3$)** δ 8.24 (d, *J* = 7.0 Hz, 2H), 8.12 (d, *J* = 8.0 Hz, 1H), 7.61 – 7.47 (m, 4H), 7.32 (ddd, *J* = 15.6, 7.7, 3.7 Hz, 2H), 7.20 (dd, *J* = 8.6, 2.1 Hz, 2H), 6.92 – 6.84 (m, 2H), 5.51 (s, 2H), 3.79 (d, *J* = 2.1 Hz, 3H), 3.01 – 2.88 (m, 2H), 2.19 (q, *J* = 13.5, 13.1 Hz, 2H), 1.73 (td, *J* = 49.5, 49.0, 13.3 Hz, 6H). **^{13}C NMR (101 MHz, CDCl$_3$)** δ 174.5, 161.1, 158.8, 151.3, 144.0, 138.8, 132.1, 131.1, 131.0, 128.7, 128.4, 127.9, 127.5, 122.8, 122.0, 114.8, 114.3, 114.1, 114.1, 111.7, 55.3, 55.3, 45.4, 36.5, 29.7, 25.8, 20.8. **IR (ATR)** ν 3675, 2958, 2925, 2907, 2850, 1692, 1629, 1597, 1510, 1251, 1172, 1130, 1107, 1039, 1020, 737, 688, 680 cm^{-1}. **HRMS (ESI)** *m/z* calcd for $C_{30}H_{28}N_2O_3$ $[M+H]^+$ 465.2178, found 465.2173.

6-Benzyl-2-(4-fluorophenyl)-4,4-dimethyl-4,6-dihydro-5*H*-[1,3]oxazino[5,6-c]quinolin-5-one (2l): Colourless solid (111 mg, 90% yield); m.p. 225.7-226.8 °C; **^{1}H NMR (400 MHz, CDCl$_3$)** δ 8.24–8.15 (m, 2H), 8.08 (dd, *J* = 8.2, 1.4 Hz, 1H), 7.55–7.47 (m, 1H), 7.38–7.16 (m, 9H), 5.59 (bs, 2H), 1.84 (s, 6H). **^{13}C NMR (101 MHz, CDCl$_3$)** δ 164.7 (d, $J_{C,F}$ = 251.4 Hz), 160.9, 150.3, 145.2, 138.6, 136.5, 131.2, 129.7 (d, $J_{C,F}$ = 8.8 Hz), 128.9, 128.0 (d, $J_{C,F}$ = 3.0 Hz), 127.3, 126.5, 122.7, 122.1, 115.5 (d, $J_{C,F}$ = 21.9 Hz), 114.9, 113.8, 111.9, 52.9, 45.9, 30.0. **IR (ATR)** ν 3027, 2963, 2912, 1639, 1598, 1546, 1510, 1491, 1323, 1168, 805, 728 cm^{-1}. **HRMS (ESI)** *m/z* calcd for $C_{27}H_{21}FN_2O_2$ $[M+H]^+$ 413.1665, found 413.1592.

37,38,39,40,41,42-Hexa-*O*-formylcalix[6]arene (4): Colourless solid (675 mg, 84% yield); m.p. 239.7-240.2 °C; **^{1}H NMR (400 MHz, CDCl$_3$)** δ 7.78 (br s, 6H), 7.16 (t, *J* = 7.5 Hz, 6H), 7.07 (d, *J* = 7.5 Hz, 12H), 3.71 (s, 12H). **^{13}C NMR (101 MHz, CDCl$_3$)** δ 158.4, 146.5, 132.3, 129.7, 126.6, 31.7. **IR (ATR)** ν 1730.51 cm^{-1}.

5,11,17,23,29,35-Hexa-(*tert*-butyl)-37,38,39,40,41,42-hexa-*O*-formylcalix[6]arene (5): Colourless solid (1048 mg, 92% yield); m.p. 221.8-222.4 °C (deg.); **^{1}H NMR (400 MHz, CDCl$_3$)** δ 7.67 (br s, 6H), 7.03 (s, 12H), 3.66 (s, 12H), 1.24 (m, 54H). **^{13}C NMR (101 MHz, CDCl$_3$)** δ 158.7, 149.1, 144.1, 131.3, 126.6, 34.4, 32.0, 31.2. **IR (ATR)** ν 2955, 1733 cm^{-1}. **ESI-MS** *m/z* calcd for $C_{72}H_{84}O_{12}$ $[M+Na]^+$ 1163.586, found 1163.778.

5,11,17,23,29,35-Hexabromo-37,38,39,40,41,42-hexa-*O*-formylcalix[6]arene (6): Colourless solid (664 mg, 52% yield); m.p. 300.2-301.8 °C (deg.); **^{1}H NMR (400 MHz, CDCl$_3$)** δ 7.91 (br s, 6H), 7.24 (s, 12H), 3.66 (s, 12H). **^{13}C NMR (101 MHz, CDCl$_3$)** δ 159.5, 145.5, 134.9, 132.4, 119.4, 30.0. **IR (ATR)** ν 2971, 1740 cm^{-1}.

References

1. Friis, S. D.; Lindhardt, A. T.; Skrydstrup, T. *Acc. Chem. Res.,* **2016**, *49*, 594–605.
2. Geitner, R.; Gurinov, A.; Huang, T. et al. *Angew. Chem. Int. Ed.*, **2021**, *60*, 3422.
3. Konishi, H.; Manabe K. *Tetrahedron*, **2019**, *60(42)*, 151147.
4. Odell, L. R.; Russo, F.; Larhed, M., *Synlett*, **2012**, 685–698.
5. Dogga, B.; Kumar, C.S.A.; Joseph, J.T. *Eur. J. Org. Chem.*, **2021**, *2021*, 309.
6. Wan, Y.; Alterman, M.; Larhed, M.; Hallberg, A. *J. Org. Chem*., **2002**, *67 (17)*, 6232-6235.
7. Mondal, K.; Halder, P.; Gopalan, G. *Org. Biomol. Chem*., **2019**, *17*, 5212-5222.
8. Morimoto, T.; Fuji, K.; Tsutsumi, K.; Kakiuchi, K. *J. Am. Chem. Soc*., **2002**, *124*, 3806–3807.
9. Korsager, S.; Taaning, R. H.; Skrydstrup, T. *J. Am. Chem. Soc*., **2013**, *135*, 2891–2894.
10. Li, H.; Neumann, H.; Beller, M.; Wu, X.-F. *Angew. Chem., Int. Ed.*, **2014**, *53*, 3183–3186.
11. Acerbi, A.; Carfagna, C.; Della Ca', N. et al. *Chem. Eur. J.*, **2018**, *24*, 4835.
12. Mancuso, R.; Miliè, R.; Della Ca', N. Gabriele, B. et al. *J. Org. Chem.*, **2019**, *84 (11)*, 7303-7311.
13. Pancrazzi, F.; Sarti, N.; Della Ca', N. et al. *Org. Lett.,* **2020**, *22*, 1569−1574.
14. Dickens, P.G.; Dove J.E.; Linnett, J.W. *Trans. Faraday Soc*., **1964**, *60*, 539-552.
15. Li, Z.; Xu, S.; Jiao, L.; Zhang, Z. et al. *J. Org. Chem.*, **2019**, *84 (15)*, 9497–9508.
16. McNulty, J.; Nair, J.J.; Robertson, A. *Org. Lett.* **2007**, *9 (22)*, 4575–4578.
17. Liu, L.; Qiang, J.; Bai, S.; Li, Y.; Miao, C.; Li, J. *Appl. Organometal. Chem*., **2017**, *31*, 3817.
18. Roy, T.; Rydfjord, J.; Sävmarker, J.; Nordeman, P. *Tetrahedron*, **2018**, *59 (13)*, 1230-1232.
19. Wan, Y.; Alterman, M.; Larhed, M.; Hallberg, A. *J. Org. Chem*., **2002**, *67 (17)*, 6232–6235.
20. Yadav, V.K.; Srivastava, V.P.; Dhar, L.; Yadav, S. *New J. Chem*., **2018**, *42*, 16281.
21. Konishi, H.; Manabe, K. *Synlett*, **2014**, *25(14)*, 1971–1986.
22. Jiang, L.-B.; Qi, J.X.; Wu, X.-F. *Tetrahedron*, **2016**, *57*, 3368–3370.
23. Wu, F.P.; Li, D.; Peng, J.B.; Wu, X.F. *Org. Lett*., **2019**, *21(14)*, 5699-5703.
24. Fu, L.Y.; Ying, J.; Qi, X.; Peng, J.B.; Wu, X.F. *J. Org. Chem.,* **2019**, *84(3)*, 1421-1429.
25. Ying, J.; Le, Z.; Wu, X.F. *Org. Lett*., **2019**, *22(1)*, 194-198.
26. Ying, J.; Wang, H.; Qi, X.; Peng, J.-B.; Wu, X.-F.*Eur. J. Org. Chem.*, **2018**, 2018, 688-692.
27. Pound, S.M.; Underwood, S.J.; Douglas, C.J. *Eur. J. Org. Chem*., **2020**, *2020*, 2448-2453.

Chapter 4. Regioselectivity Control in the Oxidative Carbonylation of *ortho*-Alkynylphenols by Palladium and Rhodium Catalysis

Introduction

Chemistry of alkynes has attracted an elevated interest in the scientific community due to its versatility for the synthesis of useful building blocks and biologically active structures.[1-2] Although alkyne-based reactions provide several attractive applications, reaction efficiency and regioselectivity sometimes become a challenge. Generally, the regioselectivity of a process is determined by the nature of the substrate. However, transition-metal catalysis has been proved to be a powerful tool to alter the usual reaction pathway, opening access to previously unapproachable scaffolds.[3-4]

Catalytic carbonylation of alkynes has been known since Walter Reppe published his work in 1930s.[5] Decades of studies revealed that the process can proceed in numerous ways, depending on the catalyst, the type of process (oxidative, additive, etc.), and the nucleophile used.[6] So, the carbonylation of alkynes in the presence of oxygen-based nucleophiles provides convenient access to a wide range of α,β-unsaturated lactones, carboxylic acids and esters.[7] Among them, coumarin- and 2-coumaranone-based biologically active and natural compounds that can be prepared using this strategy.

Coumarin is a ubiquitous structural core present in plenty of natural products.[8] Dicoumarol is a naturally occurring anticoagulant agent that depletes stores of vitamin K.[9] It became a prototype of the 4-hydroxycoumarin anticoagulant drug class which includes pharmaceuticals such as warfarin and phenprocoumon.[10] Aminocoumarins are very potent inhibitors of bacterial DNA gyrase in Gram-positive pathogens. Novobiocin, produced by the actinomycete *Streptomyces niveus*, is an orally active antibiotic belonging to the aminocoumarin group.[11] Nitrogen-containing three-cyclic coumarins possess high biological activity at the inhibition of methylenetetrahydrofolate dehydrogenase 2 (MTHFD2), which plays a key role in one-carbon (1C) metabolism in human mitochondria, and its high expression correlates with poor survival of patients with various types of cancer.[12]

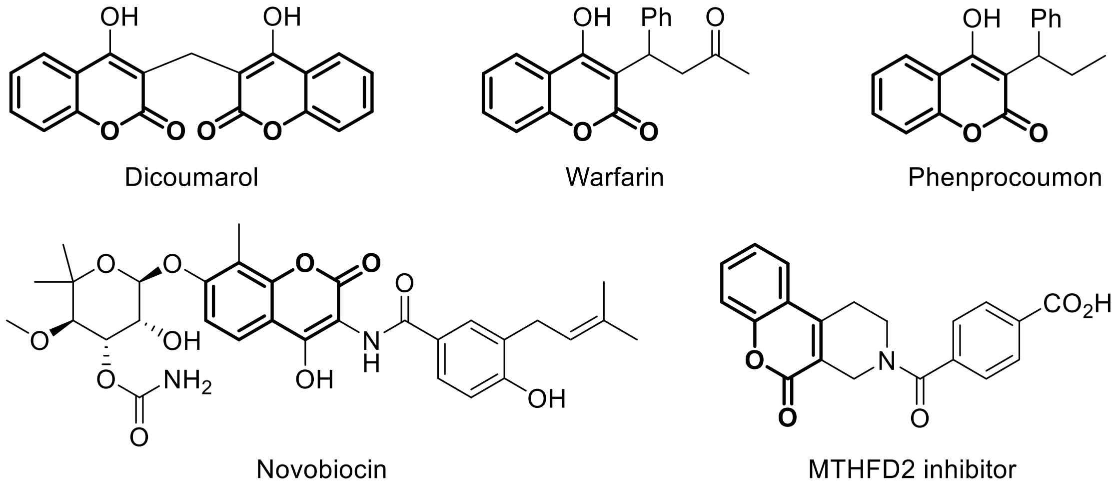

Scheme 4-1. Coumarin-Based Natural and Biologically Active Compounds.

On the other hand, naturally occurring 2-coumaranons bearing a methylene function in 3-position are extremely rare. The simplest compound is isoaurostatin isolated from *Thermomonospora alba*. Isoaurostatin was shown to inhibit the relaxation activity of calf thymus topoisomerase I in a non-competitive manner.[13] Another example is bractelactone found in *Fissistigma bracteolatum*, a plant that was widely used in traditional medicine to treat inflammatory diseases. It was demonstrated that bractelactone inhibits formyl-L-methionyl-L-leucyl-L-phenylalanine (FMLP)-induced human neutrophil activations and suppresses store-operated calcium entry in FMLP-activated cells.[14] Pterocarposide, also known as pteroisoauroside, was first isolated from *Pterocarpus marsupium*, which is used in India for the treatment of diarrhoea, toothache, fever, and skin infections.[15] A pair of photo-interconvertible isomers Suffrutine A and B extracted from the roots of *Flueggea suffruticosa*, exhibited to promote neuro-2a cell differentiation.[16]

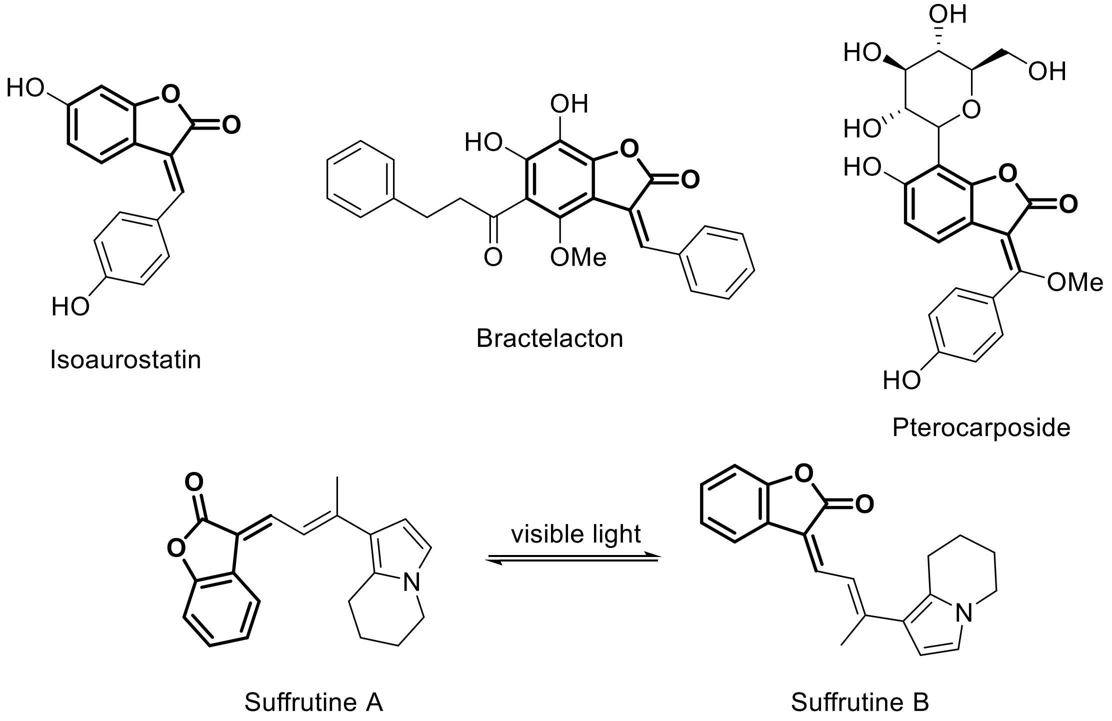

Scheme 4-2. Natural 3-Methylenebenzofuran-2(3*H*)-one-Based Compounds.

Given the importance and practical value of the abovementioned scaffolds, the development of selective and sustainable catalytic methods for their construction appears to be a burning invocation. In this chapter, we attempted to perform a divergent carbonylative synthesis starting from 2-alkynylphenol substrates in order to obtain the isomeric coumarins and 2-coumaranones with *endo* and *exo* double bonds, respectively. Creating two protocols that involve the conditions-based divergence in the carbonylative cyclisation domino reaction by merely applying different metal catalysts, we endeavor to make the carbonylative synthesis even more versatile.

Results and Discussion

Inspired by the work of Uchiyama et al.,[17] who determined the correlation between regioselectivity and acid/base effects in the intramolecular cyclisation between carboxylic acids and C≡C triple bonds, and the studies of Jiang[18] and Beller[19], who described the ligand-controlled palladium-catalysed carbonylative cyclisations, we commenced our investigation. Based on our experience,[20-22] we envisioned that 2-alkynylphenols bearing a propargylamide moiety at the *ortho*-position can undergo carbonylation intramolecular cyclisation cascade when reacted with carbon monoxide under PdI_2/KI catalysis.

Unlike 2-alkynylanilines,[22] the phenol derivative **1a** selected as a model compound demonstrated ambiguous reactivity under PdI_2/KI-based carbonylative conditions, giving the mixture of *6-endo-dig* and *5-exo-dig* cyclisation products **2a** and **3a**, respectively (Table 4-1). The process was found to be highly sensitive to changes in iodide concentration, as well as pressure applied and the ratio of gaseous mixtures. Unfortunately, regardless of all parameter variations for this system, the selectivity of the process remained low. The total yield of the products of interest **2a** and **3a** never exceeded 49%.

Table 4-1. Carbonylation of **1a** Using PdI_2/KI Catalytic System.

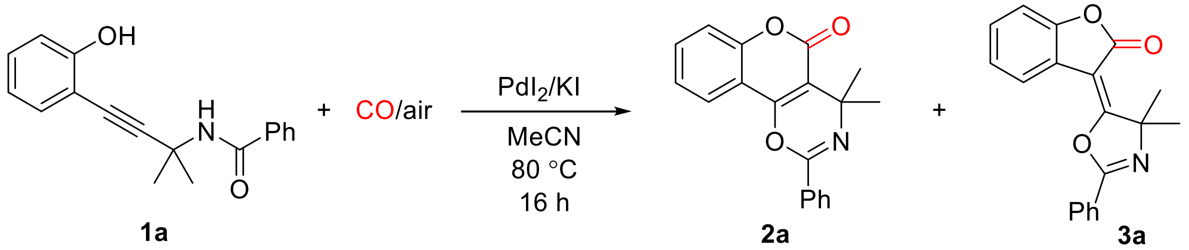

Entry	*p*(CO), bar	*p*(air), bar	KI, mol %	Conv.[a] **1a**, %	Yield[a] **2a**, %	Yield[a] **3a**, %
1	12	48	10	100	16	30
2	12	48	20	100	15	**34**
3	12	48	50	100	7	24
4	16	4	10	71	**33**	10
5	20	2	10	69	24	16
6	6	48	10	40	11	6

Reaction conditions: **1a** (0.4 mmol), PdI_2 (0.004 mmol, 1 mol%), KI, acetonitrile (0.1 M). [a]NMR yield.

These unsatisfactory results prompted us to look for new catalytic systems that would allow to implement the transformation of phenols in an efficient manner. There are few examples of the direct CO attachment to phenolic hydroxyl reported in the literature.[23-24] Oxidative carbonylation protocols described for *ortho*-arylphenols or *ortho*-vinylphenols involve the utilisation of palladium acetate as a catalyst and copper[25] or silver[26-27] salts as oxidants. The only oxidative carbonylation of *ortho*-ethynylphenols involving the activation of the *6-endo-dig* cyclisation mode was reported for 2,2'-

dihydroxydiphenylethyne[28] and 2-hydroxy-2'-aminodiphenylethyne[18] derivatives. The former was converted into coumestan with low yield (35%) by palladium chloride in combination with copper(II) chloride. The latter underwent domino carbonylation and cyclisation more efficiently under $Pd(MeCN)_2Cl_2$ and silver triflate catalysis to afford indolochromenones. Singular example of palladium-catalysed carbonylative *5-exo-dig* cyclisation of 2-alkynylphenols was described as a process, in which *ortho*-ethynylphenol initially undergoes base-promoted cyclisation to form benzofuran that consequently performs an attack on the triple bond of the unreacted substrate, followed by CO insertion and ultimate cyclisation.[29]

Taking into consideration the abovementioned reports, we carried out the new optimisation study utilising various palladium catalysts under atmospheric pressure of carbon monoxide at room temperature (Table 4-2).

Table 4-2. Optimisation Study for Pd-Catalysed Domino Carbonylation Cyclisation of **1a**.

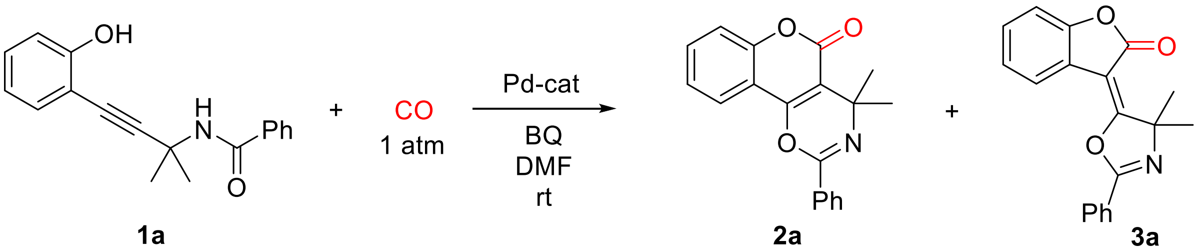

Entry	Catalyst	Ligand	Time	Conv.[a] **1a**, %	Yield[a] **2a**, %	Yield[a] **3a**
1	$Pd(OAc)_2$	-	24 h	15	9	4
2	$Pd(OAc)_2$	dppe 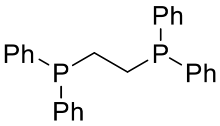	8 h	100	65	10
3	$PdCl_2$	dppe	24 h	No reaction		
4	$Pd(MeCN)_2Cl_2$	dppe	24 h	No reaction		
5	PdI_2 2.5 mol%	dppe 2.5 mol%	24 h	No reaction		
6	$Pd(OPiv)_2$	dppe	24 h	7	traces	traces
7	$Pd(TFA)_2$	dppe	24 h	10	-	9
8[c]	$Pd(OAc)_2$	dppe	6 h	100	73	20
9[d]	$Pd(OAc)_2$	dppe	6 h	100	80 (78)[b]	16
10[e]	$Pd(OAc)_2$	dppe	6 h	100	73	19

11[f]	$Pd(OAc)_2$	dppe	6 h	100	74	12
12	$Pd(OAc)_2$ 2.5 mol% + $Pd(TFA)_2$ 2.5 mol%	dppe	6 h	100	77	19
13[d]	$Pd(OAc)_2$	dppb 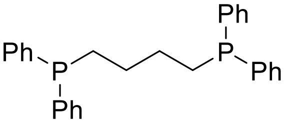	24 h	85	62	14
14[d]	$Pd(OAc)_2$	PPh_3 10 mol%	12 h	79	56	17
15[d]	$Pd(OAc)_2$	bpy 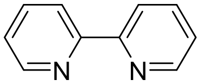	6 h	93	80	10
16[d]	$Pd(OAc)_2$	phen 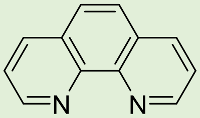	2 h	100	91 (89)[b]	6
17[d]	$Pd(OAc)_2$	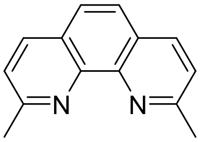	8 h	86	75	7
18[d]	$Pd(OAc)_2$	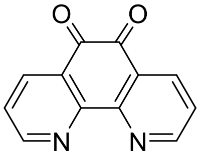	24 h	53	26	25
19[d]	$Pd(OAc)_2$		3 h	96	78	8
20[d]	$Pd(OAc)_2$	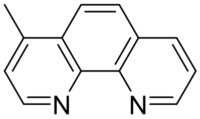	3 h	91	80	7
21[d]	$Pd(OAc)_2$	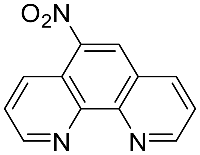	6 h	97	88	5
22[d]	$Pd(OAc)_2$	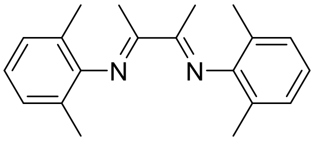	24 h	31	14	12

Reaction conditions: 1a (0.2 mmol, 1 equiv), palladium salt (0.01 mmol, 5 mol%), ligand (0.01 mmol, 5 mol%), 1,4-benzoquinone (0.24 mmol, 1.2 equiv) in DMF (2 mL) with CO balloon at RT. [a]NMR Yield. [b]Isolated yield. [c] With TFA (5 mol%). [d]With TFA (2.5 mol%). [e]With TfOH (2.5 mol%). [f]With MsOH (2.5 mol%).

We were glad to observe the formation of **2a** in 65% yield in case when the complex of palladium acetate and bis-1,2-(diphenylphosphino)ethane (dppe) was used to promote the reaction (entry 2, Table 4-2). Surprisingly, changing the counterion of palladium to halide resulted in a complete inhibition of the catalytic activity of the complex (entries 3-5, Table 4-2). Pivalate and triflate salts displayed scarce reactivity providing a conversion of the starting material of no more than 10% (entries 6-7, Table 4-2).

These results impelled us to continue our bibliographic research. Some mechanistic studies[30-32] suggested that Pd(OTf)(OAc) and Pd(TFA)(OAc) mixed salts exhibit remarkable catalytic activity. While palladium precursors such as $Pd(OTf)_2$ or $Pd(TFA)_2$ remain inactive, the introduction of a heterocounterion allows to significantly decrease the electron density at the palladium atoms, which facilitates the initial oxidative addition step of the catalytic cycle. This finding became a pivotal moment in our optimisation study.

The addition of the equimolar-to-palladium amount of trifluoroacetic acid (5 mol%) not only decreased the reaction time, but also significantly increased the selectivity towards the formation of **2a** (entry 8, Table 4-2). Lowering the quantity of TFA to 2.5 mol% resulted in an ulterior enhancement of selectivity (entry 9). The replacement of TFA with triflic or methanesulfonic acids led to a slight decrement in the yield of **2a** (entries 10-11). To exclude the plausible effect of a pH-shift in the reaction medium, we conducted an experiment using the mixture of $Pd(OAc)_2$ and $Pd(TFA)_2$ in 1:1 ratio. As the outcome was comparable to that of entry 8, we assumed that the change of acidity does not play an important role in the process.

The conclusive ligand screening revealed that the use of 1,10-phenanthroline led to a dramatic increase in the yield of **2a** (89% isolated yield) and almost complete suppression of **3a** formation (entry 16, Table 4-2). Additionally, the use of $Pd(OAc)_2$/phen/TFA catalytic system allowed to considerably reduce the reaction time, providing full conversion of **1a** in two hours.

To confirm the theory of the $L_2Pd(TFA)(OAc)$ complex effect, we conducted a series of NMR experiments. All ^{19}F NMR spectra were registered in DMF with 10% $CDCl_3$ as a solvent (Figure 4-1). Four signals observed for palladium triflate solution can be explained by the presence of various polynuclear species of palladium. Interestingly, the solution obtained by mixing palladium acetate with 0.5 equivalent of trifluoroacetic acid had the same NMR pattern as $Pd(TFA)_2$, indicating the exclusive formation of $Pd_x(TFA)_{2x}$ and thus the absence of $Pd_x(TFA)_x(OAc)_x$ species (rows 6 and 5, Figure 4-1). However, when 1,10-phenanthroline was added to both solutions, the pattern changed. Starting $Pd(TFA)_2$ formed a unique complex with 1,10-phenanthroline as one prevalent signal can be observed. The situation is different for the solution obtained from the mixture of $Pd(OAc)_2$ and TFA; apart from the less abundant signal corresponding to $Pd(TFA)_2$/phen a new major signal appeared. The evidence the formation of different types of complexes occurs becomes even clearer when the substrate **1a** is added. If classic $Pd(TFA)_2$ creates a complex with the corresponding ^{19}F signal at 76.6 ppm (row 2), the complex obtained from $Pd(OAc)_2$ and TFA has a different signal distribution, with a maximum at 75.5 ppm (row 1). A huge difference between the chemical shifts of two complexes might indicate significant differences between their electronic structure, and, consequently, their activity in the carbonylation process.

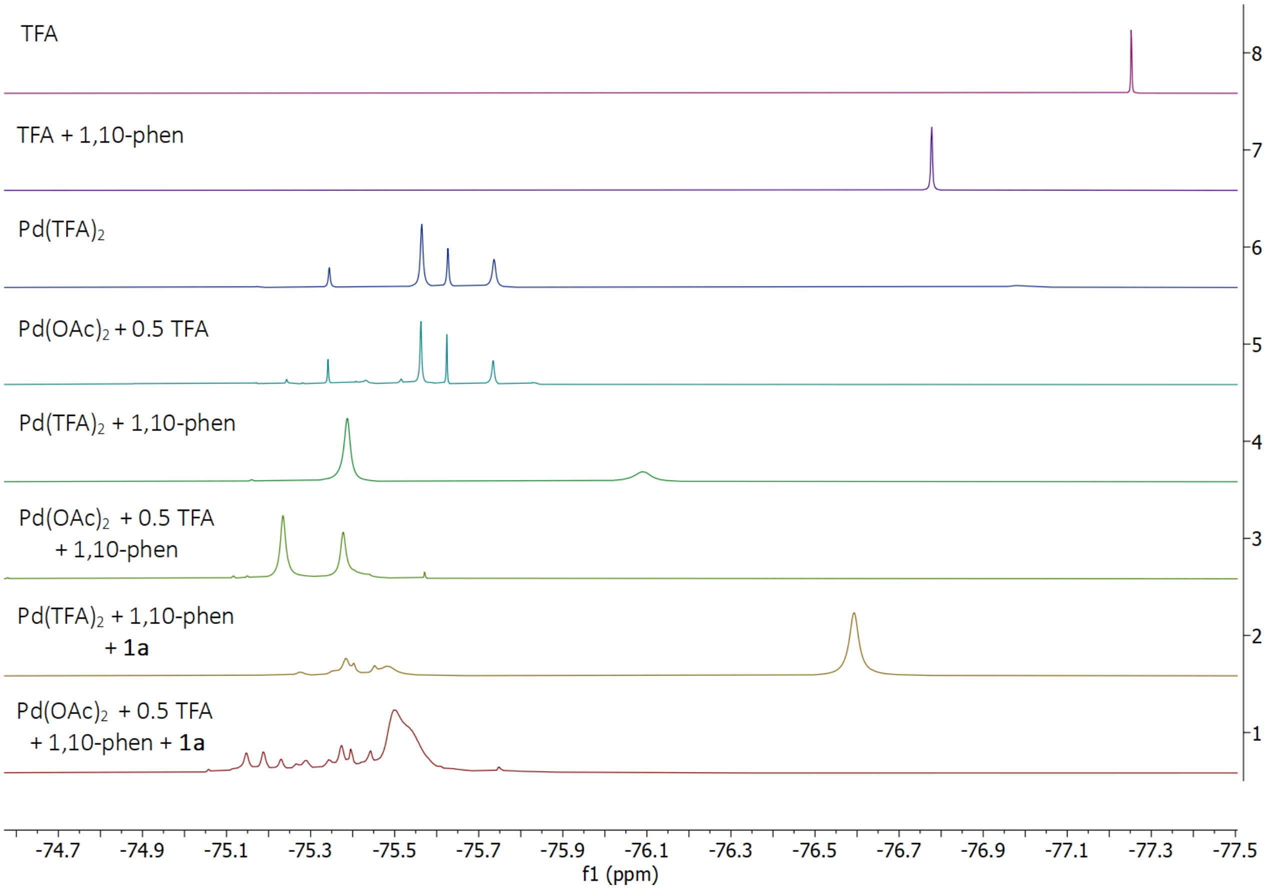

Figure 4-1. ^{19}F NMR Spectra of [Pd]-TFA Systems. NMR Conditions: 60 mM [Pd] in DMF/$CDCl_3$ (1 : 0.1).

As we aspired to find a path to regiodivergent synthesis, we continued the optimisation study to activate the *5-exo-dig* cyclisation mode of the substrate **1a**. Unfortunately, palladium catalysis has never given us satisfactory results in this direction, neither by changing ligands, nor palladium precursors and other reaction parameters. This urged us to consider other transition metals. In this context, rhodium is an attractive alternative due to its unique reactivity, including the ability to carbonylate phenol derivatives.[33-35] In particular, it was reported that *ortho*-ethynylphenols can be carbonylated by rhodium(0) carbonyl at 175 °C under 100 atm of CO to afford the mixture of coumarin and 2-coumaranone.[36] Performing a reaction under high pressure was not our intention, but we assumed that Rh(I) and Rh(III) catalysts could be suitable for the reaction under atmospheric pressure of CO.

Considering that normally rhodium-catalysed processes proceed at high temperatures, we commenced the optimisation study carrying out the reaction at 100 °C. The first result obtained with rhodium(III) acetylacetonate was extremely promising. In only two hours of reaction time the desired product of *5-exo-dig* cyclisation **3a** was isolated in 77% yield (entry 1, Table 4-3). Rhodium(III) chloride in combination with diphosphine ligands was less active in the carbonylation (entries 2 and 3), but Rh(III) pentamethylcyclopentadienyl complexes exhibited excellent selectivity towards *5-exo-dig* cyclisation. The best results were obtained using rhodium(I) cyclooctadiene complexes that provided excellent yields of **3a** in short reaction time (entries 6 and 7). Additionally, the use of $[Rh(cod)Cl]_2$ allowed to carry out the reaction at lower temperature (entry 8).

Table 4-3. Optimisation Study for Rh-Catalysed Domino Carbonylative Cyclisation of **1a**.

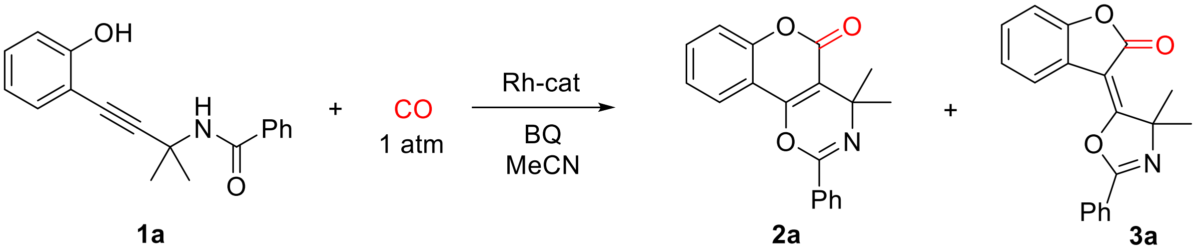

Entry	Catalyst	Ligand	Time	Conv.[a] **1a**, %	Yield[a] **2a**, %	Yield[a] **3a**, %
1	$Rh(acac)_3$	acetylacetone 3 mol %	2 h	89	7	81 (77)[b]
2	$RhCl_3 \times 3H_2O$	dppe 6 mol %	24 h	66	10	56
3	$RhCl_3 \times 3H_2O$	dppp 6 mol %	24 h	4	-	4
4	$[Cp^*RhCl_2]_2$	-	24 h	85	8	76
5	$[Cp^*Rh(MeCN)_3][SbF_6]_2$	-	24 h	100	4	93 (90)[b]
6	$Rh(cod)_2BF_4 \times H_2O$	-	6 h	100	3	95
7	$[Rh(cod)Cl]_2$	-	4 h	100	2	95
8[c]	$[Rh(cod)Cl]_2$	-	4 h	100	2	97 (94)[b]
9[c]	$[Rh(cod)Cl]_2$	1,10-phen 4 mol %	6 h	100	20	68
10[c]	$[Rh(cod)Cl]_2$	dppb 4 mol %	24 h	100	22	77

Reaction conditions: **1a** (0.2 mmol, 1 equiv), rhodium catalyst (0.004 mmol, 2 mol%), 1,4-benzoquinone (0.24 mmol, 1.2 equiv) in MeCN (2 mL) with CO balloon at 100 ˚C. [a]NMR Yield. [b]Isolated yield. [c]The reaction was carried out at 80 ˚C.

Lastly, we examined the influence of the ligands on the rhodium-catalysed process. It turned out the efficiency of the process drops as well as the selectivity towards **3a** when 1,10-phenanthroline or bis-1,4-(diphenylphosphino)butate (dppb) are introduced. Noteworthy, in all cases the product **3a** formed as a single *E*-isomer.

The developed palladium- and rhodium-catalysed protocols were applied for different substrates to study the applicability and functional-group tolerance under the optimised catalytic conditions (Table 4-4).

Table 4-4. Scope of the Substrates Obtained by Pd and Rh Catalysis.

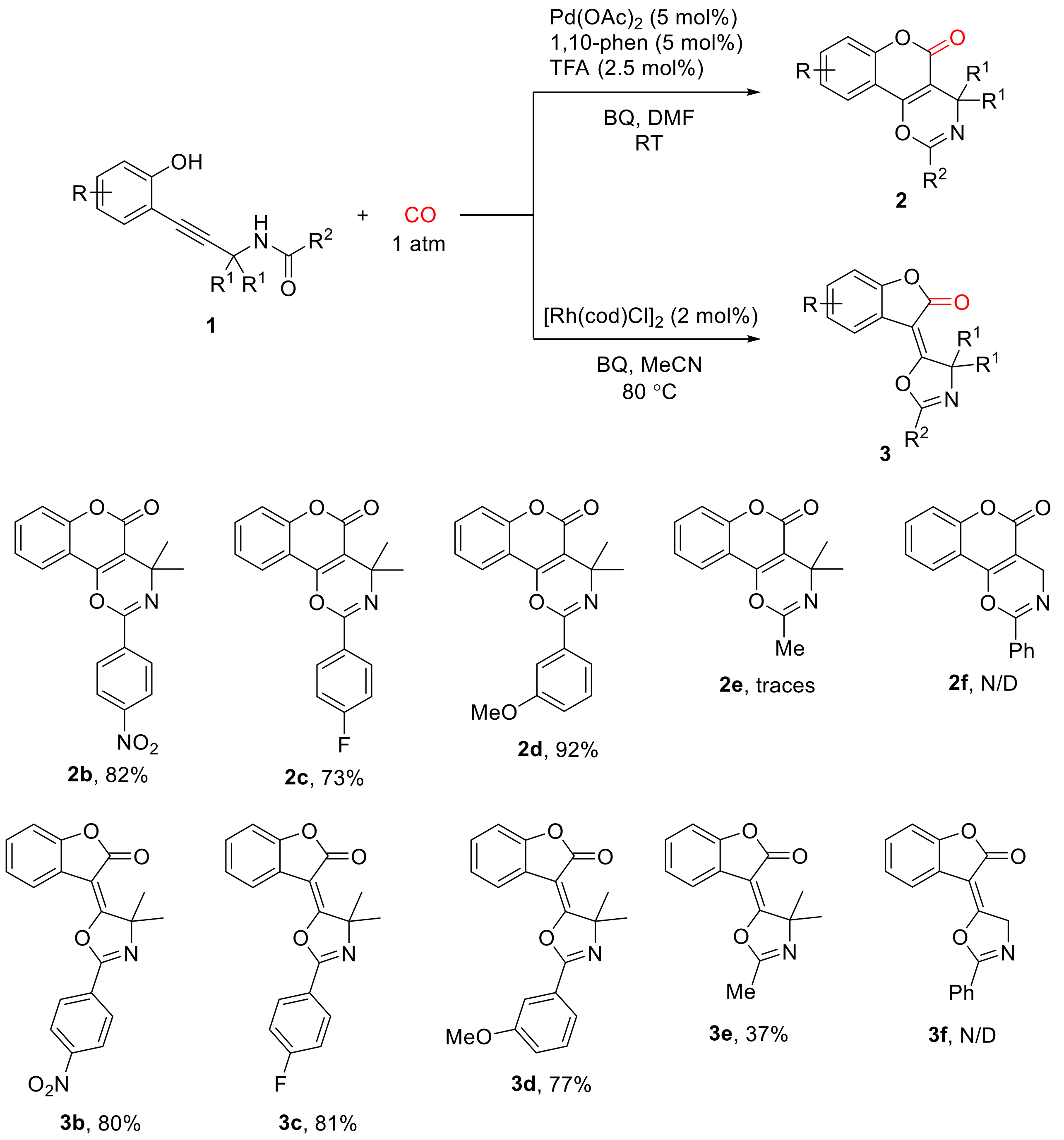

Electron-withdrawing and electron-donating substituents at the benzene ring of the amide moiety were well-tolerated by both methods. The corresponding products **2b-d** and *E*-**3b-d** were obtained in good yields (73-92%). However, when the aryl of the amide fragment was substituted with methyl, only traces of **2e** were observed under palladium catalysis, while **3e** formed in low yield (37%) by rhodium-catalysed carbonylation. It turned out that **2e** possesses low stability and easily hydrolyses to give 4-hydroxycoumarin, which was observed as a main product of the palladium-catalysed reaction. The formation of **2f** and **3f** was not observed in none of two processes. This might indicate that the Ingold-Thorpe effect of angle compression plays a fundamental role in the cyclisation step.

Our colleagues from the Research Centre for Natural Sciences in Budapest performed DFT calculations for the palladium-catalysed domino carbonylation cycloisomerisation (Scheme 4-1). The energy profile suggests that, in the initial step, *6-endo-dig* cyclisation has lower energy barrier, while *5-exo-dig* pathway requires more energy (27.6 kcal/mol vs 23.1 kcal/mol). This correlates with the experimental data as *6-endo-dig* product is favoured under palladium catalysis.

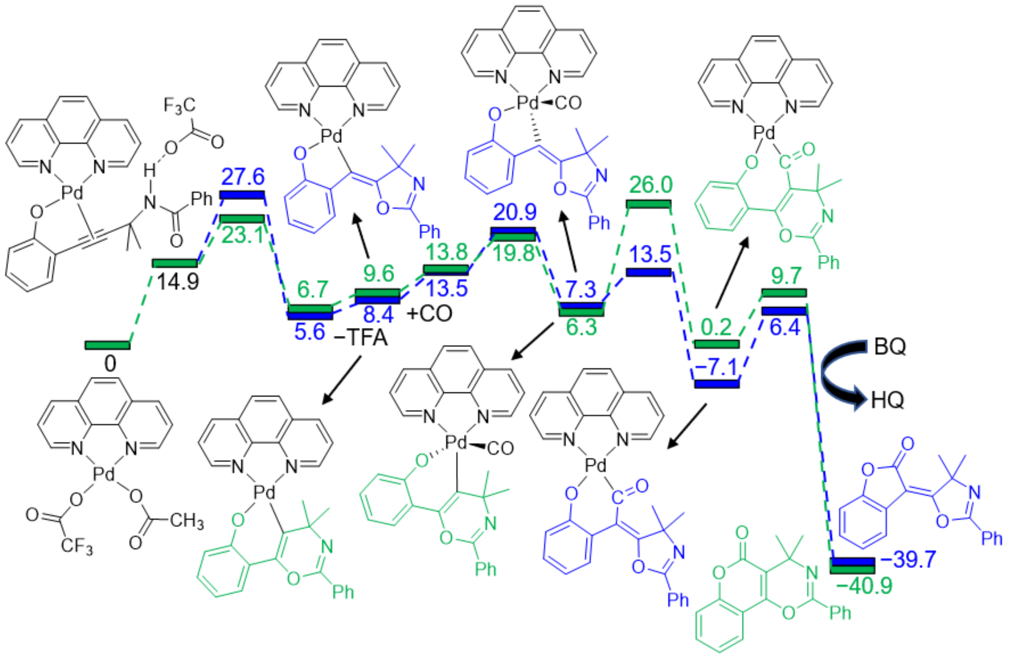

Scheme 4-1. Energy Profile of the Palladium-Catalysed Carbonylation of **1a**.

To unequivocally determine the structures of the obtained compounds X-ray analysis of the products **2a**, **3a** and **3e** was performed. As we suggested, **2a** is a product of *6-endo-dig* cyclisation forming under palladium catalysis (Figure 4-2), while **3a** and **3e** are (*E*)-3-(oxazol-5(4*H*)-ylidene)benzofuran-2(3*H*)-one derivatives obtained by Rh-catalysed carbonylative *5-exo-dig* cyclisation sequence (Figures 4-3 and 4-4).

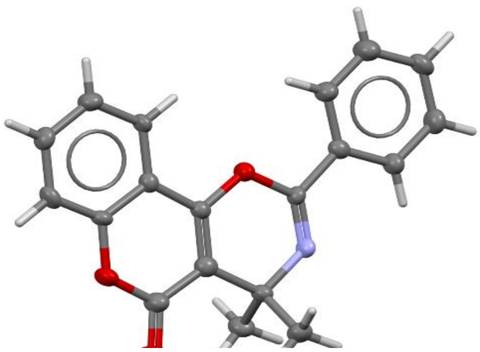

Figure 4-2. Structure of **2a** Obtained by X-ray Analysis.

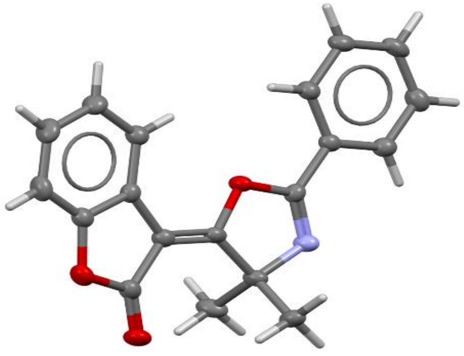

Figure 4-3. X-ray Structure of **3a**.

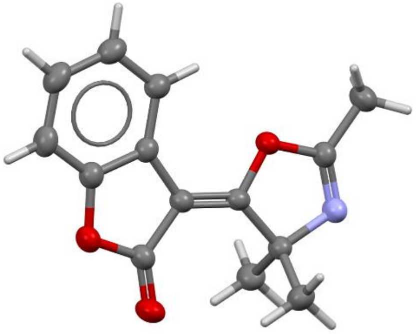

Figure 4-4. X-ray Structure of **3e**.

Conclusions

Selective and sustainable catalytic methods for the synthesis of coumarin and 2-coumaranone-based structures are herein reported. Starting from phenol derivatives bearing a propargylamide moiety in *ortho*-position, a catalyst-directed divergent reactivity has been accessed by palladium and rhodium catalysis. Carbonylative cyclisation cascade proceeded through the *6-endo-dig* pathway when a palladium-based catalytic system was used, while a rhodium complex directed the process towards the *5-exo-dig* cyclisation mode. Highly selective formation of the novel 4*H*,5*H*-chromeno[3,4-*e*][1,3]oxazin-5-ones and (*E*)-3-(oxazol-5(4*H*)-ylidene)benzofuran-2(3*H*)-ones has been achieved under mild conditions. A detailed DFT study has been performed for the palladium catalysed process.

Experimental Part

Preparation of 2-Iodophenylacetates (O-Acylation):[37]

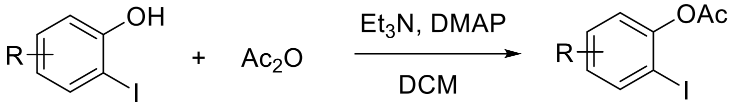

To a 50 mL flask was added a solution of a 2-iodophenol (4 mmol), dimethylaminopyridine (DMAP, 0.2 mmol, 24 mg), and Et_3N (7.2 mmol, 1 mL) in 8 mL of DCM. Then acetic anhydride (4.8 mmol, 450 µL) was added dropwise to the stirring solution. The reaction was monitored by TLC. When the starting 2-iodophenol was consumed (in 1-3 h), the resulting solution was poured into a cold 1M NaCl solution. The organic layer was extracted with DCM (2x10 mL), dried over anhydrous Na_2SO_4 and filtered. Solvent evaporation afforded 2-iodophenylacetate that was used without purification.

Preparation of Propargylamides (N-Acylation):[22]

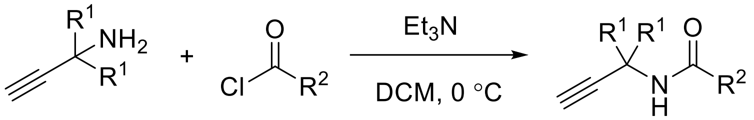

In a 100 mL flask, a solution of a propargylamine (5 mmol) and Et_3N (7.2 mmol, 1 mL) in 15 mL of DCM was cooled to 0 ˚C. Acyl chloride (5.05 mmol) was added dropwise to the stirring solution. The reaction was monitored by TLC. When the starting propargylamine was consumed (in 10-30 min), the resulting solution was poured into a 1M NH_4Cl solution. The organic layer was extracted with DCM (2x15 mL), dried over anhydrous Na_2SO_4 and filtered. Solvent evaporation afforded propargylamide that was used without purification.

Synthesis of 2-(3-Propargylamide)aryl Acetates (Sonogashira Coupling):[38]

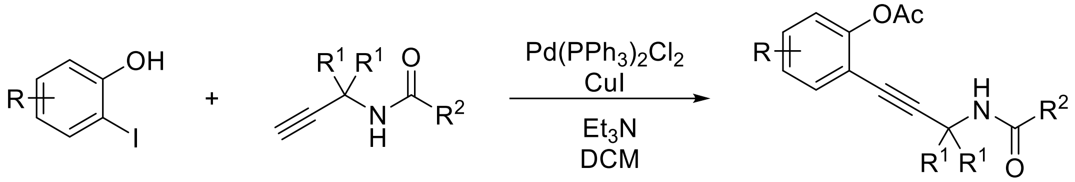

In a 50 mL Schlenk tube under N_2, a 2-iodophenylacetate (2 mmol, 1 equiv), and a propargylamide (2.1 mmol, 1.05 equiv) were dissolved in 1-3 mL of DCM. Then $Pd(PPh_3)_2Cl_2$ (0.04 mmol, 28 mg), Et_3N (36 mmol, 5 mL), and, lastly, CuI (0.1 mmol, 18 mg) were added. The Schlenk tube was sealed and the reaction mixture was stirred at 45 ˚C for 2-6 h. When the 2-iodophenylacetate was fully consumed, the mixture was filtered through a thin pad of Celite® and poured into a 1M NH_4Cl solution. The organic layer was extracted with DCM (3x10 mL), dried over anhydrous Na_2SO_4, filtered and concentrated in vacuo. Flash column chromatography on silica gel (hexane/EtOAc mixtures in 1:10 – 1:2 ratios as eluent) afforded pure 2-(3-propargylamide)aryl acetate.

Synthesis of 2-(3-Propargylamide)phenols ***1a-l*** *(Phenol Deprotection):*[38]

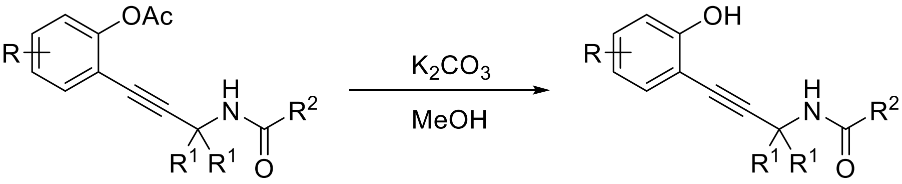

1

In a 50 mL flask, the solution of 2-(3-propargylamide)aryl acetate (1 mmol, 1 equiv) in 3 mL methanol was cooled to 0 ˚C. Potassium carbonate (2 mmol, 276 mg) was added to the stirring solution. When the starting acetate was fully converted (in 10-20 min, TLC control), methanol was evaporated under reduced pressure, and the residue was diluted with 15 mL of 0.5 M NH_4Cl solution. The organic phase was extracted with EtOAc (3x10 mL), dried over anhydrous Na_2SO_4 and filtered. Solvent evaporation afforded pure 2-(3-propargylamide)phenol **1**.

*General Procedure for the Synthesis of 4H,5H-Chromeno[3,4-e][1,3]oxazin-5-ones **2a-d**:*

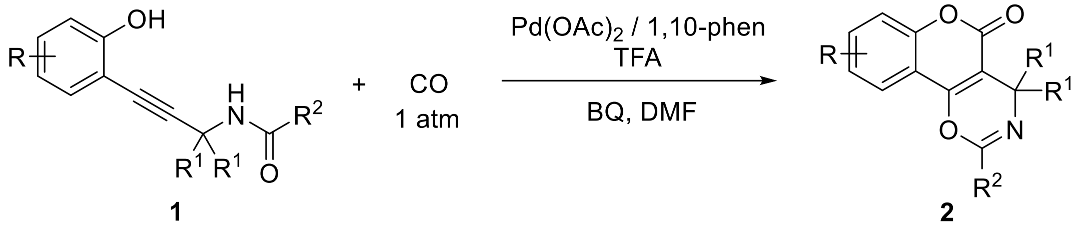

In a 45 mL Schlenk tube under N$_2$, palladium acetate (0.01 mmol, 2.2 mg) and 1,10-phenanthroline (0.01 mmol, 1.8 mg) were dissolved in 2 mL of a 2.5 µM trifluoroacetic acid solution in dry DMF (0.005 mmol, 0.38 µL of TFA in 2 mL of DMF). The solution was stirred for 15 minutes at room temperature and then **1** (0.2 mmol, 1 equiv) was added, followed by the addition of 1,4-benzoquinone (0.24 mmol, 1.2 equiv). The reaction was purged with CO for ~30 seconds and, finally, a balloon charged with CO (1 atm) was attached to the tube. Full conversion of **1** was observed after 2-4 hours of reaction time. The resulting mixture was filtered through a pad of Celite® and concentrated in vacuo. The product **2** was isolated by flash column chromatography on silica gel using mixtures of hexane/DCM (4:1 – 1:3 ratios) as eluent.

*General Procedure for the Synthesis of (E)-3-(Oxazol-5(4H)-ylidene)benzofuran-2(3H)-ones **3a-e**:*

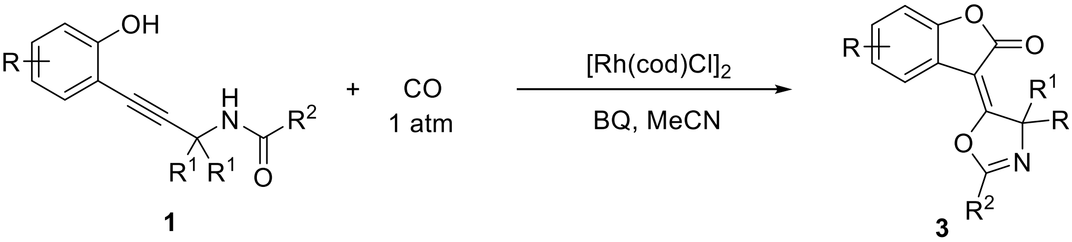

In a 45 mL Schlenk tube under N$_2$, chloro(1,5-cyclooctadiene)rhodium(I) dimer (0.004 mmol, 2 mg), **1** (0.2 mmol, 1 equiv) and 1,4-benzoquinone (0.24 mmol, 1.2 equiv) were dissolved in 2 mL of dry acetonitrile. The reaction was purged with CO for ~30 seconds and, finally, a balloon charged with CO (1 atm) was attached to the tube. The reaction mixture was heated at 80 ˚C for 2-6 hours. The resulting mixture was filtered through a pad of Celite® and concentrated in vacuo. The product **3** was isolated by flash column chromatography on silica gel using mixtures of hexane/DCM (4:1 – 1:3 ratios) as eluent.

Table 4-5. Crystallographic Data and Structure Refinement.

Identification code	2a	3a	3e
Empirical formula	$C_{19}H_{16}NO_3$	$C_{19}H_{15}NO_3$	$C_{14}H_{13}NO_3$
Formula weight	306.33	305.32	243.25
Temperature/K	150.0	150.0	200.00
Crystal system	orthorhombic	triclinic	monoclinic
Space group	$Cmc2_1$	P-1	$P2_1/m$
a/Å	6.851(9)	7.0158(14)	7.9781(3)
b/Å	20.24(2)	10.611(3)	6.7272(2)

c/Å	10.748(14)	10.847(3)	11.0238(4)
α/°	90	102.103(8)	90
β/°	90	106.891(8)	94.605(2)
γ/°	90	93.349(8)	90
Volume/Å^3	1491(3)	749.3(3)	589.74(4)
Z	4	2	2
ρ_{calc}g/cm^3	1.365	1.353	1.370
μ/mm^{-1}	0.093	0.092	0.798
F(000)	644.0	320.0	256.0
Crystal size/mm^3	0.8 × 0.7 × 0.3	0.24 × 0.23 × 0.18	0.6 × 0.4 × 0.3
Radiation	MoKα (λ = 0.71073)	MoKα (λ = 0.71073)	CuKα (λ = 1.54178)
2Θ range for data collection/°	4.024 to 52.816	3.958 to 52.904	8.046 to 148.682
Index ranges	$-6 \le h \le 8$, $-24 \le k \le 25$, $-12 \le l \le 13$	$-8 \le h \le 8$, $-13 \le k \le 13$, $-13 \le l \le 13$	$-9 \le h \le 9$, $-8 \le k \le 8$, $-13 \le l \le 13$
Reflections collected	4467	23830	8113
Independent reflections	1524 R_{int} = 0.0236, R_{sigma} = 0.0259	3083 R_{int} = 0.0609, R_{sigma} = 0.0339	1307 R_{int} = 0.0364, R_{sigma} = 0.0227
Data/restraints/parameters	1524/1/137	3083/0/210	1307/0/109
Goodness-of-fit on F^2	1.106	1.102	1.053
Final R indexes [I>=2σ (I)]	R_1 = 0.0396, wR_2 = 0.0951	R_1 = 0.0526, wR_2 = 0.1127	R_1 = 0.0366, wR_2 = 0.0915
Final R indexes [all data]	R_1 = 0.0462, wR_2 = 0.0994	R_1 = 0.0668, wR_2 = 0.1186	R_1 = 0.0452, wR_2 = 0.1005
Largest diff. peak/hole / e Å^{-3}	0.18/-0.32	0.22/-0.23	0.23/-0.20

DFT computational study details:

Software: Gaussian16.[39]

The DFT calculations were performed using the M06 functional.[40]

The geometry optimizations were carried out with the 6-31+G* basis set for the nonmetal atoms.[41]

The palladium was treated with the LANL2DZ basis set and effective core potential (ECP),[42] where the basis was expanded with two additional polarization (f) functions.

To evaluate the nature of the stationary points and to obtain free energy corrections, frequency calculations were performed using the RRHO approximation.

The electronic energies were refined with the 6-311++G(3df,3pd) basis for nonmetals.[43]

Solvation free energies (DMF solvent) were calculated using the Solvation Model Based on Density (SMD) approach.[44]

***N*-(4-(2-Hydroxyphenyl)-2-methylbut-3-yn-2-yl)benzamide (1a):** Colourless solid (474 mg, 85% overall yield after Sonogashira coupling and phenol deprotection); m.p. 126.3-128.7 ˚C; **^{1}H NMR (400 MHz, CDCl$_3$)** δ 8.02 – 7.91 (br s, 1H), 7.83 – 7.77 (m, 2H), 7.54 – 7.48 (m, 1H), 7.46 – 7.39 (m, 2H), 7.28 – 7.19 (m, 2H), 6.98 (dd, *J* = 8.3, 1.1 Hz, 1H), 6.82 (td, *J* = 7.5, 1.2 Hz, 1H), 6.42 (br s, 1H), 1.80 (s, 6H). **^{13}C NMR (101 MHz, CDCl$_3$)** δ 167.4, 159.0, 134.4, 131.8, 130.3, 130.1, 128.6 (2C), 127.1 (2C), 119.3, 115.2, 109.2, 98.4, 77.6, 48.1, 29.4 (2C). **HRMS (ESI)** m/z calcd for $C_{18}H_{17}NO_2$ [M+H]$^+$: 280.1259, found: 280.1261. **IR (ATR diamond, neat):** *v* 3321.4, 3256.3, 2986.2, 2971.2, 2929.0, 1646.6, 1573.9, 1531.6, 1487.5, 1461.5, 1312.4, 1291.3, 1240.0, 1214.2, 1179.2, 1158.5, 1028.8, 888.5, 755.3, 721.5, 691.9, 654.5 cm^{-1}.

***N*-(4-(2-Hydroxyphenyl)-2-methylbut-3-yn-2-yl)benzamide (2b):** Light yellow solid (261 mg, 68% overall yield after Sonogashira coupling and phenol deprotection); m.p. 52.6-54.0 ˚C; **^{1}H NMR (400 MHz, CDCl$_3$)** δ 8.22 – 8.15 (m, 2H), 7.94 – 7.87 (m, 2H), 7.76 (s, 1H), 7.23 (t, *J* = 7.8 Hz, 2H), 6.94 (dd, *J* = 7.9, 1.3 Hz, 1H), 6.82 (td, *J* = 7.6, 1.1 Hz, 1H), 6.74 (s, 1H), 1.81 (s, 6H). **^{13}C NMR (101 MHz, CDCl$_3$)** δ 165.5, 158.6, 149.6, 139.9, 130.5, 130.3, 128.3 (2C), 123.8 (2C), 119.7, 115.1, 108.9, 97.9, 77.8, 48.7, 29.3 (2C). **HRMS (ESI)** m/z calcd for $C_{18}H_{16}N_2O_4$ [M+H]$^+$: 324.1110, found: 324.1113. **IR (ATR diamond, neat):** *v* 3321.7, 2982.0, 2937.1, 2863.5, 1650.7, 1600.9, 1521.0, 1483.8, 1345.0, 1291.0, 1210.9, 1179.1, 1107.0, 1031.0, 1013.9, 866.3, 854.4, 754.2, 720.3 cm^{-1}.

4-Fluoro-*N*-(4-(2-hydroxyphenyl)-2-methylbut-3-yn-2-yl)benzamide (2c): Colourless solid (496 mg, 79% overall yield after Sonogashira coupling and phenol deprotection); m.p. 122.9-123.1 ˚C; **^{1}H NMR (400 MHz, CDCl$_3$)** δ 7.99 (s, 1H), 7.81 – 7.72 (m, 2H), 7.24 (ddd, *J* = 15.3, 7.6, 1.7 Hz, 2H), 7.04 (t, *J* = 8.6 Hz, 2H), 6.96 (dd, *J* = 8.2, 1.1 Hz, 1H), 6.82 (td, *J* = 7.5, 1.1 Hz, 1H), 6.57 (s, 1H), 1.78 (s, 6H). **^{13}C NMR (101 MHz, CDCl$_3$)** δ 166.5, 166.1, 163.6, 158.8, 130.6, 130.5, 130.3, 130.2, 129.5, 129.4, 119.5, 115.7, 115.5, 115.1, 109.2, 98.5, 77.5, 48.2, 29.3. **HRMS (ESI)** m/z calcd for $C_{18}H_{16}FNO_2$ [M+H]$^+$: 298.1165, found: 298.1163. **IR (ATR diamond, neat):** *v* 3289.6, 2982.6, 1633.6, 1603.0, 1536.6, 1483.9, 1315.6, 1215.3, 1157.4, 845.5, 751.5 cm^{-1}.

2-Bromo-*N*-(4-(2-hydroxyphenyl)-2-methylbut-3-yn-2-yl)benzamide (2d): Colourless solid (516 mg, 72% overall yield after Sonogashira coupling and phenol deprotection); m.p. 121.6-122.2 ˚C; **^{1}H NMR (400 MHz, CDCl$_3$)** δ 7.49 (ddd, *J* = 14.8, 7.8, 1.5 Hz, 2H), 7.31 – 7.16 (m, 4H), 6.92 (dd, *J* = 8.3, 1.1 Hz, 1H), 6.81 (td, *J* = 7.5, 1.2 Hz, 1H), 6.63 (s, 1H), 1.75 (s, 6H). **^{13}C NMR (101 MHz, CDCl$_3$)** δ 167.5, 158.9, 137.3, 133.3, 131.4, 130.3, 130.3, 129.6, 127.6, 119.4, 119.3, 115.2, 109.3, 98.2, 77.6, 48.5, 29.2 (2C). **HRMS (ESI)** m/z calcd for $C_{18}H_{16}BrNO_2$ [M+H]$^+$: 358.0364, found: 358.0366. **IR (ATR diamond, neat):** *v* 3389.5, 3253.1, 2987.7, 1625.7, 1528.4, 1485.8, 1434.6, 1321.3, 1210.8, 1025.9, 757.5, 749.2 cm^{-1}.

***N*-(4-(2-Hydroxyphenyl)-2-methylbut-3-yn-2-yl)-3-methoxybenzamide (2e):** Colourless solid (556 mg, 90% overall yield after Sonogashira coupling and phenol deprotection); m.p. 106.6-107.6 ˚C; **^{1}H NMR (400 MHz, CDCl$_3$)** δ 8.14 (br s, 1H), 7.38 – 7.17 (m, 5H), 6.97 (tdd, *J* = 5.5, 2.7, 1.1 Hz, 2H), 6.82 (td, *J* = 7.4, 1.1 Hz, 2H), 3.76 (s, 3H), 1.78 (s, 6H). **^{13}C NMR (101 MHz, CDCl$_3$)** δ 167.6, 159.7, 158.9, 135.8, 130.3, 130.2, 129.6, 119.5, 119.1, 117.9, 115.1, 112.4, 109.4, 98.8, 77.4, 55.4, 48.1, 29.3 (2C). **HRMS (ESI)** m/z calcd for $C_{19}H_{19}NO_3$ [M+H]$^+$: 310.1365, found: 310.1366. **IR (ATR diamond, neat):** *v* 3384.6, 3220.1, 2989.3, 2940.4, 2834.5, 1636.1, 1585.5, 1519.9, 1485.1, 1463.1, 1307.3, 1288.8, 1244.4, 1211.4, 1178.3, 1035.0, 860.3, 867.5, 755.1 cm^{-1}.

***N*-(4-(2-Hydroxyphenyl)-2-methylbut-3-yn-2-yl)benzamide (2f):** Colourless solid (347 mg, 80% overall yield after Sonogashira coupling and phenol deprotection); m.p. 161.9-162.3 ˚C; **^{1}H NMR (400 MHz, $CDCl_3$)** δ 7.84 (s, 1H), 7.22 (dh, *J* = 6.8, 1.7 Hz, 2H), 6.95 (dd, *J* = 8.7, 1.2 Hz, 1H), 6.80 (td, *J* = 7.5, 1.2 Hz, 1H), 5.91 (s, 1H), 2.03 (s, 3H), 1.66 (s, 6H). **^{13}C NMR (101 MHz, $CDCl_3$)** δ 170.2, 159.0, 130.2, 130.0, 119.3, 115.2, 109.1, 98.5, 77.38, 47.6, 29.3 (2C), 24.1. **HRMS (ESI)** m/z calcd for $C_{13}H_{15}NO_2$ [M+H]$^+$: 217.1103, found: 217.1103. **IR (ATR diamond, neat):** *v* 3336.8, 3074.9, 2975.8, 2755.9, 2609.0, 1650.7, 1586.0, 1446.1, 1381.7, 1229.0, 1184.2, 752.2 cm^{-1}.

***N*-(3-(2-Hydroxyphenyl)prop-2-yn-1-yl)benzamide (2g):** Colourless solid (292.5 mg, 58% overall yield after Sonogashira coupling and phenol deprotection); m.p. 141.2-142.4 ˚C; **^{1}H NMR (400 MHz, $CDCl_3$)** δ 7.89 – 7.78 (m, 2H), 7.57 – 7.38 (m, 5H), 7.26 (dtd, *J* = 19.5, 7.3, 1.3 Hz, 2H), 6.95 (t, *J* = 5.7 Hz, 1H), 6.65 (s, 1H), 4.77 (d, *J* = 5.6 Hz, 2H). **^{13}C NMR (101 MHz, $CDCl_3$)** δ 167.5, 155.0, 154.1, 134.8, 134.0, 131.7, 128.6 (2C), 128.3, 127.9, 127.1 (2C), 124.2, 122.9, 121.0, 111.1, 104.3, 37.5. **HRMS (ESI)** m/z calcd for $C_{16}H_{13}NO_2$ [M+H]$^+$: 252.0946, found: 252.0946. **IR (ATR diamond, neat):** *v* 3672.2, 3274.5, 2987.5, 2900.5, 1620.1, 1568.9, 1536.7, 1487.3, 1240.6, 1173.7, 1076.1, 756.0, 693.6, 645.9 cm^{-1}.

***N*-(1-((2-Hydroxyphenyl)ethynyl)cyclohexyl)benzamide (2h):** Colourless solid (480 mg, 75% overall yield after Sonogashira coupling and phenol deprotection); m.p. 66.8-67.9 ˚C; **^{1}H NMR (400 MHz, $CDCl_3$)** δ 7.91 (br s, 1H), 7.81 (dd, *J* = 7.2, 1.8 Hz, 2H), 7.58 – 7.48 (m, 1H), 7.44 (t, *J* = 7.7 Hz, 2H), 7.33 – 7.19 (m, 2H), 6.98 (dd, *J* = 8.3, 1.1 Hz, 1H), 6.82 (td, *J* = 7.5, 1.1 Hz, 1H), 6.33 (s, 1H), 2.39 (dd, *J* = 11.1, 5.3 Hz, 2H), 1.90 – 1.65 (m, 7H), 1.45 – 1.26 (m, 1H). **^{13}C NMR (101 MHz, $CDCl_3$)** δ 167.2, 159.0, 134.6, 131.8, 130.3, 130.2, 128.6 (2C), 127.0 (2C), 119.3, 115.2, 109.4, 97.0, 79.5, 52.4, 37.5, 25.3, 22.6. **HRMS (ESI)** m/z calcd for $C_{21}H_{21}NO_2$ [M+H]$^+$: 320.1572, found: 320.1571. **IR (ATR diamond, neat):** *v* 3314.4, 2931.6, 2856.8, 1637.6, 1571.1, 1515.9, 1482.5, 1445.3, 1289.1, 1186.4, 1029.1, 752.0, 712.4 cm^{-1}.

***N*-(4-(5-Acetyl-2-hydroxyphenyl)-2-methylbut-3-yn-2-yl)benzamide (2i):** Colourless solid (541 mg, 84% overall yield after Sonogashira coupling and phenol deprotection); m.p. 149.0-149.4 ˚C; **^{1}H NMR (400 MHz, $CDCl_3$)** δ 8.67 (br s, 1H), 7.92 – 7.84 (m, 2H), 7.84 – 7.79 (m, 2H), 7.57 – 7.49 (m, 1H), 7.49 – 7.40 (m, 2H), 7.01 (d, *J* = 8.6 Hz, 1H), 6.50 (s, 1H), 2.54 (s, 3H), 1.80 (s, 6H). **^{13}C NMR (101 MHz, $CDCl_3$)** δ 196.3, 167.6, 163.2, 134.2, 132.0, 131.3, 131.0, 129.2, 128.7 (2C), 127.1 (2C), 115.4, 109.5, 99.0, 76.8, 48.1, 29.3, 28.8 (2C), 26.3. **HRMS (ESI)** m/z calcd for $C_{20}H_{19}NO_3$ [M+H]$^+$: 322.1365, found: 322.1366. **IR (ATR diamond, neat):** *v* 3356.0, 3215.3, 2983.8, 1668.8, 1652.4, 1562.3, 1534.0, 1315.7, 1209.0, 893.0, 831.0, 714.1, 691.5 cm^{-1}.

Methyl 3-(3-benzamido-3-methylbut-1-yn-1-yl)-4-hydroxybenzoate (2j): Colourless solid (595 mg, 88% overall yield after Sonogashira coupling and phenol deprotection); m.p. 126.3-127.0 ˚C; **^{1}H NMR (400 MHz, $CDCl_3$)** δ 7.97 (d, *J* = 2.2 Hz, 1H), 7.91 (dd, *J* = 8.7, 2.2 Hz, 1H), 7.84 – 7.76 (m, 2H), 7.54 – 7.47 (m, 1H), 7.42 (dd, *J* = 8.3, 6.9 Hz, 2H), 6.98 (d, *J* = 8.7 Hz, 1H), 6.54 (s, 1H), 3.87 (s, 3H), 1.79 (s, 6H). **^{13}C NMR (101 MHz, $CDCl_3$)** δ 167.6, 166.5, 163.0, 134.2, 132.3, 132.0, 128.7 (2C), 127.1 (2C), 121.4, 115.2, 109.5, 98.9, 76.8, 51.9, 48.0, 29.3 (2C). **HRMS (ESI)** m/z calcd for $C_{20}H_{19}NO_4$ [M+H]$^+$: 338.1314, found: 338.1314.

IR (ATR diamond, neat): *v* 3381.6, 3255.4, 2982.0, 2944.6, 1712.7, 1655.2, 1525.0, 1438.4, 1315.6, 1214.5, 1112.8, 767.6, 723.5, 695.8 cm^{-1}.

1-(4-(2-Hydroxyphenyl)-2-methylbut-3-yn-2-yl)-3-phenylurea (2k): Colourless solid (473 mg, 80% overall yield after Sonogashira coupling and phenol deprotection); m.p. 156.7-157.4 ˚C; **^{1}H NMR (400 MHz, CDCl$_3$)** δ 8.09 (s, 1H), 7.33 – 7.18 (m, 5H), 7.10 – 7.02 (m, 1H), 6.92 (dd, *J* = 18.8, 8.1 Hz, 2H), 6.82 (td, *J* = 7.6, 1.8 Hz, 1H), 5.42 (d, *J* = 7.7 Hz, 1H), 1.62 (s, 6H). **^{13}C NMR (101 MHz, CDCl$_3$)** δ 158.8, 155.4, 138.0, 130.2, 130.1, 129.3 (3C), 124.2, 121.4 (2C), 119.5, 115.1, 109.4, 99.6, 47.6, 29.7 (2C). **HRMS (ESI)** m/z calcd for $C_{18}H_{18}N_2O_2$ [M+H]$^+$: 295.1368, found: 295.1366. **IR (ATR diamond, neat):** *v* 3391.8, 3253.4, 3092.5, 3043.4, 2986.2, 1626.2, 1593.2, 1553.4, 1482.9, 1434.8, 1285.9, 1237.4, 1206.1, 1171.1, 1030.0, 753.3, 737.9, 655.0 cm^{-1}.

***N*-(4-(5-Chloro-8-hydroxyquinolin-7-yl)-2-methylbut-3-yn-2-yl)benzamide (2l):** Olive green solid (621 mg, 85% overall yield after Sonogashira coupling and phenol deprotection); m.p. 135.3-136.8 ˚C; **^{1}H NMR (400 MHz, CDCl$_3$)** δ 8.86 (dd, *J* = 4.3, 1.5 Hz, 1H), 8.46 (dd, *J* = 8.5, 1.4 Hz, 1H), 7.87 – 7.78 (m, 2H), 7.58 – 7.38 (m, 5H), 6.52 (s, 1H), 1.92 (s, 6H). **^{13}C NMR (101 MHz, CDCl$_3$)** δ 166.8, 153.7, 149.2, 138.6, 134.8, 133.2, 131.6, 129.2, 128.5 (2C), 127.0 (2C), 126.4, 122.8, 120.3, 105.5, 99.7, 76.5, 49.0, 29.1 (2C). HRMS (ESI) m/z calcd for $C_{21}H_{17}ClN_2O_2$ [M+H]$^+$: 365.0979, found: 365.0976. **IR (ATR diamond, neat):** *v* 3280.9, 2979.3, 2901.3, 1643.6, 1526.4, 1487.0, 1454.6, 1361.5, 1291.7, 1187.8, 1155.8, 1048.9, 946.2, 788.5, 723.6, 713.3 cm^{-1}.

4,4-Dimethyl-2-phenyl-4*H*,5*H*-chromeno[3,4-*e*][1,3]oxazin-5-one (2a): Colourless solid (54 mg, 89%); m.p. 148.5-149.1 ˚C; **^{1}H NMR (400 MHz, CDCl$_3$)** δ 8.17 – 8.11 (m, 2H), 7.97 – 7.91 (m, 1H), 7.65 – 7.49 (m, 4H), 7.43 – 7.36 (m, 2H), 1.77 (s, 6H). **^{13}C NMR (101 MHz, CDCl$_3$)** δ 159.9, 153.8, 153.0, 145.4, 132.4, 131.6, 131.0, 128.5 (2C), 128.0 (2C), 127.8, 127.5, 124.2, 122.5, 116.7, 113.4, 107.1, 52.1, 29.8 (2C). **HRMS (ESI)** m/z calcd for $C_{19}H_{15}NO_3$ [M+H]$^+$: 305.1052, found: 305.1051. **IR (ATR diamond, neat):** *v* 2962.8, 2926.0, 2855.3, 1709.6, 1692.5, 1626.0, 1609.5, 1577.1, 1449.3, 1370.4, 1268.1, 1097.4, 1011.2, 891.4, 751.7, 689.1 cm^{-1}.

4,4-Dimethyl-2-(4-nitrophenyl)-4*H*,5*H*-chromeno[3,4-*e*][1,3]oxazin-5-one (2b): Colourless solid (57 mg, 82%); m.p. 237.5-237.9 ˚C; **^{1}H NMR (400 MHz, CDCl$_3$)** δ 8.40 – 8.29 (m, 4H), 7.91 (dd, *J* = 7.9, 1.6 Hz, 1H), 7.65 (ddd, *J* = 8.2, 7.3, 1.6 Hz, 1H), 7.46 – 7.38 (m, 2H), 1.78 (s, 6H). **^{13}C NMR (101 MHz, CDCl$_3$)** δ 159.6, 153.3, 153.0, 149.7, 144.0, 136.7, 132.7, 128.5 (2C), 124.4, 123.7 (2C), 122.3, 116.9, 113.0, 107.1, 52.7, 29.7 (2C). **HRMS (ESI)** m/z calcd for $C_{19}H_{14}N_2O_5$ [M+H]$^+$: 350.0903, found: 350.0905. **IR (ATR diamond, neat):** *v* 3104.7, 2973.9, 2924.8, 2868.0, 1763.4, 1713.2, 1692.7, 1626.9, 1518.9, 1379.7, 1341.2, 1301.6, 1271.1, 1259.8, 1175.5, 1098.6, 1031.7, 1005.0, 990.1, 890.8, 866.7, 763.2, 704.0 cm^{-1}.

2-(4-Fluorophenyl)-4,4-dimethyl-4*H*,5*H*-chromeno[3,4-*e*][1,3]oxazin-5-one (2c): Colourless solid (47 mg, 73%); m.p. 177.6-181.6 ˚C; **^{1}H NMR (400 MHz, CDCl$_3$)** δ 8.18 – 8.11 (m, 2H), 7.93 – 7.88 (m, 1H), 7.65 – 7.59 (m, 1H), 7.43 – 7.36 (m, 2H), 7.23 – 7.16 (m, 2H), 1.75 (s, 6H). **^{13}C NMR (101 MHz, CDCl$_3$)** δ 166.1, 163.6, 159.8, 153.6, 153.0, 144.6, 132.4, 129.8, 129.7, 127.2, 127.1, 124.2, 122.4, 116.8, 115.7, 115.5, 113.3, 107.1, 52.1, 29.8 (2C). **HRMS (ESI)** m/z calcd for $C_{19}H_{14}FNO_3$ [M+H]$^+$: 324.0958, found: 324.0959.

IR (ATR diamond, neat): ν 3317.3, 3145.6, 2969.8, 2929.0, 1714.0, 1689.6, 1607.6, 1509.1, 1370.4, 1271.4, 1289.2, 1155.4, 1096.7, 1029.6, 1011.1, 858.6, 750.0, 729.7 cm^{-1}.

2-(3-Methoxyphenyl)-4,4-dimethyl-4*H*,5*H*-chromeno[3,4-*e*][1,3]oxazin-5-one (2d): Colourless solid (62 mg, 92%); m.p. 184.6-185.8 ˚C; **^{1}H NMR (400 MHz, CDCl$_3$)** δ 7.95 – 7.89 (m, 1H), 7.72 (dt, *J* = 7.8, 1.1 Hz, 1H), 7.67 (dd, *J* = 2.7, 1.5 Hz, 1H), 7.64 – 7.59 (m, 1H), 7.45 – 7.35 (m, 3H), 7.10 (ddd, *J* = 8.3, 2.7, 1.0 Hz, 1H), 3.93 (s, 3H), 1.76 (s, 6H). **^{13}C NMR (101 MHz, CDCl$_3$)** δ 159.9, 159.7, 153.7, 153.0, 145.3, 132.4, 129.5, 124.3, 122.5, 119.9, 117.4, 116.7, 113.4, 112.9, 107.1, 55.5, 52.1, 29.8 (2C). **HRMS (ESI)** m/z calcd for $C_{20}H_{17}NO_4$ [M+H]$^+$: 336.1158, found: 336.1157. **IR (ATR diamond, neat):** ν 2973.9, 2924.8, 2851.3, 1761.2, 1676.5, 1651.6, 1604.1, 1586.7, 1459.6, 1426.1, 1293.9, 1241.1, 1181.3, 1155.0, 1055.5, 1019.3, 969.9, 889.4, 779.7, 751.7, 715.2, 680.9 cm^{-1}.

(*E*)-3-(4,4-Dimethyl-2-phenyloxazol-5(4*H*)-ylidene)benzofuran-2(3*H*)-one (3a): Colourless solid (59 mg, 97%); m.p. 151.6-152.1 ˚C; **^{1}H NMR (400 MHz, CDCl$_3$)** δ 8.16 – 8.10 (m, 2H), 7.83 (dd, *J* = 7.4, 1.5 Hz, 1H), 7.68 – 7.62 (m, 1H), 7.59 (dd, *J* = 8.3, 6.6 Hz, 2H), 7.36 – 7.24 (m, 2H), 7.15 (dd, *J* = 7.8, 1.2 Hz, 1H), 1.91 (s, 6H). **^{13}C NMR (101 MHz, CDCl$_3$)** δ 176.3, 167.5, 158.0, 132.7, 129.0 (2C), 128.4 (3C), 128.3, 123.9, 123.4, 123.1, 110.3, 75.6, 23.4 (2C). **HRMS (ESI)** m/z calcd for $C_{19}H_{15}NO_3$ [M+H]$^+$: 305.1052, found: 305.1052. **IR (ATR diamond, neat):** ν 3068.0, 2972.5, 2933.0, 2867.6, 1761.6, 1681.4, 1652.1, 1615.5, 1462.4, 1451.3, 1284.0, 1231.1, 1176.5, 1149.7, 1036.1, 1007.9, 966.9, 918.8, 885.3 770.6, 743.0, 683.5 cm^{-1}.

(*E*)-3-(4,4-Dimethyl-2-(4-nitrophenyl)oxazol-5(4*H*)-ylidene)benzofuran-2(3*H*)-one (3b): Colourless solid (56 mg, 80%); m.p. 281.9-282.9 ˚C; **^{1}H NMR (400 MHz, CDCl$_3$)** δ 8.48 – 8.41 (m, 2H), 8.34 – 8.28 (m, 2H), 7.81 – 7.74 (m, 1H), 7.36 (td, *J* = 7.8, 1.5 Hz, 1H), 7.32 – 7.26 (m, 1H), 7.19 – 7.14 (m, 1H), 1.92 (s, 6H). **^{13}C NMR (101 MHz, CDCl$_3$)** δ 175.0, 167.2, 156.4, 151.8, 150.2, 131.1, 129.4 (2C), 128.8, 124.1 (2C), 124.0, 123.1, 123.0, 110.5, 100.5, 76.1, 23.5 (2C). **HRMS (ESI)** m/z calcd for $C_{19}H_{14}N_2O_5$ [M+H]$^+$: 350.0903, found: 350.0906. **IR (ATR diamond, neat):** ν 3301.0, 3072.0, 2922.0, 2855.3, 1756.3, 1676.9, 1646.2, 1528.3, 1456.1, 1346.5, 1279.1, 1182.8, 1166.0, 1022.6, 1005.7, 971.2, 861.6, 752.7 cm^{-1}.

(*E*)-3-(2-(4-Fluorophenyl)-4,4-dimethyloxazol-5(4*H*)-ylidene)benzofuran-2(3*H*)-one (3c): Colourless solid (53 mg, 81%); m.p. 151.6-152.1 ˚C; **^{1}H NMR (400 MHz, CDCl$_3$)** δ 8.16 – 8.10 (m, 2H), 7.80 – 7.76 (m, 1H), 7.33 (td, *J* = 7.7, 1.5 Hz, 1H), 7.29 – 7.23 (m, 3H), 7.17 – 7.12 (m, 1H), 1.89 (s, 6H). **^{13}C NMR (101 MHz, CDCl$_3$)** δ 176.0, 167.4, 166.7, 164.1, 157.1, 151.7, 130.8, 130.7, 128.4, 123.9, 123.3, 123.1, 121.7, 121.6, 116.4, 116.2, 110.4, 99.7, 75.7, 23.6 (2C). **HRMS (ESI)** m/z calcd for $C_{19}H_{14}FNO_3$ [M+H]$^+$: 324.0958, found: 324.0960. **IR (ATR diamond, neat):** ν 2982.0, 2933.0, 2871.7, 1770.9, 1760.0, 1681.7, 1654.0, 1603.1, 1506.8, 1462.6, 1283.6, 1240.4, 1176.0, 1157.3, 1023.3, 1009.3, 965.1, 951.3, 843.1, 778.3, 742.2, 669.6 cm^{-1}.

(*E*)-3-(2-(3-methoxyphenyl)-4,4-dimethyloxazol-5(4*H*)-ylidene)benzofuran-2(3*H*)-one (3d): Colourless solid (52 mg, 77%); m.p. 151.6-152.1 ˚C; **^{1}H NMR (400 MHz, CDCl$_3$)** δ 7.81 (dd, *J* = 7.6, 1.4 Hz, 1H), 7.69 (dt, *J* = 7.7, 1.2 Hz, 1H), 7.64 (dd, *J* = 2.6, 1.5 Hz, 1H), 7.49 (t, *J* = 8.0 Hz, 1H), 7.35 – 7.23 (m, 2H), 7.20 – 7.12 (m, 2H), 3.94 (s, 3H), 1.90 (s, 6H). **^{13}C NMR (101 MHz, CDCl$_3$)** δ 176.2, 167.5, 159.9, 158.0, 151.7, 130.1, 128.3, 126.5, 123.9, 123.4, 123.1, 120.7, 119.0, 113.1, 110.3, 99.6, 75.6, 55.6, 23.5 (2C). **HRMS**

(ESI) m/z calcd for $C_{20}H_{17}NO_4$ $[M+H]^+$: 336.1158, found: 336.1156. **IR (ATR diamond, neat):** *v* 2973.9, 2924.8, 2851.3, 1761.2, 1676.5, 1651.6, 1604.1, 1586.7, 1459.6, 1426.1, 1293.9, 1241.1, 1181.3, 1055.5, 1019.3, 969.9, 889.4, 779.7, 751.7, 715.2, 680.9 cm^{-1}.

(*E*)-3-(2,4,4-Trimethyloxazol-5(4*H*)-ylidene)benzofuran-2(3*H*)-one (3e): Colourless solid (18 mg, 37%); m.p. 131.5-133.1 ˚C; **^{1}H NMR (400 MHz, $CDCl_3$)** δ 7.67 (ddd, *J* = 7.6, 1.4, 0.6 Hz, 1H), 7.31 – 7.25 (m, 1H), 7.18 (td, *J* = 7.6, 1.1 Hz, 1H), 7.11 (dt, *J* = 7.9, 0.8 Hz, 1H), 2.35 (s, 3H), 1.78 (s, 6H). **^{13}C NMR (101 MHz, $CDCl_3$)** δ 176.5, 167.5, 158.4, 151.6, 128.2, 123.7, 123.3, 123.2, 110.2, 99.0, 75.2, 23.2 (2C), 13.8. **HRMS (ESI)** m/z calcd for $C_{14}H_{13}NO_3$ $[M+H]^+$: 243.0895, found: 243.0896. **IR (ATR diamond, neat):** *v* 3256.0, 2979.0, 2923.9, 2855.3, 1762.1, 1699.5, 1651.8, 1612.2, 1544.5, 1458.0, 1251.2, 1176.5, 1110.4, 1015.8, 976.9, 846.4, 780.9, 754.0, 712.4 cm^{-1}.

References

1. Boyarskiy, V.P.; Ryabukhin, D.S.; Bokach, N.A.; Vasilyev, A.V. *Chem. Rev.*, **2016**, *116*, 5894.
2. Yoshida, H. *ACS Catal*., **2016**, *6*, 1799.
3. Karandeep Singh, K.; Malviya, B.K.; Roy, T.K. et al. *J. Org. Chem.*, **2018**, *83 (1)*, 57–68.
4. Zheng, Z.; Wang, Z.; Wang, Y.; Zhang, L. *Chem. Soc. Rev.*, **2016**, *45*, 4448.
5. Kiss, G. *Chem. Rev.*, **2001**, *101*, 3435−3456.
6. Quintero-Duque, S.; Dyballa, K.M.; Fleischer, I. *Tetrahedron*, **2015**, 56, 2634-2650.
7. Doherty, S.; Knight, J.G.; Smyth, C.H. Modern Carbonylation Methods, **2008**.
8. Stefanachi, A.; Leonetti, F.; Pisani, L.; Catto, M.; Carotti, A. *Molecules,* **2018**, *23*, 250.
9. Timson, D.J. *Curr. Drug Targets*, **2017**, *18 (5)*, 500-510.
10. Au, N.; Rettie, A.E. *Drug Metab. Rev.*, **2008**, *40 (2),* 355-375.
11. May, J.M.; Owens, T.W.; Mandler, M.D. et al. *J. Am. Chem. Soc*., **2017**, *139 (48)*, 17221–17224.
12. May, J.M.; Owens, T.W.; Mandler, M.D. et al. *ACS Med. Chem. Lett.*, **2019**, *10*, 893−898.
13. Venkateswarlu, S.; Panchagnula, G.K.; Guraiah, M.B. et al. *Tetrahedron*, **2005**, *61 (12)*, 3013-3017.
14. Wu, Y.-C.; Sureshbabu, M.; Fang, Y.-C. et al. *Toxicol. Appl. Pharmacol.*, **2013**, *266 (3)*, 399-407.
15. Handa, S.S.; Singh, R.; Maurya, R. *Tetrahedron*, **2000**, *41 (10)*, 1579-1581.
16. Wu, Z.-L.; Zhao, B.-X.; Huang, X.-J. *Angew. Chem.*, **2014**, *126*, 5906 –5909.
17. Uchiyama, M.; Ozawa, H.; Takuma, K. et al. *Org. Lett.*, **2006**, *8*, 5517.
18. Ding, D.; Zhu, G.; Jiang, X. *Angew. Chem. Int. Ed.*, **2018**, *57*, 9028.
19. Ge, Y.; Ye, F.; Liu, J.; Beller, M. et al. *Angew. Chem. Int. Ed.*, **2020**, *59*, 21585.
20. Acerbi, A.; Carfagna, C.; Della Ca', N. et al. *Chem. Eur. J.*, **2018**, *24*, 4835.
21. Mancuso, R.; Miliè, R.; Della Ca', N. Gabriele, B. et al. *J. Org. Chem.*, **2019**, *84 (11)*, 7303-7311.
22. Pancrazzi, F.; Sarti, N.; Della Ca', N. et al. *Org. Lett.,* **2020**, *22*, 1569−1574.
23. Kuniyasu, H.; Yoshizawa, T.; Kambe, N., *Tetrahedron*, **2010**, *51 (52)*, 6818-6821.
24. Arcadi, A.; Cacchi, S.; Fabrizi, G.; Moro, L. *Eur. J. Org. Chem.*, **1999**, *1999*, 1137-1141.
25. Shin, Y.; Yoo, C.; Moon, Y.; Lee, Y.; Hong, S. *Chem. Asian J.*, **2015**, *10*, 878-881.
26. Luo, S.; Luo, F.-X.; Zhang, X.-S.; Shi, Z.-J. *Angew. Chem. Int. Ed.*, **2013**, *52*, 10598-10601.
27. Lee, T.-H.; Jayakumar, J.; Cheng, C.-H.; Chuang, S.-C. *Chem. Commun*., **2013**, *49*, 11797-11799.
28. Hiroya, K.; Suzuki, N.; Yasuhara, A. et al. *J. Chem. Soc., Perkin Trans. 1*, **2000**, *24*, 4339–4346.
29. Luo, Y.; Wu, J. *Org. Lett.*, **2011**, *13 (21)*, 5858–5861.
30. Wang, D.; Stahl, S.S. *J. Am. Chem. Soc*., **2017**, *139 (16)*, 5704–5707.
31. Beckers, I.; Henrion, M.; De Vos, D.E. *ChemCatChem*, **2020**, *12*, 90.
32. Váňa, J.; Lang, J.; Šoltésová, M. et al. *Dalton Trans.*, **2017**, *46*, 16269.
33. Park, K.H.; Jung, I.G.; Chung, Y.K. *Synlett*, **2004**, *14*, 2541–25442.
34. Gulías, M.; Marcos-Atanes, D.; Font, M. et al. *Org. Process Res. Dev*., **2019**, *23*, 1669−1673.
35. Ai, H.-J.; Wang, H.; Li, C.-L.; Wu, X.-F. *ACS Catalysis,* **2020**, *10 (9)*, 5147-5152.
36. Yoneda, E.; Sugioka, T.; Takahashi, S. et al. *J. Chem. Soc. Perkin Trans. 1*, **1998**, 477-483.
37. Costello, J.P.; Ferreira, E.M. *Org. Lett*., **2019**, *21 (24)*, 9934 – 9939.
38. Hirner, J.J.; Faizi, D.J.; Blum, S.A. *J. Am. Chem. Soc*., **2014**, *136 (12)*, 4740 – 4745.

39. Frisch, M. J.; Trucks, G. W.; Schlegel, H.B. et al. *Gaussian, Inc., Wallingford CT*, **2016**.
40. Zhao, Y.; Truhlar, D. G. *Theor. Chem. Acc.*, **2007**, *120*, 215–241.
41. Clark, T.; Chandrasekhar, J.; Spitznagel, G. W.; Schleyer, P.V.R. *J. Comput. Chem.*, **1983**, *4*, 294–301.
42. Schuchardt, K. L.; Didier, B. T.; Elsethagen, T. et al. *J. Chem. Inf. Model.*, **2007**, *47*, 1045–1052.
43. Krishnan, R.; Binkley, J. S.; Seeger, R.; Pople, J. A. *J. Chem. Phys.*, **1980**, *72*, 650–654.
44. Marenich, A. V.; Cramer, C. J.; Truhlar, D. G. *J. Phys. Chem. B*, **2009**, *113*, 6378–6396.

Chapter 5. Visible-Light-Induced Oxidative Dearomatization of 2-Naphthylamines

Introduction

Photocatalysis as a synthetic methodology in organic chemistry has seen a remarkable expansion, as can be noted by the number of relevant publications in recent years. The specialty of photocatalysis is owed by the fact that the energy used for the bond construction is provided by light, one of the most abundant and renewable sources. Additionally, the versatility of the photocatalytic approach, given the possibility to perform both reductive and oxidative transformations and get the access to peculiar structures in highly selective manner, makes it an attractive choice for planning the synthesis.

As for oxidative photoredox-catalysis, previous research has demonstrated great success in using molecular oxygen under mild conditions either as a terminal oxidant for the catalyst reoxidation,[1-3] dehydrogenation of the starting material,[4-8] or incorporation of oxygen in the final products of the reaction.[8-16] Conventional oxidants are highly reactive species and usually are solid reagents (Cornforth reagent, *m*-CPBA, copper(II) or silver(I) salts,…), which makes them easy to handle and employ even at room temperature. However, their use in stoichiometric quantities brings the formation of large quantities of waste that needs to be disposed of, resulting in the increase of the production cost and the emergence of purification issues. On the other hand, the use of oxygen represents an economical and green alternative to classic oxidants due to its low cost, safety, high abundance, and, most importantly, the fact it leaves no toxic residues. Before photocatalysis, the thermal activation of oxygen, relatively stable in its ground state of triplet, had always been an issue due to the lack of selectivity and efficiency control at high temperatures and/or pressures. Altering the mechanism of singlet state formation by the involvement of light has become a gamechanger as it allowed to perform processes without special equipment and in a safe and efficient manner.

Aromatic compounds are generally considered low reactive due to their particular stability gained by the resonance energy. Oxidative photocatalysis allows these molecules to be activated through radical pathway, resulting in the formation of reactive intermediate species, which can be easily converted into dearomatized carbocycles. Thus, complex three-dimensional structures can be obtained starting from available two-dimensional aromatic molecules. Phenols and naphthols exhibit well reactivity under photocatalytic conditions, due to the presence of electron-rich hydroxy-groups.

Resorcinol derivatives were shown to undergo oxidative dearomatization under flavin mononucleotide (FMN) catalysis using molecular oxygen as oxidant (Scheme 5-1).[17] The transformation proceeded with high selectivity toward the formation of *ortho*-quinols. However, the presence of an aldehyde function was found to be strictly indispensable. Also, electron-withdrawing substituents were found to completely suppress the reaction.

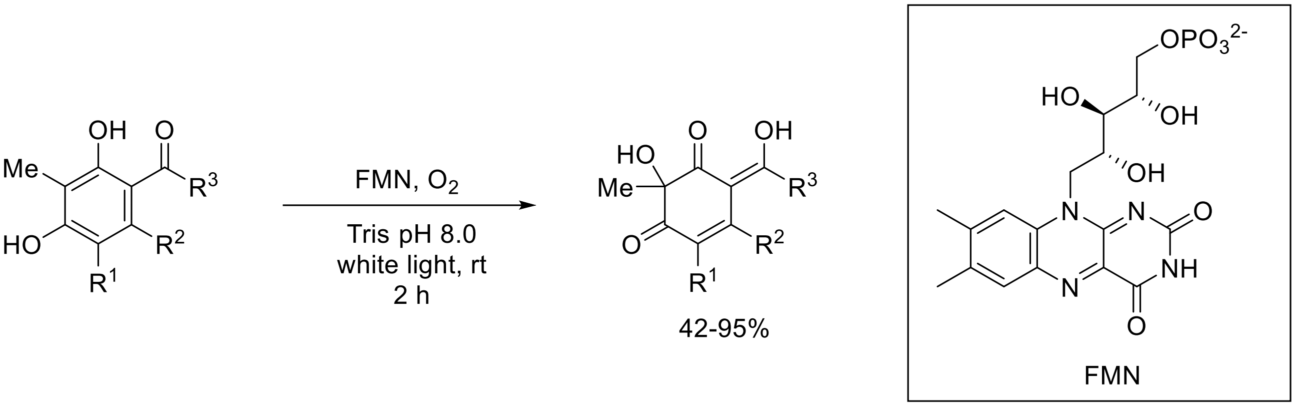

Scheme 5-1. Photocatalysed Oxidation of Resorcinol Derivatives.

β-Naphthol derivatives were successfully dearomatized by acridine-based catalyst under aerobic conditions (Scheme 5-2).[18] The intermolecular transformation of starting naphthols and *N*-hydrocycarbamates afforded exclusive formation of cyclic ketones with a stereogenic centre in α-position. Contrastingly to the previous rapid resorcinol oxidation, the reaction time for naphthols was extended up to 72 hours in some cases.

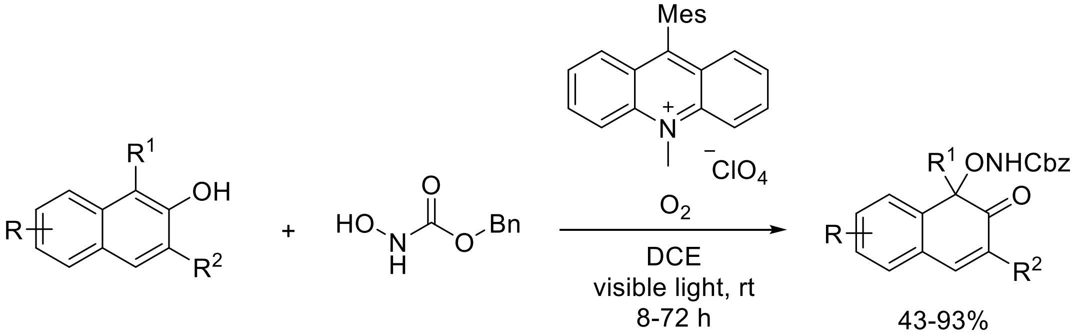

Scheme 5-2. Photocatalysed Dearomatization of 2-Naphthols.

Electron-rich heterocycles can also undergo aerobic dearomatization. Visible-light-promoted oxyamidation of indole derivatives was demonstrated to proceed with high chemo- and diastereoselectivity under Ru(bpy)$_3$Cl$_2$ catalysis, giving tetrahydro-5*H*-indolo[2,3-*b*]quinolinols.[19]

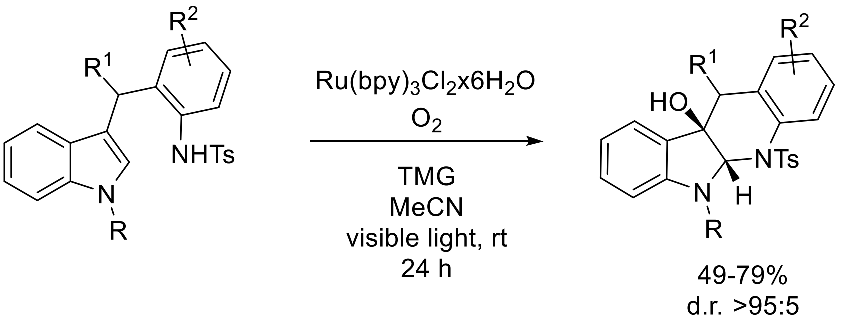

Scheme 5-3. Aerobic Oxyamidation of Indoles.

As for oxidative dearomatization of naphthylamine derivatives, only one example of photocatalytic transformation has been reported to date. The aerobic photooxidation of 2,3-dihydro-1*H*-perimidines led to the formation of mixture of 1,2-dihydroperimidinones under $Ru(bpy)_3{}^{2+}$ catalysis (Scheme 5-4).[20] Strangely, the counterion of the ruthenium complex was never mentioned in the publication.

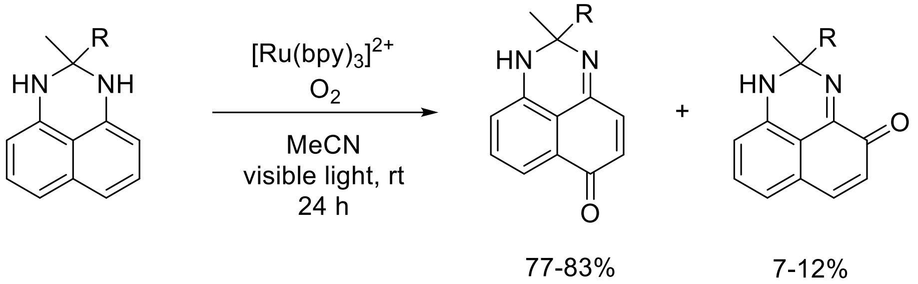

Scheme 5-4. Aerobic Oxidation of Dihydroperimidines.

Previously our research group has demonstrated that variously benzo[*b*]naphtho[1,2-*f*]azepines can be efficiently oxidised to give benzo[*b*]naphtho[1,2-f]azepin-13a-ols (Scheme 5-5). The reaction reaches completion in 24 hours when catalysed by $Ru(bpy)_3Cl_2$ using 2,6-lutidine as a base and DMSO as a solvent. The reaction conditions are very mild, in fact the process tolerates various functional groups, including halogens and trifluoromethoxy- and trifluoromethyl-groups.

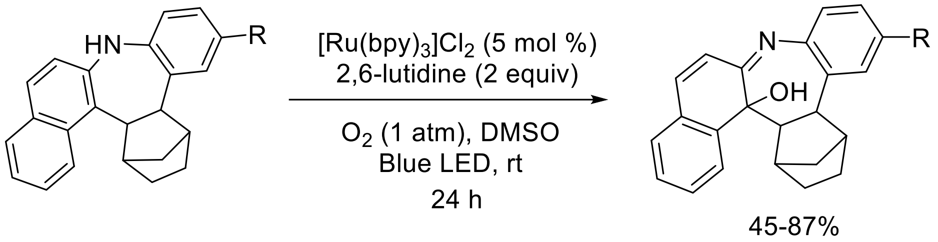

Scheme 5-5. Photocatalytic Oxidation of Benzo[*b*]naphtho[1,2-*f*]azepines.

In the course of the present study we decided to broaden the field of applicability of the photocatalytic process developed for benzo[*b*]naphtho[1,2-*f*]azepines by expanding the scope to 2-naphthylamine derivatives. We tested different solvents, bases and catalysts to define the limits of the photo-dearomatization process and make it as sustainable as possible.

Results and Discussion

Radical oxidation of *N*-arylnaphthyl-2-amines is known to proceed in many ways.[21] Once the *N*-radical is generated, at least five different products can form, varying from naphthoquinones to dibenzocarbazoles, naphthalenediamines etc. (Scheme 5-6). Usually, aerobic radical processes are completely spontaneous, and the outcome mainly depends on the concentration of the reactive species and oxygen. Even under mild conditions shifting the selectivity towards one single direction is quite a challenging task.

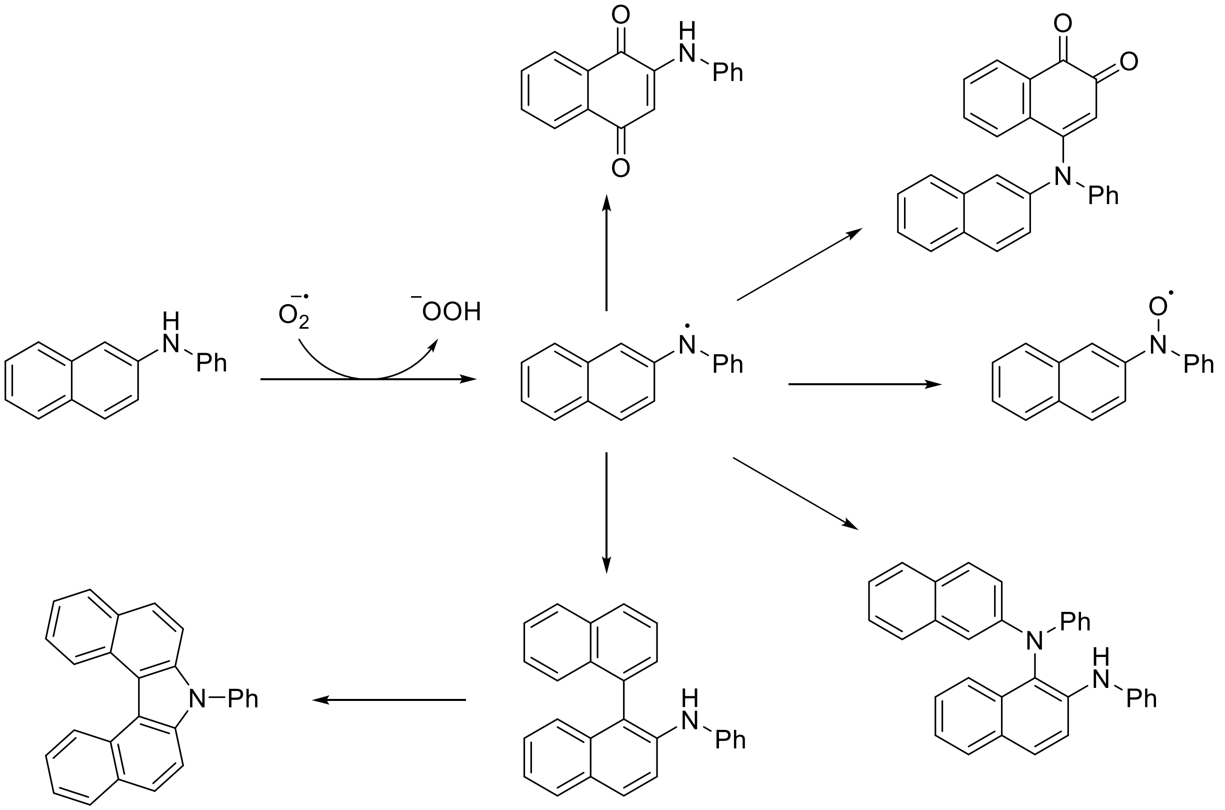

Scheme 5-6. Radical Oxidation Pathways of *N*-Phenylnaphthalen-2-amine.

Considering this, we revised the substitution pattern of 2-naphthylamine. By attaching a substituent at 1-position of the naphthylamine, we aspired to partially limit the chaotic state of the oxidation process. The designed model substrate, *N*,1-diphenylnaphtanele-2-amine **3a**, was synthetised in accordance with the sequence illustrated in Scheme 5-7. The bromination step proceeded smoothly with excellent yields, and the Suzuki coupling with phenylboronic acid afforded **3a** in 77% yield.

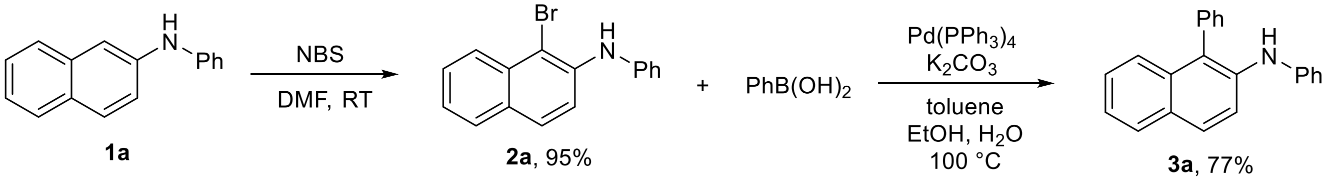

Scheme 5-7. Synthesis of the Model Compound **3a**.

The photocatalysed dearomatization of **3a** was carried out in a 50 mL Schlenk tube at room temperature under atmospheric pressure of oxygen (balloon). Preliminary experiments showed that the increased surface area of the solution and effective volume of oxygen enhance the efficiency of the process, allowing full conversion in reduced reaction times. The light irradiation was provided by an LED strip (18 W), and the temperature control was implemented by installing air coolers (ventilators) inside the light reactor. As tris(bipyridine)ruthenium(II) chloride previously demonstrated best results for the photooxidation of benzo[*b*]naphtho[1,2-*f*]azepines, we commenced the optimisation study using it as a catalyst (Table 5-1).

Table 5-1. Optimisation Study for Photocatalysed Dearomatization of **3a**.

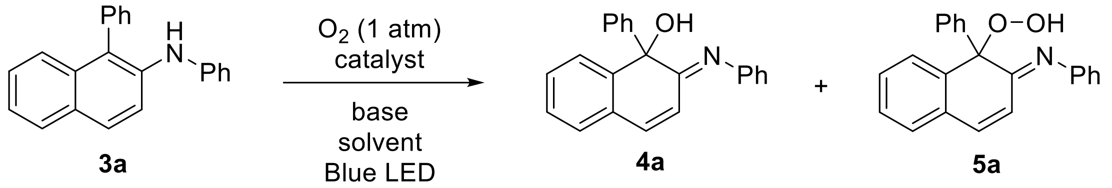

Entry	Catalyst	Base	Solvent	Time	Conv.[a] **3a**, %	Yield[a] **4a**, %	Yield[a] **5a**, %
1	$Ru(bpy)_3Cl_2{\times}6H_2O$	-	MeCN	48 h	75	5	57
2[b]	$Ru(bpy)_3Cl_2{\times}6H_2O$	-	MeCN	24 h	98	5	**83 (80)**[c]
3	$Ru(bpy)_3Cl_2{\times}6H_2O$	2,6-lutidine (2 equiv)	MeCN	48 h	78	3	58
4	$Ru(bpy)_3Cl_2{\times}6H_2O$	DIPEA (2 equiv)	MeCN	24 h	98	29	17
5	$Ru(bpy)_3Cl_2{\times}6H_2O$	DIPEA (1 equiv)	MeCN	48 h	99	34	27
6	$Ru(bpy)_3Cl_2{\times}6H_2O$	DIPEA (0.5 equiv)	MeCN	48 h	99	33	49
7	$Ru(bpy)_3Cl_2{\times}6H_2O$	**Cs_2CO_3 (2 equiv)**	MeCN	24 h	64	**37**	18
8	$Ru(bpy)_3Cl_2{\times}6H_2O$	Cs_2CO_3 (1 equiv)	MeCN	24 h	56	33	15
9	$Ru(bpy)_3Cl_2{\times}6H_2O$	Cs_2CO_3 (2 equiv)	**EtOH**	24 h	73	**57**	-
10	$Ru(bpy)_3Cl_2{\times}6H_2O$	K_2CO_3 (2 equiv)	EtOH	48 h	89	53	-
11	$Ru(bpy)_3Cl_2{\times}6H_2O$	DIPEA (2 equiv)	EtOH	48 h	81	54	-
12	$Ru(bpy)_3Cl_2{\times}6H_2O$	-	EtOH	48 h	67	18	-
13	**$Ru(bpy)_3(PF_6)_2$**	Cs_2CO_3 (2 equiv)	EtOH	24 h	100	**62**	-

14^{b}	$Ru(bpy)_3(PF_6)_2$	Cs_2CO_3 (2 equiv)	EtOH	24 h	100	**71 (67)**^{c}	-
15^{b}	$Ru(bpy)_3(PF_6)_2$	Cs_2CO_3 (2 equiv)	MeOH	24 h	100	40	-
16^{b}	$Ru(bpy)_3(PF_6)_2$	Cs_2CO_3 (2 equiv)	PrOH	24 h	100	43	-
17^{b}	$Ru(bpy)_3(PF_6)_2$	Cs_2CO_3 (2 equiv)	CF_3CH_2OH	24 h	98	-	-
18^{b}	$Ru(bpy)_3(PF_6)_2$	Cs_2CO_3 (2 equiv)	THF	24 h	5	-	-
19^{b}	$Ru(bpy)_3(PF_6)_2$	Cs_2CO_3 (2 equiv)	toluene	24 h	22	5	-
20^{b}	$Ru(bpy)_3Cl_2 \times 6H_2O$	Cs_2CO_3 (2 equiv)	EtOH	24 h	100	60	-
21^{b}	Eosin Y	Cs_2CO_3 (2 equiv)	EtOH	24 h	65	23	-
22^{b}	2,4,6-Triphenylpyrylium tetrafluoroborate	Cs_2CO_3 (2 equiv)	EtOH	24 h	-	-	-
23^{b}	$(Ir[dF(CF_3)ppy]_2(dtbpy))PF_6$	Cs_2CO_3 (2 equiv)	EtOH	24 h	56	16	-
24^{b,d}	$Ru(bpy)_3(PF_6)_2$	Cs_2CO_3 (2 equiv)	EtOH	24 h	-	-	-
25^{b}	-	Cs_2CO_3 (2 equiv)	EtOH	24 h	-	-	-
26^{b,e}	$Ru(bpy)_3(PF_6)_2$	Cs_2CO_3 (2 equiv)	EtOH	24 h	77	45	-

Conditions: 3a (0.1 mmol), catalyst (5 mol%), base, solvent (c 0.1 M) under O_2 (1 atm). ^{a}NMR yield ^{b}Concentration c 0.03 M. ^{c}Isolated yield. ^{d}In the dark. ^{c}Under air.

The primary tests revealed that when the reaction is carried out in the absence of base in acetonitrile (entries 1,2, Table 5-1), the desired product **4a** forms in low 5% yield, while the major product of the reaction is hydroperoxide **5a**. Interestingly, in contrast to classic peroxides, the product **5a** exhibited distinctive stability as the attempts to convert it into alcohol by using an iron(II) solution or aluminium oxide failed.

The addition of organic bases as 2,6-lutidine or DIPEA in various concentrations (entries 3-6, Table 5-1) did not overturn the results as **5a** remained the main reaction product. When two equivalents of caesium carbonate were added instead (entry 7), for the first time the selectivity of the process shifted towards the predominant formation of the target imino alcohol **4a**. Reducing the quantity of caesium carbonate worsened the efficiency of the process (entry 8), while replacing acetonitrile with ethanol significantly improved the yield of **4a** (57%, entry 9). Moreover, in ethanol the formation of the hydroperoxide **5a** was completely suppressed. Subsequent replacement of caesium carbonate with potassium carbonate and DIPEA did not have positive effect of the outcome of the reaction (entries 10, 11). The exchange of the counterion of $Ru(bpy)_3^{2+}$ complex to hexafluorophosphate brought a 5% increase in the yield of **4a** (entry 13), and the following dilution of the reaction mixture by passing from 0.1 M to 0.03 M concentration of the substrate in ethanol resulted in the best formation of **4a** ever achieved (67% isolated yield, entry 14). Further solvent (entries 15-19) and catalyst (entries 20-23) screening did not bring any enhancements to the efficiency or selectivity. The importance of light irradiation and the catalyst was demonstrated by carrying out an experiment in the dark (entry 24) and in the absence of ruthenium complex (entry 25). The substitution of oxygen atmosphere with air led to a decrease in the yield of **4a** by 26% (entry 26).

Once the optimisation study was concluded, we proceeded with the synthesis of different starting materials. Initially, to synthetise *N*-aryl-substituted naphtalene-2-amines, Buchwald-Hartwig amination was performed for 2-bromonaphthalene and aniline derivatives (Scheme 5-8). The products **1b-f** were obtained in moderate to good yields.

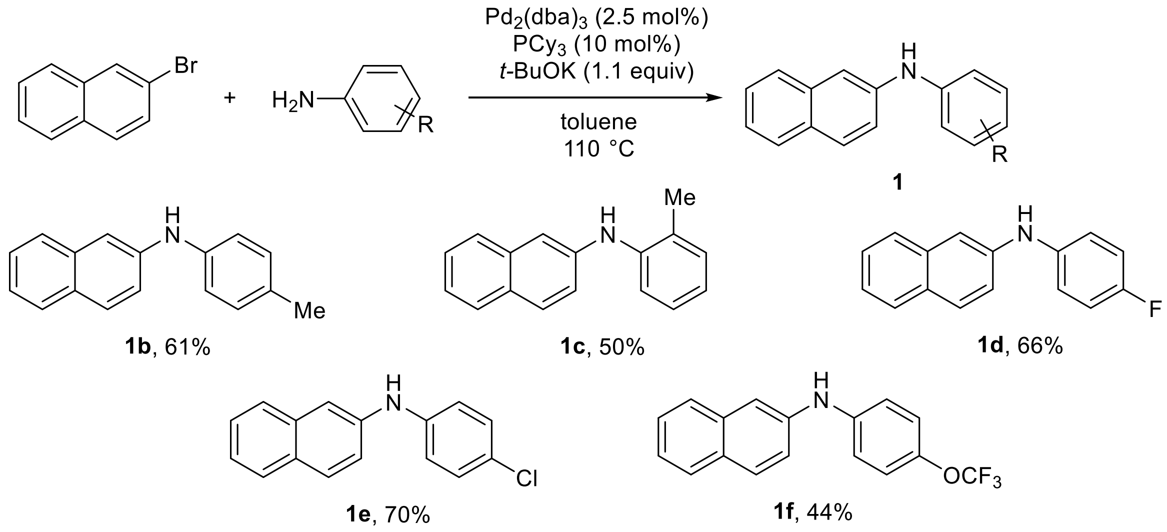

Scheme 5-8. Buchwald-Hartwig Amination.

To prepare compounds **1h** and **1u**, the coupling was performed using BrettPhos Pd G4 catalyst as tris(dibenzylideneacetone)dipalladium(0) exhibited scarce catalytic activity in promoting the corresponding reactions. Quantitative formation of **1h** was observed under new Buchwald coupling conditions, while **1v** was isolated in modest 40% yield (Scheme 5-9).

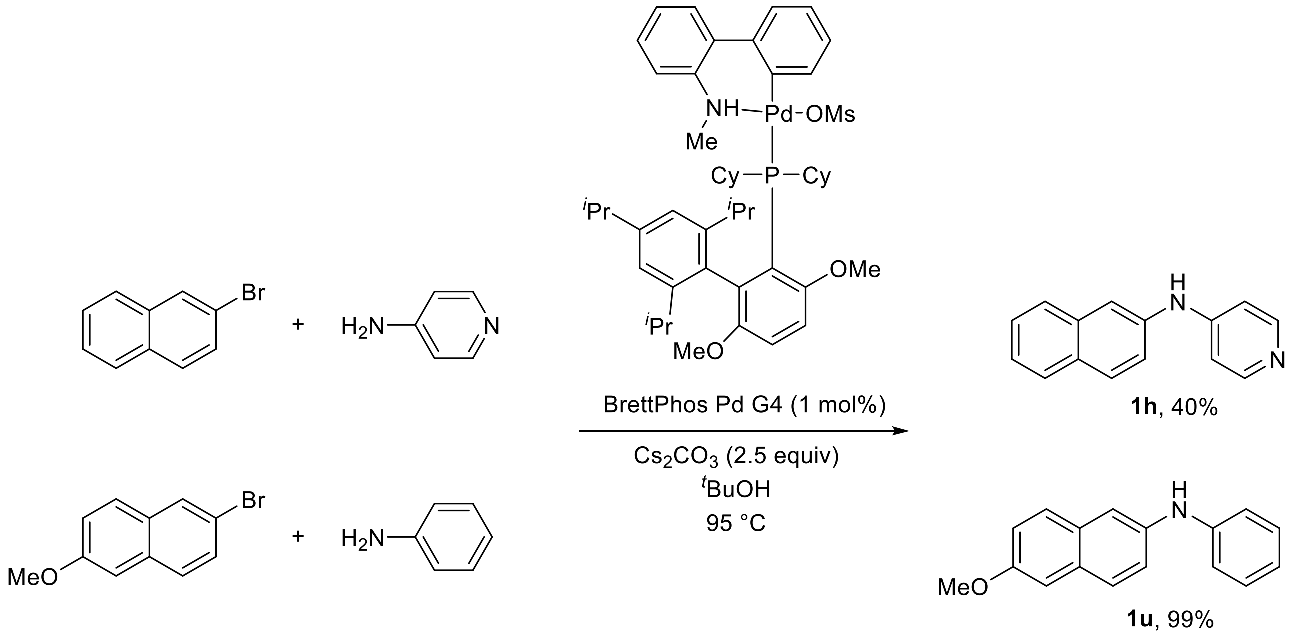

Scheme 5-9. Buchwald-Hartwig Amination Catalysed by BrettPhos Pd G4.

For the synthesis of *N*-methyl and *N*-benzyl-substituted naphthylamines, the classic Bucherer reaction was carried out. Starting from 2-naphthol and ammonia or methylamine, 2-naphthylamine and *N*-methylnaphthalene-2-amine were obtained in 60% and 80% yield, respectively (Scheme 5-10). The former was introduced into the reductive amination reaction with benzaldehyde, affording *N*-benzyl-naphthalene-2-amine in 88% yield.

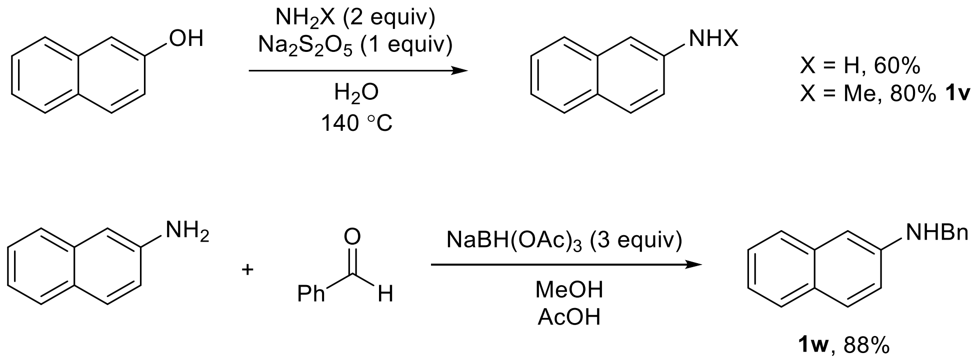

Scheme 5-10. Preparation of Naphthylamines **1v** and **1w**.

Next, the obtained *N*-substituted naphtalene-2-amines were brominated or iodinated with *N*-bromo or *N*-iodosuccinimide, respectively (Scheme 5-11). Generally, the halogenation proceeded well for all substrates, except for 2,2'-dinaphthylamine that gave a mixture of mono- and dibrominated products, resulting in a reduced formation of the desired monobrominated compound **2g**, which was isolated in 34% yield. Remarkably, the selectivity of the halogenation was found to be extremely high as the substitution only occurred at the 1-position of naphthalene.

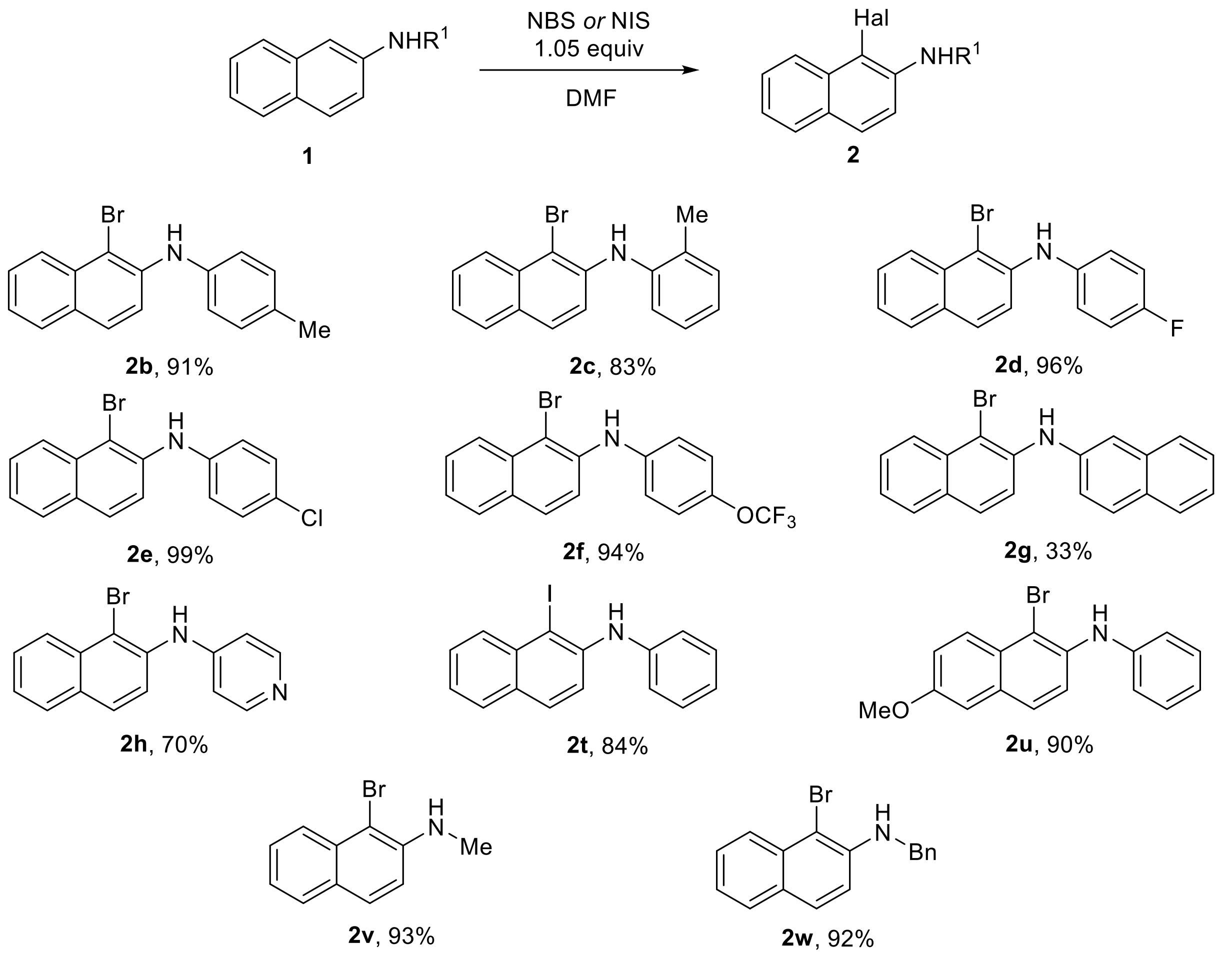

Scheme 5-11. Halogenation of 2-Naphthyamines.

The last step in the synthesis of substrates 3 was Suzuki cross-coupling performed for all brominated naphthalene-2-amines using boronic acids or their pinacol esters. The yields of 3 mainly depended on the substitution pattern of naphthalene and steric hindrance in the reagents as the presence of *ortho*-substituents led to a discrete formation of products 3c, 3j, 3o, and 3u (Scheme 5-12).

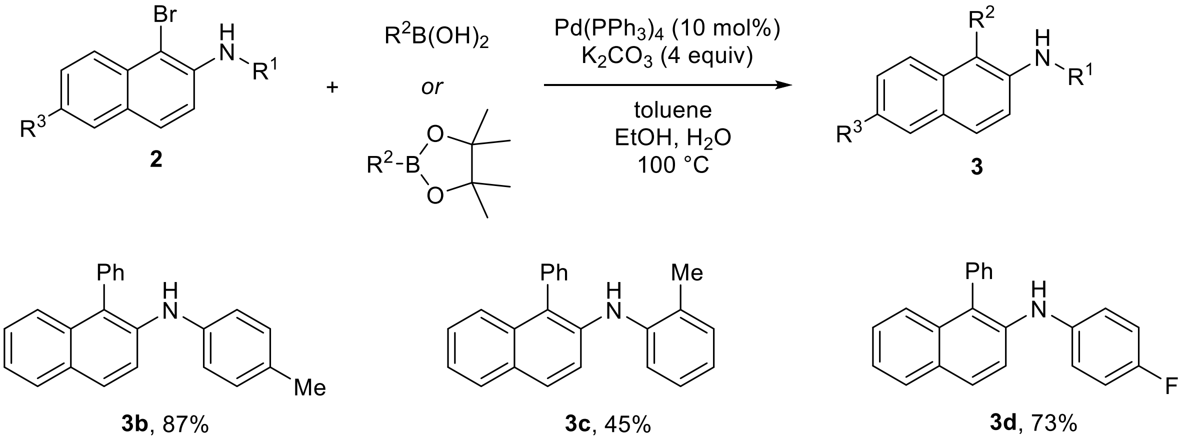

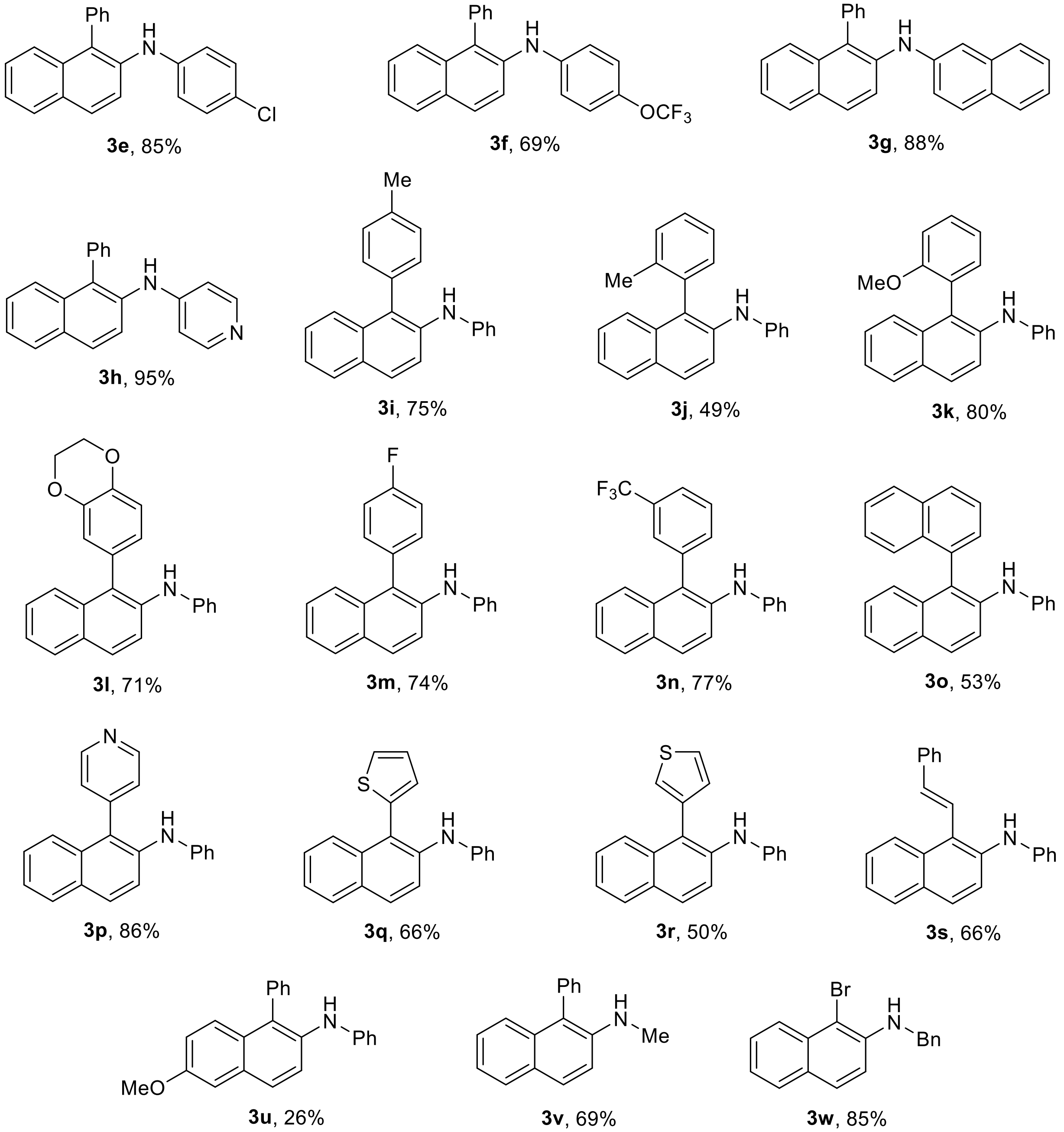
3e, 85%
3f, 69%
3g, 88%
3h, 95%
3i, 75%
3j, 49%
3k, 80%
3l, 71%
3m, 74%
3n, 77%
3o, 53%
3p, 86%
3q, 66%
3r, 50%
3s, 66%
3u, 26%
3v, 69%
3w, 85%

Scheme 5-12. Scope of the Substrates 3 Obtained by Suzuki Coupling.

No reaction was observed when 2,6-dimethylphenylboronic acid was introduced in the cross-coupling, evidently due to the abovementioned steric issues. Unfortunately, the attempts to attach an alkyl substituent at 1-position of naphthalene under Suzuki conditions failed as no product formation was detected when ethylboronic acid and isobutylboronic acid or its pinacol ester were introduced into the reaction (Scheme 5-13).

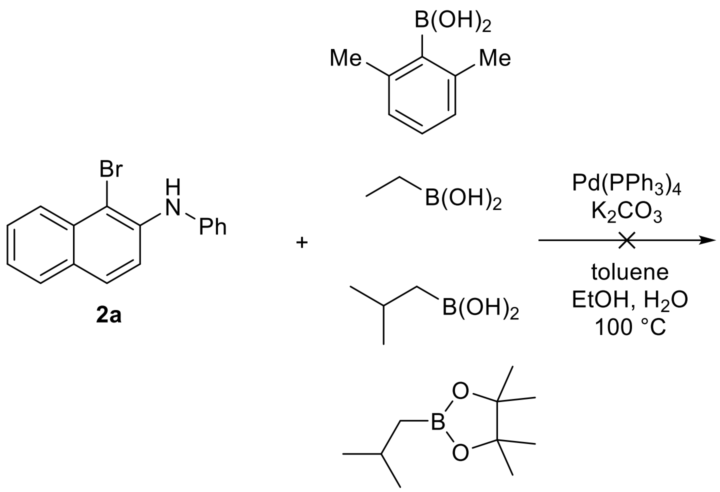

Scheme 5-13. Unsuccessful Attempts to Perform Suzuki Reaction.

Lastly, the substrate **3t** was prepared by Sonogashira coupling of phenylacetylene and 1-iodo-*N*-phenylnaphthalen-2-amine **2t** (Scheme 5-14). The reaction required to be carried out under unusually harsh conditions, at 120 ˚C and with high catalyst loading. After 4 hours of reaction time the product **3t** was isolated in 60% yield.

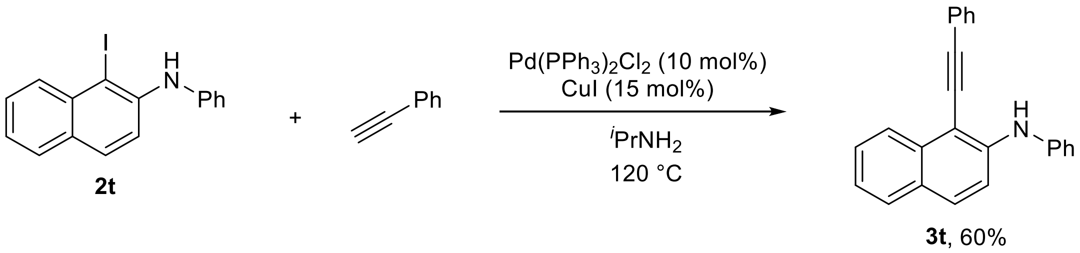

Scheme 5-14. Preparation of **3t** by Sonogashira Coupling.

The twenty-two prepared substrates **3b-w** were tested under the optimised photocatalytic conditions (Scheme 5-15). As many of them were poorly soluble in pure ethanol, some reactions were carried out in the mixture of ethanol and acetonitrile in ratio 2:1.

We found out that the presence of an aryl substituent at the amino group (R^1) was absolutely essential. The dinaphthyl substrate **3g** was fully converted but gave a multicomponent mixture with a low content of the desired **4g**. The substrate **3h** with attached pyridine ring did not react in any manner and was almost fully recovered.

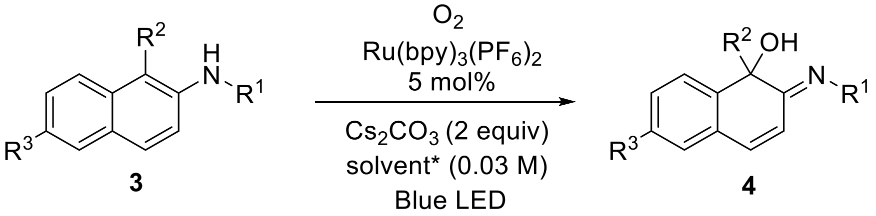

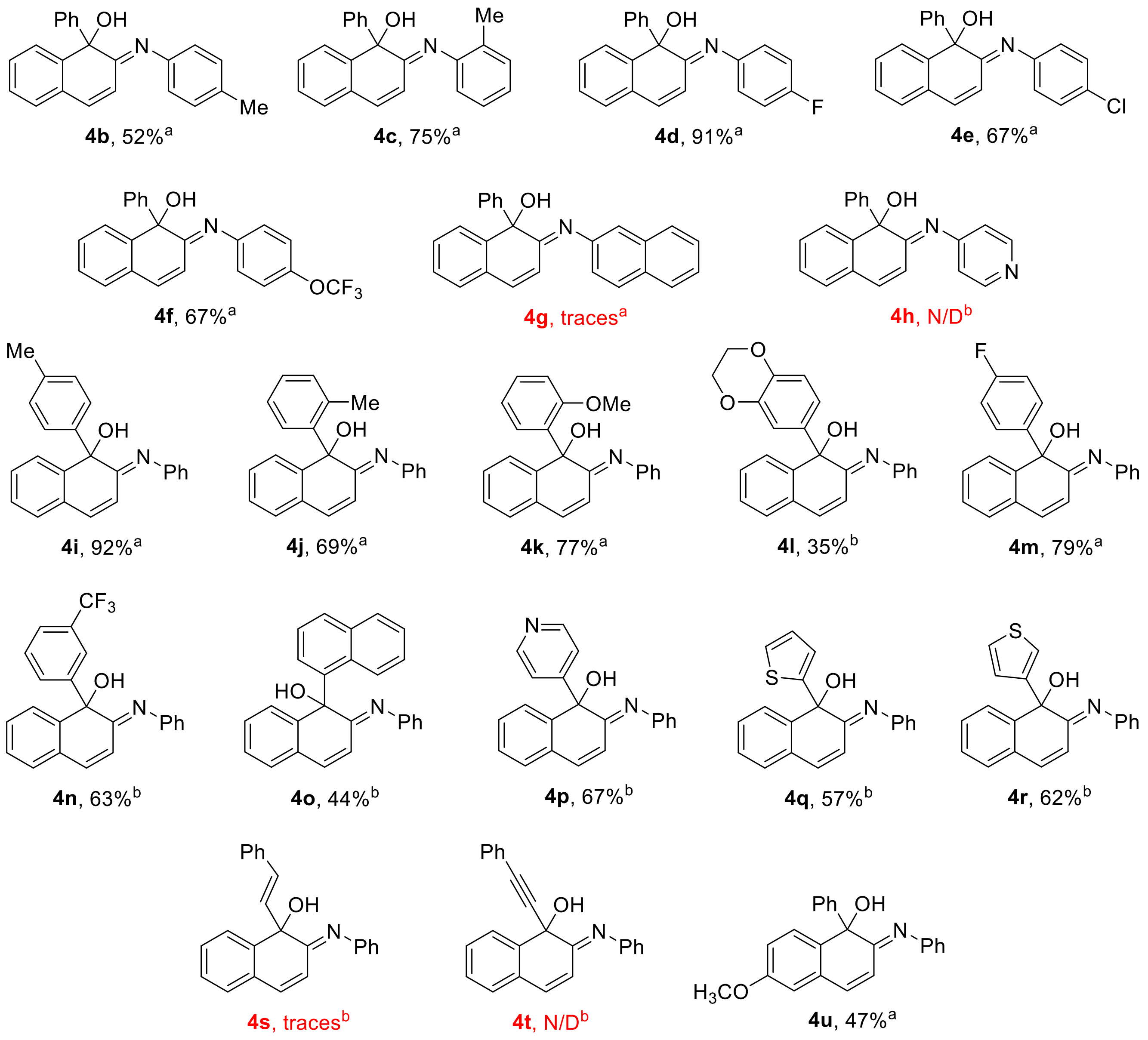

*The reaction was carried out: [a]in absolute ethanol; [b]in ethanol and acetonitrile mixture (2:1 ratio).

Scheme 5-15. Photocatalysed Dearomatization of Naphthalene-2-amines.

Higher variety of substituents at 1-position of naphthylamines (R^2) were tolerated under photocatalytic conditions. Halogen-substituted substrates **3m-n** were successfully transformed into imino alcohols **4m-n** with good yields (63-79%). 1-Naphthyl-substituted naphthalene-2-amine **3o** was dearomatized to afford **4o** in 44% yield. Also, pyridine and thienyl-substituted naphthylamines **3p-r** were transformed into corresponding imino alcohols **4p-r** with moderate yields (57-67%).

Naphthylamine bearing a styrene moiety **3s** was completely degraded under ruthenium photocatalysis and gave a multicomponent mixture, while naphthylamine with a phenylacetylene fragment **4t** exhibited particular stability and was recovered with minimal loss. This stability can be explained by an extra conjugation with acetylene moiety resulting in higher dearomatization energy barrier. The presence of an electron-donating substituent at 6-position of naphthalene (R^3) had a negative impact on the yield of the dearomatized product **4u**.

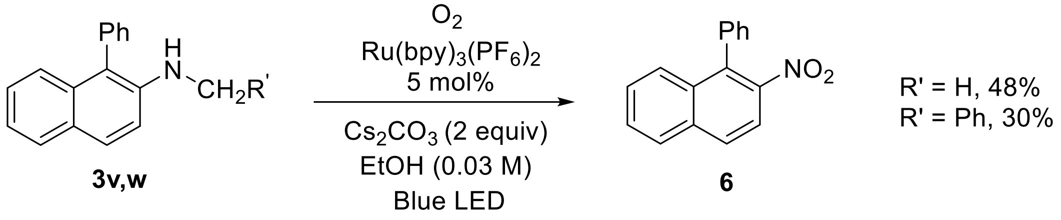

Scheme 5-16. Photooxidation of **3v** and **3w**.

No dearomatization products were observed when **3v** and **3w** were tested under photooxidative conditions (Scheme 5-16). Methyl and benzyl substituents at the amino group turned out to be labile under ruthenium photocatalysis as nitronaphthalene **6** was observed as the main product of the oxidation of the corresponding substrates. To the best of our knowledge, this is the first example of photocatalytic conversion of secondary amines into nitro-compounds.

To unequivocally determine the structures of the obtained products, X-ray analysis was performed for **4a**, **4m**, and **5a**. As we assumed, **4a** and **4m** are (*E*)-imino alcohols, while **5a** is an (*E*)-imino hydroperoxide.

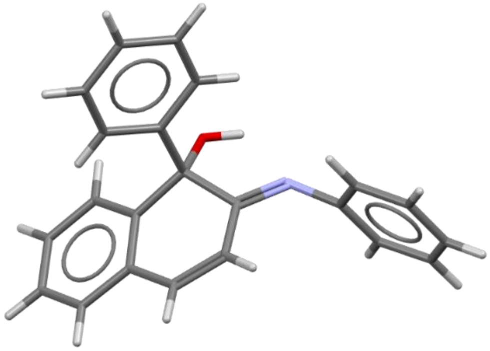

Figure 5-1. X-Ray Structure of **4a**.

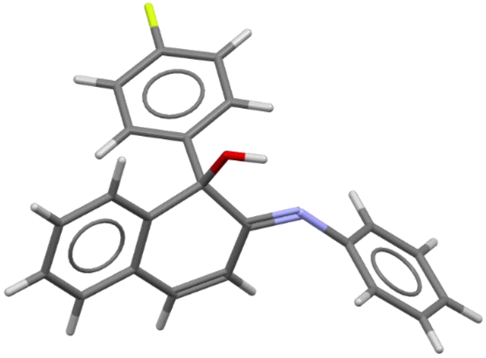

Figure 5-2. X-Ray Structure of **4m**.

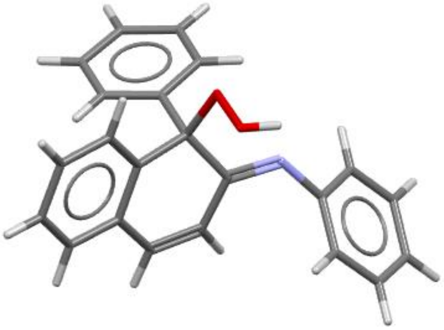

Figure 5-3. X-Ray Structure of **5a**.

In the end we decided to compare the new catalytic system with the previously developed one for the oxidative dearomatization of benzo[*b*]naphtho[1,2-*f*]azepine **7a** (Scheme 5-17). It turned out that under both conditions **8a** forms in similar yields (45-46%), which is not equal for the substrates **3** that cannot be efficiently dearomatized under conditions (A).

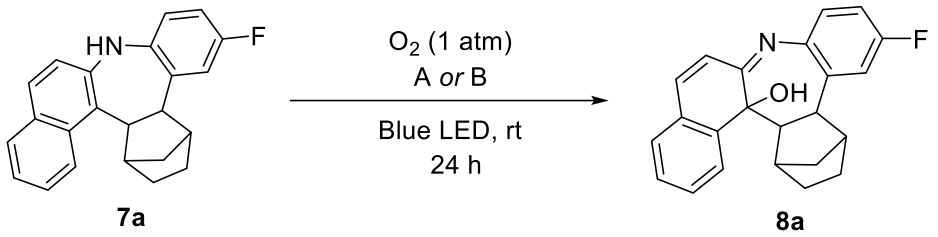

Reaction conditions:
A) $[Ru(bpy)_3]Cl_2$ (5 mol%), 2,6-lutidine (2 equiv), DMSO (0.1 M) 45%
B) $[Ru(bpy)_3]PF_6$ (5 mol%), Cs_2CO_3 (2 equiv), EtOH (0.03 M) 46%

Scheme 5-17. Dearomatization of **7a** Under Different Photocatalytic Conditions.

Possible reaction pathways include oxidative (Scheme 5-18) and reductive (Scheme 5-19) quenching of ruthenium. Here we provide both plausible mechanisms. The determination of the correct reaction route requires a thorough study of redox potentials of ruthenium complexes and substrates in each step.

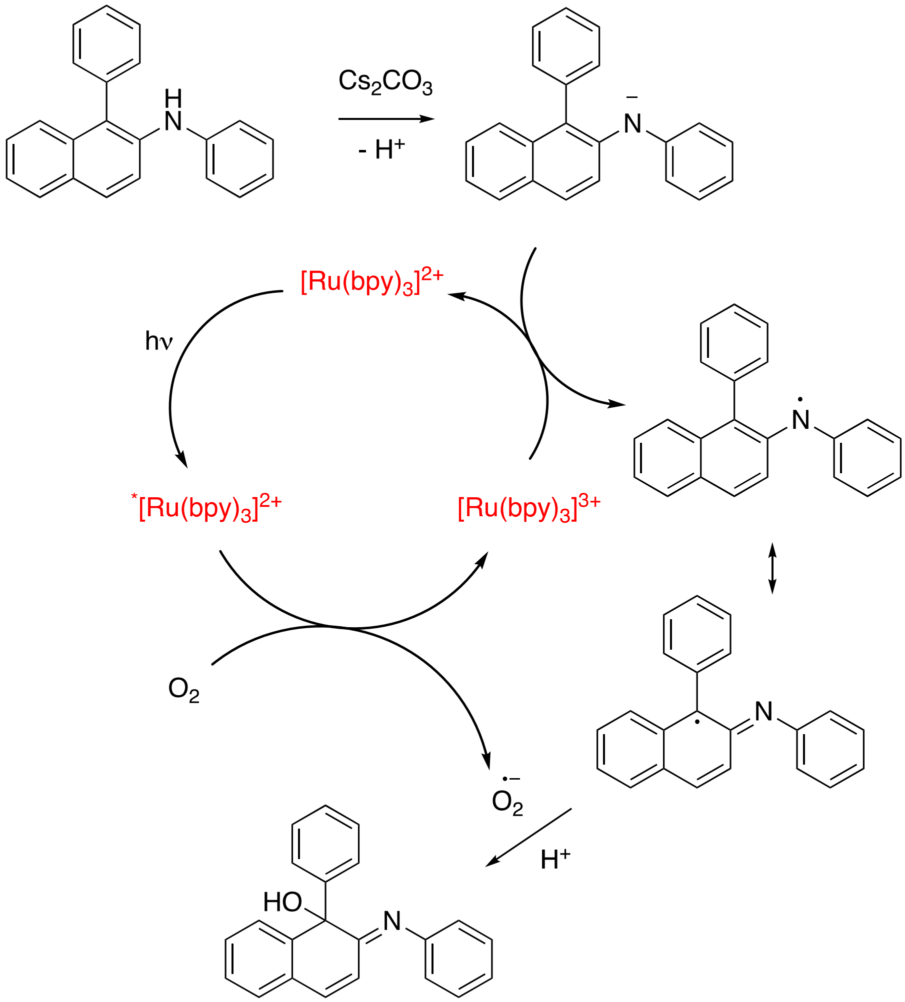

Scheme 5-18. Oxidative Quenching.

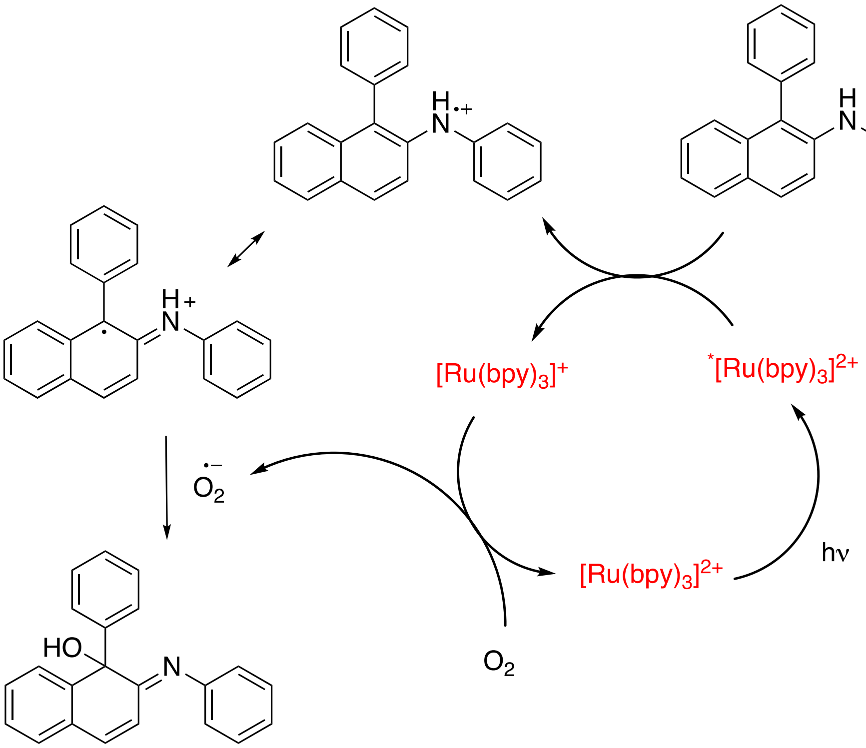

Scheme 5-18. Reductive Quenching.

Conclusions

New photocatalytic methodology has been developed for the synthesis of previously unavailable (*E*)-2-imino-1,2-dihydronaphthalen-1-ols. The protocol excludes the involvement of toxic oxidants and is promoted by oxygen. Visible light is used as an energy source for the C-O bond construction and dearomatization of the aromatic system of naphthalene. The limitations of the process have been explored on 24 examples, and the exact structures of the obtained products were determined by a complex of analyses, including X-ray analysis. Two plausible reaction mechanisms are provided.

Experimental Part

Preparation of N-Arylnaphthalene-2-amines ***1b-f*** *(Buchwald-Hartwig Cross-Coupling):*[22]

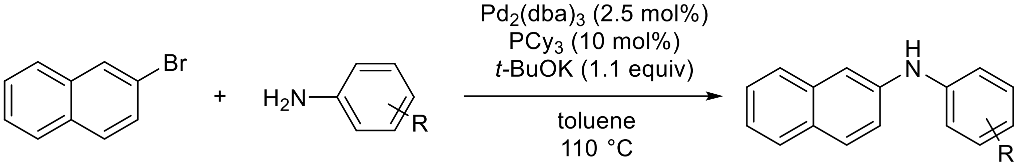

1

Under N$_2$, a 50 mL Schlenk tube was charged with Pd$_2$(dba)$_3$ (57 mg, 0.0625 mol), PCy$_3$ (70 mg, 0.25 mmol) and ^{t}BuOK (308 mg, 2.75 mmol). Then 2-bromonaphtalene (518 mg, 2.5 mmol) and an aniline (2.5 mmol) were added, followed by the addition of anhydrous toluene (10 mL). The tube was sealed, and the stirring mixture was heated up to 110 °C. The reaction was monitored by TLC. When the reagents were consumed (after 24-48 hours), the reaction mixture was cooled to room temperature, and filtered through a pad of Celite®. The solvent was removed under reduced pressure, and the products were isolated by flash column chromatography on silica gel using mixtures of hexane/ethyl acetate as eluent.

Preparation of N-Arylnaphthamines ***1h*** *and* ***1u*** *(Buchwald Coupling Catalysed by BrettPhos Pd G4):*[23]

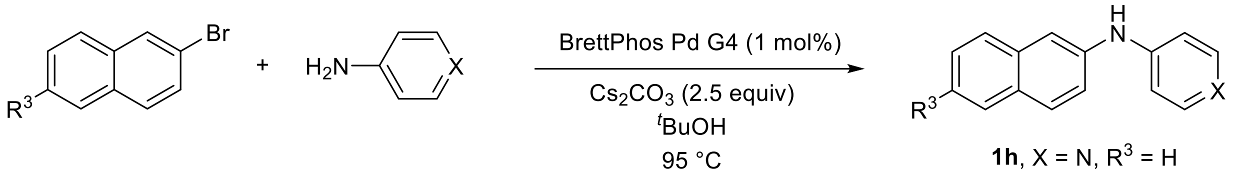

1h, X = N, R^3 = H
1u, X = CH, R^3 = OMe

Under N_2, a 50 mL Schlenk tube was charged with BrettPhos Pd G4 (0.01 mmol, 9.2 mg) and Cs_2CO_3 (1.6 g, 5 mmol). Then a 2-bromonaphthalene (2 mmol) and an aromatic amine (2 mmol) were added, followed by the addition of ^{t}BuOH (8 mL). The tube was sealed, and the stirring mixture was heated up to 95 °C. The reaction was monitored by TLC. When the reagents were consumed (after 16-24 hours), the reaction mixture was cooled to room temperature, and filtered through a pad of Celite®. The solvent was removed under reduced pressure, and the products were isolated by flash column chromatography on silica gel using DCM/methanol (10:1) mixture as eluent for **1h**, and hexane/ethyl acetate (5:2) mixture for **1u**.

Preparation of 2-Naphthylamine and N-Methyl-naphthalene-2-amine ***1v*** *(Bucherer Reaction):*[24]

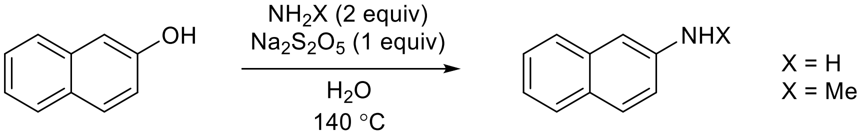

A 45 mL autoclave equipped with a magnetic stirrer was charged with 2-naphthol (720 mg, 5 mmol), a 30% aqueous solution of ammonia or methylamine (1 mL) and sodium metabisulfite (950 mg, 5 mmol) dissolved in 2.5 mL of water. Then the autoclave was flushed with nitrogen and sealed. The mixture was heated at 140 °C overnight and then cooled down to room temperature. The mixture was washed with a 5% aqueous solution of KOH (20 mL) and filtered through a Buchner filter. Organic layer was extracted with DCM (4x10 mL) and dried over anhydrous Na_2SO_4. The solvent was removed under reduced pressure, and the products were isolated by flash column chromatography on silica gel using mixtures of hexane/ethyl acetate as eluent.

Preparation of N-Benzyl-naphthalene-2-amine ***1w*** *(Reductive Amination):*[25]

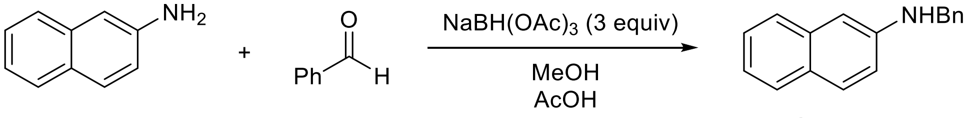

1w, 88%

In a 50 mL flask naphthalene-2-amine (143 mg, 1 mmol) was dissolved in 5 mL of methanol. Then benzaldehyde (122 µL, 1.2 mmol) and acetic acid (2 mL) were added. The reaction mixture was cooled down to 0 °C, and sodium triacetoxyborohydride (636 mg, 3 mmol) was added portionwise within 30 minutes. The mixture was stirred at room temperature for 2 hours and then poured into 20 mL of saturated $NaHCO_3$ solution. Organic phase was extracted with ethyl acetate (3x7 mL) and dried over anhydrous Na_2SO_4. The solvent was removed under reduced pressure, and flash column chromatography on silica gel was performed using hexane/ethyl acetate (12:1) mixture as eluent to afford pure **1w** (205 mg, 88% yield).

Preparation of 1-Bromonaphthalene-2-amines ***2a-s,u*** *and 1-Iodo-N-phenylnaphthalene-2-amine* ***2t*** *(Halogenation):*[25]

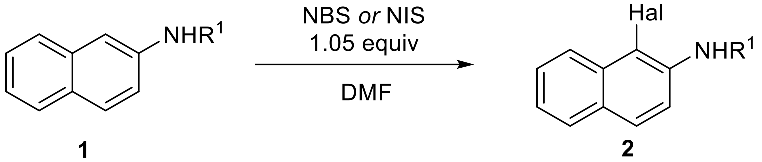

In a 50 mL flask, to a solution of naphthalene-2-amine **1** (1.2 mmol) dissolved in 1.5 mL of DMF was added dropwise a solution of *N*-bromosuccinimide (224 mg, 1.26 mmol) or *N*-iodoosuccinimide (284 mg, 1.26 mmol) in 1.5 mL of DMF. The reaction was monitored by TLC. When **1** was fully consumed, the mixture was poured into a saturated aqueous solution of LiCl. Organic phase was extracted with ethyl acetate (2x7 mL) and dried over anhydrous Na_2SO_4. The solvent was removed under reduced pressure, and the products were isolated by flash column chromatography on silica gel using mixtures of hexane/ethyl acetate as eluent.

Preparation of 1-Substituted Naphthalene-2-amines ***3a-s,u*** *(Suzuki Cross-Coupling):*

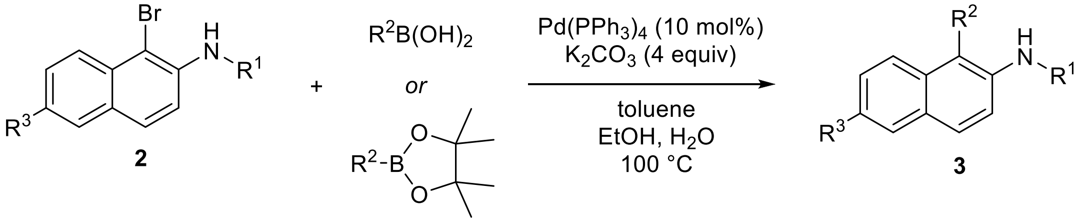

Under N_2, a 50 mL Schlenk tube was charged with $Pd(PPh_3)_4$ (92 mg, 0.08 mmol), K_2CO_3 (455 mg, 3.3 mmol), 1-bromonaphthalene-2-amine **2** (0.8 mmol) and a boronic acid or a pinacol ester of boronic acid (1 mmol). The mixture was dissolved in an emulsion of 6 mL of toluene, 1.5 mL of ethanol and 1 mL of water. The tube was sealed, and the mixture was heated at 100 °C until **2** was fully consumed (16-24 h). Then the reaction mixture was cooled down to room temperature, filtered through a pad of Celite® and poured into 15 mL of 1 M solution of NH_4Cl. Organic layer was extracted with DCM (2x15 mL), dried over anhydrous Na_2SO_4. The solvent was removed under reduced pressure, and the products were isolated by flash column chromatography on silica gel using mixtures of hexane/DCM as eluent.

*Preparation of N-Phenyl-1-(phenylethynyl)naphthalen-2-amine **3t** (Sonogashira Coupling):*[25]

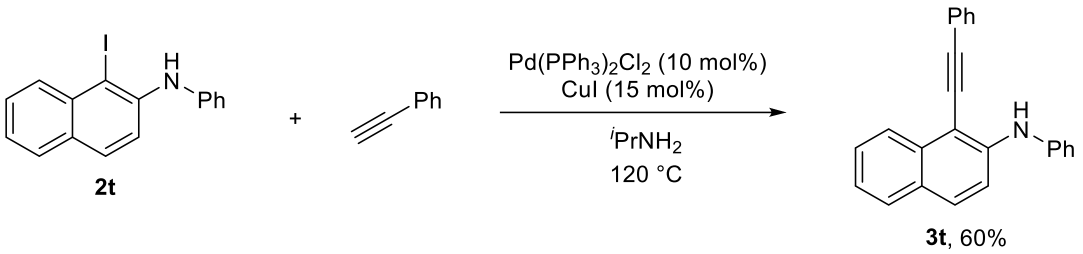

Under N_2, a 100 mL Schlenk flask was charged with *N*-phenyl-1-iodonaphthalen-2-amine **2t** (345 mg, 1 mmol) dissolved in 12 mL of $^{i}PrNH_2$. Then phenylacetylene (329 µL, 3 mmol) and $Pd(PPh_3)_2Cl_2$ (70 mg, 0.1 mmol) were added, followed by the addition of CuI (29 mg, 0.15 mmol). The flask was sealed, and the mixture was stirred at 120 °C for 4 hours. Then the reaction mixture was cooled down to room temperature, filtered through a pad of Celite® and poured into 15 mL of 1 M solution of NH_4Cl. Organic layer was extracted with DCM (2x15 mL), dried over anhydrous Na_2SO_4. The solvent was removed under reduced pressure, and flash column chromatography on silica gel was performed using hexane/DCM (9:1) mixture as eluent to afford pure **3t** (191 mg, 60% yield).

*General Procedure for the Photocatalysed Dearomatization to Obtain **4**:*

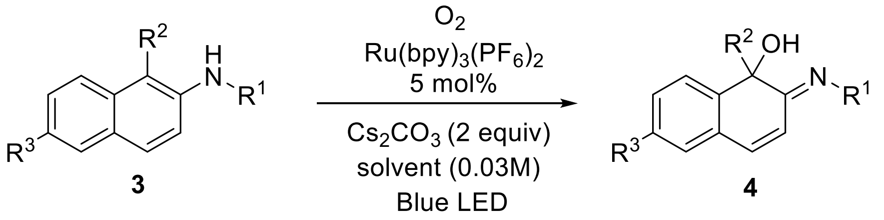

In a 50 mL Schlenk tube, a 1-substituted *N*-arylnaphthalene-2-amine **3** (0.2 mmol) was dissolved in 6-7 mL of ethanol (when insoluble, 2 mL of acetonitrile and 4-5 mL of ethanol). Then $Ru(bpy)_3(PF_6)_2$ (8,6 mg, 0.01 mmol) and caesium carbonate (130 mg, 0.4 mmol) were added. The tube was purged with O_2 for ~30 seconds, and a balloon charged with O_2 (1 atm) was attached as a reserve. The stirring mixture was irradiated with 18 W blue LEDs at room temperature for 24-36 hours. When **3** was fully consumed, the mixture was diluted with 5 mL of DCM and filtered through a pad of Celite®. The solvents were removed under reduced pressure, and the products were isolated by flash column chromatography on silica gel using mixtures of hexane/ethyl acetate or hexane/DCM as eluent.

*Photocatalysed Dearomatization to Obtain **5a**:*

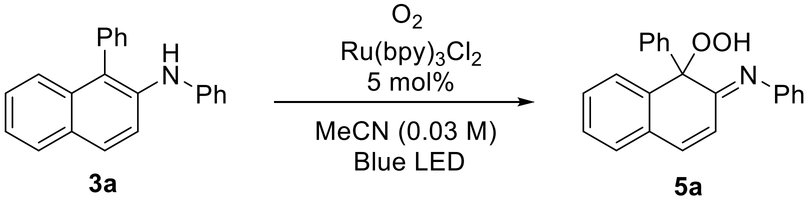

In a 50 mL Schlenk tube, *N*,1-diphenylnaphthalene-2-amine **3a** (59 mg, 0.2 mmol) and Ru(bpy)$_3$Cl$_2$ (6.4 mg, 0.01 mmol) were dissolved in 7 mL of acetonitrile. The tube was purged with O_2 for ~30 seconds, and a balloon charged with O_2 (1 atm) was attached as a reserve. The stirring mixture was irradiated with 18 W blue LEDs at room temperature for 24hours. When **3a** was fully consumed, the mixture was diluted with 5 mL of DCM and filtered through a pad of Celite®. The solvents were removed under reduced pressure, and flash column chromatography on silica gel was performed using hexane/ethyl acetate (9:1) mixture as eluent to afford pure **5a** (52 mg, 80% yield).

Table 5-2. Crystallographic Data and Structure Refinement.

Identification code	4a	4m	5a
Empirical formula	$C_{22}H_{17}NO$	$C_{22}H_{16}FNO$	$C_{22}H_{17}NO_2$
Formula weight	311.36	329.36	327.36
Temperature/K	200.0	200.00	200.0
Crystal system	triclinic	triclinic	triclinic
Space group	P-1	P-1	P-1
a/Å	9.5687(4)	9.4877(3)	8.9188(8)
b/Å	10.2374(5)	10.2155(3)	10.4222(10)
c/Å	10.3857(5)	10.2710(3)	36.886(3)
α/°	79.852(2)	80.1940(10)	90.818(3)
β/°	63.610(2)	67.3820(10)	90.019(3)
γ/°	63.274(2)	63.8840(10)	94.889(3)
Volume/Å^3	813.63(7)	825.10(4)	3415.9(5)
Z	2	2	8
ρ_{calc}g/cm^3	1.271	1.326	1.273
μ/mm^{-1}	0.078	0.089	0.649
F(000)	328.0	344.0	1376.0
Crystal size/mm^3	0.1 × 0.1 × 0.06	0.5 × 0.3 × 0.2	0.1 × 0.04 × 0.03
Radiation	MoKα (λ = 0.71073)	MoKα (λ = 0.71073)	CuKα (λ = 1.54178)
2Θ range for data collection/°	4.38 to 52.83	4.296 to 52.854	7.19 to 89.05
Index ranges	$-11 \le h \le 10$, $-12 \le k \le 11$, $-12 \le l \le 12$	$-11 \le h \le 11$, $-12 \le k \le 12$, $-12 \le l \le 11$	$-8 \le h \le 8$, $-9 \le k \le 9$, $-33 \le l \le 33$
Reflections collected	8585	8445	18349
Independent reflections	3299 R_{int} = 0.0675, R_{sigma} = 0.0772	3303 R_{int} = 0.0219, R_{sigma} = 0.0272	5323 R_{int} = 0.0668, R_{sigma} = 0.0744
Data/restraints/parameters	3299/0/218	3303/0/227	5323/0/905
Goodness-of-fit on F^2	1.021	1.048	1.083
Final R indexes [I>=2σ (I)]	R_1 = 0.0494, wR_2 = 0.1110	R_1 = 0.0404, wR_2 = 0.0981	R_1 = 0.0723, wR_2 = 0.2048

Final R indexes [all data]	$R_1 = 0.0708$, $wR_2 = 0.1238$	$R_1 = 0.0471$, $wR_2 = 0.1023$	$R_1 = 0.1153$, $wR_2 = 0.2349$
Largest diff. peak/hole / e Å^{-3}	0.22/-0.19	0.23/-0.16	0.43/-0.30

***N*,1-Diphenylnaphthalen-2-amine (3a):** Colourless solid (182 mg, 77% yield); m.p. 104.2-104-8°C; **^{1}H NMR (400 MHz, $CDCl_3$)** δ 7.94-7.85 (m, 2H); 7.73 (d, 1H, J=8.9Hz) 7.74 (t, 2H, J=7.4Hz); 7.59-7.46 (m, 4H); 7.46-7.38 (m, 2H); 7.34 (t, 2H; J=7.8Hz); 7.13 (d, 2H, J=7.5Hz); 7.05 (t, 1H, J=7.3Hz); 5.62 (br s, 1H). **^{13}C NMR (101 MHz, $CDCl_3$)** δ: 143.6, 138.1, 136.8, 134.0, 131.1, 129.5, 129.5, 128.5, 128.1, 128.0, 126.5, 125.5, 125.1, 123.6, 121.6, 119.1, 118.7. **HRMS (ESI)** m/z calcd for $C_{22}H_{17}N$ [M+H]$^+$: 296.1439, found: 296.1442. **IR (ATR diamond, neat):** *ν* 3414.1, 3061.3, 3019.8, 2920.9, 2851.3, 1593.8, 1509.9, 1313.0, 811.2, 746.0, 693.3 cm^{-1}.

1-Phenyl-*N*-(*p*-tolyl)naphthalen-2-amine (3b): Brown oil (215 mg, 87% yield); **^{1}H NMR (400 MHz, $CDCl_3$)** δ 7.92 – 7.82 (m, 2H), 7.70 – 7.60 (m, 3H), 7.59 – 7.44 (m, 4H), 7.42 – 7.37 (m, 2H), 7.17 (d, *J* = 8.1 Hz, 2H), 7.06 (d, *J* = 8.2 Hz, 2H), 2.41 (s, 3H). **^{13}C NMR (101 MHz, $CDCl_3$)** δ 140.7, 138.6, 136.6, 133.8, 131.6, 131.1, 129.9, 129.4, 129.0, 128.4, 128.0, 127.9, 126.3, 124.9, 124.5, 123.2, 119.7, 118.4, 20.8. **HRMS (ESI)** m/z calcd for $C_{23}H_{19}N$ [M+H]$^+$: 310.1596, found: 310.1594. **IR (ATR diamond, neat):** *ν* 3403.1, 3051.8, 3022.2, 2918.1, 2859.4, 1595.8, 1509.0, 1295.8, 809.1, 704.0 cm^{-1}.

1-Phenyl-*N*-(*o*-tolyl)naphthalen-2-amine (3c): Colourless solid (111 mg, 45% yield); m.p. 116.0-117.2 °C; **^{1}H NMR (400 MHz, $CDCl_3$)** δ 7.94 – 7.85 (m, 2H), 7.70 – 7.64 (m, 2H), 7.62 – 7.50 (m, 5H), 7.47 – 7.38 (m, 3H), 7.30 – 7.24 (m, 2H), 7.06 (td, *J* = 7.4, 1.3 Hz, 1H), 5.42 (s, 1H), 2.17 (s, 3H). **^{13}C NMR (101 MHz, $CDCl_3$)** δ 141.6, 139.0, 136.9, 133.9, 131.1, 131.0, 129.5, 129.1, 129.0, 128.5, 128.1, 128.0, 126.9, 126.5, 124.9, 124.3, 123.2, 122.4, 119.1, 118.5, 17.9. **HRMS (ESI)** m/z calcd for $C_{23}H_{19}N$ [M+H]$^+$: 310.1596, found: 310.1596. **IR (ATR diamond, neat):** *ν* 3062.0, 2923.1, 2853.8, 1626.3, 1593.2, 1484.0, 1444.1, 1393.9, 1045.5, 812.2, 754.3, 698.0 cm^{-1}.

***N*-(4-Fluorophenyl)-1-phenylnaphthalen-2-amine (3d):** Colourless solid (183 mg, 73% yield); m.p. 90.3-91.4 °C; **^{1}H NMR (400 MHz, $CDCl_3$)** δ 7.82 – 7.74 (m, 2H), 7.55 (t, *J* = 7.4 Hz, 2H), 7.47 (t, *J* = 8.3 Hz, 2H), 7.41 – 7.37 (m, 2H), 7.37 – 7.27 (m, 3H), 7.05 – 6.88 (m, 4H). **^{13}C NMR (101 MHz, $CDCl_3$)** δ 159.7, 157.3, 139.4, 139.4, 138.7, 136.6, 133.8, 131.0, 129.4, 129.1, 128.5, 128.0, 127.9, 126.4, 124.9, 124.6, 123.3, 121.5, 121.4, 118.1, 116.1, 115.8. **HRMS (ESI)** m/z calcd for $C_{22}H_{16}FN$ [M+K]$^+$: 352.0904, found: 352.0904. **IR (ATR diamond, neat):** *ν* 3403.2, 3053.4, 1619.2, 1595.0, 1501.9, 1342.3, 814.0, 763.2, 744.1, 703.9 cm^{-1}.

***N*-(4-Chlorophenyl)-1-phenylnaphthalen-2-amine (3e):** Colourless solid (224 mg, 85% yield); m.p. 104.4-105.9 °C; **^{1}H NMR (400 MHz, $CDCl_3$)** δ 7.95 – 7.85 (m, 2H), 7.68 – 7.59 (m, 3H), 7.59 – 7.54 (m, 1H), 7.53 – 7.40 (m, 5H), 7.28 (d, *J* = 8.6 Hz, 2H), 7.01 (d, *J* = 8.6 Hz, 2H). **^{13}C NMR (101 MHz, $CDCl_3$)** δ 142.4, 137.5, 136.6, 133.9, 131.0, 129.6, 129.5, 129.4, 128.7, 128.1, 126.6, 126.1, 126.1, 125.2, 123.8, 119.6, 119.1. **HRMS (ESI)** m/z calcd for $C_{22}H_{16}ClN$ [M+H]$^+$: 330.1050, found: 330.1049. **IR (ATR diamond, neat):** *ν* 3416.3, 3053.1, 2923.4, 1619.0, 1589.2, 1488.9, 1306.8, 1173.1, 1086.3, 816.2, 710.0, 702.1, 693.4 cm^{-1}.

1-Phenyl-*N*-(4-(trifluoromethoxy)phenyl)naphthalen-2-amine (3f): Light brown solid (209 mg, 69% yield); m.p. 87.0-87.4 °C; **^{1}H NMR (400 MHz, CDCl$_3$)** δ 7.88 – 7.80 (m, 2H), 7.62 – 7.54 (m, 3H), 7.54 – 7.48 (m, 1H), 7.46 – 7.33 (m, 5H), 7.12 (d, *J* = 7.6 Hz, 2H), 7.00 (d, *J* = 9.0 Hz, 2H), 5.55 (s, 1H). **^{13}C NMR (101 MHz, CDCl$_3$)** δ 143.3, 142.6, 137.4, 136.5, 133.8, 130.9, 129.6, 129.4, 128.6, 128.1, 126.6, 126.2, 125.2, 123.8, 122.4, 122.0, 119.4, 119.0, 119.0.

FT-IR (cm^{-1}): 3416 (stretch N-H); 3064 (stretch C-H aromatico); 1590 (bend N-H); 1505 (C-C aromatico); 1252 (stretch C-F/C-O); 1162 (stretch C-F/C-O); 816; 750; 696. **HRMS (ESI)** m/z calcd for $C_{22}H_{16}F_3NO$ [M+K]$^+$: 418.0821, found: 418.0822. **IR (ATR diamond, neat):** *ν* 3416.0, 3064.0, 1590.4, 1504.9, 1252.0, 1162.3, 816.4, 749.7, 696.8 cm^{-1}.

***N*-(Naphthalen-2-yl)-1-phenylnaphthalen-2-amine (3g):** Light yellow solid (289.5 mg, 88% yield); m.p. 135.0-137.4 ˚C; **^{1}H NMR (400 MHz, CD$_2$Cl$_2$)** δ 7.91 – 7.86 (m, 2H), 7.77 (td, *J* = 9.0, 8.5, 2.0 Hz, 3H), 7.67 (dd, *J* = 8.2, 1.1 Hz, 1H), 7.64 – 7.57 (m, 2H), 7.56 – 7.50 (m, 1H), 7.49 – 7.31 (m, 8H), 7.17 (dd, *J* = 8.8, 2.3 Hz, 1H), 5.80 (s, 1H). **^{13}C NMR (101 MHz, CD$_2$Cl$_2$)** δ 141.5, 137.8, 136.6, 134.6, 133.8, 130.8 (2C), 129.7, 129.3 (2C), 129.0, 128.4, 127.9, 127.9, 127.5, 126.4, 126.3, 125.0, 123.6, 123.5, 120.4, 119.6, 111.9. **HRMS (ESI)** m/z calcd for $C_{26}H_{16}N$ [M+H]$^+$: 346.1517, found: 346.1520. **IR (ATR diamond, neat):** *ν* 3393.0, 3051.6, 2916.7, 1615.9, 1592.7, 1485.4, 1415.4, 1287.4, 1069.2, 854.1, 816.1, 750.2, 702.9, 697.4 cm^{-1}.

***N*-(1-Phenylnaphthalen-2-yl)pyridin-4-amine (3h):** Colourless waxy solid (161 mg, 95% yield); **^{1}H NMR (400 MHz, CD$_2$Cl$_2$)** δ 8.22 (d, *J* = 5.5 Hz, 2H), 7.94 (t, *J* = 7.5 Hz, 2H), 7.68 (d, *J* = 8.7 Hz, 1H), 7.60 – 7.31 (m, 9H), 6.76 (d, *J* = 5.8 Hz, 2H), 6.22 (s, 1H). **^{13}C NMR (101 MHz, CD$_2$Cl$_2$)** δ 151.13, 149.94 (2C), 136.1, 134.6, 133.6, 131.0, 130.5 (2C), 129.0 (2C), 128.6, 128.0, 127.9, 126.5, 125.7, 124.9, 121.9, 109.7 (2C). **HRMS (ESI)** m/z calcd for $C_{21}H_{16}N_2$ [M+H]$^+$: 297.1313, found: 297.1313. **IR (ATR diamond, neat):** *ν* 3645.5, 3401.0, 3209.4, 3049.7, 3049.7, 3027.7, 2959.5, 2922.2, 1918.0, 1708.2, 1588.0, 1503.7, 1340.1, 1312.8, 1212.4, 1028.7, 992.4, 811.7, 759.4, 697.1 cm^{-1}.

***N*-Phenyl-1-(*p*-tolyl)naphthalen-2-amine (3i):** Colourless solid (185 mg, 75% yield); m.p. 104.1-104.9 °C; **^{1}H NMR (400 MHz, CDCl$_3$)** δ 7.91 – 7.83 (m, 2H), 7.72 (d, *J* = 8.9 Hz, 1H), 7.55 – 7.50 (m, 1H), 7.46 – 7.37 (m, 6H), 7.37 – 7.30 (m, 2H), 7.15 – 7.10 (m, 2H), 7.04 (t, *J* = 7.3 Hz, 1H), 2.56 (s, 3H). **^{13}C NMR (101 MHz, CDCl$_3$)** δ 143.7, 138.2, 137.6, 134.1, 133.6, 131.0, 130.2, 129.5, 128.4, 128.1, 126.4, 125.4, 125.2, 123.5, 121.5, 119.0, 118.7, 21.5. **HRMS (ESI)** m/z calcd for $C_{23}H_{19}N$ [M+H]$^+$: 310.1596, found: 310.1598. **IR (ATR diamond, neat):** *ν* 3409.8, 3048.0, 3027.2, 2917.3, 1592.9, 1498.2, 1302.8, 810.2, 746.4, 694.1 cm^{-1}.

***N*-Phenyl-1-(*o*-tolyl)naphthalen-2-amine (3j):** Colourless solid (121 mg, 49% yield); m.p. 116.5-117.1 °C; **^{1}H NMR (400 MHz, CDCl$_3$)** δ 7.92 – 7.84 (m, 2H), 7.72 (d, *J* = 8.9 Hz, 1H), 7.52 – 7.42 (m, 3H), 7.42 – 7.25 (m, 6H), 7.17 – 7.10 (m, 2H), 7.04 (t, *J* = 7.3 Hz, 1H), 2.13 (s, 3H). **^{13}C NMR (101 MHz, CDCl$_3$)** δ 143.2, 138.3, 138.1, 135.9, 131.2, 130.9, 129.4, 129.3, 128.3, 128.3, 128.1, 126.9, 126.5, 124.7, 124.0, 123.3, 121.7, 119.0, 19.7. **HRMS (ESI)** m/z calcd for $C_{23}H_{19}N$ [M+K]$^+$: 348.1155, found: 348.1153. **IR (ATR diamond, neat):** *ν* 3400.2, 3048.1, 3017.1, 2918.7, 2857.6, 1593.4, 1494.5, 1342.0, 1304.2, 809.9, 730.3, 692.1 cm^{-1}.

1-(2-Methoxyphenyl)-*N*-phenylnaphthalen-2-amine (3k): Colourless solid (258.6 mg, 80% yield); m.p. 43.2-45.6 ˚C; **^{1}H NMR (400 MHz, CDCl$_3$)** δ 7.83 – 7.76 (m, 2H), 7.58 (d, *J* = 8.9 Hz, 1H), 7.48 (ddd, *J* = 8.4, 7.5, 1.8 Hz, 1H), 7.35 – 7.18 (m, 6H), 7.17 – 7.09 (m, 2H), 7.03 – 6.97 (m, 2H), 6.93 – 6.87 (m, 1H), 5.64 (s, 1H), 3.68 (s, 3H). **^{13}C NMR (101 MHz, CDCl$_3$)** δ 159.7, 145.8, 140.5, 135.8, 134.5, 131.5, 131.4, 131.1 (2C), 130.1, 129.8, 128.1, 126.8, 126.8, 125.2, 124.5, 123.2, 122.9, 121.2, 120.2 (2C), 113.6, 57.5, 55.9, 55.6, 55.3, 55.1, 54.8. **HRMS (ESI)** m/z calcd for $C_{23}H_{19}NO$ [M+H]$^+$: 326.1467, found: 326.1468. **IR (ATR diamond, neat):** *v* 3399.0, 3051.7, 2929.0, 2835.0, 1618.1, 1592.6, 1494.2, 1416.3, 1342.8, 1240.7, 1023.6, 810.3, 737.2, 691.0 cm^{-1}.

1-(2,3-Dihydrobenzo[*b*][1,4]dioxin-6-yl)-*N*-phenylnaphthalen-2-amine (3l): Colourless solid (201 mg, 71% yield); m.p. 66.4-68.7 ˚C; **^{1}H NMR (400 MHz, CD$_2$Cl$_2$)** δ 7.85 – 7.76 (m, 2H), 7.60 (d, *J* = 8.9 Hz, 1H), 7.49 – 7.43 (m, 1H), 7.39 – 7.24 (m, 4H), 7.12 – 7.03 (m, 3H), 6.98 (tt, *J* = 7.3, 1.2 Hz, 1H), 6.91 (d, *J* = 2.0 Hz, 1H), 6.86 (dd, *J* = 8.2, 2.1 Hz, 1H), 5.74 (s, 1H), 4.42 – 4.31 (m, 4H). **^{13}C NMR (101 MHz, CD$_2$Cl$_2$)** δ 144.3, 143.5, 143.5, 138.3, 134.0, 129.5, 129.2 (3C), 128.1, 127.8, 126.2, 124.9, 124.7, 123.7, 123.2, 121.4, 119.5, 118.6 (2C), 118.0, 64.6 (2C). **HRMS (ESI)** m/z calcd for $C_{24}H_{19}NO_2$ [M+H]$^+$: 354.1416, found: 354.1417. **IR (ATR diamond, neat):** *v* 3399.0, 3051.7, 2929.0, 2835.0, 1618.1, 1592.6, 1494.2, 1416.3, 1342.8, 1240.7, 1023.6, 810.3, 737.2, 691.0 cm^{-1}.

1-(4-Fluorophenyl)-*N*-phenylnaphthalen-2-amine (3m): Colourless solid (185 mg, 74% yield); m.p. 90.1-91.4 °C; **^{1}H NMR (400 MHz, CDCl$_3$)** δ 7.89 – 7.81 (m, 2H), 7.67 (d, *J* = 8.9 Hz, 1H), 7.45 – 7.36 (m, 5H), 7.35 – 7.26 (m, 4H), 7.09 (d, *J* = 7.5 Hz, 2H), 7.02 (t, *J* = 7.3 Hz, 1H). **^{13}C NMR (101 MHz, CDCl$_3$)** δ 163.7, 161.3, 143.3, 138.2, 133.9, 132.8, 132.7, 132.4, 132.4, 129.4, 129.4, 128.6, 128.1, 126.5, 124.8, 124.3, 123.5, 121.7, 119.0, 118.7, 116.6, 116.4. **HRMS (ESI)** m/z calcd for $C_{22}H_{16}FN$ [M+H]$^+$: 314.1345, found: 314.1346. **IR (ATR diamond, neat):** *v* 3406.8, 3053.2, 2918.1, 2861.4, 1613.7, 1595.5, 1408.1, 1342.5, 1299.0, 809.1, 745.4, 704.3 cm^{-1}.

***N*-Phenyl-1-(3-(trifluoromethyl)phenyl)naphthalen-2-amine (3n):** Colourless oil (232.5 mg, 77% yield); **^{1}H NMR (400 MHz, CD$_2$Cl$_2$)** δ 7.96 – 7.86 (m, 4H), 7.79 (t, *J* = 7.7 Hz, 1H), 7.76 – 7.72 (m, 2H), 7.48 – 7.41 (m, 3H), 7.40 – 7.33 (m, 2H), 7.17 – 7.12 (m, 2H), 7.12 – 7.04 (m, 1H), 5.61 (s, 1H). **^{13}C NMR (101 MHz, CD$_2$Cl$_2$)** δ 143.3, 138.5, 137.9, 134.8, 133.7, 131.6 (q, CCF_3), 130.1, 129.5, 129.4 (2C), 129.2 (CF_3), 129.1, 128.2, 128.1, 128.0 (q, $CHCCF_3$), 126.8, 125.8 (CF_3), 124.8 (q, $CHCCF_3$), 124.4, 124.1, 123.9, 123.7, 123.2, 123.1 (CF_3), 121.8, 119.1, 118.9 (2C), 118.4 (CF_3). **HRMS (ESI)** m/z calcd for $C_{23}H_{16}F_3N$ [M+H]$^+$: 364.1235, found: 364.1237. **IR (ATR diamond, neat):** *v* 3403.1, 3051.6, 2978.0, 2929.0, 2875.8, 1619.1, 1593.1, 1495.5, 1416.7, 1298.8, 1251.1, 1121.5, 1067.6, 807.4, 738.2, 692.2 cm^{-1}.

***N*-Phenyl-[1,1'-binaphthalen]-2-amine (3o):** Colourless solid (106 mg, 53% yield); m.p. 134.8-138.0 ˚C; **^{1}H NMR (400 MHz, CD$_2$Cl$_2$)** δ 8.10 – 8.00 (m, 2H), 7.96 – 7.86 (m, 2H), 7.75 – 7.68 (m, 2H), 7.55 (ddd, *J* = 9.5, 6.8, 1.3 Hz, 2H), 7.49 – 7.43 (m, 1H), 7.35 (tdd, *J* = 8.0, 6.7, 1.3 Hz, 2H), 7.24 (ddq, *J* = 8.3, 5.0, 1.7, 1.2 Hz, 3H), 7.08 – 6.99 (m, 3H), 6.95 (tt, *J* = 7.3, 1.2 Hz, 1H), 5.48 (s, 1H). **^{13}C NMR (101 MHz, CD$_2$Cl$_2$)** δ 143.1, 139.2, 134.4, 134.3, 134.2, 132.7, 129.2, 129.2 (2C), 129.0, 128.6, 128.5, 128.5, 127.9, 126.5, 126.3, 126.3, 126.2, 125.5, 124.9, 123.2, 122.3, 121.6, 119.0 (2C), 118.3. **HRMS (ESI)** m/z calcd for $C_{26}H_{19}N$

[M+H]$^+$: 346.1517, found: 346.1518. **IR (ATR diamond, neat):** *ν* 3399.0, 3047.5, 2961.6, 2919.1, 2850.1, 1593.0, 1495.3, 1411.9, 1343.5, 1259.0, 1088.3, 1076.2, 1011.5, 805.9, 784.1, 736.0, 692.2 cm^{-1}.

***N*-Phenyl-1-(pyridin-4-yl)naphthalen-2-amine (3p):** Light yellow solid (274.5 mg, 86% yield); m.p. 178.1-179.2 ˚C; **^{1}H NMR (400 MHz, DMSO)** δ 8.73 – 8.65 (m, 2H), 7.94 – 7.86 (m, 2H), 7.52 (d, *J* = 8.9 Hz, 1H), 7.43 – 7.33 (m, 4H), 7.33 – 7.21 (m, 2H), 7.20 – 7.12 (m, 2H), 6.93 – 6.87 (m, 2H), 6.78 (tt, *J* = 7.3, 1.1 Hz, 1H), 5.76 (s, 1H). **^{13}C NMR (101 MHz, DMSO)** δ 150.4 (2C), 145.5, 145.2, 138.4, 132.8, 130.0, 129.7, 129.5 (2C), 128.6, 127.3, 126.6 (2C), 126.0, 124.4, 124.4, 122.2, 120.0, 117.1 (2C). **HRMS (ESI)** m/z calcd for $C_{21}H_{16}N_2$ [M+H]$^+$: 297.1313, found: 297.1312. **IR (ATR diamond, neat):** *ν* 3395.1, 3051.6, 2929.0, 2835.0, 1937.1, 1593.1, 1494.4, 1416.9, 1279.0, 1241.3, 1024.3, 809.5, 739.4, 691.4 cm^{-1}.

***N*-Phenyl-1-(thiophen-2-yl)naphthalen-2-amine (3q):** Colourless waxy solid (254.3 mg, 66% yield); **^{1}H NMR (400 MHz, CD_2Cl_2)** δ 7.88 (dd, *J* = 8.3, 2.0 Hz, 2H), 7.74 – 7.67 (m, 2H), 7.64 (dd, *J* = 5.2, 1.2 Hz, 1H), 7.52 – 7.32 (m, 5H), 7.25 (dd, *J* = 3.4, 1.2 Hz, 1H), 7.22 – 7.15 (m, 2H), 7.14 – 7.07 (m, 1H), 6.07 (s, 1H). **^{13}C NMR (101 MHz, CD_2Cl_2)** δ 143.2, 140.9, 137.2, 135.5, 130.0, 129.7 (2C), 129.6, 129.3, 128.4, 128.3, 127.8, 127.2, 125.0, 123.7, 122.5, 119.9 (2C), 118.2, 116.2, 54.4, 54.2, 54.1, 53.8, 53.6, 53.3. **HRMS (ESI)** m/z calcd for $C_{22}H_{15}NS$ [M+H]$^+$: 302.0925, found: 302.0923. **IR (ATR diamond, neat):** *ν* 3391.1, 3043.5, 2916.7, 1616.3, 1590.9, 1495.6, 1415.9, 1299.5, 1144.7, 1025.8, 820.7, 750.4, 700.2 cm^{-1}.

***N*-Phenyl-1-(thiophen-3-yl)naphthalen-2-amine (3r):** Colourless waxy solid (273.5 mg, 50% yield); **^{1}H NMR (400 MHz, CD_2Cl_2)** δ 7.92 – 7.85 (m, 2H), 7.71 (d, *J* = 9.0 Hz, 1H), 7.68 – 7.60 (m, 2H), 7.50 – 7.40 (m, 3H), 7.40 – 7.33 (m, 2H), 7.26 (dd, *J* = 4.9, 1.3 Hz, 1H), 7.19 – 7.13 (m, 2H), 7.07 (tt, *J* = 7.3, 1.1 Hz, 1H), 5.91 (s, 1H). **^{13}C NMR (101 MHz, CD_2Cl_2)** δ 143.5, 139.0, 136.5, 134.3, 130.0, 129.4 (2C), 129.3, 128.6, 128.1, 127.0, 126.6, 125.3, 124.9, 123.5, 121.6, 119.9, 118.8 (2C), 118.7. **HRMS (ESI)** m/z calcd for $C_{22}H_{15}NS$ [M+H]$^+$: 302.0925, found: 302.0921. **IR (ATR diamond, neat):** *ν* 3394.5, 3097.1, 3043.4, 1615.0, 1591.8, 1496.6, 1415.9, 1301.6, 1078.0, 1024.0, 855.8, 750.7, 690.9 cm^{-1}.

***(E)-N*-Phenyl-1-styrylnaphthalen-2-amine (3s):** Light yellow solid (175 mg, 66%); m.p. 142.0-143.8 ˚C; **^{1}H NMR (400 MHz, CD_2Cl_2)** δ 8.13 (dq, *J* = 8.5, 0.8 Hz, 1H), 7.86 – 7.80 (m, 1H), 7.75 (dd, *J* = 8.9, 0.8 Hz, 1H), 7.67 – 7.62 (m, 2H), 7.60 (d, *J* = 8.9 Hz, 1H), 7.52 – 7.29 (m, 8H), 7.18 – 7.11 (m, 2H), 7.07 – 6.97 (m, 2H), 6.17 (br s, 1H). **^{13}C NMR (101 MHz, CD_2Cl_2)** δ 143.4, 138.3, 137.2, 136.4, 133.0, 129.7, 129.4 (2C), 128.8 (2C), 128.3, 128.2, 128.0, 126.5 (2C), 126.5, 124.3, 123.5, 123.1, 121.6, 121.3, 118.9, 118.4 (2C). **HRMS (ESI)** m/z calcd for $C_{24}H_{19}N$ [M+H]$^+$: 322.1517, found: 322.1518. **IR (ATR diamond, neat):** *ν* 3410.5, 3050.5, 2924.6, 2855.3, 1696.9, 1593.4, 1497.0, 1307.5, 1240.0, 1024.5, 809.4, 740.0, 692.4 cm^{-1}.

***N*-Phenyl-1-(phenylethynyl)naphthalen-2-amine (3t):** Light yellow solid (192 mg, 60% yield); m.p. 114.0-117.5 ˚C; **^{1}H NMR (400 MHz, $CDCl_3$)** δ 8.28 (dq, *J* = 8.4, 0.9 Hz, 1H), 7.79 – 7.71 (m, 2H), 7.69 – 7.65 (m, 2H), 7.63 – 7.18 (m, 10H), 7.12 (tt, *J* = 7.2, 1.2 Hz, 1H), 6.90 (br s, 1H). **^{13}C NMR (101 MHz, CD_2Cl_2)** δ 144.2, 141.5 139.1, 138.4, 135.6, 129.7 (2C), 129.6, 129.5 (2C), 128.5 (2C), 128.5, 128.4, 127.9 (2C), 127.4, 124.7, 123.5, 123.3, 123.0, 115.6, 102.7. **HRMS (ESI)** m/z calcd for $C_{24}H_{17}N$ [M+H]$^+$: 320.1361, found: 320.1363. **IR (ATR diamond, neat):** *ν* 3386.8, 3057.6, 2197.2, 1888.0, 1738.8, 1619.4, 1594.4, 1495.9, 1386.2, 1307.6, 1177.2, 1024.2, 804.2, 751.5, 739.2, 699.0 cm^{-1}.

6-Methoxy-N,1-diphenylnaphthalen-2-amine (3u): Colourless waxy solid (62 mg, 26% yield); **^{1}H NMR (400 MHz, CD_2Cl_2)** δ 7.77 (d, *J* = 8.9 Hz, 1H), 7.67 – 7.56 (m, 3H), 7.56 – 7.49 (m, 1H), 7.46 – 7.40 (m, 2H), 7.39 – 7.33 (m, 1H), 7.31 – 7.21 (m, 3H), 7.09 – 6.99 (m, 3H), 6.95 (tt, *J* = 7.3, 1.1 Hz, 1H), 5.51 (s, 1H), 3.96 (s, 3H). **^{13}C NMR (101 MHz, CD_2Cl_2)** δ 156.3, 144.4, 136.8, 135.9, 130.8 (2C), 130.7, 129.3 (2C), 129.2 (3C), 129.1, 127.8, 127.1, 127.0, 126.7, 120.7, 120.6, 118.6, 117.5 (2C), 106.3, 55.3. **HRMS (ESI)** m/z calcd for $C_{23}H_{19}NO$ $[M+H]^+$: 326.1467, found: 326.1468. **IR (ATR diamond, neat):** *v* 3403.1, 3051.6, 3027.0, 2930.2, 2830.9, 1624.3, 1593.7, 1495.2, 1371.8, 1237.7, 1033.2, 851.7, 823.1, 747.1, 701.5, 691.9 cm^{-1}.

***N*-Methyl-1-phenylnaphthalen-2-amine (3v):** Colourless oil (96.8 mg, 69% yield); **^{1}H NMR (400 MHz, $CDCl_3$)** δ 7.85 (d, *J* = 8.9 Hz, 1H), 7.77 (dt, *J* = 7.9, 1.2 Hz, 1H), 7.61 – 7.55 (m, 2H), 7.51 – 7.45 (m, 1H), 7.40 – 7.34 (m, 2H), 7.28 – 7.16 (m, 4H), 3.78 (s, 1H), 2.91 (s, 3H). **^{13}C NMR (101 MHz, $CDCl_3$)** δ 154.0, 143.9, 137.1, 133.5, 131.3 (2C), 129.4 (2C), 128.9, 127.9, 127.6, 127.0, 126.2, 124.0, 121.6, 119.6, 113.2, 31.2, 18.9. **HRMS (ESI)** m/z calcd for $C_{17}H_{15}N$ $[M+H]^+$: 234.1204, found: 234.1205. **IR (ATR diamond, neat):** *v* 3424.5, 3052.1, 2912.0, 2883.4, 2819.4, 1616.1, 1595.7, 1512.8, 1495.3, 1340.6, 1296.2, 1169.8, 1152.3, 1022.4, 807.8, 745.2, 703.8 cm^{-1}.

***N*-Benzyl-1-phenylnaphthalen-2-amine (3w):** Colourless solid (219 mg, 85% yield); m.p. 145.6-152.0 ˚C; **^{1}H NMR (400 MHz, CD_2Cl_2)** δ 7.76 (dd, *J* = 8.7, 2.9 Hz, 2H), 7.66 – 7.60 (m, 2H), 7.56 – 7.49 (m, 1H), 7.46 – 7.40 (m, 2H), 7.38 – 7.19 (m, 8H), 7.15 (d, *J* = 8.9 Hz, 1H), 4.49 (br s, 2H), 4.32 (s, 1H). **^{13}C NMR (101 MHz, CD_2Cl_2)** δ 142.7, 140.0, 137.1, 133.7, 131.2 (2C), 129.5 (2C), 128.8, 128.7, 128.5 (2C), 127.8, 127.7, 127.5, 127.2, 126.9 (2C), 126.1, 125.8, 123.9, 121.7, 119.9, 114.1, 47.9. **HRMS (ESI)** m/z calcd for $C_{23}H_{19}N$ $[M+H]^+$: 310.1517, found: 310.1514. **IR (ATR diamond, neat):** *v* 3429.5, 3055.7, 2923.0, 2853.0, 1619.6, 1597.9, 1496.2, 1341.5, 1295.0, 1026.4, 809.5, 745.3, 700.5 cm^{-1}.

(*E*)-1,2-Dihydro-1-phenyl-2-(phenylimino)naphthalen-1-ol (4a): Yellow solid (42 mg, 67% yield); m.p. 105.9-106.8 °C; **^{1}H NMR (400 MHz, $CDCl_3$)** δ 7.78 (dd, *J* = 7.7, 1.4 Hz, 1H), 7.46 (td, *J* = 7.6, 1.5 Hz, 1H), 7.43 – 7.23 (m, 9H), 7.17 (t, *J* = 7.4 Hz, 1H), 6.97 (d, *J* = 10.0 Hz, 1H), 6.87 (dd, *J* = 8.1, 1.0 Hz, 2H), 6.18 (d, *J* = 10.0 Hz, 1H), 5.76 (s, 1H). **^{13}C NMR (101 MHz, $CDCl_3$)** δ 170.3, 148.3, 144.9, 142.1, 138.9, 130.6, 130.1, 128.9, 128.3, 128.2, 128.2, 127.6, 127.2, 125.7, 124.7, 120.8, 117.3. **HRMS (ESI)** m/z calcd for $C_{22}H_{17}NO$ $[M+H]^+$: 312.1388, found: 312.1384. **IR (ATR diamond, neat):** *v* 3440.1, 3373.2, 2029.2, 2950.9, 1726.1, 1594.2, 1487.3, 1444.5, 1215.3, 1159.4, 752.0, 696.2, 507.1 cm^{-1}.

(*E*)-2-(*p*-Tolylimino)-1,2-dihydro-1-phenylnaphthalen-1-ol (4b): Yellow solid (34 mg, 52% yield); m.p. 102.8-103.7 °C; **^{1}H NMR (400 MHz, $CDCl_3$)** δ 7.79 (d, *J* = 8.2 Hz, 1H), 7.46 (td, *J* = 7.5, 1.4 Hz, 1H), 7.39 (td, *J* = 7.4, 1.3 Hz, 1H), 7.37 – 7.25 (m, 6H), 7.17 (d, *J* = 8.0 Hz, 2H), 6.95 (d, *J* = 10.0 Hz, 1H), 6.79 (d, *J* = 8.2 Hz, 2H), 6.22 (d, *J* = 10.0 Hz, 1H), 5.83 (s, 1H), 2.38 (s, 3H). **^{13}C NMR (101 MHz, $CDCl_3$)** δ 170.0, 145.6, 144.9, 142.1, 138.6, 134.4, 130.7, 130.1, 129.5, 128.2, 128.1, 127.6, 127.2, 125.7, 120.9, 117.4, 21.0. **HRMS (ESI)** m/z calcd for $C_{23}H_{19}NO$ $[M+H]^+$: 326.1545, found: 326.1545. **IR (ATR diamond, neat):** *v* 3317.4, 3023.2, 2973.1, 1623.1, 1503.0, 1392.4, 1051.5, 809.3, 759.6, 696.0, 513.4 cm^{-1}.

(*E*)-2-(*o*-Tolylimino)-1,2-dihydro-1-phenylnaphthalen-1-ol (4c): Yellow oil (49 mg, 75% yield); **^{1}H NMR (400 MHz, $CDCl_3$)** δ 7.64 (d, *J* = 7.6 Hz, 1H), 7.32 (td, *J* = 7.4, 1.4 Hz, 1H), 7.28 – 7.22 (m, 3H), 7.19 – 6.98 (m, 6H), 6.93 (td, *J* = 7.4, 1.4 Hz, 1H), 6.82 (d, *J* = 9.9 Hz, 1H), 6.51 (dd, *J* = 7.7, 1.4 Hz, 1H), 5.94 (d, *J* = 9.9

Hz, 1H), 5.68 (s, 1H), 1.90 (s, 3H). **^{13}C NMR (101 MHz, CDCl$_3$)** δ 170.0, 147.0, 145.1, 142.3, 138.8, 130.9, 130.6, 130.2, 129.3, 128.2, 128.2, 127.6, 127.3, 126.2, 125.6, 124.7, 119.8, 117.4, 17.9. **HRMS (ESI)** m/z calcd for $C_{23}H_{19}NO$ [M+H]$^+$: 326.1545, found: 326.1542. **IR (ATR diamond, neat):** *v* 3021.1, 2921.3, 1625.9, 1594.3, 1483.1, 1185.4, 1053.0, 810.4, 732.2, 696.1, 623.4 cm^{-1}.

(*E*)-2-(4-Fluorophenylimino)-1,2-dihydro-1-phenylnaphthalen-1-ol (4d): Yellow oil (60 mg, 91% yield); **^{1}H NMR (400 MHz, CDCl$_3$)** δ 7.77 (d, *J* = 7.6 Hz, 1H), 7.46 (td, *J* = 7.5, 1.5 Hz, 1H), 7.39 (td, *J* = 7.5, 1.4 Hz, 1H), 7.36 – 7.22 (m, 6H), 7.13 – 7.02 (m, 2H), 6.99 (d, *J* = 10.0 Hz, 1H), 6.88 – 6.78 (m, 2H), 6.17 (d, *J* = 10.0 Hz, 1H), 5.70 (s, 1H). **^{13}C NMR (101 MHz, CDCl$_3$)** δ 170.8, 161.4, 159.0, 144.8, 144.3, 144.2, 142.1, 139.2, 130.5, 130.3, 128.3, 128.2, 128.2, 127.7, 127.2, 125.6, 122.4, 122.3, 117.0, 115.8, 115.6, 77.1. **HRMS (ESI)** m/z calcd for $C_{22}H_{16}FNO$ [M+H]$^+$: 330.1294, found: 330.1297. **IR (ATR diamond, neat):** *v* 3392.0, 3063.4, 1624.9, 1498.2, 1446.1, 1394.1, 1208.9, 1054.2, 767.2, 695.9, 519.5, 496.1 cm^{-1}.

(*E*)-2-(4-Chlorophenylimino)-1,2-dihydro-1-phenylnaphthalen-1-ol (4e): Yellow solid (46 mg, 67% yield); m.p. 93.4-94.3 °C; **^{1}H NMR (400 MHz, CDCl$_3$)** δ 7.65 (d, *J* = 7.7 Hz, 1H), 7.34 (td, *J* = 7.5, 1.5 Hz, 1H), 7.27 (td, *J* = 7.5, 1.4 Hz, 1H), 7.25 – 7.10 (m, 8H), 6.88 (d, *J* = 10.0 Hz, 1H), 6.75 – 6.63 (m, 2H), 6.02 (d, *J* = 10.0 Hz, 1H), 5.51 (s, 1H). **^{13}C NMR (101 MHz, CDCl$_3$)** δ 171.1, 146.9, 144.7, 142.1, 139.4, 130.4, 130.3, 130.1, 129.0, 128.3, 128.2, 127.7, 127.2, 125.6, 122.2, 116.9, 77.2. **HRMS (ESI)** m/z calcd for $C_{22}H_{16}ClNO$ [M+Na]$^+$: 368.0818, found: 368.0819. **IR (ATR diamond, neat):** *v* 3407.0, 3060.0, 3029.3, 1626.1, 1590.7, 1481.3, 1445.6, 1302.1, 1194.0, 1089.4, 1054.5, 1010.0, 842.4, 806.8, 756.1, 697.4, 510.2 cm^{-1}.

(*E*)-2-(4-(Trifluoromethoxy)phenylimino)-1,2-dihydro-1-phenylnaphthalen-1-ol (4f): Yellow solid (53 mg, 67% yield); m.p. 92.8-93.9 °C; **^{1}H NMR (400 MHz, CDCl$_3$)** δ 7.79 (d, *J* = 7.7 Hz, 1H), 7.48 (td, *J* = 7.5, 1.4 Hz, 1H), 7.40 (td, *J* = 7.5, 1.4 Hz, 1H), 7.37 – 7.26 (m, 6H), 7.22 (d, *J* = 7.8 Hz, 2H), 7.02 (d, *J* = 10.0 Hz, 1H), 6.91 – 6.83 (m, 2H), 6.16 (d, *J* = 10.0 Hz, 1H), 5.64 (s, 1H). **^{13}C NMR (101 MHz, CDCl$_3$)** δ 171.3, 147.1, 146.1, 144.7, 142.1, 139.6, 130.4, 128.4, 128.3, 128.3, 127.7, 127.2, 125.6, 122.0, 121.8, 119.3, 116.9, 77.2. **HRMS (ESI)** m/z calcd for $C_{22}H_{16}F_3NO_2$ [M+H]$^+$: 396.1211, found: 396.1216. **IR (ATR diamond, neat):** *v* 3401.0, 3063.0, 1626.4, 1497.4, 1394.4, 1253.0, 1151.9, 1054.2, 856.6, 806.8, 755.3, 697.1 cm^{-1}.

(*E*)-2-(Phenylimino)-1-(*p*-tolyl)-1,2-dihydronaphthalen-1-ol (4i): Yellow oil (60 mg, 92% yield); **^{1}H NMR (400 MHz, CDCl$_3$)** δ 7.79 (d, *J* = 7.6 Hz, 1H), 7.46 (td, *J* = 7.5, 1.4 Hz, 1H), 7.41 – 7.33 (m, 3H), 7.29 (d, *J* = 8.1 Hz, 1H), 7.22 (d, *J* = 8.3 Hz, 2H), 7.16 (t, *J* = 7.4 Hz, 1H), 7.09 (d, *J* = 7.8 Hz, 2H), 6.95 (d, *J* = 10.0 Hz, 1H), 6.87 (dd, *J* = 8.3, 1.2 Hz, 2H), 6.17 (d, *J* = 10.0 Hz, 1H), 5.72 (s, 1H), 2.32 (s, 3H). **^{13}C NMR (101 MHz, CDCl$_3$)** δ 170.3, 148.4, 142.3, 142.0, 138.8, 137.4, 130.5, 130.1, 129.0, 128.9, 128.2, 128.1, 127.1, 125.7, 124.6, 120.8, 117.3, 77.0, 21.0. **HRMS (ESI)** m/z calcd for $C_{23}H_{19}NO$ [M+H]$^+$: 326.1545, found: 326.1543. **IR (ATR diamond, neat):** *v* 3362.0, 3062.0, 3029.4, 1634.1, 1592.0, 1481.8, 1392.1, 1188.6, 1054.2, 907.3, 807.0, 727.8, 695.0, 507.9 cm^{-1}.

(*E*)-2-(Phenylimino)-1-(*o*-tolyl)-1,2-dihydronaphthalen-1-ol (4j): Yellow oil (45 mg, 69% yield); **^{1}H NMR (400 MHz, CDCl$_3$)** δ 7.77 (dd, *J* = 7.6, 1.8 Hz, 1H), 7.40 – 7.20 (m, 9H), 7.20 – 7.09 (m, 2H), 7.03 (d, *J* = 10.0 Hz, 1H), 6.81 (d, *J* = 7.4 Hz, 2H), 6.36 (d, *J* = 10.0 Hz, 1H), 3.91 (s, 1H), 2.13 (s, 3H). **^{13}C NMR (101 MHz, CDCl$_3$)** δ 170.4, 149.3, 143.5, 141.1, 137.7, 135.8, 131.8, 130.7, 130.0, 128.9, 128.9, 128.4, 128.2, 127.6, 126.2, 125.5, 124.3, 120.2, 117.3, 77.3, 20.6. **HRMS (ESI)** m/z calcd for $C_{23}H_{19}NO$ [M+H]$^+$: 326.1545, found: 326.1544. **IR (ATR diamond, neat):** *v* 3370.0, 3061.0, 3029.0, 1633.9, 1590.9, 1480.3, 1394.4, 1187.5, 1053.0, 907.1, 806.8, 722.3 cm^{-1}.

***(E)*-1-(2-Methoxyphenyl)-2-(phenylimino)-1,2-dihydronaphthalen-1-ol (4k):** Yellow solid (53 mg, 77% yield); m.p. 43.2-45.6 ˚C; **^{1}H NMR (400 MHz, CDCl$_3$)** δ 7.84 (dt, *J* = 7.7, 1.2 Hz, 1H), 7.45 (dd, *J* = 5.8, 3.3 Hz, 1H), 7.37 – 7.23 (m, 6H), 7.14 – 7.03 (m, 2H), 6.98 (d, *J* = 10.0 Hz, 1H), 6.83 (d, *J* = 8.1 Hz, 1H), 6.80 – 6.73 (m, 2H), 6.35 (d, *J* = 10.0 Hz, 1H), 4.05 (s, 1H), 3.63 (d, *J* = 0.9 Hz, 3H). **^{13}C NMR (101 MHz, CDCl$_3$)** δ 171.2, 156.1, 149.7, 140.5, 136.9 (2C), 135.9, 130.6, 129.4, 128.8, 128.8 (2C), 128.6, 127.9, 127.8, 126.2, 123.9, 120.6, 120.3, 117.4, 111.5, 74.8, 55.2. **HRMS (ESI)** m/z calcd for $C_{23}H_{19}NO_2$ [M+H]$^+$: 342.1416, found: 342.1416. **IR (ATR diamond, neat):** *v* 3325.5, 3006.6, 2969.8, 2929.0, 2904.4, 2830.8, 1627.7, 1584.0, 1483.1, 1462.5, 1244.3, 1045.4, 1028.2, 927.5, 763.4, 747.5, 734.8, 696.2 cm^{-1}.

***(E)-1*-(2,3-Dihydrobenzo[*b*][1,4]dioxin-6-yl)-2-(phenylimino)-1,2-dihydronaphthalen-1-ol (4l):** Yellow solid (25.5 mg, 35% yield); m.p. 66.4-68.7 ˚C; **^{1}H NMR (400 MHz, CDCl$_3$)** δ 7.78 (d, *J* = 7.6 Hz, 1H), 7.49 – 7.42 (m, 1H), 7.36 (td, *J* = 7.6, 3.6 Hz, 3H), 7.27 (d, *J* = 6.5 Hz, 1H), 7.20 – 7.14 (m, 1H), 6.95 (d, *J* = 10.0 Hz, 1H), 6.93 – 6.87 (m, 2H), 6.87 – 6.74 (m, 3H), 6.18 (d, *J* = 10.0 Hz, 1H), 5.74 (s, 1H), 4.22 (m, 4H). **^{13}C NMR (101 MHz, CDCl$_3$)** δ 170.5, 147.9, 143.13, 143.0, 142.1, 139.1 (2C), 138.1, 130.4, 130.2, 128.9 (2C), 128.3, 128.1, 127.1, 124.8, 121.0, 119.0, 117.2, 117.0, 115.1, 76.7, 64.4, 64.3. **HRMS (ESI)** m/z calcd for $C_{24}H_{19}NO_3$ [M+H]$^+$: 370.1365, found: 370.1367. **IR (ATR diamond, neat):** *v* 3386.8, 3059.7, 2973.9, 2929.0, 2875.8, 1732.7, 1625.6, 1589.6, 1500.5, 1483.8, 1283.3, 1253.1, 1066.6, 1051.0, 891.9, 808.3, 753.4, 739.6, 698.3 cm^{-1}.

(*E*)-1-(4-Fluorophenyl)-2-(phenylimino)-1,2-dihydronaphthalen-1-ol (4m): Yellow solid (52 mg, 79% yield); m.p. 102.8-103.5 °C; **^{1}H NMR (400 MHz, CDCl$_3$)** δ 7.77 (d, *J* = 7.5 Hz, 1H), 7.47 (td, *J* = 7.5, 1.5 Hz, 1H), 7.43 – 7.29 (m, 6H), 7.18 (t, *J* = 7.4 Hz, 1H), 7.01 – 6.93 (m, 3H), 6.86 (d, *J* = 7.1 Hz, 2H), 6.18 (d, *J* = 10.0 Hz, 1H), 5.75 (s, 1H). **^{13}C NMR (101 MHz, CDCl$_3$)** δ 170.1, 163.5, 161.0, 148.2, 141.9, 140.7, 140.7, 138.9, 130.5, 130.3, 129.0, 128.3, 128.3, 127.6, 127.5, 127.1, 124.8, 120.8, 117.2, 115.1, 114.9, 76.6. **HRMS (ESI)** m/z calcd for $C_{22}H_{16}FNO$ [M+H]$^+$: 330.1294, found: 330.1290. **IR (ATR diamond, neat):** *v* 3396.0, 3067.0, 2922.1, 2852.4, 1625.0, 1593.2, 1502.3, 1392.0, 1301.8, 1221.9, 1160.3, 1047.4, 814.1,765.1 cm^{-1}.

***(E)*-2-(Phenylimino)-1-(3-(trifluoromethyl)phenyl)-1,2-dihydronaphthalen-1-ol (4n):** Yellow oil (47.7 mg, 63% yield); **^{1}H NMR (400 MHz, CDCl$_3$)** δ 7.79 – 7.69 (m, 2H), 7.55 – 7.31 (m, 8H), 7.21 – 7.14 (m, 1H), 7.00 (d, *J* = 10.0 Hz, 1H), 6.88 – 6.80 (m, 2H), 6.20 (d, *J* = 10.0 Hz, 1H), 5.76 (s, 1H). **^{13}C NMR (101 MHz, CDCl$_3$)** δ 169.6, 148.2, 146.2, 141.4, 139.0, 130.7 (q, CCF_3), 130.4 (2C), 129.0 (3C), 128.7, 128.5, 128.4, 128.2 (CF_3), 127.2, 125.5 (CF_3), 124.8, 124.5 (q, $CHCCF_3$), 122.8 (CF_3), 122.5 (q, $CHCCF_3$), 120.7 (2C), 120.0 (CF_3), 117.1, 76.6. **HRMS (ESI)** m/z calcd for $C_{23}H_{16}F_3NO$ [M+H]$^+$: 380.1184, found: 380.1187. **IR (ATR diamond, neat):** *v* 3346.0, 3076.1, 2920.8, 2855.3, 1625.7, 1591.2, 1453.8, 1389.9, 1331.5, 1316.3, 1170.8, 1119.2, 1098.8, 1056.0, 910.5, 761.1, 691.0 cm^{-1}.

***(E)*-2-(Phenylimino)-[1,1'-binaphthalen]-1(2*H*)-ol (4o):** Colourless solid (31.5 mg, 44% yield); m.p. 134.8-138.0 ˚C; **^{1}H NMR (400 MHz, CDCl$_3$)** δ 8.02 (dd, *J* = 7.4, 1.2 Hz, 1H), 7.85 (ddd, *J* = 8.8, 6.4, 1.3 Hz, 2H), 7.78 (dd, *J* = 8.6, 1.2 Hz, 1H), 7.54 (dd, *J* = 8.2, 7.3 Hz, 1H), 7.44 – 7.31 (m, 5H), 7.30 – 7.23 (m, 3H), 7.16

– 7.04 (m, 2H), 6.67 – 6.61 (m, 2H), 6.40 (d, *J* = 10.0 Hz, 1H). **^{13}C NMR (101 MHz, CDCl$_3$)** δ 170.7, 149.6, 141.4, 141.2, 137.4, 134.5, 130.6, 130.3, 130.0, 129.0, 128.9, 128.8, 128.7 (2C), 128.6 (2C), 125.7, 125.5, 125.2, 124.9, 124.2, 124.1, 119.9 (2C), 117.4, 76.9. **HRMS (ESI)** m/z calcd for $C_{26}H_{19}NO$ [M+H]$^+$: 362.1467, found: 362.1466. **IR (ATR diamond, neat):** *v* 3415.4, 3370.4, 3051.2, 3010.7, 2920.8, 2855.3, 1620.2, 1589.0, 1482.5, 1396.9, 1213.6, 1057.8, 996.1, 957.9, 797.6, 775.7, 755.3, 721.5, 696.7 cm^{-1}.

***(E)*-2-(Phenylimino)-1-(pyridin-4-yl)-1,2-dihydronaphthalen-1-ol (4p):** Yellow solid (29 mg, 67%); m.p. 178.0-179.2 ˚C; **^{1}H NMR (400 MHz, CD$_2$Cl$_2$)** δ 8.52 – 8.46 (m, 2H), 7.73 – 7.66 (m, 1H), 7.50 – 7.34 (m, 5H), 7.34 – 7.29 (m, 2H), 7.24 – 7.15 (m, 1H), 7.07 (d, *J* = 10.0 Hz, 1H), 6.90 – 6.81 (m, 2H), 6.22 (d, *J* = 10.0 Hz, 1H), 5.67 (s, 1H). **^{13}C NMR (101 MHz, CD$_2$Cl$_2$)** δ 169.1, 153.9, 149.7 (2C), 148.2, 141.0, 139.3, 130.4, 130.2, 129.0 (2C), 128.5, 128.5, 126.9, 124.8, 120.6 (2C), 120.3 (2C), 117.0, 76.3. **HRMS (ESI)** m/z calcd for $C_{21}H_{16}N_2O$ [M+H]$^+$: 313.1263, found: 313.1261. **IR (ATR diamond, neat):** *v* 3063.2, 3077.9, 3023.2, 2923.2, 2921.8, 1592.3, 1521.8, 1482.5, 1360.9, 1270.4, 1155.8, 1027.9, 925.9, 818.5, 800.6, 750.8, 697.0 cm^{-1}.

***(E)*-2-(Phenylimino)-1-(thiophen-2-yl)-1,2-dihydronaphthalen-1-ol (4q):** Yellow waxy solid (36 mg, 57% yield); **^{1}H NMR (400 MHz, CDCl$_3$)** δ 7.94 (dd, *J* = 7.7, 1.3 Hz, 1H), 7.49 (td, *J* = 7.6, 1.4 Hz, 1H), 7.44 – 7.36 (m, 3H), 7.31 – 7.26 (m, 1H), 7.21 (ddt, *J* = 14.9, 7.2, 1.2 Hz, 2H), 6.99 – 6.91 (m, 3H), 6.86 (dd, *J* = 5.1, 3.6 Hz, 1H), 6.73 (dd, *J* = 3.6, 1.3 Hz, 1H), 6.24 (d, *J* = 10.0 Hz, 1H), 5.83 (s, 1H). **^{13}C NMR (101 MHz, CDCl$_3$)** δ 168.9, 150.5, 148.2, 141.5, 138.7, 130.0, 129.9, 129.0 (2C), 128.5, 128.4, 126.7, 126.5, 125.7, 125.0, 124.8, 120.8 (2C), 116.8, 75.1. **HRMS (ESI)** m/z calcd for $C_{20}H_{15}NOS$ [M+H]$^+$: 317.0874, found: 317.0877. **IR (ATR diamond, neat):** *v* 3660.7, 3378.6, 3068.0, 2990.3, 2900.3, 1675.1, 1626.5, 1591.4, 1483.0, 1451.9, 1393.0, 1224.0, 1190.0, 1047.3, 801.2, 696.6 cm^{-1}.

***(E)*-2-(Phenylimino)-1-(thiophen-3-yl)-1,2-dihydronaphthalen-1-ol (4r):** Yellow solid (39 mg, 62% yield); m.p. 118.3-126.0 ˚C; **^{1}H NMR (400 MHz, CDCl$_3$)** δ 7.86 (dd, *J* = 7.6, 1.3 Hz, 1H), 7.47 (td, *J* = 7.5, 1.4 Hz, 1H), 7.38 (tt, *J* = 7.3, 1.2 Hz, 3H), 7.31 – 7.12 (m, 4H), 6.97 – 6.83 (m, 4H), 6.21 (d, *J* = 9.9 Hz, 1H), 5.69 (s, 1H). **^{13}C NMR (101 MHz, CDCl$_3$)** δ 169.5, 148.4, 146.8, 142.0, 138.7, 130.0, 129.0 (2C), 128.3, 128.2, 126.7, 126.2, 125.7, 124.7, 121.8, 120.8 (2C), 117.0, 75.5. **HRMS (ESI)** m/z calcd for $C_{20}H_{15}NOS$ [M+H]$^+$: 317.0874, found: 317.0876. **IR (ATR diamond, neat):** *v* 3660.7, 3360.3, 2988.0, 2921.1, 1625.7, 1594.2, 1485.0, 1448.7, 1392.2, 1232.0, 1190.9, 1140.2, 1045.5, 781.6, 758.0, 726.8 703.0 cm^{-1}.

***(E)*-6-Methoxy-1-phenyl-2-(phenylimino)-1,2-dihydronaphthalen-1-ol (4u):** Yellow waxy solid (27 mg, 47%); **^{1}H NMR (400 MHz, CDCl$_3$)** δ 7.68 (d, *J* = 8.5 Hz, 1H), 7.39 – 7.24 (m, 7H), 7.19 – 7.13 (m, 1H), 6.99 (dd, *J* = 8.5, 2.6 Hz, 1H), 6.91 (d, *J* = 10.0 Hz, 1H), 6.89 – 6.81 (m, 3H), 6.18 (d, *J* = 10.0 Hz, 1H), 5.70 (s, 1H), 3.89 (s, 3H). **^{13}C NMR (101 MHz, CDCl$_3$)** δ 170.4, 159.4, 148.4, 145.2, 138.8, 134.2, 131.6, 128.9 (2C), 128.5, 128.2 (2C), 127.6, 125.7 (2C), 124.7, 120.8 (2C), 117.8, 115.1, 113.7, 76.8, 55.5. **HRMS (ESI)** m/z calcd for $C_{23}H_{19}NO_2$ [M+H]$^+$: 342.1416, found: 342.1417. **IR (ATR diamond, neat):** *v* 3673.0, 3382.7, 2994.3, 2965.7, 2916.7, 2835.0, 1730.7, 1673.4 1628.1, 1612.9, 1566.2, 1488.6, 1316.1, 1268.9, 1166.6, 1118.9, 1036.8, 856.0, 825.5, 806.0, 756.1, 698.0 cm^{-1}.

(*E*)-1-Hydroperoxy-*N*,1-diphenylnaphthalen-2(1*H*)-imine (5a): Orange solid (52 mg, 80% yield); **^{1}H NMR (400 MHz, CDCl$_3$)** δ 10.65 (br s, 1H), 7.96 (dd, *J* = 7.7, 1.3 Hz, 1H), 7.54 (td, *J* = 7.6, 1.4 Hz, 1H), 7.45 (td, *J* = 7.5, 1.3 Hz, 1H), 7.42 – 7.26 (m, 8H), 7.21 – 7.16 (m, 1H), 6.96 – 6.89 (m, 2H), 6.85 (d, *J* = 10.1 Hz, 1H), 6.16 (d, *J* = 10.1 Hz, 1H). **^{13}C NMR (101 MHz, CDCl$_3$)** δ 168.8, 148.6, 139.2, 138.9, 137.8, 132.3, 129.8, 129.2, 129.0, 128.9, 128.8, 128.5, 128.3, 128.2, 127.6, 127.4, 125.7, 124.7, 120.8, 118.8, 117.3, 89.9. **HRMS (ESI)** m/z calcd for $C_{22}H_{17}NO_2$ [M+H]$^+$: 328.1338, found: 328.1342.

2-Nitro-1-phenylnaphthalene (6): Colourless oil (24 mg, 48% yield); **^{1}H NMR (400 MHz, CDCl$_3$)** δ 7.99 (td, *J* = 8.5, 0.9 Hz, 2H), 7.94 (d, *J* = 8.9 Hz, 1H), 7.70 – 7.62 (m, 2H), 7.58 – 7.50 (m, 4H), 7.41 – 7.33 (m, 2H). **^{13}C NMR (101 MHz, CDCl$_3$)** δ 146.7, 134.8, 134.7, 134.6, 132.5, 129.4 (2C), 129.1, 128.5 (3C), 128.4, 128.3, 128.1, 127.8, 120.0. **HRMS (ESI)** m/z calcd for $C_{16}H_{11}NO_2$ [M+H]$^+$: 250.0790, found: 250.0787. **IR (ATR diamond, neat):** *ν* 3202.8, 3133.3, 3050.8, 2969.8, 2916.7, 1919.8, 1589.3, 1504.9, 1429.4, 1341.9, 1212.4, 993.9, 812.5, 759.0, 698.3 cm^{-1}.

References

1. Lin, S.; Ischay, M.A.; Fry, C.G.; Yoon, T.P. *J. Am. Chem. Soc.*, **2011**, *133*, *48*, 19350–19353.
2. Zoller, J.; Fabry, D.C.; Ronge, M.A.; Rueping, M. *Angew. Chem. Int. Ed.,* **2014**, *53*, 13264-13268.
3. Magallanes, G.; Karka¨, D.M.; Bosque, I. et al. *ACS Catal.*, **2019**, *9*, 2252−2260.
4. Cheng, Y.; Yang, J.; Qu, Y.; Li, P. *Org. Lett.*, **2012**, *14 (1)*, 98–101.
5. To, W.-P.; Liu, Y.; Lau, T.-C.; Che, C.-M. *Chem. Eur. J.*, **2013**, *19*, 5654-5664.
6. Itoh, A.; Yamaguchi, T.; Nobuta, T. et al. *Synlett*, **2014**, *25(10)*, 1453–1457.
7. Daniel, M.; Fensterbank, L.; Goddard, J.-P.; Ollivier, C. *Org. Chem. Front*., **2014**, *1*, 551-555.
8. Yang, D.; Shi, Q.; Shen, J.; Li, Z. et al. *RSC Adv*., **2021**, *11*, 18966-18973.
9. Parrish, J.D.; M.A.; Lu, Z.; Guo, S.; Peters, N.R.; Yoon, T.P.; Org. Lett., **2012**, *14 (6)*, 1640–1643.
10. Zou, Y.-Q.; Chen, J.-R.; Xiao, W.-J. et al. *Angew. Chem. Int. Ed*., **2012**, *51*, 784-788.
11. Han, J.W.; Jung, J.; Lee, Y.-M.; Nam, W.; Fukuzumi, S.; *Chem. Sci*., **2017**, *8*, 7119-7125.
12. Vo, N.T.; Mekmouche, Y.; Tron, T.; Aukauloo, A. et al. *Angew. Chem. Int. Ed.*, **2019**, *58*, 16023.
13. Torregrosa-Chinillach, A.; Chinchilla, R. *Molecules*, **2021**, *26(4)*, 974.
14. Zhu, S.; Das, A.; Bui, L.; Rueping, M. et al. *J. Am. Chem. Soc.*, **2013**, *135 (5)*, 1823–1829.
15. Ding, W.; Zhou, Q.-Q.; Xuan, J.; Xiao, J.-W. et al. *Tetrahedron*, **2014**, *55*, 4648–4652.
16. Wang, D.; Li, J.; Cai, S.; Chen, J.; Zhao, Y. *Synlett*, **2014**, *25*, 1626–1628.
17. Dockrey, S.A.B.; Narayan, A.R.H. *Org. Lett.*, **2020**, *22*, 3712−3716.
18. Cheng, Y.-Z.; Zhou, K.; Zhu, M.; Li, L.-A.-C.; Zhang, X.; You, S.-L. *Chem. Eur. J.* **2018**, *24*, 12519.
19. An, J.; Zou, Y.-Q.; Yang, Q.-Q.; Wang, Q.; Xiao, W.-J. *Adv. Synth. Catal.*, **2013**, *355*, 1483-1489.
20. Wu, C.; Liou, T.; Wei, H.; Tsai, P.; Yang, D. *Tetrahedron*, **2014**, *70 (44)*, 8219–8225.
21. Forrester, A.R.; Fullerton J.D.; McConnachie, G. *J. Chem. Soc., Perkin Trans. 1*, **1983**, 2711-2715.
22. Yu, M.; Wang, M.; Chen, X.; Hong, B.; Zhang, X.; Cheng, C. *J. Chem. Res.*, **2005**, *9*, 558–560.
23. Balestri, D.; Bacchi, A.; Scilabra, P.; Pelagatti, P. *Inorganica Chim. Acta*, **2018**, *470*, 416-422.
24. Macháček, J.P.; Jansa, V.; Svobodová, P. et al. *Eur. J. Org. Chem.,* **2008**, *2008*, 3272-3278.
25. Zhang, L.; Shen, J.; Wu, S.; Zhong, G.; Wang, Y.-B.; Tan, B.; *Angew. Chem. Int. Ed.,* **2020**, *59*, 23077.